**EVALUATION OF SAMPLING PROCEDURES FOR SPATIAL ANALYSIS OF SURFACE AND EDAPHIC PROPERTIES ON SPORTS FIELDS**

by

CHASE MATTHEW STRAW

(Under the Direction of Gerald M. Henry)

## ABSTRACT

Spatial variation of surface and edaphic properties on sports fields are challenging to control due to dependency of foot traffic. The term "performance testing" is a method to quantify these properties to assist in more efficient management decisions. However, minimal testing procedures have been identified to detect variability of a property in space. The recent introduction of a mobile multi-sensor device, for use in turfgrass, allows for rapid data collection and the use of geostatistics for spatial analysis. Several sample grid sizes of soil moisture (volumetric water content, VWC), soil compaction (penetration resistance), and plant performance (normalized difference vegetative index, NDVI) were measured with the mobile device and spatially evaluated on six community sports fields. An appropriate sample grid size was identified for each property. Preliminary comparison of mobile and handheld data collection methods indicate the need for more spatial research using handheld devices.

INDEX WORDS: GIS, GPS, NDVI, VWC, Geostatistics, Penetration resistance, Spatial variability, Sports fields, Turfgrass

# EVALUATION OF SAMPLING PROCEDURES FOR SPATIAL ANALYSIS OF SURFACE AND EDAPHIC PROPERTIES ON SPORTS FIELDS

by

CHASE MATTHEW STRAW

B.S., University of Kentucky, 2010

A Thesis Submitted to the Graduate Faculty of The University of Georgia in Partial Fulfillment of the Requirements for the Degree

MASTER OF SCIENCE

ATHENS, GEORGIA

2014

© 2014

Chase M. Straw

All Rights Reserved

**EVALUATION OF SAMPLING PROCEDURES FOR SPATIAL ANALYSIS OF SURFACE AND EDAPHIC PROPERTIES ON SPORTS FIELDS**

by

CHASE MATTHEW STRAW

| | |
|---|---|
| Major Professor: | Gerald M. Henry |
| Committee: | Robert N. Carrow<br>Van Cline |

Electronic Version Approved:

Maureen Grasso
Dean of the Graduate School
The University of Georgia
May 2014

## ACKNOWLEDGEMENTS

First and foremost, I would like to thank my wonderful wife for her unwavering support. Choosing to further my education has led us both to new experiences that have made us grow even stronger together than we were before. You inspire me to pursue my goals and are my strength through every day. I love you and deeply appreciate all the sacrifices you have made to make this possible.

I would also like to thank my entire family. This experience has led us away from them geographically, but they have always shown support and provided positive encouragement.

I would like to express my gratitude to Dr. Gerald Henry for allowing me the opportunity to further my education. He has opened many doors for me in my time working with him and I truly appreciate everything he has done. I take pride in having him as a major professor and look forward to continuing our friendship.

Thank you to my other committee members, Dr. Robert Carrow and Dr. Van Cline, for offering their expertise and always being available for advice and support.

Thank you to Mark Holder and Tom Popps for allowing me to use their sports fields and accommodating me during data collection.

Last, but certainly not least, I would like to thank the Toro Company. Special thanks to Dr. Van Cline, Kathy Rice, and Troy Carson for all their insight, analysis, and technical support. It has been a pleasure having the opportunity to work with you all.

## TABLE OF CONTENTS

Page

ACKNOWLEDGEMENTS ..... iv

CHAPTER

1 INTRODUCTION AND LITERATURE REVIEW ..... 1

2 EVALUATION OF SAMPLING PROCEDURES FOR SPATIAL ANALYSIS OF SOIL MOISTURE ON SPORTS FIELDS ..... 27

3 EVALUATION OF SAMPLING PROCEDURES FOR SPATIAL ANALYSIS OF SOIL COMPACTION ON SPORTS FIELDS ..... 108

4 EVALUATION OF SAMPLING PROCEDURES FOR SPATIAL ANALYSIS OF PLANT PERFORMANCE ON SPORTS FIELDS ..... 190

5 PRELIMINARY COMPARISON OF MOBILE AND HANDHELD SAMPLING DEVICES FOR MEASURING SURFACE AND EDAPHIC PROPERTIES ON SPORTS FIELDS ..... 272

6 CONCLUSIONS ..... 292

7 APPENDIX ..... 295

# CHAPTER 1

# INTRODUCTION AND LITERATURE REVIEW

## Background – Management of Natural Turf Sports Fields

Due to the well documented health benefits of regular physical activity (Fletcher et al., 1996; World Health Organization, 2003; Britain and Donaldson, 2004) there has been an increase of participation in sports and exercise in the United States over the last few decades (US Youth Soccer, 2012; National Collegiate Athletic Association, NCAA, 2013; National Federation of State High School Associations, 2013). Sports activities can take place on almost any surface and within limited space (Stiles et al., 2009). However, at all levels which sports are played (professional, collegiate, community, etc.) a quality playing surface is desired to encourage fair play, maximize enjoyment, and minimize the risk of injury (Baker and Canaway, 1993). Thus, for sports played on natural turf, there is an importance for proper management practices to provide expected quality.

Sports turf managers aspire to produce homogeneous playing conditions across the entire area (Caple et al., 2012). The major stresses on the field are associated with foot traffic from game play (Madison, 1971). The term traffic is general in nature and includes both wear and soil compaction stresses (Carrow and Petrovic, 1992). Wear is the injury inflicted to a turf from pressure, scuffing, or tearing on the turfgrass tissues (Carrow and Petrovic, 1992). Soil compaction is defined as the pressing together of soil particles, resulting in a more dense soil mass with less pore space (Beard, 1973). Madison (1971) noted that compaction causes an

overall decline in growth, vigor, quality, and persistence of the turf by influencing factors that affect growth, such as soil aeration, soil strength, and plant and soil moisture relationships.

To combat foot traffic stress, management involves an integrated approach of several techniques, including primary cultural practices such as mowing, fertilization, irrigation, and cultivation. These practices should encourage growth and provide a sufficient root zone that will enhance turf stability for athletic play. Furthermore, cultural practices should focus on managing both surface and edaphic properties relative for the play of sports (Holmes and Bell, 1986). These properties have shown to influence, presumably, the two most important components of managing a sports field; player safety and field playability (Baker, 1999; Caple et al., 2012). Player safety is related to player-surface interactions such as surface hardness (the hardness of the playing surface), soil compaction, traction (the amount of grip footwear has on the turf), soil moisture (amount of moisture in the soil profile) and turf performance (turf evenness, coverage, uniformity, and density) (Bell et al., 1985; Baker and Canaway, 1993). Field playability is related to ball-surface interactions such as rebound height (how well the ball rebounds from the surface), smoothness (evenness of the surface), and speed of the surface (speed of ball movement across the surface) (Bell et al., 1985; Baker and Canaway, 1993).

Previous research has shown that surface and edaphic properties associated with player and surface interactions have a strong influence on one another. For example, Baker (1991) found that surface hardness was dependent on soil moisture (higher surface hardness with lower amounts of soil moisture). Gibbs et al. (1989) observed that traction was related to the amount of root material present (decreased traction as turf is lost from a field). Holmes and Bell (1986) showed that ball rebound was correlated with surface hardness (higher rebound with harder surfaces). Additionally, Richards and Baker (1992) determined ball roll was influenced by height

of turf (less ball roll with higher mowing). The importance of implementing a balanced management approach is vital due to the impact these interactions can have on athletes and the game.

## Performance Testing of Natural Turf Sports Fields

The term "performance testing" (i.e. site assessment) is receiving increasing attention as a method to quantify the performance of sports field properties (McAuliffe, 2008; Stiles et al., 2009; Carrow et al., 2010). Performance testing has primarily been focused on synthetic surfaces with the assumption that natural turf surfaces are a benchmark for safety (Stiles et al., 2009; Fédération Internationale de Football Association, FIFA, 2012). However, on natural turf fields, the magnitude and frequency of spatial variations are considerably greater and more challenging to control because of dependency on the level of foot traffic (Baker, 1991). Performance standards were first proposed by Bell, Baker, and Canaway (1985) and the final report from the Natural Turf Pitch Prototypes Advisory Panel was published in 1992 (Adams et al., 1992). However, the research did not produce a code of practice or management plan (Jennings-Temple et al., 2006).

Recently, two case studies have been published to emphasize the need for future research and the importance of performance testing on natural turf sports fields. The first case study, by McAuliffe (2008), specified that a major driving force for performance testing and standards in Australia is the demand by authorities for safer playing conditions, because of fear of litigation. McAuliffe proposed the creation of surface performance standards to be measurable and clearly defined. Having measurable/objective, rather than subjective, methods of measuring surface properties provide greater clarity with regard to what is being specified. For example, using terms such as "hard", "slippery", or "uneven" are subjective based on an individual's personal

assessment (McAuliffe, 2008). A number of other practical uses were listed, including; defining the quality and safety of the field, providing a basis for tendering out work, enabling auditing, evaluating the progress over time, comparing fields, providing a basis for negotiating a contract, and resolving disputes.

The second case study, Bartlett et al. (2009), proposed performance testing be split into four broad categories: 1) comparison between fields; 2) assessment of facility; 3) ability for better management decisions, and; 4) research in design, function, or injury risk. Category 1 testing involves set surface standards to deliver client expectations and to protect against litigation in sports related injuries. Category 2 and 3 are somewhat similar in which identifying deficiencies in the playing surface can lead to better management decisions and thus improvements in facility (Baker et al., 1998). Category 4 testing is the least common and is used to inform the other 3 categories of testing the player perception of surface quality (Fleming et al., 2005), sports injury epidemiology, and sports equipment and development (Dixon et al., 1999; Nigg et al., 2001; Dixon et al., 2008; Stiles et al., 2009).

These studies describe performance testing from the standpoint of player safety and field playability. However, turf managers world-wide are also interested in ways to improve input efficiency of primary cultural practices to minimize costs and reduce any potential negative environmental aspects (Beard and Kenna, 2008; Carrow and Duncan, 2008). To do so in agriculture, the concepts of precision agriculture (PA) and precision conservation (PC) have been developed and based on the premise of site-specific management. PA involves applying inputs, such as water, fertilizer, and pesticides, only where, when, and in the amount needed by the plant (Bouma et al., 1999; Corwin and Lesch, 2005; Bullock et al., 2007). PC was developed out of

PA to assist in making the best management decisions related to conservation and sustainability of agriculture, rangeland, and natural areas (Delgado and Berry, 2008).

As a parallel to PA and PC, the concept of precision turfgrass management (PTM) has recently been suggested for enhanced input efficiency and management decisions in turfgrass (Stowell and Gelernter, 2006, 2008; Carrow et al., 2007; Bell and Xiong, 2008; Krum, 2008; Carrow et al., 2010; Krum et al., 2010). Complex turf sites already practice some degree of PTM. For example, on golf courses, greens, tees, fairways, and roughs all have unique management requirements (Carrow et al., 2010). Similarly, for sports fields, depending on turf species, soil class, usage, level of sport, and the sport itself being played, management requirements can significantly differ from field to field. However, the evolution of PTM is based on acquiring detailed site information by intensive site assessment to offer an even more precise and efficient management of inputs, such as sub-areas with a sports field, than is currently practiced (Carrow et al., 2010). Performance testing can be viewed as the site assessment referred to in the PTM concept.

## Performance Testing Methods

### *Surface hardness*

Surface hardness is essentially a measurement of 'firmness' of the playing surface, which includes stiffness (i.e. how much it deforms under a given load) and resilience (i.e. how much energy is returned to the player) (Bell et al., 1985). Monitoring surface hardness is particularly important, from a player's perspective, to cover the conditions of player to surface impact that relate to running, falling, and injury prevention (Baker and Canaway, 1993). Additionally, ball-surface interactions, such as ball bounce and ball roll, have been significantly correlated with surface hardness (Holmes and Bell, 1986; Baker, 1991).

Tests involve dropping a missile of known mass from a standard height, with a mounted linear accelerometer (Gramckow, 1968; Clegg, 1976; American Society for Testing and Materials (ASTM), 2010a). The maximum acceleration during the impact (relative to gravity) is recorded and that value is commonly reported as g-max (Holmes and Bell, 1986; Baker et al., 1998; Baker, 1991; ASTM, 2010a). It is important to consider the missile mass, with greater masses being more appropriate when conditions deeper in the soil surface are expected to influence hardness. Common missile masses used on sports fields include 0.5-kg, 2.25-kg, and 4.5-kg (Lush, 1985; Baker, 1991; Bartlett et al., 2009; ASTM, 2010a).

*Soil Compaction*

A strong correlation has been observed between surface hardness and soil compaction in turf (Baker, 1991). Beard (1973) noted that the majority of compaction in turfgrass situations occurs in the top 8 cm of the soil surface, mostly in the upper 3 cm. Furthermore, in compacted soil, turf roots are prevented from growing deep within the soil surface (Carrow and Petrovic, 1992), which can greatly increase the chance of creating divots when players make athletic maneuvers.

Soil compaction on sports fields has been measured using multiple techniques. One of the more common methods is the use of a penetrometer device (Holmes and Bell, 1986; Bengough et al., 2000; Flitcroft et al., 2010; Caple et al., 2012). There are various forms of penetrometers available and most allow for data to be obtained in a reasonable time. A penetrometer uses a cylindrical tip (also referred to as "cone") of a certain length to measure the penetration resistance of the soil at a certain depth (i.e. the force it takes to insert the cone into the soil to a specific depth) (Holmes and Bell, 1986).

Penetration resistance can, in principal, be estimated from the bulk mechanical properties of the soil (Bengough et al., 2000). Soil bulk density is an indicator of soil compaction and is defined as the mass of total soil divided by the volume it occupies (Black and Hartge, 1986). Therefore, higher bulk densities indicate a higher penetration resistance and a more compacted soil. A result of high bulk density is a decline in pore space from macropores to micropores, thus also influencing air-water relationship (Carrow and Petrovic, 1992). Perhaps the first determination of bulk density was done by collecting a known volume of soil and measuring the weight after drying (Black and Hartge, 1986).

A third technique is a nondestructive method to measure soil bulk density using gamma ray attenuation (Gardner, 1986). This method has been adapted to a portable surface moisture-density gauge that has been used effectively in turfgrass traffic research (McNitt and Landschoot, 2001). The gamma source is positioned at a specific depth within the soil by insertion into an access hole. Gamma rays are transmitted through the soil to detectors located within the gauge and the average density between the gamma source and the detectors is determined (Troxler Electron Laboratories, Inc., 2003).

*Traction*

Traction is an indication of the horizontal forces that are applied to turf, which are typically linear or rotational (Bell et al., 1985; Baker, 1999). Sports involve running and turning, therefore it is essential that there is sufficient grip between the players footwear and the playing surface to prevent slipping or falling (Bell et al., 1985; Baker, 1999). Alternatively, excessive grip may increase the incidence of knee and ankle injuries (Baker et al., 1998).

One of the first traction measuring techniques was a studded disc apparatus utilized by Canaway (1975) to measure the torque necessary to shear the turf. Canaway and Bell (1986)

described a more improved studded-boot apparatus with a 40-kg mass and two handled torque wrench to measure the force needed to cause the turf to fail. Additionally, McNitt et al. (1997) developed the Pennfoot apparatus to measure both linear and rotational traction of the athletic shoe-field surface interface on natural turf as well as other playing surfaces (Middour, 1992; Brosnan et al., 2009).

Traction can also be determined by means of shear vanes (Shildrick, 1981; Stier et al., 1999). The Clegg Shear Tester is a device for quantifying shear strength related to divot removal through measuring the force required by pulling a blade (up to 50 mm wide and inserted as deep as 40 mm) through the turf surface in an arching motion (Chivers and Aldous, 2003; Sherratt et al., 2005).

*Soil moisture*

Multiple researchers have shown the amount of moisture in the soil can have a significant impact on surface hardness, soil compaction, and traction on a sports field (Holmes and Bell, 1986; Baker, 1991; Carrow and Petrovic, 1992). Carrow and Petrovic (1992) stated that when the soil moisture content is at or near saturation, traffic will have a maximum effect on soil compaction due to soil particle orientation that causes reduction in pore space. Holmes and Bell (1986) conducted traction tests concluding significant (negative) correlations with soil moisture.

One of the first methods of measuring soil moisture was collecting a soil core and measuring the ‘wet’ and ‘dry’ weight to determine a percentage. More recently, time-domain reflectometry (TDR) and capacitance sensors have been used for determining soil moisture by measuring changes in the soil dielectric constant (ε) as water contents fluctuate (Leib et al., 2003). TDR sensors produce a high frequency voltage pulse that is transmitted and reflected along metal probes when inserted into the soil. The velocity of the transmitted pulse in the soil,

which is primarily dependent on VWC, determines the ε. Water has a significantly higher ε than air (ε = 80 and 1, respectively), thus the permittivity and corresponding pulse velocity are closely related to the soil water content (Plauborg et al., 2005). Capacitance sensors determine ε by measuring the charge time of a capacitor which uses that soil as a dielectric. These methods typically express soil moisture as percent volumetric water content (%VWC).

*Turf performance*

Turf performance qualities (evenness, coverage, uniformity, and density) are critical in terms of player-surface impacts. In particular, turf coverage was found to increase traction (Jennings-Temple et al., 2006) and decrease surface hardness (Holmes and Bell, 1986). Additionally, unexpected changes in the surface can cause a player to stumble, slip, or fall (Baker, 1999). These qualities can also influence ball-surface interactions, such as ball roll and vertical ball bounce (Baker, 1999).

Two common methods have been utilized to measure surface evenness; 1) the use of a straight edge to record localized changes in evenness (McClements and Baker, 1994), and 2) a profile gauge based on a series of independently moving rods in a frame that are displaced by surface undulations (Baker, 1999). Turf coverage has been assessed visually using quadrat frames to find percent coverage within each quadrat (Bartlett et al., 2009; Institute of Groundsmanship, IOG, 2014). Furthermore, a method by Haggar et al. (1983) has been used by researchers to evaluate ground cover using spectral reflectance sensors. The operation of the sensor depends on measuring the radiance ratio of red (R) and near-infrared (IR) of the form [(R + IR)/IR]. This ratio is higher for green canopies than for soil.

Most recently, a more broad assessment of turf performance has been reported by Trenholm et al. (1999) using a spectral reflectance methodology referred to as normalized

difference vegetative index (NDVI). NDVI has been shown to be significantly associated with visual turf quality, density, and shoot tissue injury (Trenholm et al., 1999). NDVI sensors are equipped with internal light emitting diodes and a photodiode optical detector that measures the reflectance of red (R = 660 nm) and near-infrared (NIR = 770 nm) spectra used to calculate a vegetative index {NDVI = $[(R_{770} - R_{660})/(R_{770} + R_{660})]$} (Krum et al., 2010). Healthy plants have greater NIR and lower R reflectance than plants under stress. Bell et al. (2002) concluded that measuring NDVI can lead to reduction of inputs, increased turf uniformity, and provide early detection of plant stress.

## Performance Testing Procedures

Minimal procedures have been published to identify performance test locations on natural turf sports fields. The ASTM F1936 is a standard specification of test point locations for impact attenuation (i.e. surface hardness) measured in the field (ASTM, 2010b). The specification describes test locations for all sports played on natural turf in America (football, soccer, lacrosse, field hockey). Generally, 10 test points are recommended in the proximity of areas such as end zones and goals, wings (a certain distance from the center line and sideline), middle of field, and one location outside the in-bound lines. Three consecutive missile drops at each test location are suggested and visual estimates of turf cover (0-100%) as well as soil moisture (dry, damp, wet, saturated, etc.) are encouraged (ASTM, 2010b).

Additionally, The Performance Quality Standards (PQS) is a concept in Europe, developed by Dury (1997), to provide a complete picture of a stated facility (such as a football pitch), with the surface, sub-surface, and playing aspects being clearly defined. The IOG provides PQS test methods to assess an extensive number of parameters (total of 19) (Bartlett et al., 2009; IOG, 2014). For each parameter, sampling numbers and test locations vary by sport.

The values from each location are averaged to determine performance of that parameter. For overall performance, the values are written in an evaluation table then compared to the benchmark standard. Points are allocated to rate for quality (5 points for "high" quality; 1 point for "basic" quality). Points are then totaled and compared to a set scale (high, standard, basic, below standard) to determine what the level of quality is, on the whole, for the field (IOG, 2014).

Researchers that have evaluated performance qualities have used similar test procedure with slight variations in methodologies (Bell and Holmes, 1988; Baker and Bell, 1986; Holmes and Bell, 1986; McClements and Baker, 1994; Jennings-Temple et al., 2006; Bartlett et al., 2009). These studies collected data from 3-12 locations across their fields, with 1-10 tests per location area. The sample scheme from this research was generally developed from the assumption that foot traffic on a sports field creates an approximate diamond shape wear pattern (with majority of wear being in the center of the field and around goals) (Holmes and Bell, 1986). To take into account of inherent variability, samples were collected from sites on the field thought to receive high, intermediate, and low levels of wear (Holmes and Bell, 1986). Summary statistics (mean, min, max, standard deviation, etc.) were the primary determinate of central tendency and variability for the data.

## Spatial Analysis of Natural Sports Fields

Previously described sampling methods are designed to be 'low technology' to enable wide usage; however, a consequence of making data assessment easier to conduct and interpret can mask variability of the data for the entire field (Bartlett et al., 2009). Geostatistics is a form of statistics used to analyze spatial data which are applied in environmental science fields such as mineral resource mapping and precision farming in agriculture (James and Goodwin, 2003; Taylor et al., 2003; Emery and González, 2007). Global Positioning Systems (GPS) enable the

data to be imported into powerful Geographic Information System (GIS) programs for spatial analysis using geostatistics. GPS is a radio-navigation system providing continuous location (i.e., latitude, longitude, and altitude) information to an unlimited number of users (U.S. Coast Guard Navigation Center).

Specifically, two geostatistical techniques, variograms and interpolation, are commonly used. A variogram (also referred to as semivariogram) is a function of the distance and direction separating measured points used to quantify the spatial autocorrelation (also referred to as spatial dependence) of the data set (ESRI, 2004). The semivariogram represents half the difference squared of the values between each pair of points (i.e. semivariance) at different distances then fits a model to the empirically derived data points (Webster and Oliver, 2007). The semivariogram is based on Tobler's Law, also known as the first law of geography, which states, "Everything is related to everything else, but near things are more related than distant things" (Tobler, 1970). Therefore, semivariance is generally low when two locations are close to each other and increases as the distance between the locations grow until at some point the locations become independent.

It is important to note that the most determining factor for an accurate semivariogram, and the one in which we have the most control over, is the sample size that it is based on (Oliver and Webster, 2014). Typically, the more data you have the greater the accuracy. Oliver and Webster (2014) demonstrated, from repeated grid sampling of a large two-dimensional simulated field, that confidence intervals narrow as the number of data samples increases and the distance between the data samples decreases. They concluded that semivariograms generated from fewer than 100 data samples were unreliable.

Secondly, interpolation can be used to create continuous surface maps of the data for visual assessment. To create a continuous surface map of a certain phenomenon, predictions are made for locations in the study area based on the semivariogram and spatial arrangement of measured values that are nearby (ESRI, 2004). Kriging is a common interpolation method that forms weights from surrounding measured values to predict values at unmeasured locations (ESRI, 2004). With kriging interpolation, the closest measured values have the most influence on weights.

Currently, only Miller (2004), and most recently Caple et al. (2012), have used geostatistical methods to characterize spatial structure of performance qualities on natural turf sports fields. Both studies used handheld devices for data collection. Miller (2004) evaluated the surface hardness of two soccer fields (one sand-based and one native soil) using a grid pattern of 80 cells. Each cell was 10 m x 10 m and surface hardness data was taken at the center using a Clegg Impact Soil Tester (Jolimont, Western, Australia) with a 2.25-kg missile. Semivariograms were generated to show differences in spatial structure of surface hardness on the sand-based and native-soil fields. These results concluded that native soils may be influenced by field usage more than sand-based soils. Graphic presentation of kriged data was useful to visually determine spatial patterns, especially those influenced by something other than normal foot traffic patterns.

Caple et al. (2012) performed a more robust geostatistical analysis surveying three sports fields of different soil textures at the beginning, middle, and end of season using 135 or 150 samples of five parameters [volumetric water content, penetration resistance, shear resistance, peak deceleration (surface hardness), and surface energy absorption]. With exception of penetration resistance, all parameters exhibited random variation, defined by the semivariograms. Caple et al. (2012) described that random variation should be placed into

context of surface performance applicable to foot traffic by athletes, as that the measured parameters will vary on a small spatial scale. The kriged interpolation maps provided visual assessment and confirmed random variation in the surface.

GIS is more commonly used in agriculture to implement the PA concept (Rhoades et al., 1999; Corwin and Lesch, 2005; Thomsen et al., 2007). To recall, site-specific management is the first premise of PA, to apply inputs only where needed, when needed and at the amount needed (Bouma et al., 1999; Corwin and Lesch, 2005; Bullock et al., 2007). Spatial areas for agriculture extend much farther than that of a sports field, therefore mobile sensor platforms have been developed for more efficient sampling and more precise spatial analysis. The most widely used mobile field sensor platforms in agriculture are those that record soil electrical conductivity ($EC_a$), especially by electromagnetic induction (EM), to map (i.e. interpolate) spatial variation (Rhoades, 1993; Corwin and Lesch, 2005). However, indications of VWC from $EC_a$ are crude and not as reliable as measurements of VWC by TDR (Carrow and Duncan, 1998). Recently, a relatively rapid stop-and-go TDR unit for mapping soil VWC has been developed to record measurements over 15-30 ha in 8 h (Thomsen et al., 2007). Remote sensing indices such as NDVI have also been used on a frequent basis at ground level, in the air, or by satellites to estimate crop cover, green plant biomass, and leaf area index (Trenholm et al., 1999; Hunsaker et al., 2003).

To date, only one study using a mobile platform on sports fields has been conducted. Freeland et al. (2008) used a ground penetrating radar (GPR) towed behind an electric golf cart to conduct a rapid survey method for mapping soil compaction on a collegiate football field. The GPR system has a control unit with software and data recording capability, and has the high-speed electronics to generate, receive, and process electrical pulses sent and received from an

antenna. The antenna receives the electrical pulse and forms and transmits it as an electromagnetic pulse into the subsurface. Reflections of the subsurface are displayed on a computer monitor and materials that have high ($EC_a$), such as wet clay, will attenuate signals very rapidly permitting only shallow penetration depths (Freeland et al., 2008). Conversely, materials with lower $EC_a$, such as dry sand, do not attenuate the signal and allow much greater penetration depths (Freeland et al., 2008). A soil horizon that is compacted will have a different ε from the surrounding non-compacted horizon, thus reflecting radar to a greater degree due primarily to reduced pore space, altering both volumetric air and water content (Freeland et al., 2008). A Clegg Impact Soil Tester (CIST) was also used to complement the survey by evaluating surface hardness on a 9.14 m x 9.14 m grid across the field, totaling 77 locations. While interpolation techniques were used for visual assessment, variograms were not provided to quantify spatial dependence of the data. Additionally, plant performance information was not provided to determine relationships.

Flitcroft et al. (2010) and Krum et al. (2010) are the only researchers to use a mobile multi-sensor device on a turfgrass site (golf course fairway). Data collection was performed in both studies using the Toro Mobile Multi-Sensor (TMM) prototype data acquisition unit [now patented as the Toro Precision Sense 6000 (PS6000)] (The Toro Company, Bloomington, MN). The PS6000 was affixed to and maneuvered with a utility vehicle, traversing the fairways by making passes at approximately 2.5 m in a traverse at an operating speed of 2.7 to 3.3 km $h^{-1}$ with measurements made while moving. The PS6000 simultaneously measures VWC (%), compaction (penetration resistance; N in m kg $s^{-2}$), and NDVI (unit-less with best = 1.0) all while using GPS to geo-reference longitudinal and latitudinal location of samples. Variograms and kriging were used to spatially analyze the data for mapping of penetration resistance for site-

specific cultivation on one golf course fairway (Flitcroft et al., 2010) and to identify site-specific-management units (SSMUs) on two golf course fairways (Krum et al., 2010). By utilizing spatial data, the concept of PTM can be implemented to make informed management decisions.

## Conclusions

Performance testing of natural turf sports fields is receiving increasing attention due to the magnitude and frequency of temporal variations with associated surface and edaphic properties. Data generated can provide an assessment of field conditions to assist in making more informed management decisions to reduce inputs. Previous sampling methods are designed for wide usage; however, making data assessment easier to conduct and interpret can greatly mask variability of the data across the entire field. Therefore, the use of geostatistics for spatial analysis would best explain variability in space.

Site-specific information is the first requirement of PTM, using spatial analysis, and can be best obtained with mobile platforms. To the author's knowledge, the PS6000 is the first and only mobile multi-sensor unit with GPS capability for use on turfgrass sites. One advantage of the PS6000 is unlimited sampling intensity. The use of handheld devices for extreme data sampling has been deemed time, cost, and labor intensive. However, to date, mobile devices are not abundantly available for commercial use, thus limiting data collection to handheld sensors in most instances. Furthermore, a standard procedure using either type of apparatus has not been implemented for spatial analysis of sports fields. Therefore, various sampling procedures should be evaluated.

## References


Adams, W.A., R.J. Gibbs, S. Baker, and D. Lance. 1992. Making the most of natural turf pitches. A national survey of winter games pitches with high quality drainage designs. Natural Turf Pitches Prototypes Advisory Panel Report No. 10, Sports Council.

American Society for Testing and Materials (ASTM). 2010a. F1702–10, Measuring impact-attenuation characteristics of natural playing surface systems using a lightweight portable apparatus. Annual book of ASTM standards. American Society for Testing Materials, West Conshohocken, PA.

American Society for Testing and Materials (ASTM). 2010b. F1936–10, Standard specification of impact attenuation of turf playing systems as measured in the field. Annual book of ASTM standards. American Society for Testing Materials, West Conshohocken, PA.

Baker, S.W., and M.J. Bell. 1986. The playing characteristics of natural turf and synthetic turf surfaces for association football. J. Sports Turf Res. Inst. 62:9-35.

Baker, S.W. 1991. Temporal variation of selected mechanical properties of natural turf football pitches. J. Sports Turf Res. Inst. 67:83-92.

Baker, S.W., and P.M Canaway. 1993. Concepts of playing quality: criteria and management. Int. Turfgrass Soc. Res. J. 7:172-181.

Baker, S.W., A.R. Cole, and S.L. Thornton. 1998. Performance standards and the interpretation of playing quality for soccer in relation to rootzone composition. J. Sports Turf Res. Inst. 64:120-132.

Baker, S. 1999. The playing quality of turfgrass sports surfaces. p. 231-244. *In* Aldous D. (Ed.) International Turf Management Handbook. Butterworth Heinemann Press, Oxford (UK).

Bartlett, M.D., I.T. James, M. Ford, and M. Jennings-Temple. 2009. Testing natural turf sports surfaces: the value of performance quality standards. Proceedings of the Institution of Mechanical Engineers, Part P. J. Sports Eng. and Technol. 223:21-29.

Beard, J.B. 1973. Turfgrass: Science and culture. Prentice Hall Inc., Englewood Cliffs, NJ.

Beard, J.B., and M.P. Kenna. 2008. Water quality and quantity issues for turfgrasses in urban landscapes. CAST Special Publication 27. Ames, Iowa: Council for Agriculture Science and Technology.

Bell, M.J., S.W. Baker, and P.M. Canaway. 1985. Playing quality of sports surfaces: A review. J. Sports Turf Res. Inst. 61:26-45.

Bell, M.J., and G. Holmes. 1988. The playing quality of association football pitches. J. Sports Turf Res. Inst. 61:19-47.

Bell, G.E., D.L. Martin, M.L. Stone, J.B. Solie, and G.V. Johnson. 2002. Turf area mapping using vehicle-mounted optical sensors. Crop Sci. 42:648-651.

Bell, G.E., and X. Xiong. 2008. The history, role, and potential of optical sensing for practical turf management. p. 641-660. *In* M. Pessarakli (Ed.), Handbook of turfgrass management and physiology. CRC Press, NY.

Bengough, A.G., D.J. Campbell, and M.F. O'Sullivan. 2000. Penetrometer techniques in relation to soil compaction and root growth. p. 377-403. *In* Smith, K.A., and C.E Mullins (Eds.), Soil and Environmental Analysis. 2nd ed. Marcel Dekker, NY.

Black, G.R., and K.H. Hartge. 1986. Bulk density. p. 363-375. *In* A. Klute (Ed.), Methods of soil analysis. Part 1. 2nd ed. Agron. Monogr. 9. ASA and SSSA, Madison, WI.

Bouma, J., J. Stoorvogel, B.J. van Alphen, and H.W.G. Booltink. 1999. Pedology, precision agriculture, and the changing paradigm of agricultural research. Soil Sci. 63.6:1763-1768.

Britain, G., and L.J. Donaldson. 2004. At least five a week: evidence on the impact of physical activity and its relationship to health. Department of Health, Physical Activity, Health Improvement, and Prevention. http://webarchive.nationalarchives.gov.uk/20130107105354/http://www.dh.gov.uk/prod_consum_dh/groups/dh_digitalassets/@dh/@en/documents/digitalasset/dh_4080981.pdf (accessed 25 Feb 2014).

Brosnan, J.T., and J. Deputy. 2009. Preliminary observations on the traffic tolerance of four seashore paspalum cultivars compared to hybrid bermudagrass. Hort. Technol. 19(2): 423-426.

Bullock, D.S., N. Kitchen, and D.G., Bullock. 2007. Multidisciplinary teams: a necessity for research in precision agriculture systems. Crop Sci. 47:1765-1769.

Canaway, P.M. 1975. Fundamental techniques in the study of turfgrass wear: an advance report on research. J. Sports Turf Res. Inst. 51:104-115.

Canaway, P.M., and M.J. Bell. 1986. Technical note: an apparatus for measuring traction and friction on natural and artificial playing surfaces. J. Sports Turf Res. Inst. 62:211-214.

Caple, M., I. James, and M. Bartlett. 2012. Spatial analysis of the mechanical behaviour of natural turf sports pitches. Sports Eng. 15:143-157.

Carrow, R.N., and A.M. Petrovic. 1992. Effects of traffic on turfgrasses. p. 285-330. *In* Carrow, R.N and R.C. Shearman (Eds.), Turfgrass. ASA, Madison, WI.

Carrow, R.N., V. Cline, and J. Krum. 2007. Monitoring spatial variability in soil properties and turfgrass stress: applications and protocols. Proc. of 28th Int. Irrigation Show, 9-11 Dec. 2007, San Diego, CA.

Carrow, R.N., and R.R. Duncan. 2008. Turfgrass BPMs for water resources: holistic-systems approach. *In* M. Kenna and J.B. Beard (Eds.), Water quality and quantity issues for turfgrasses in urban landscapes (pp. 273-294). Ames, IA: Council for Agricultural Science and Technology. CAST Special Pub. 27.

Carrow, R.N., J.M Krum, I. Flitcroft, and V. Cline. 2010. Precision turfgrass management: challenges and field applications for mapping turfgrass soil and stress. Precis. Agric. 11:115-134.

Chivers, I.H., and D.E. Aldous. 2003. Performance monitoring of grassed playing surfaces for Australian rules football. J. Turfgrass and Sports Surf. Sci. 79:73-80.

Clegg, B. 1976. An impact testing device for in situ base course evaluation. Proc. of the Australian Road Research Board. August 1976. 8:1-6.

Corwin, D.L., and S.M. Lesch. 2005. Apparent soil electrical conductivity measurements in agriculture. Comput. Electron. Agric. 46:103-133.

Delgado, J.A., and J.K. Berry. 2008. Advances in precision conservation. Advances in Agron. 98:1-44.

Dixon, S.J., M.E. Batt, and A.C. Collop. 1999. Artificial playing surfaces research: a review of medical, engineering and biomechanical aspects. Int. J. Sports Med. 20:209-218.

Dixon, S.J., I.T. James, K. Blackburn, N. Pettican, and D. Low. 2008. Influence of footwear and soil density on loading within the shoe and soil surface during running. Proceedings of the Institution of Mechanical Engineers, part P: J. Sports Eng. Technol. 222:1-10.

Dury, P.L.K. 1997. Grounds maintenance: managing outdoor sport and landscape facilities. Thorogood, London.

Emery, X., and K. González. 2007. Incorporating the uncertainty in geological boundaries into mineral resources evaluation. J. Geol. Soc. India. 69:29–38.

ESRI. 2004. ArcGIS 9: Using ArcGIS Geostatistical Analyst. ESRI, Redlands, CA.

Fédération Internationale de Football Association (FIFA). 2012. FIFA quality concept for football turf. Fédération Internationale de Football Association. http://www.fifa.com/mm/document/afdeveloping/pitchequip/fqc_football_turf_folder_342.pdf (accessed 31 March 2014).

Fleming, P.R., C. Young, J.R. Roberts, R. Jones, and N. Dixon. 2005. Human perceptions of artificial surfaces for field hockey. Sports Eng. 8:121-136.

Flitcroft, I., J. Krum, R. Carrow, K. Rice, T. Carson, and V. Cline. 2010. Spatial mapping of penetrometer resistance on turfgrass soils for site-specific cultivation. Proc. CD of the 10th Int. Conference on Prec. Ag., Denver, CO. 18-21 July, 2010. ISPA, Monticello, IL.

Fletcher, G.F., G. Balady, S.N. Blair, et al. 1996. Statement on exercise: benefits and recommendations for physical activity programs for all Americans. A statement for health professionals by the Committee on Exercise and Cardiac Rehabilitation of the Council on Clinical Cardiology, American Heart Association. Circulation. 94:857-862.

Freeland, R.S., J.C. Sorochan, M.J. Goddard, and J.S. McElroy. 2008. Using ground-penetrating radar to evaluate soil compaction of athletic turfgrass fields. Appl. Eng. Agric. 24:509-514.

Gardner, W.H. 1986. Water content. *In* C. A. Black (Ed.) Methods of soil analysis, Part 1. Am. Soc. Agron. pp. 82-127.

Gibbs, R.J., W.A. Adams, and S.W Baker. 1989. Factors affecting the surface stability of a sand rootzone. *In* H. Takotoh (Ed.), Proceedings of 6th Intl. Turfgrass Res. Conf.

Tokyo, Japan, pp. 189-191.

Gramckow, J. 1968. Athletic field quality studies. Cal-Turf Inc., Camarillo, CA.

Haggar, R.J., C.J. Stent, and S. Isaac. 1983. A prototype hand-held patch sprayer for killing weeds, activated by spectral differences in crop/weed canopies. J. Agric. Eng. Res. 28:349-358.

Holmes, G., and M.J. Bell. 1986. A pilot study of the playing quality of football pitches. J. Sports Turf Res. Inst. 62:74-91.

Hunsaker, D.J., P.J. Pinter Jr, E.M. Barnes, and B.A. Kimball. 2003. Estimating cotton evapotranspiration crop coefficients with a multispectral vegetation index. Irrig. Sci. 22:95-104.

Institute of Groundsmanship (IOG). 2014. Performance Quality Test (PQS) Methods. http://www.iog.org/train-education/Technical-Library/Performance+Quality+Standards/PQS+Methods+of+Test (accessed 25 Feb 2014).

James, I.T., and R.J. Godwin. 2003. Soil, water and yield relationships in developing strategies for the precision application of nitrogen fertiliser to winter barley. Biosyst. Eng. 84:467-480.

Jennings-Temple, M., P. Leeds-Harrison, and I. James. 2006. An investigation into the link between soil physical conditions and the playing quality of winter sports pitch rootzones. *In* The engineering of sport 6. 1:315-320. Springer, NY.

Krum, J.M. 2008. Spatial site assessment of soil moisture and plant status on golf courses. M.S. thesis. Univ. of Georgia, Athens, GA.

Krum, J.M., R.N. Carrow, and K. Karnok. 2010. Spatial mapping of complex turfgrass sites: Site-specific management units and protocols. Crop Sci. 50:301-315.

Leib, B.G., J.D. Jabro, and G.R. Matthews. 2003. Field evaluation and performance comparison of soil moisture sensors. Soil Sci. 168:396-409.

Lush, W.M. 1985. Objective assessment of turf cricket pitches using an impact hammer. J. Sports Turf Res. Inst. 61:71-79.

Madison, L.H. 1971. Principle of turfgrass culture. Van Nostrand Reinhold Co., NY.

McAuliffe, K.W. 2008. The role of performance testing and standards in the sports turf industry: A case study approach. *In* J.C. Stier, L. Han, and D. Li (Eds.). Proceedings of 2nd international conference on turfgrass management and sports fields (pp. 391-398). Int. Soc. Hort. Sci. Belgium.

McClements, I., and S.W. Baker. 1994. The playing quality of rugby pitches. J. Sports Turf Res. Inst. 70:29-43.

McNitt, A.S., R.O. Middour, and D.V. Waddington. 1997. Development and evaluation of a method to measure traction on turfgrass surfaces. J. Test. Eval. 25:99-107.

McNitt, A.S., and P.J. Landschoot. 2001. The effects of soil reinforcing inclusions in an athletic field rootzone. Int. Turfgrass Soc. Res. J. 9:565-572.

Middour, R.O. 1992. Development and evaluation of a method to measure traction on turfgrass surfaces. M.S. Thesis. Pennsylvania State Univ., University Park, PA.

Miller, G.L. 2004. Analysis of soccer field surface hardness. *In* P.A. Nektarios (Ed.), Proceedings of the first International Conference on Turfgrass Management and Science for Sports Fields. ISHS, Leuven, pp. 287-294.

National Collegiate Athletic Association (NCAA). 2013. Participation Rates Continue To Rise. National Collegiate Athletic Association http://www.ncaa.org/about/resources/media-center/news/participation-rates-continue-rise. (accessed 25 Feb 2014).

National Federation of State High School Associations. 2013. 2012-2013 High School Athletics Participation Survey. http://www.nfhs.org/WorkArea/linkit.aspx?LinkIdentifier=id&ItemID=9627&libID=9648. (accessed 25 Feb 2014).

Nigg, B.M., and J.M Wakeling. 2001. Impact forces and muscle tuning: a new paradigm. Exerc. Sport Sci. Rev. 29:37-41.

Oliver, M.A., and R. Webster. 2014. A tutorial guide to geostatistics: Computing and modelling variograms and kriging. Catena. 113:56-69.

Plauborg, F., B.V Iversen, and P.E. Laerke. 2005. In situ comparison of three dielectric soil moisture sensors in drip irrigated sandy soils. Vadose Zone J. 4:1037-1047.

Richards, C.W., and S.W. Baker. 1992. Technical note. The effect of sward height on ball roll properties for Association Football. J. Sports Turf Res. Inst. 68:124-124.

Rhoades, J.D., F. Chanduvi, and S.M. Lesch. 1999. Soil salinity assessment: Methods and interpretation of electrical conductivity measurements. FAO Irrigation and Drainage Paper 57. Food and Agric. Organ. of the United Nations. Rome, Italy.

Sherratt, P J., J.R. Street, and D.S. Gardner. 2005. Effects of biomass accumulation on the playing quality of a Kentucky bluegrass stabilizer system used for sports fields. Agron. J. 97:1107-1114.

Shildrick, J.P. 1981. Shoot numbers, stem bases and persistence in artificially-worn perennial ryegrass cultivars. J. Sports Turf Res. Inst. 57:84-107.

Stier, J.C., J.N. Rogers, J.R. Crum, and P.E. Rieke. 1999. Flurprimidol effects on Kentucky bluegrass under reduced irradiance. Crop Sci. 39:1423-1430.

Stiles, V.H., I.T. James, S.J. Dixon, and I.N. Guisasola. 2009. Natural turf surfaces. Sports Med. 39(1):65-84.

Stowell, L., and W. Gelernter. 2006. Sensing the future. Golf Course Manage. 74(3):107-110.

Stowell, L., and W. Gelernter. 2008. Evaluation of a Geonics EM38 and NTech GreenSeeker sensor array for use in precision turfgrass management. *In* Abstracts, GSA-SSSA-ASACSSA-GCAGS Int. Annu. Meet., Houston, TX, 5-9 Oct. 2008. ASA-CSSA-SSSA, Madison, WI.

Taylor, J.C., G.A. Wood, R. Earl, and R.J. Godwin. 2003. Soil factors and their influence on within-field crop variability, part II: spatial analysis and determination of management zones. Biosyst. Eng. 84:441-453.

Thomsen, A., K. Schelde, P. Drøscher, and F. Steffensen. 2007. Mobile TDR for geo-referenced measurement of soil water content and electrical conductivity. Precis. Agric. 8:213-223.

Tobler W.R. 1970. A computer movie simulating urban growth in the Detroit region. Econ. Geogr. 46:234–240.

Trenholm, L.E., R.N. Carrow, and R.R. Duncan. 1999. Relationship of multispectral radiometry data to qualitative data in turfgrass research. Crop Sci. 39:763-769.

Troxler Laboratories, Inc. 2003. RoadReader™ Nuclear Density Gauge Models 3430 & 3440 product brochure. http://www.troxlerlabs.com/downloads/pdfs/3430-40/3430-40_brochure.pdf (accessed 31 March 2014).

US Youth Soccer. 2012. Key Statistics. US Youth Annual Registration of Players. http://www.usyouthsoccer.org/media_kit/keystatistics/ (accessed 25 Feb 2014).

Webster, R., and Oliver, M.A. 2007. Geostatistics for environmental scientists. John Wiley & Sons, Hoboken, NJ.

World Health Organization. 2003. Health and development through physical activity and sport. http://whqlibdoc.who.int/hq/2003/WHO_NMH_NPH_PAH_03.2.pdf (accessed 25 Feb 2014).

# CHAPTER 2

# EVALUATION OF SAMPLING PROCEDURES FOR SPATIAL ANALYSIS OF SOIL MOISTURE ON SPORTS FIELDS[1]

[1] Straw, C.M., G.M. Henry, R.N. Carrow, V. Cline. To be submitted to *Crop Science.*

Abstract

Pressure from society for water conservation and the effects of soil moisture on surface properties has led to the need for improved management regimes on sports fields. The term "performance testing" is a method to quantify surface and edaphic properties of sports fields, such as volumetric water content (VWC). Previous procedures have used handheld devices to collect data from minimal locations (6-12). The low number of samples restricts analysis of variability over the entire area. Geostatistics is a branch of statistics that uses semivariograms and interpolation, generated from intense data sampling, for analysis of a given variable in space. The Toro Precision Sense 6000 (PS6000), a mobile multi-sensor device with Global Positioning System (GPS) capability, has recently been introduced for use on turfgrass sites. The PS6000's ability for rapid sampling and geo-referenced data allows for the use of geostatistical methods to conduct spatial analysis. However, there is limited research of sampling procedures or protocols for use on sports fields. The PS6000 was used to measure VWC on three 'Tifway 419' hybrid bermudagrass (*Cynodon dactylon* x *C. transvaalensis*) sports fields in Roswell, Georgia and three 'TifSport' hybrid bermudagrass sports fields in Watkinsville, Georgia during the summer of 2013. Various levels of sample sizes were manipulated, using Geographic Information System (GIS) software, from the initial 2.4 m x 2.4 m sample grid. Spatial analysis of VWC was conducted on all sample sizes and compared within each field to evaluate an appropriate sampling procedure. In general, as the sample grid sizes became larger, the strength of the semivariograms and the accuracy and detail of the surface maps minimized. A minimal sample grid size of 9.6 m x 4.8 m was determined, with subsequently decreasing grid sizes providing a more accurate and detailed site-specific analysis.

## Introduction

Managers of natural turf sports fields aspire to produce homogeneous playing conditions with consistent surface and edaphic properties across the field (Caple et al., 2012). An integrated approach utilizing several techniques is needed to achieve homogeneity; including, primary cultural practices such as irrigation, mowing, fertilization, and aerification. Irrigation management is of particular importance, not only for turf growth, but also due to societal pressure for more efficient regimes to conserve water. Furthermore, soil moisture has been shown to effect surface properties, such as hardness and traction, which can decrease player safety and field playability (Holmes and Bell, 1986; Baker, 1991). Therefore, turf managers are interested in finding ways to improve water use efficiency and how to better evaluate soil moisture distribution on their sports fields.

An earlier method of measuring soil moisture involved collecting a soil core to determine a percentage from "wet" and "dry" weights. More recently, time-domain reflectometry (TDR) and capacitance sensors have been used for determining soil moisture by measuring changes in the soil dielectric constant (ε) as water contents fluctuate (Leib et al., 2003). TDR sensors produce a high frequency voltage pulse that is transmitted and reflected along metal probes when inserted into the soil. The velocity of the transmitted pulse in the soil, which is primarily dependent on volumetric water content (VWC), determines the ε. Water has a significantly higher ε than air (ε = 80 and 1, respectively), thus the permittivity and corresponding pulse velocity are closely related to the soil water content (Plauborg et al., 2005). Capacitance sensors determine ε by measuring the charge time of a capacitor which uses that soil as a dielectric. These methods typically express soil moisture as percent volumetric water content (%VWC).

A procedure to quantify the surface and edaphic properties of sports fields, such as VWC, is termed "performance testing" (i.e. site assessment) (McAuliffe, 2008; Stiles et al., 2009; Carrow et al., 2010). Performance testing involves collecting data samples at multiple locations across a field to better understand the variability of the property of interest. Minimal standards have been established to identify sampling locations. One procedure is the American Society for Testing and Materials (ASTM) F1936, which identifies test locations to measure only surface hardness (ASTM, 2010). The Performance Quality Standards (PQS) provides a test procedure for a wide range of parameters, but soil moisture is not included (Institute of Groundsmanship, IOG, 2014). Researchers that have evaluated soil moisture on sports fields have collected samples from only six to twelve locations (Holmes and Bell, 1986; Bell and Holmes, 1988; McClements and Baker, 1994). Summary statistics (mean, min, max, standard deviation, etc.) were used to determine central tendency and variability of the data. However, performance properties can vary significantly across an area due to dynamic interactions of use, management, climate, plant, and soil factors (Taylor et al., 2007). Thus, the low number of sample locations restricts detailed analysis and may mask small scale variability on a field.

Variability of a property in space is better explained using geostatistics. Geostatistics provides a number of statistical techniques to evaluate spatial data which has been utilized in environmental science fields such as mineral resource mapping and precision farming in agriculture (James and Goodwin, 2003; Taylor et al., 2003; Emery and González, 2007). Global Positioning Systems (GPS) enable the data to be geo-referenced (i.e. record of longitudinal and latitudinal location) and imported into Geographic Information Systems (GIS) where geostatistics can be implemented.

Specifically, two geostatistical techniques, variograms and interpolation, are commonly used. A variogram (also referred to as semivariogram) is a function of the distance and direction separating measured points used to quantify the spatial autocorrelation (also referred to as spatial dependence) of the data set (ESRI, 2004). The semivariogram represents half the difference squared of the values between each pair of points (i.e. semivariance) at different distances then fits a model to the empirically derived data points (Webster and Oliver, 2007).

It is important to note that the most determining factor for an accurate semivariogram, and the one in which we have the most control over, is the sample size that it is based on (Oliver and Webster, 2014). Typically, the more data you have the greater the accuracy. Oliver and Webster (2014) demonstrated, from repeated grid sampling of a large two-dimensional simulated field, that confidence intervals narrow as the number of data samples increases and the distance between the data samples decreases. They concluded that semivariograms generated from fewer than 100 data samples were unreliable.

Secondly, interpolation creates continuous surface maps of the data for visual assessment. To do so, predictions are made for locations in the study area based on the semivariogram and spatial arrangement of measured values that are nearby (ESRI, 2004). Kriging is a common interpolation method that forms weights from surrounding measured values to predict values at unmeasured locations (ESRI, 2004). With kriging interpolation, the closest measured values have the most influence on weights. Much like the semivariogram, sample size can greatly influence the accuracy and detail of a kriged surface map.

GIS is more common in agriculture to implement the precision agriculture (PA) concept (Rhoades, 1999; Corwin and Lesch, 2005; Thomsen et al., 2007). PA involves applying inputs, such as water, fertilizers, and pesticides, only where, when, and in the amount needed by the

plant (Bouma et al., 1999; Corwin and Lesch, 2005; Bullock et al., 2007). As a parallel to PA, the concept of precision turfgrass management (PTM) is gaining increasing attention for enhanced input efficiency and management decisions in turfgrass (Stowell and Gelernter, 2008; Carrow et al., 2007; Bell and Xiong, 2008; Krum, 2008; Carrow et al., 2010; Krum et al., 2010). PTM was developed and based on the premise of site-specific management. To a certain degree, complex turf sites already use some degree of PTM. For example, on sports fields, management can differ significantly depending on turf species, soil class, field usage, level of sport, and the sport itself being played. However, the evolution of PTM is based on acquiring detailed site information by intensive data sampling to offer an even more precise and efficient management of inputs, such as sub-areas within a sports field, than is currently practiced now (Carrow et al., 2010). Performance testing can be viewed as the site assessment referred to in the PTM concept.

To date, only Miller (2004), Freeland et al. (2008), and most recently Caple et al. (2012), have used geostatistical methods to analyze spatial variability of surface and edaphic properties on natural turf sports fields. Research by Miller (2004) evaluated only surface hardness, while the study by Freeland et al. (2008) evaluated surface hardness and soil compaction. Caple et al. (2012) conducted a spatial analysis on multiple surface properties. VWC, along with soil compaction, traction, surface hardness, and surface energy absorption were evaluated on three sports fields of different soil textures at the beginning, middle, and end of the season using 135 or 150 samples. Aside from Freeland et al. (2008), who used an electric golf cart to tow a Ground Penetrating Radar (GPR) for the rapid assessment of soil compaction, the other studies used handheld devices for data collection. However, handheld devices have been deemed timely, costly, and labor intensive for such extensive sampling.

In agriculture, mobile platforms, with built in sensors, have been developed for efficient sampling and more precise spatial analysis. For example, a relatively rapid stop-and-go TDR unit for mapping (i.e. surveying) soil VWC has been developed to record measurements over 15-30 ha in 8 h (Thomsen et al., 2007). In turfgrass, the Toro Precision Sense 6000 (PS6000) (The Toro Company, Bloomington, MN) was recently developed for rapid sampling on complex turfgrass sites. The PS6000 simultaneously measures VWC (%), soil compaction (penetration resistance; N in m kg $s^{-2}$), and plant performance (normalized difference vegetative index, NDVI; unit-less with best = 1.0) all while using GPS to geo-reference longitudinal and latitudinal location of samples.

Currently, the only researcher to utilize the PS6000 for mapping of VWC is Krum et al. (2010) and Flitcroft et al. (2010). Krum et al.'s (2010) study used geostatistical techniques to identify site-specific management units (SSMU's) on two golf course fairways. SSMU's classify areas of similar soil and landscape properties that result in similar plant response, input-use efficiency, and environmental impact (Boydell and McBratney, 1999; Corwin and Lesch, 2005; and Krum et al., 2010). SSMU's are foundational to efficient management in PA and PTM because they identify "trouble" locations to aide in the application of inputs as well as potentially identify deficiencies in irrigation systems. Evaluation of VWC surface maps, before and after a routine irrigation practices, can provide insight in faults into the system down to individual irrigation heads that could not be detected otherwise. Deficiencies can include clogged nozzles, inadequate system pressure, or poor irrigation head spacing. Flitcroft et al. (2010) evaluated the spatial relationship of VWC and penetration resistance to determine site-specific cultivation areas on a golf course fairway.

Mobile multi-sensor devices to conduct performance tests with spatial analysis have yet to be utilized on sports fields, but can be fundamental in developing a site-specific, comprehensive sports turf management program. Site-specific information is the first requirement of spatial analysis. To the author's knowledge, the PS6000 is the first and only mobile multi-sensor device, with GPS capability, for use on turfgrass sites. However, there are currently few available for use, thus limiting data collections to handheld devices in most instances. Furthermore, an efficient sampling procedure, using either methodology, has yet to be implemented for an accurate spatial analysis. Therefore, the primary objective of this study was to utilize the PS6000 to evaluate 7 different sample grid sizes, and a sample size of 7 locations resembling previous performance testing methods, to define an effective, science-based grid spacing for an accurate spatial analysis of VWC on natural turf sports fields.

## Materials and Methods

### *Description of sports fields*

Research was conducted at the Grimes Bridge Soccer Complex in the city of Roswell, GA and Oconee Veterans Park in Watkinsville, GA. A total of six community level sports fields were used between the two locations (Tables A-1 and A-2, Appendix). The Roswell location included three 'Tifway 419' hybrid bermudagrass (*Cynodon dactylon* x *C. transvaalensis*) fields mowed two times a week at 2.54 cm with a reel mower. The Watkinsville location included three 'TifSport' hybrid bermudagrass fields also mowed two times a week at 2.54 cm with a reel mower. All fields evaluated had sandy loam soils and field size ranged from 60-64 m x 95-104 m.

Soccer was the primary sport played on all fields at both locations (Table A-1, Appendix). Fields in Roswell were constructed in tiers, with field 1 being at the top, field 2 in the

middle, and field 3 below. Two concrete walls approximately 9.1 m and 3.0 m high separates fields 1 and 2, and fields 2 and 3, respectively. Field 1 is open to the public while fields 2 and 3 remain gated throughout the day and are solely used for scheduled practice and games. Fields in Watkinsville were designed in a flat open area (4.2 ha) and laid in close proximity to one another. Field 1 is directly north of field 3 with the south end zone of 1 being approximately 22.9 m from the north end zone of 3. Field 2 is centered approximately 22.9 m east of 1 and 3. All fields in Watkinsville are open to the public.

Data collection in Roswell followed one day after significant rainfall, thus each field was semi-saturated. In Watkinsville data was collected two days after rainfall, thus VWC was lower than at Roswell, but still near field capacity. The distribution of VWC does not resemble manual irrigation patterns at either location.

*Data collection*

VWC data was collected in Roswell on 9 May, 2013 and in Watkinsville on 10 May, 2013 (Table A-1, Appendix). The PS6000 was used to measure VWC on all six fields. The PS6000 is a mobile device equipped to attach to the hitch of a utility vehicle. Measurements are made approximately every 2.4 m while traversing the field at a speed of 2.7 to 3.3 km $h^{-1}$. Passes downfield were made 2.4 m apart; therefore measurements were collected using an approximate 2.4 m x 2.4 m sample grid, which resulted in 997-1,189 readings per field. Data was recorded using an on-board computer and displayed in a spreadsheet format.

Soil moisture measurements were based on a capacitance sensor (The Toro Company, Bloomington, MN) modified for use on the PS6000 that measured VWC at a 0-10 cm depth. To ensure soil penetration at 10 cm, two custom stainless steel probes of 9.53 mm diameter, 3.3 cm spacing, and 10 cm length were installed on the sensor. The sensor is attached to one end of a

shaft on the PS6000, while a bolt is connected to the opposite end. When the PS6000 is moving forward, the wheel-driven shaft rotates in a circular fashion. The sensor's probes enter the soil and the bolt passes by a series of magnets that triggers the data loggers to take a measurement (Krum et al., 2010). A NovAtel GPS (NovAtel Inc., Alberta, Canada), attached to the PS6000, was used to gather latitude and longitude information for the data.

The ArcGIS version 10.1 GIS and mapping software (ArcMap) was used to develop, display, analyze and interpret maps of the PS6000 VWC data (ESRI, Redlands, CA). Using the editor tool in ArcMap, samples were removed from the initial 2.4 m x 2.4 m sampling grid to create the various sample sizes evaluated in this study. For each field, a total of 8 sample sizes were manipulated including 7 sampling grids and a sampling pattern that resembles test procedures from previous non-spatial performance testing research (Table 2.1-2.4; Figure 2.1a-2.48a).

*Statistical analysis*

Analysis of field data was done in three components. First, summary statistics were produced to evaluate central tendency, frequency distribution, and variability of data from each sample size on all fields. The mean is commonly used to measure central tendency and is calculated by:

$$\bar{x} = \frac{\sum x}{n} \qquad \text{[Eq. 2.1]}$$

where $\sum x$ is the sum of all values and $n$ is the number of samples taken. Comparison of means between sample sizes within each field was done using one-way ANOVA and Fisher's Protected LSD ($P < 0.05$). Data analysis was performed using the 'agricolae' package (Mendiburu, 2014) in R version 2.15.2 statistical software (R Development Core Team, 2008). Skewness is a

measure of degree of symmetry and determines the extent of even or uneven data distribution in relation to the mean:

$$\text{Skewness} = \frac{\sum(X_i - \overline{\text{X}})^3}{ns^3} \quad \text{[Eq. 2.2]}$$

Kurtosis measures the degree of flatness or peakness of a data set:

$$\text{Kurtosis} = \frac{\sum(X_i - \overline{\text{X}})^4}{ns^4} \quad \text{[Eq. 2.3]}$$

Histograms (not shown) were also produced to visually assess the central tendency and shape of data distribution.

The range is the simplest measure of data variability and is simply the difference between the highest and the lowest value in the data set. The standard deviation (SD) shows how much variation of the data there is from the mean and can be found using:

$$s = \sqrt{\frac{\sum(\text{X}_i - \overline{\text{X}})^2}{n}} \quad \text{[Eq. 2.4]}$$

where $\text{X}_i$ is the value of observation *i*. The standard error of the mean (SE) is the level of dispersion of the data from the mean and is calculated:

$$\text{SE}_{\bar{X}} = \frac{s}{\sqrt{n}} \quad \text{[Eq. 2.5]}$$

The coefficient of variability (CV) is different from standard deviation in that it is expressed as a percentage of the mean and consequently allows for analysis between data sets with different absolute values. Therefore, the CV is valuable as a relative index of data dispersion:

$$\text{CV} = \frac{s}{\overline{\text{X}}}(100) \quad \text{[Eq. 2.6]}$$

Next, semivariograms were created by plotting the semivariance, $\gamma(h)$, between each pair of data. Semivariance is quantified using the equation:

$$\gamma(h) = \frac{1}{2N(h)} \sum_{i=1}^{N(h)} [z(x_i) - z(x_i + h)]^2 \qquad \text{[Eq. 2.7]}$$

where $N(h)$ is the number of pairs of data separated by a lag distance $h$, and $z$ is the value of the given measurement at location $x_i$. The lag distance $h$ is the spatial range between two data points. If a grid survey is used for sampling it is common to use the sample grid spacing as $h$ (Oliver and Webster, 2014). Therefore, when constructing the semivariograms of the sample grids in this study, the respective grid spacing was used as $h$. For the sample pattern not following a grid survey, $h$ was found using the Average Nearest Neighbor tool in the Spatial Statistics toolbox of ArcMap (ESRI, Redlands, CA).

The range ($A_0$), nugget ($C_0$), sill ($C_0 + C$), and partial sill ($C$) are important components of a semivariogram and are used to describe the parameters of spatial structure. The range is the finite lag distance where spatial dependency occurs (i.e. at distances beyond the range there is little to no correlation among variables). The nugget is the value that intercepts the y axis and represents independent error, measurement error, and/or microscale variation at spatial scales that are too small to detect. The sill represents the total variance of the dataset; at large distances variables become uncorrelated and the sill of the semivariogram is equal to the variance of the random variable. The partial sill is the sill minus the nugget.

There are several models that can be fit to describe semivariograms; the spherical model is considered the most commonly used model for describing spatial data and was used to fit the semivariograms in this study (Jian, 1996). This model has linear behavior at small separation distances near the origin, but flattens out at larger distances and reaches the sill at the range (Isaaks, 1989). The spherical model is calculated by:

$$\gamma(h) = \begin{cases} 0, & h = 0 \\ C_0 + (C - C_0)\left\{\frac{3h}{2A_0} - \frac{1}{2}\left(\frac{h}{A_0}\right)^3\right\}, & 0 \le h \le A_0 \\ C_0 + (C - C_0), & h \ge A_0 \end{cases} \qquad \text{[Eq. 2.8]}$$

where $C_0$ is the nugget ($C_0 \geq 0$), $C$ is the sill ($C \geq 0$), $A_0$ is the range ($A_0 \geq 0$), and $h$ is the lag distance as defined in Eq. 2.7 (Jian, 1996).

Lastly, visual assessment of the measured parameters was done using kriging, with the Geostatistical Analyst extension of ArcMap, to create prediction surface maps (ESRI, Redlands, CA). The formula for kriging is:

$$\hat{Z}(x_0) = \sum_{i=1}^{N} \lambda_i z(x_i) \qquad \text{[Eq. 2.9]}$$

where $\hat{Z}(x_0)$ is the predicted value at the prediction location, $N$ is the number of measured values, $\lambda_i$ is an unknown weight for the measured value at the $i$th location, and $z(x_i)$ is the measured value at the $i$th location (ESRI, 2004). There are various models of kriging, for this study simple kriging was used. Simple kriging assumes the model:

$$\hat{Z}(x) = \mu + \varepsilon(x) \qquad \text{[Eq. 2.10]}$$

where $\hat{Z}(x)$ is the variable of interest, $\mu$ is the known mean constant, and $\varepsilon(x)$ is formed from autocorrelated errors.

Following kriging, cross-validation was conducted to provide summary statistics in order choose the most plausible model. Cross-validation is the process by which each of the $N$ data points is omitted in turn from the set of data and its value is predicted using the chosen kriging model (Oliver and Webster, 2014). Three statistics of interest are calculated; the mean error (ME), the root mean squared error (RMSE), and the root mean square standardized error (RMSSE). The ME is the average difference between each measured and predicted value:

$$\frac{1}{N}\sum_{i=1}^{N} z(x_i) - \hat{Z}(x_i) \qquad \text{[Eq. 2.11]}$$

The RMSE indicates how closely the model predicts the measured values:

$$\frac{1}{N}\sum_{i=1}^{N} \{z(x_i) - \hat{Z}(x_i)\}^2 \qquad \text{[Eq. 2.12]}$$

Lastly, the RMSSE is the RMSE divided by the corresponding kriging variance:

$$\frac{1}{N}\sum_{i=1}^{N} \frac{\{z(x_i) - \hat{Z}(x_i)\}^2}{\hat{\sigma}_K^2(x_i)} \qquad \text{[Eq. 2.13]}$$

where $\hat{\sigma}_K^2(x_i)$ is the kriging variance. RMSSE should be close to 1 if the prediction standard errors are valid (ESRI, 2004).

## Results

*Descriptive statistics*

According to Fisher's Protected LSD, significant differences in mean were only observed between sample grid sizes at Roswell field 2 and Watkinsville field 3 (Table 2.1 and 2.2, respectively). At Roswell 2, the 19.2 m x 9.6 m and 19.2 m x 19.2 m sample grid sizes were significantly different than the 7 sample size. All other sample grids were statistically similar to each evaluated grid size and the 7 sample size. At Watkinsville 3, with exception of the 19.2 m x 9.6 m sample grid, all evaluated sample grid sizes had statistically similar means. Furthermore, the 2.4 m x 2.4 m, 2.4 m x 4.8 m, and 4.8 m x 4.8 m sample grid sizes had statistically similar means to all evaluated sample sizes except the 19.2 m x 9.6 m sample grid.

Positive skewness indicates the mass of the distribution is concentrated on the left side of the histogram (i.e. lower VWC values). A negative skewness indicates the mass of distribution is concentrated on the right side histogram (i.e. higher VWC values). With the exception of only one or two instances per field, skewness for all sample sizes tended to be positive (Table 2.1 and

2.2). These results indicate the mass distribution of VWC concentrated toward lower values. A skewness of 0 would exhibit perfect symmetry and data falling within -1 and 1 are said to be normally distributed. All sample sizes within each field exhibited normal distribution.

A kurtosis value > 3.0 indicates a leptokurtic (peaked) distribution, a value of 3.0 is a mesokurtic (normal) distribution, and < 3.0 is a platykurtic (flat) distribution (McGrew and Monroe, 2009). On Roswell fields 1 and 3, all sample sizes exhibited platykurtic distributions and on field 2 the sample sizes exhibited both platykurtic and leptokurtic distributions (Table 2.1). On Watkinsville field 3, all sample sizes had platykurtic distributions and fields 1 and 2 the sample sizes exhibited both platykurtic and leptokurtic distributions (Table 2.2). The leptokurtic distributions indicate that the mass of the values are concentrated around the mean, while the platykurtic distribution indicates the values are more spread out.

Although the mean, skewness, and kurtosis can be a useful tool in understanding the data, they provide little information about variability. The range is considered the simplest method to determine variability; with wide ranges indicating more. In general, for all fields, the VWC range decreased as sample grid sizes became larger (Table 2.1 and 2.2). This result is expected, since low and high values can be omitted from the dataset as more samples are removed to create larger grid sizes. The occurrences when range did not change with increasing sample grid size could be attributed to the high and low values not being removed as the grid size increased. The ranges for the 7 sample sizes were significantly smaller than all grid sizes for all fields, except Roswell 1, indicating that accounted variability of the area is reduced with such a small sample size (Table 2.1 and 2.2).

The SD, SE, and CV are all common measures of data variability. SD and CV tended to not differ dramatically within sample sizes on each field (Table 2.1 and 2.2). The SD and CV for

the 7 sample size on all fields were less than that of the sample grids. SE increased as sample size decreased for all fields. Smaller SE indicates less sampling error and is primarily influenced by sample size. Therefore, this result was expected.

*Spatial analysis*

**S**emivariograms were generated for all sample sizes on each field to describe parameters of spatial structure (Figure 2.1c-2.48c). The range represents the distance, at which once beyond, a pair of samples is no longer correlated. Sampling distances should be less than the range if data are to be spatially correlated for interpolation. The ranges for all sample sizes on each field were greater than the sampling distance used indicating all were sufficient (Table 2.3 and 2.4; Figure 2.1c-2.48c).

The nugget and sill provide information to determine error and variability of the models, respectively. A trend in nugget and sill values between sample grid sizes on each field was not observed (Table 2.3 and 2.4). Nugget and sill values also varied from field to field. For all fields the sample grid with the highest nugget value was the 19.2 m x 19.2 m, with exception of Roswell 3 in which the 19.2 m x 9.6 m sample grid had the highest (Table 2.3 and 2.4). Sample sizes of 7 indicated a pure nugget for all fields except Watkinsville 1 (Table 2.3 and 2.4). Pure nuggets occur when the nugget equals the sill which indicates that the distance between sampling intervals is too large and the scale of spatial dependency is determined in ranges less than the shortest sampling distance. It is not recommended to conduct interpolation on a pure nugget (Oliver and Webster, 2014). The sample size of 7 on Watkinsville 1 exhibited a relatively low nugget value (Table 2.3), however further assessment will indicate this is still a poor model. Furthermore, no trend was observed with the sill on any fields (Table 2.3 and 2.4).

It is common to use the nugget/sill ratio of each dataset to assess the strength of spatial dependence (< 25% indicates strong spatial dependence, 25-75% indicates moderate spatial dependence, and > 75% indicates weak spatial dependence) (Cambardella et al., 1994). A large ratio can indicate that substantial measurement errors are present or the need of a more intense sampling, or both (Oliver and Webster, 2014). A pure nugget semivariogram would have a nugget/sill ratio of 1:1. The extent of spatial dependency for each model indicates the reliability of interpolation values.

At Roswell, the 2.4 m x 2.4 m and 2.4 m x 4.8 m sample grids exhibited strong spatial dependence for all fields (Table 2.3). On Roswell 1 the 9.6 m x 9.6 m sample grid, on Roswell 2 the 9.6 m x 4.8 m sample grid, and on Roswell 3 all other sample grids also showed strong spatial dependence (Table 2.3). All other sample grid sizes for each field had moderate spatial dependence (Table 2.3). The sample sizes of 7 in Roswell all indicated pure nuggets, which demonstrate weak spatial dependence (Figures 2.8c, 2.16c, and 2.24c; Table 2.3).

At Watkinsville field 1, all sample sizes have moderate spatial dependence (Table 2.4). Fields 2 and 3 both exhibited strong spatial dependence with the 2.4 m x 2.4 m sample grid (Table 2.4). On Watkinsville 2 the 9.6 m x 4.8 m sample grid and on Watkinsville 3 the 9.6 m x 9.6 m sample grid also exhibited strong spatial dependence (Table 2.4). All other sample grids, with exception of the 9.6 m x 9.6 m and 19.2 m x 19.2 m sample grids on Watkinsville 2, had moderate spatial dependence (Table 2.4). Weak spatial dependence was shown for those sample grids. Pure nuggets were observed for the 19.2 m x 19.2 m sample grid and the sample size of 7 on Watkinsville 2, as well as the sample size of 7 on Watkinsville 3, indicating weak spatial dependence (Figures 2.39c, 2.40c, and 2.48c, respectively; Table 2.4).

*Visual assessment and cross validation*

The 2.4 m x 2.4 m sample grid provides the most detailed visual assessment by map results of VWC variability for all fields at both locations (Figure 2.1b, 2.9b, 2.17b, 2.25b, 2.33b, and 2.41b). In Roswell, detailed variability holds from the 2.4 m x 2.4 m to 4.8 m x 4.8 m sample grid sizes on all fields, with minimum changes in surface maps (Figure 2.1b-2.3b, 2.9b-2.11b, and 2.17b-2.19b). The 9.6 m x 4.8 m sample grid is when variability tends to decline, but would still be considered acceptable for most situations (Figure 2.4b, 2.12b, and 2.20b). The 9.6 m x 9.6 m, 19.2 m x 9.6 m, and 19.2 m x 19.2 m sample grid sizes did provide similar VWC patterns as smaller sample grid sizes (Figure 2.5b-2.7b, 2.13b-2.15b, and 2.21b-2.23b). However, the short-range variability was not accounted for, resulting in a less detailed visual assessment. The sample size of 7 on all three fields showed no spatial variation of VWC, which is a result of exhibiting pure nugget semivariograms (Figure 2.8b and c, 2.16b and c, and 2.24b and c).

All Watkinsville fields had minimal differences of VWC variability in surface maps with 2.4 m x 2.4 m and 4.8 m x 2.4 m sample grid sizes (Figure 2.25b, 2.26b, 2.33b, 2.34b, 2.41b, and 2.42b). On Watkinsville fields 1 and 2 variability began to decline and continued to decline as sample grid size increased from the 4.8 m x 4.8 m sample grid size (Figures 2.27b-2.31b and 2.35b-2.39b, respectively). For Watkinsville field 2, the 19.2 m x 19.2 m sample grid and the 7 sample size exhibited no spatial variation of VWC, as indicated by a pure nugget semivariogram (Figures 2.39b and c and 2.40b and c, respectively). Only slight variations in VWC occurred between sample grid sizes of 2.4 m x 2.4 m and 9.6 m x 9.6 m on Watkinsville 3 (Figures 2.41b-2.45b). Variability began to decline at the 19.2 m x 9.6 m sample grid size until reaching no variation with the pure nugget sample size of 7 (Figures 2.46b-2.48b, and 2.48c).

Following kriging, cross-validation is conducted to provide prediction errors. The ME should be close to zero if the predicted values are centered around the measurement values (unbiased predictions). The ME varied between sample grids on all fields (Tables 2.3 and 2.4). Pure nugget semivariograms exhibited an ME of 0, but these models have already been observed as an unacceptable option.

If predicted values being close to measured values would result in a low RMSE. In Roswell the larger sample grid sizes tended to have a larger RMSE than the smaller sample grids (Table 2.3). At Watkinsville a similar trend was observed except on field 1 where there was little variation of RMSE between sample sizes (Table 2.4). The RMSE on the sample sizes of 7 were similar to the mid-sized sample grids, with exception of Watkinsville fields 1 and 2, in which they were the smallest of all sizes.

RMSSE varied between sample sizes on all fields. If RMSSE are greater than 1, the variability in the predictions is underestimated; if the RMSSE are less than 1, the variability in the predictions is overestimated. The 2.4 m x 2.4 m sample grid size was the only to continuously show differences greater than 1 on each field indicating the predictions were underestimated (Table 2.3 and 2.4). No other general trend was observed on any field.

## Discussion

Descriptive statistics and geostatistical techniques provide a comprehensive insight of the spatial variation of VWC on sports fields. Often, as seen with previous methods of performance testing, the mean is the determinate statistic to quantify performance of a given variable on a sports field; although it is highly unpractical to predict the true value. In theory, a higher sampling intensity would be a better prediction than a low sampling intensity. However, of the six fields evaluated, four showed no significant differences in VWC mean between sample sizes.

These results suggest that the central tendency of a field can be approximated with lower sampling numbers; however variability of VWC in space across the field is masked.

Spatial variability was better defined using geostatistics. Ideally, the best type of model will have a low nugget with a high sill. This would indicate that greater micro-scale variability is accounted for with less measurement error and also provide a low nugget/sill ratio indicating strong spatial dependence. Furthermore, generated semivariograms are based on Tobler's Law, also known as the first law of geography, which states, "Everything is related to everything else, but near things are more related than distant things" (Tobler, 1970). This indicates semivariance is generally low when two locations are close to each other and increases as the distance between the locations grow until at some point the locations become independent. Therefore, smaller sample grid sizes would be expected to result in a lower nugget and potentially stronger spatial dependence. Although the nugget/sill ratio can warn us of measurement errors and/or micro-scale variability, it tells us nothing about the underlying variation of properties that vary continuously in space (Oliver and Webster, 2014). This phenomenon is better explained with interpolation.

Generated surface maps from kriging interpolation provide the best visual indication of VWC variation in space. Our study showed that, in general, as sample grid size increased, variability decreased. Results indicated that larger sample grid sizes, such as 9.6 m x 9.6 m and 19.2 m x 9.6 m, are capable of showing similar trends across a field as smaller sample grid sizes. However, these mask detailed variability in certain locations and provide a less accurate and detailed surface map. Thus, sampling schemes should be chosen relative to the desired degree of accounted variability, with smaller sample grid sizes providing the most accuracy and detail.

Detailed spatial information is important when identifying why small (or large) areas of extreme (high or low) values are exhibited for a particular property.

The ME, RMSE, and RMSSE, obtained from cross-validation are good indicators of prediction errors and should be used when considering models. However, they depend on the scale of the data and should not be the underlining decision maker. The combination of descriptive statistics, geostatistics, and general knowledge of the site conditions and use before spatial analysis can aide in interpretation of the interpolated data and selecting the best model (Oliver and Webster, 2014).

It is important to emphasize that data collection and spatial analysis in this study was conducted after rainfall events when fields were at field capacity. At field capacity the spatial distribution of soil VWC is most influenced by soil particle size, the turf, and drainage properties (Starr, 2005; Duffera et al., 2007; Krum et al., 2010). In contrast, at less than field capacity (during a dry period), VWC spatial distribution is a function of irrigation system design, operation, or malfunction; with soil particle size, the turf , and drainage properties impacting VWC distribution to a lesser extent. Therefore, data collection at field capacity would be most beneficial for follow up on-site assessment review of specific areas to determine cause of any soil, turf, or drainage issues associated with excessively low or high VWC. It may also give clues to irrigation issues, but to a lesser degree than data collection at less than field capacity. Thus, for spatial analysis of VWC on sports fields, data collection at both field capacity and less than field capacity, give the most robust information. Since our study only evaluated sample procedures for spatial analysis of VWC at field capacity, further research should evaluate sample procedures for spatial analysis of VWC at less than field capacity to determine an appropriate protocol for data collection under such conditions.

Comparison of results to previous research is difficult, since, to the author's knowledge, Caple et al. (2012) is the only researcher to conduct spatial analysis of VWC on sports fields. However, the purpose of their study was not to compare sampling schemes. The 135 or 150 samples used in that study exhibited random variation of VWC across each. Semivariogram data was not shown for VWC; therefore comparison of spatial dependency at that sample size cannot be made with our results. Furthermore, handheld devices that were used for data collection may be time, cost, and labor intensive for certain facilities. The PS6000 was capable of sampling a soccer field using the 2.4 m x 2.4 m grid (~1000-1100 samples) in approximately 1 h and would be more practical for use of mapping multiple sports fields.

This, however, does not completely disregard the use of handheld devices to spatially analyze a smaller number of fields. Our results found a minimal sampling procedure of 9.6 m x 4.8 m (~140-160 samples) can provide an acceptably accurate spatial analysis and could be feasibly done using handheld devices. However, the sample grids used in this study were manipulated in GIS from data collected with the PS6000. Future research should consider using handheld devices, at these sampling grids, to determine if they correlate with analyses conducted in this study.

Moreover, spatial analysis of sports fields by Miller (2004) and Caple et al. (2012) evaluated variability of surface and edaphic properties for various soil classes. Miller (2004) observed higher uniformity of surface hardness on sand-based fields than that of native soil. Caple et al. (2012) detected greater spatial and temporal uniformity of sand rootzone fields compared to clay loam and loamy sand for all observed properties. This consistency may be due to sand soils exhibiting greater infiltration rates, resilient modules, and shear strength that are less sensitive to changes in water content compared to soils with greater proportions of clay

(Baker and Gibbs, 1989; Guisasola et al., 2010; Caple et al., 2011). Due to the observed uniformity of properties on sand-based fields, a smaller sample grid may be required to account for short-range variability between samples. Our study only evaluated fields with sandy loam soils; therefore, further research of varying sampling schemes at locations with different soil classes should be conducted for comparisons.

## Conclusions

Performance tests to spatially analyze surface and edaphic properties, such as VWC, on sports fields can be fundamental in determining "trouble" areas. Spatial analysis when fields are at field capacity, and less than field capacity, provides robust information to determine cause of any irrigation system, soil, turf, or drainage issues associated with excessively low or high VWC areas. As a result, site-specific sports turf management programs can be implemented to increase player safety and field playability, and reduce inputs.

Previous methods of performance testing on sports fields used a minimal amount of samples across a field; however to better assess the variability of a property, as well as the relationship between properties, spatial analysis using geostatistics is more appropriate. The most important factor in determining the reliability, or accuracy, of a semivariogram is the sample size on which it is based (Oliver and Webster, 2014). In general, the more data you have the greater the accuracy and detail. It is for this reason that mobile sensor platforms are the most practical means of data collection over larger areas, because of the ability to sample more intensely and the addition of an equipped GPS for geo-referencing. With a mobile platform, like the PS6000, the user may sample as intensely as desired. Our results suggest that at minimum a 9.6 m x 4.8 m sample grid size (~140-160 samples) be utilized for spatial analysis of VWC on sports fields using geostatistical techniques. For the PS6000, this exact sample grid is not achievable in the

field because samples are collected every 2.4 m. Therefore, we suggest distances between passes downfield be 4.8 m (~4.8 m x 2.4 m sample grid) or at most 9.6 m (~9.6 m x 2.4 m sample grid). However, due to the relatively short time for data collection with the PS6000 (~1 h per field), an intense sample grid such as 2.4 m x 2.4 m would be most beneficial and give the most detail.

Furthermore, to date, mobile sensors are not abundantly available for commercial use. Sports fields differ from agriculture and golf courses with respect to the area managed. Use of the more commonly available handheld devices to spatially analyze sports field properties could be feasible if a standard procedure or protocol is implemented with the most important component being sampling grid size. However, the sample grids used in this study were manipulated in GIS from data collected with the PS6000. Future research should consider a comparison of spatial analyses, using sample grids from this study, between handheld and mobile devices.

## References

American Society for Testing and Materials (ASTM). 2010. F1936–10, Standard specification of impact attenuation of turf playing systems as measured in the field. Annual book of ASTM standards. American Society for Testing Materials, West Conshohocken, PA.

Baker, S.W., and R.J. Gibbs. 1989. Levels of use and the playing quality of winter games pitches of different construction types: case studies at Nottingham and Warrington. J. Sports Turf Res. Inst. 65:9-33.

Baker, S.W. 1991. Temporal variation of selected mechanical properties of natural turf football pitches. J. Sports Turf Res. Inst. 67:83-92.

Bell, M.J., and G. Holmes. 1988. The playing quality of association football pitches. J. Sports Turf Res. Inst. 61:19-47.

Bell, G.E., and X. Xiong. 2008. The history, role, and potential of optical sensing for practical turf management. p. 641-660. *In* M. Pessarakli (Ed.), Handbook of turfgrass management and physiology. CRC Press, NY.

Bouma, J., J. Stoorvogel, B.J. van Alphen, and H.W.G. Booltink. 1999. Pedology, precision agriculture, and the changing paradigm of agricultural research. Soil Sci. 63.6:1763-1768.

Boydell, B., and A.B. McBratney. 1999. Identifying potential within-field management zones from cotton yield estimates. P. 331-341. *In* J.V. Stafford (ed.) Precision agriculture '99. Proc. Eur. Conf. on Precision Agric. Odense Congress Cent., Denmark. 11-15 July 1999. SCI, London.

Bullock, D.S., N. Kitchen, and D.G., Bullock. 2007. Multidisciplinary teams: a necessity for research in precision agriculture systems. Crop Sci. 47:1765-1769.

Cambardella, C.A., T.B. Moorman, T.B. Parkin, D.L. Karlen, J.M. Novak, R.F. Turco, and A.E. Konopka. 1994. Field-scale variability of soil properties in central Iowa soils. Soil Sci. Soc. Am. J. 58:1501-1511.

Caple, M.C., I.T. James, M.D. Bartlett, and D.I. Bartlett. 2011. Development of a simplified dynamic testing device for turfed sports surfaces. In Proceedings of the Institution of Mechanical Engineers, Part P: J. Sports Eng. Technol. 225:103-109.

Caple, M., I. James, and M. Bartlett. 2012. Spatial analysis of the mechanical behaviour of natural turf sports pitches. Sports Eng. 15:143-157.

Carrow, R.N., V. Cline, and J. Krum. 2007. Monitoring spatial variability in soil properties and turfgrass stress: applications and protocols. Proc. of 28th Int. Irrigation Show, 9-11 Dec. 2007, San Diego, CA.

Carrow, R.N., J.M Krum, I. Flitcroft, and V. Cline. 2010. Precision turfgrass management: challenges and field applications for mapping turfgrass soil and stress. Precis. Agric, 11:115-134.

Corwin, D.L., and S.M. Lesch. 2005. Apparent soil electrical conductivity measurements in agriculture. Comput. Electron. Agric. 46:103-133.

Duffera, M., J.G. White, and R. Weisz. 2007. Spatial variability of Southeastern U.S. Coastal Plain soil physical properties: Implications for site-specific management. Geoderma 137:327-339.

Emery, X., and K. González. 2007. Incorporating the uncertainty in geological boundaries into mineral resources evaluation. J. Geol. Soc. India. 69:29–38.

ESRI. 2004. ArcGIS 9: Using ArcGIS Geostatistical Analyst. ESRI, Redlands, CA.

Flitcroft, I., J. Krum, R. Carrow, K. Rice, T. Carson, and V. Cline. 2010. Spatial mapping of penetrometer resistance on turfgrass soils for site-specific cultivation. Proc. CD of the 10th Int. Conf. on Prec. Ag., Denver, CO. 18-21 July, 2010. ISPA, Monticello, IL.

Freeland, R.S., J.C. Sorochan, M.J. Goddard, and J.S. McElroy. 2008. Using ground-penetrating radar to evaluate soil compaction of athletic turfgrass fields. Appl. Eng. Agric. 24:509-514.

Guisasola, I., I. James, V. Stiles, and S. Dixon. 2010. Dynamic behaviour of soils used for natural turf sports surfaces. Sports Eng.12:111-122.

Holmes, G., and M.J. Bell. 1986. A pilot study of the playing quality of football pitches. J. Sports Turf Res. Inst. 62:74-91.

Institute of Groundsmanship (IOG). 2014. Performance Quality Test (PQS) Methods. http://www.iog.org/train-education/Technical-

Library/Performance+Quality+Standards/PQS+Methods+of+Test (accessed 25 Feb 2014).

Isaaks, E.H., and R.M Srivastava. 1989. Applied geostatistics. Oxford University Press. New York, NY.

James, I.T., and R.J. Godwin. 2003. Soil, water and yield relationships in developing strategies for the precision application of nitrogen fertiliser to winter barley. Biosyst. Eng. 84:467-480.

Jian, X., R.A. Olea, and Y.S. Yu. 1996. Semivariogram modeling by weighted least squares. Comput. Geosci. 22:387-397.

Krum, J.M. 2008. Spatial site assessment of soil moisture and plant status on golf courses. M.S. thesis. Univ. of Georgia, Athens, GA.

Krum, J.M., R.N. Carrow, and K. Karnok. 2010. Spatial mapping of complex turfgrass sites: Site-specific management units and protocols. Crop Sci. 50:301-315.

Leib, B.G., J.D. Jabro, and G.R. Matthews. 2003. Field evaluation and performance comparison of soil moisture sensors. Soil Sci. 168:396-409.

McAuliffe, K.W. 2008. The role of performance testing and standards in the sports turf industry: A case study approach. *In* J.C. Stier, L. Han, and D. Li (Eds.). Proceedings of 2nd international conference on turfgrass management and sports fields (pp. 391-398). Int. Soc. Hort. Sci. Belgium.

McClements, I., and S.W. Baker. 1994. The playing quality of rugby pitches. J. Sports Turf Res. Inst. 70:29-43.

McGrew Jr., J.C., and C.B. Monroe. 2009. An introduction to statistical problem solving in geography. Waveland Press, Long Grove, IL.

Mendiburu, F. (2014). agricolae: Statistical Procedures for Agricultural Research. R package version 1.1-7. http://CRAN.R-project.org/package=agricolae (accessed 1 April 2014).

Miller, G.L. 2004. Analysis of soccer field surface hardness. *In* P.A. Nektarios (Ed.), Proceedings of the first International Conference on Turfgrass Management and Science for Sports Fields. ISHS, Leuven, pp. 287-294.

Oliver, M.A., and R. Webster. 2014. A tutorial guide to geostatistics: Computing and modelling variograms and kriging. Catena. 113:56-69.

Plauborg, F., B.V Iversen, and P.E. Laerke. 2005. In situ comparison of three dielectric soil moisture sensors in drip irrigated sandy soils. Vadose Zone J. 4:1037-1047.

R Development Core Team. 2008. R: A language and environment for statistical computing. R Foundation for Statistical Computing, Vienna, Austria. http://www.R-project.org (accessed 1 April 2014).

Rhoades, J.D., F. Chanduvi, and S.M. Lesch. 1999. Soil salinity assessment: Methods and interpretation of electrical conductivity measurements. FAO Irrigation and Drainage Paper 57. Food and Agric. Organ. of the United Nations. Rome, Italy.

Starr, G.C. 2005. Assessing temporal stability and spatial variability of soil water patterns with implications for precision water management. Agric. Water Manage. 72:223-243.

Stiles, V.H., I.T. James, S.J. Dixon, and I.N. Guisasola. 2009. Natural turf surfaces. Sports Med. 39(1):65-84.

Stowell, L., and W. Gelernter. 2008. Evaluation of a Geonics EM38 and NTech GreenSeeker sensor array for use in precision turfgrass management. *In* Abstracts, GSA-SSSA-ASACSSA-GCAGS Int. Annu. Meet., Houston, TX, 5-9 Oct. 2008. ASA-CSSA-SSSA, Madison, WI.

Taylor, J.C., G.A. Wood, R. Earl, and R.J. Godwin. 2003. Soil factors and their influence on within-field crop variability, part II: spatial analysis and determination of management zones. Biosyst. Eng. 84:441-453.

Taylor, J.A., A.B. McBratney, and B.M. Whelan. 2007. Establishing management classes for broadacre agricultural production. Agron. J. 99:1366-1376.

Tobler W.R. 1970. A computer movie simulating urban growth in the Detroit region. Econ. Geogr. 46:234–240.

Thomsen, A., K. Schelde, P. Drøscher, and F. Steffensen. 2007. Mobile TDR for geo-referenced measurement of soil water content and electrical conductivity. Precis. Agric. 8:213-223.

Webster, R., and Oliver, M.A. 2007. Geostatistics for environmental scientists. John Wiley & Sons, Hoboken, NJ.

**Table 2.1.** Descriptive statistics of percent volumetric water content (%VWC) on fields at Roswell for evaluated sample sizes on 9 May, 2013.

| Sample size | Sample Grid | Mean (±SE)[†] [‡] | Min[§] | Max[¶] | Range | SD[#] | CV[††] (%) | Skewness | Kurtosis |
|---|---|---|---|---|---|---|---|---|---|
| Roswell 1 | | | | | | | | | |
| | | %VWC | | | | | | | |
| 1121 | 2.4 m x 2.4 m | 37.9 ± 0.22a | 23.8 | 61.5 | 37.6 | 7.21 | 19.0 | 0.63 | 2.85 |
| 584 | 4.8 m x 2.4 m | 37.6 ± 0.29a | 23.8 | 60.1 | 37.2 | 7.11 | 18.9 | 0.50 | 2.61 |
| 295 | 4.8 m x 4.8 m | 37.5 ± 0.41a | 23.8 | 58.9 | 35.1 | 6.99 | 18.7 | 0.43 | 2.49 |
| 160 | 9.6 m x 4.8 m | 37.8 ± 0.52a | 23.8 | 58.9 | 35.1 | 6.63 | 17.5 | 0.34 | 2.82 |
| 83 | 9.6 m x 9.6 m | 37.9 ± 0.72a | 25.8 | 58.9 | 33.1 | 6.60 | 17.4 | 0.30 | 2.80 |
| 47 | 19.2 m x 9.6 m | 37.6 ± 1.08a | 25.8 | 58.9 | 33.1 | 7.41 | 19.7 | 0.47 | 2.81 |
| 24 | 19.2 m x 19.2 m | 38.4 ± 1.58a | 27.3 | 58.9 | 31.6 | 7.73 | 20.1 | 0.54 | 2.98 |
| 7 | N/A | 36.3 ± 1.99a | 28.3 | 42.8 | 14.4 | 5.25 | 14.5 | -0.35 | 1.83 |
| Roswell 2 | | | | | | | | | |
| | | %VWC | | | | | | | |
| 1189 | 2.4 m x 2.4 m | 53.7 ± 0.32ab | 31.5 | 93.6 | 62.0 | 10.97 | 20.4 | 0.79 | 3.24 |
| 616 | 4.8 m x 2.4 m | 53.8 ± 0.45ab | 34.6 | 90.2 | 55.6 | 11.10 | 20.6 | 0.76 | 2.94 |
| 308 | 4.8 m x 4.8 m | 54.1 ± 0.64ab | 34.6 | 90.2 | 55.6 | 11.24 | 20.8 | 0.78 | 3.08 |
| 154 | 9.6 m x 4.8 m | 54.2 ± 0.89ab | 35.2 | 90.2 | 55.0 | 11.04 | 20.4 | 0.91 | 3.55 |
| 77 | 9.6 m x 9.6 m | 54.1 ± 1.26ab | 35.2 | 90.2 | 55.0 | 11.06 | 20.4 | 0.75 | 3.25 |
| 44 | 19.2 m x 9.6 m | 56.8 ± 1.74a | 40.4 | 90.2 | 49.8 | 11.51 | 20.3 | 0.66 | 2.88 |
| 24 | 19.2 m x 19.2 m | 57.1 ± 2.61a | 40.7 | 90.2 | 49.5 | 12.80 | 22.4 | 0.72 | 2.88 |
| 7 | N/A | 47.0 ± 2.94b | 35.4 | 58.6 | 23.3 | 7.77 | 16.5 | -0.02 | 2.10 |
| Roswell 3 | | | | | | | | | |
| | | %VWC | | | | | | | |
| 997 | 2.4 m x 2.4 m | 57.2 ± 0.44a | 32.7 | 99.8 | 67.0 | 13.72 | 24.0 | 0.72 | 2.81 |
| 519 | 4.8 m x 2.4 m | 57.2 ± 0.63a | 33.1 | 98.0 | 64.9 | 14.44 | 25.2 | 0.83 | 2.83 |
| 259 | 4.8 m x 4.8 m | 57.4 ± 0.93a | 33.1 | 97.6 | 64.5 | 14.97 | 26.1 | 0.85 | 2.79 |
| 139 | 9.6 m x 4.8 m | 58.8 ± 1.32a | 33.1 | 97.6 | 64.5 | 15.58 | 26.5 | 0.66 | 2.53 |
| 70 | 9.6 m x 9.6 m | 58.0 ± 1.80a | 33.1 | 97.5 | 64.4 | 15.08 | 26.0 | 0.65 | 2.46 |
| 40 | 19.2 m x 9.6 m | 57.6 ± 2.53a | 33.1 | 97.5 | 64.4 | 16.00 | 27.8 | 0.61 | 2.39 |
| 20 | 19.2 m x 19.2 m | 56.0 ± 3.50a | 33.1 | 81.7 | 48.7 | 15.67 | 28.0 | 0.37 | 1.65 |
| 7 | N/A | 52.4 ± 3.98a | 33.1 | 65.8 | 32.7 | 10.52 | 20.1 | -0.68 | 2.79 |

[†] Within columns, means followed by the same letter are not significantly different at $p \leq 0.05$ according to Fisher's Protected LSD test.
[‡] SE, standard error
[§] Min, minimum
[¶] Max, maximum
[#] SD, standard deviation
[††] CV, coefficient of variability

**Table 2.2.** Descriptive statistics of percent volumetric water content (%VWC) on fields at Watkinsville for evaluated sample sizes on 10 May, 2013.

| Sample size | Sample Grid | Mean (±SE)[†‡] | Min[§] | Max[¶] | Range | SD[#] | CV[††] (%) | Skewness | Kurtosis |
|---|---|---|---|---|---|---|---|---|---|
| Watkinsville 1 | | | | | | | | | |
| | | %VWC | | | | | | | |
| 1066 | 2.4 m x 2.4 m | 21.3 ± 0.10a | 4.7 | 33.2 | 28.5 | 3.31 | 15.5 | 0.03 | 3.96 |
| 535 | 4.8 m x 2.4 m | 21.2 ± 0.14a | 4.7 | 33.2 | 28.5 | 3.32 | 15.7 | -0.15 | 4.46 |
| 263 | 4.8 m x 4.8 m | 21.4 ± 0.20a | 13.6 | 33.2 | 19.6 | 3.25 | 15.2 | 0.38 | 3.41 |
| 142 | 9.6 m x 4.8 m | 21.6 ± 0.28a | 14.2 | 31.6 | 17.4 | 3.29 | 15.2 | 0.37 | 2.90 |
| 75 | 9.6 m x 9.6 m | 21.8 ± 0.41a | 14.2 | 31.6 | 17.4 | 3.54 | 16.3 | 0.47 | 2.88 |
| 43 | 19.2 m x 9.6 m | 21.8 ± 0.54a | 14.2 | 31.6 | 17.4 | 3.53 | 16.2 | 0.44 | 3.36 |
| 24 | 19.2 m x 19.2 m | 22.2 ± 0.71a | 15.8 | 28.3 | 12.5 | 3.45 | 15.6 | 0.11 | 2.43 |
| 7 | N/A | 20.3 ± 1.11a | 16.4 | 25.6 | 9.2 | 2.94 | 14.4 | 0.57 | 2.72 |
| Watkinsville 2 | | | | | | | | | |
| | | %VWC | | | | | | | |
| 1053 | 2.4 m x 2.4 m | 21.1 ± 0.09a | 10.3 | 32.4 | 22.1 | 2.87 | 13.6 | 0.31 | 3.61 |
| 526 | 4.8 m x 2.4 m | 21.3 ± 0.12a | 13.6 | 32.4 | 18.8 | 2.87 | 13.5 | 0.24 | 3.56 |
| 260 | 4.8 m x 4.8 m | 21.4 ± 0.17a | 14.1 | 31.1 | 17.0 | 2.74 | 12.8 | 0.11 | 3.20 |
| 139 | 9.6 m x 4.8 m | 21.4 ± 0.24a | 14.1 | 31.1 | 17.0 | 2.87 | 13.4 | 0.08 | 3.59 |
| 74 | 9.6 m x 9.6 m | 21.6 ± 0.33a | 14.1 | 29.2 | 15.1 | 2.80 | 13.0 | -0.08 | 3.21 |
| 43 | 19.2 m x 9.6 m | 22.0 ± 0.41a | 15.9 | 29.2 | 13.3 | 2.71 | 12.3 | 0.02 | 3.52 |
| 24 | 19.2 m x 19.2 m | 21.9 ± 0.65a | 15.9 | 29.2 | 13.3 | 3.20 | 14.6 | 0.10 | 2.98 |
| 7 | N/A | 22.9 ± 0.85a | 19.2 | 25.2 | 5.9 | 2.24 | 9.8 | -0.49 | 1.92 |
| Watkinsville 3 | | | | | | | | | |
| | | %VWC | | | | | | | |
| 1101 | 2.4 m x 2.4 m | 19.3 ± 0.09a | 9.3 | 28.9 | 19.5 | 3.15 | 16.4 | 0.20 | 2.75 |
| 555 | 4.8 m x 2.4 m | 19.4 ± 0.13a | 9.3 | 28.9 | 19.5 | 3.17 | 16.4 | 0.18 | 2.98 |
| 283 | 4.8 m x 4.8 m | 19.3 ± 0.18a | 12.3 | 28.8 | 16.5 | 3.07 | 15.9 | 0.23 | 2.90 |
| 152 | 9.6 m x 4.8 m | 19.7 ± 0.26ab | 12.3 | 28.8 | 16.5 | 3.22 | 16.4 | 0.26 | 2.89 |
| 76 | 9.6 m x 9.6 m | 19.8 ± 0.41ab | 12.3 | 28.1 | 15.9 | 3.58 | 18.0 | 0.16 | 2.44 |
| 43 | 19.2 m x 9.6 m | 20.5 ± 0.56b | 12.3 | 28.1 | 15.9 | 3.64 | 17.7 | 0.05 | 2.54 |
| 24 | 19.2 m x 19.2 m | 20.4 ± 0.70ab | 12.3 | 26.9 | 14.6 | 3.45 | 16.9 | -0.12 | 2.82 |
| 7 | N/A | 19.8 ± 1.15ab | 14.8 | 24.0 | 9.2 | 3.03 | 15.3 | -0.17 | 2.38 |

[†] Within columns, means followed by the same letter are not significantly different at $p \leq 0.05$ according to Fisher's Protected LSD test.
[‡] SE, standard error
[§] Min, minimum
[¶] Max, maximum
[#] SD, standard deviation
[††] CV, coefficient of variability

**Table 2.3.** Geostatistical model parameters for percent volumetric water content (%VWC) on fields at Roswell for evaluated sample sizes on 9 May, 2013.

| Sample size | Sample Grid | Model | Nugget ($C_0$) | Sill ($C_0 + C$) | Nugget/Sill (%) | Spatial dependence[†] | Range (m) | ME[‡] | RMSE[§] | RMSSE[¶] |
|---|---|---|---|---|---|---|---|---|---|---|
| Roswell 1 | | | | | | | | | | |
| 1121 | 2.4 m x 2.4 m | Spherical | 10.5 | 57.2 | 18.4 | Strong | 36.4 | -0.017 | 4.3 | 1.07 |
| 584 | 2.4 m x 4.8 m | Spherical | 10.7 | 55.6 | 19.2 | Strong | 36.2 | -0.033 | 3.9 | 0.94 |
| 295 | 4.8 m x 4.8 m | Spherical | 15.9 | 55.3 | 28.8 | Moderate | 47.5 | -0.043 | 4.3 | 0.88 |
| 160 | 9.6 m x 4.8 m | Spherical | 16.4 | 47.9 | 34.2 | Moderate | 39.6 | -0.095 | 4.5 | 0.89 |
| 83 | 9.6 m x 9.6 m | Spherical | 5.9 | 46.2 | 12.8 | Strong | 32.1 | -0.103 | 4.8 | 1.00 |
| 47 | 19.2 m x 9.6 m | Spherical | 18.3 | 65.4 | 28.0 | Moderate | 46.4 | -0.846 | 7.0 | 0.97 |
| 24 | 19.2 m x 19.2 m | Spherical | 45.7 | 64.1 | 71.3 | Moderate | 54.9 | -0.615 | 7.4 | 0.96 |
| 7 | N/A | Spherical | 27.6 | 27.6 | 100.0 | Weak | 86.7 | 0 | 4.9 | 0.93 |
| Roswell 2 | | | | | | | | | | |
| 1189 | 2.4 m x 2.4 m | Spherical | 11.6 | 120.1 | 9.7 | Strong | 19.1 | -0.033 | 6.7 | 1.21 |
| 616 | 2.4 m x 4.8 m | Spherical | 15.1 | 92.5 | 16.3 | Strong | 15.1 | -0.078 | 6.4 | 1.04 |
| 308 | 4.8 m x 4.8 m | Spherical | 33.4 | 115.8 | 28.8 | Moderate | 26.9 | -0.044 | 8.0 | 1.04 |
| 154 | 9.6 m x 4.8 m | Spherical | 31.1 | 137.8 | 22.6 | Strong | 51.0 | -0.052 | 7.7 | 1.05 |
| 77 | 9.6 m x 9.6 m | Spherical | 57.9 | 143.5 | 40.3 | Moderate | 68.8 | -0.216 | 9.1 | 1.00 |
| 44 | 19.2 m x 9.6 m | Spherical | 71.6 | 148.9 | 48.1 | Moderate | 62.2 | -0.031 | 9.4 | 0.92 |
| 24 | 19.2 m x 19.2 m | Spherical | 76.4 | 190.9 | 40.0 | Moderate | 77.1 | -0.450 | 10.8 | 0.93 |
| 7 | N/A | Spherical | 60.4 | 60.4 | 100.0 | Weak | 98.8 | 0 | 7.2 | 0.93 |
| Roswell 3 | | | | | | | | | | |
| 997 | 2.4 m x 2.4 m | Spherical | 38.2 | 197.1 | 19.4 | Strong | 39.3 | -0.053 | 8.0 | 1.07 |
| 519 | 2.4 m x 4.8 m | Spherical | 28.9 | 265.0 | 10.9 | Strong | 62.0 | -0.028 | 7.2 | 1.04 |
| 259 | 4.8 m x 4.8 m | Spherical | 28.9 | 307.9 | 9.4 | Strong | 71.9 | -0.027 | 7.9 | 1.04 |
| 139 | 9.6 m x 4.8 m | Spherical | 23.8 | 330.8 | 7.2 | Strong | 71.9 | 0.044 | 8.6 | 1.09 |
| 70 | 9.6 m x 9.6 m | Spherical | 30.0 | 224.3 | 13.4 | Strong | 43.5 | -0.183 | 8.4 | 0.87 |
| 40 | 19.2 m x 9.6 m | Spherical | 47.9 | 249.4 | 19.2 | Strong | 49.5 | -0.784 | 10.1 | 0.88 |
| 20 | 19.2 m x 19.2 m | Spherical | 32.2 | 306.0 | 10.5 | Strong | 68.5 | -1.330 | 9.9 | 0.82 |
| 7 | N/A | Spherical | 110.6 | 110.6 | 100.0 | Weak | 88.8 | 0 | 9.7 | 0.93 |

[†] Spatial dependence is described as strong, moderate, or weak for nugget/sill ratios <25%, 25-75%, or >75%, respectively.
[‡] ME, mean prediction error.
[§] RMSE, root-mean square prediction error.
[¶] RMSSE, root-mean square standardized prediction error.

**Table 2.4.** Geostatistical model parameters for percent volumetric water content (%VWC) on fields at Watkinsville for evaluated sample sizes on 10 May, 2013.

| Sample size | Sample Grid | Model | Nugget ($C_0$) | Sill ($C_0 + C$) | Nugget/Sill (%) | Spatial dependence[†] | Range (m) | ME[‡] | RMSE[§] | RMSSE[¶] |
|---|---|---|---|---|---|---|---|---|---|---|
| Watkinsville 1 | | | | | | | | | | |
| 1066 | 2.4 m x 2.4 m | Spherical | 5.4 | 11.0 | 49.1 | Moderate | 20.6 | -0.004 | 2.7 | 1.05 |
| 535 | 2.4 m x 4.8 m | Spherical | 4.8 | 11.0 | 43.6 | Moderate | 16.4 | -0.011 | 2.9 | 1.07 |
| 263 | 4.8 m x 4.8 m | Spherical | 3.1 | 10.9 | 28.4 | Moderate | 19.6 | -0.016 | 2.7 | 1.10 |
| 142 | 9.6 m x 4.8 m | Spherical | 5.1 | 12.0 | 42.5 | Moderate | 50.4 | 0 | 2.6 | 0.99 |
| 75 | 9.6 m x 9.6 m | Spherical | 3.6 | 14.4 | 25.1 | Moderate | 49.5 | 0.003 | 2.9 | 1.08 |
| 43 | 19.2 m x 9.6 m | Spherical | 4.5 | 14.0 | 32.2 | Moderate | 58.3 | 0.005 | 3.0 | 1.03 |
| 24 | 19.2 m x 19.2 m | Spherical | 7.3 | 12.6 | 58.0 | Moderate | 66.1 | 0.085 | 3.3 | 1.00 |
| 7 | N/A | Spherical | 3.8 | 11.4 | 32.9 | Moderate | 83.6 | 0.237 | 2.2 | 0.81 |
| Watkinsville 2 | | | | | | | | | | |
| 1053 | 2.4 m x 2.4 m | Spherical | 1.6 | 8.1 | 19.8 | Strong | 6.5 | 0.016 | 2.6 | 1.12 |
| 526 | 2.4 m x 4.8 m | Spherical | 3.4 | 7.6 | 44.7 | Moderate | 10.8 | 0.008 | 2.4 | 1.01 |
| 260 | 4.8 m x 4.8 m | Spherical | 2.3 | 7.5 | 30.7 | Moderate | 14.1 | 0.006 | 2.4 | 1.08 |
| 139 | 9.6 m x 4.8 m | Spherical | 1.5 | 8.5 | 17.6 | Strong | 13.5 | 0.048 | 2.6 | 1.06 |
| 74 | 9.6 m x 9.6 m | Spherical | 6.5 | 7.7 | 84.4 | Weak | 17.9 | 0.016 | 2.8 | 0.99 |
| 43 | 19.2 m x 9.6 m | Spherical | 4.3 | 7.4 | 58.1 | Moderate | 24.9 | 0.025 | 2.6 | 0.98 |
| 24 | 19.2 m x 19.2 m | Spherical | 10.2 | 10.2 | 100.0 | Weak | 85.1 | 0 | 3.1 | 0.98 |
| 7 | N/A | Spherical | 5.0 | 5.0 | 100.0 | Weak | 95.4 | 0 | 2.1 | 0.93 |
| Watkinsville 3 | | | | | | | | | | |
| 1101 | 2.4 m x 2.4 m | Spherical | 1.2 | 9.9 | 12.1 | Strong | 16.1 | -0.002 | 2.4 | 1.35 |
| 555 | 2.4 m x 4.8 m | Spherical | 3.7 | 10.0 | 37.0 | Moderate | 19.8 | 0.003 | 2.4 | 1.01 |
| 283 | 4.8 m x 4.8 m | Spherical | 4.6 | 9.7 | 47.4 | Moderate | 28.0 | 0.003 | 2.4 | 0.93 |
| 152 | 9.6 m x 4.8 m | Spherical | 3.3 | 10.9 | 30.3 | Moderate | 25.5 | 0.040 | 2.4 | 0.95 |
| 76 | 9.6 m x 9.6 m | Spherical | 2.0 | 12.8 | 15.6 | Strong | 22.6 | -0.019 | 2.8 | 0.96 |
| 43 | 19.2 m x 9.6 m | Spherical | 3.4 | 13.4 | 25.8 | Moderate | 27.8 | 0.066 | 3.1 | 0.98 |
| 24 | 19.2 m x 19.2 m | Spherical | 8.3 | 13.0 | 63.8 | Moderate | 66.5 | 0.140 | 3.4 | 0.99 |
| 7 | N/A | Spherical | 9.2 | 9.2 | 100.0 | Weak | 88.5 | 0 | 2.8 | 0.93 |

[†] Spatial dependence is described as strong, moderate, or weak for nugget/sill ratios <25%, 25-75%, or >75%, respectively.
[‡] ME, mean prediction error.
[§] RMSE, root-mean square prediction error.
[¶] RMSSE, root-mean square standardized prediction error.

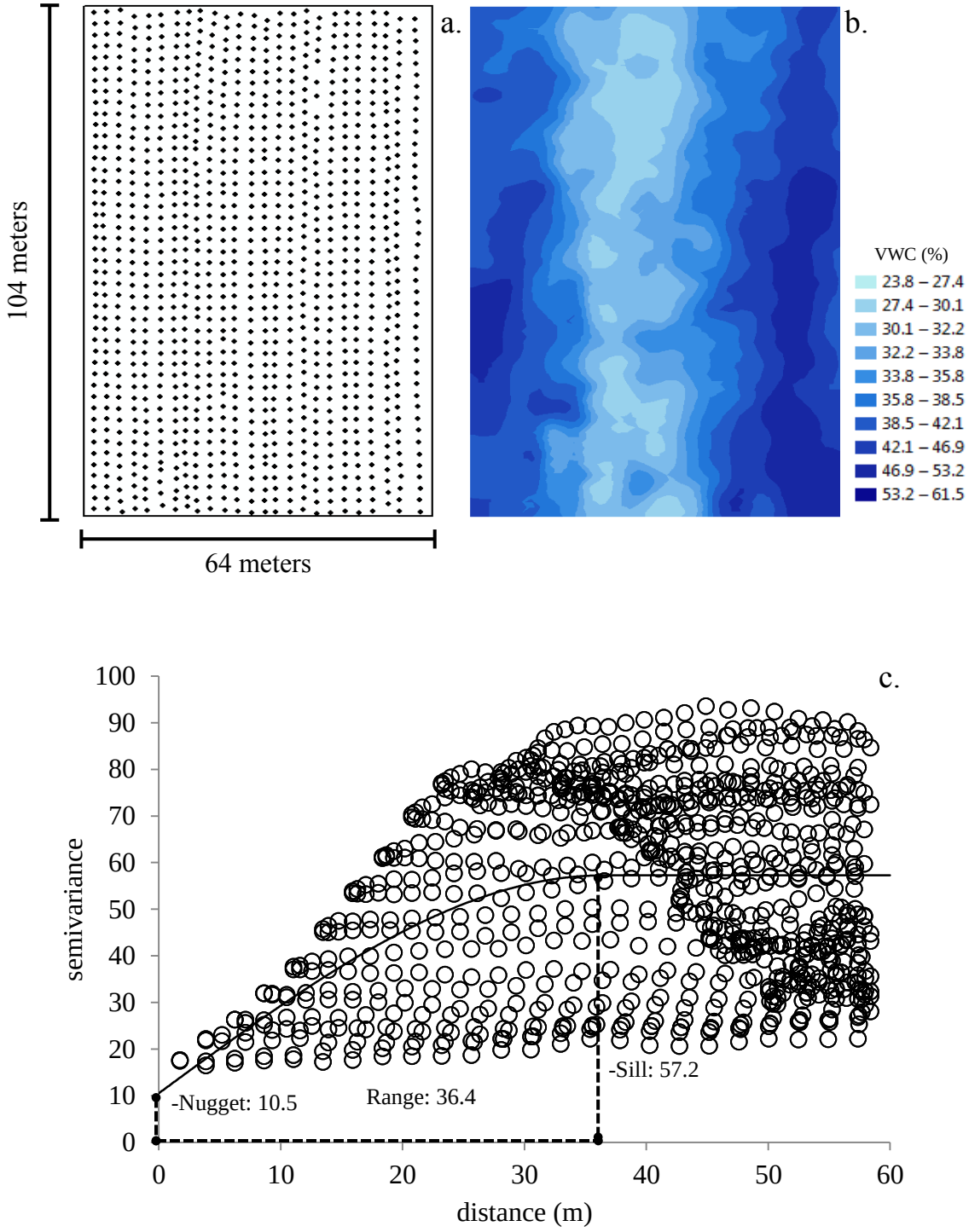


Figure 2.1. (a) Sampling locations (approximately 2.4 m x 2.4 m grid; 1121 samples), (b) kriged prediction map and (c) semivariogram including the fitted spherical model of percent volumetric water content (%VWC) on Roswell field 1.

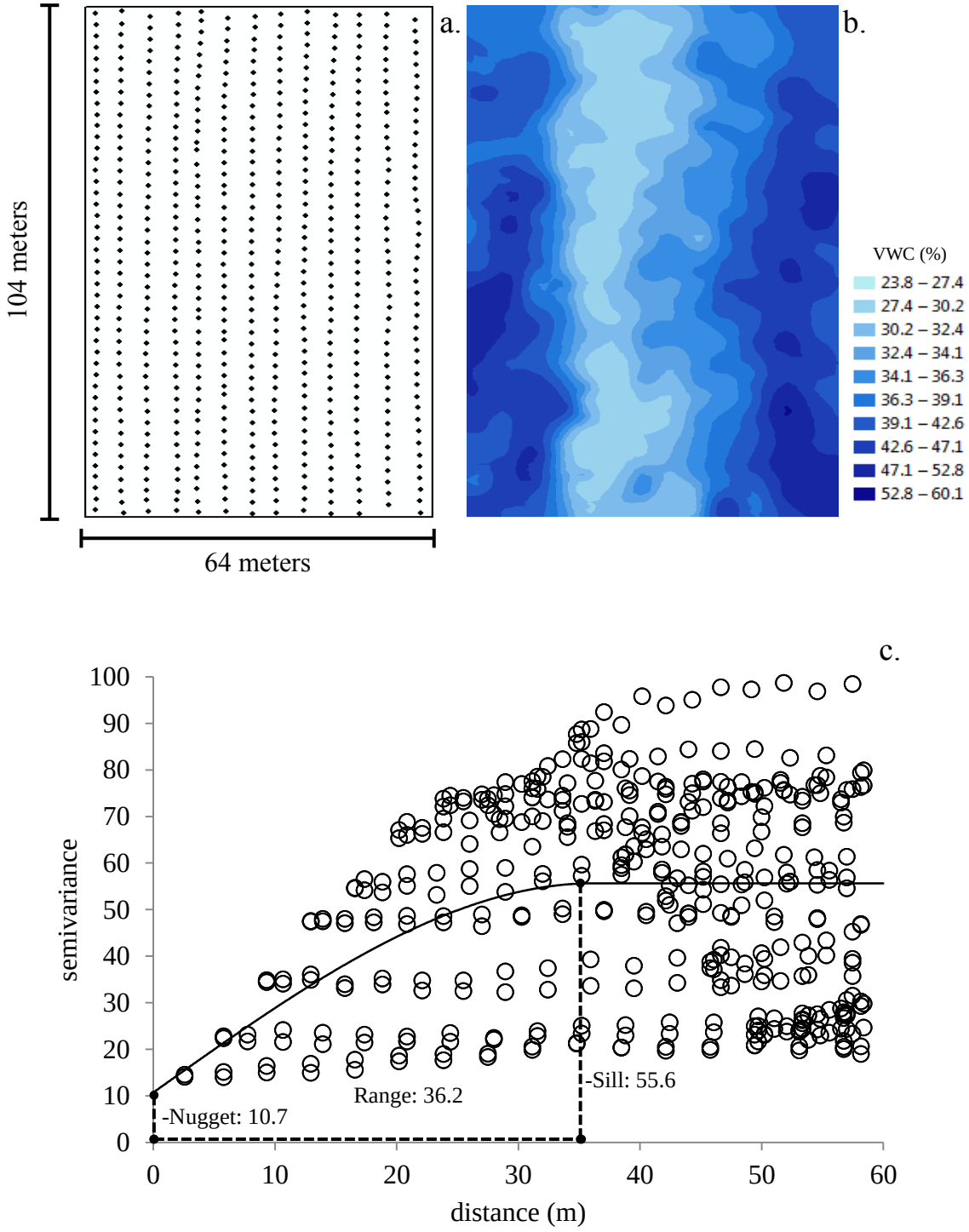


Figure 2.2. (a) Sampling locations (approximately 4.8 m x 2.4 m grid; 584 samples), (b) kriged prediction map and (c) semivariogram including the fitted spherical model of percent volumetric water content (%VWC) on Roswell field 1.

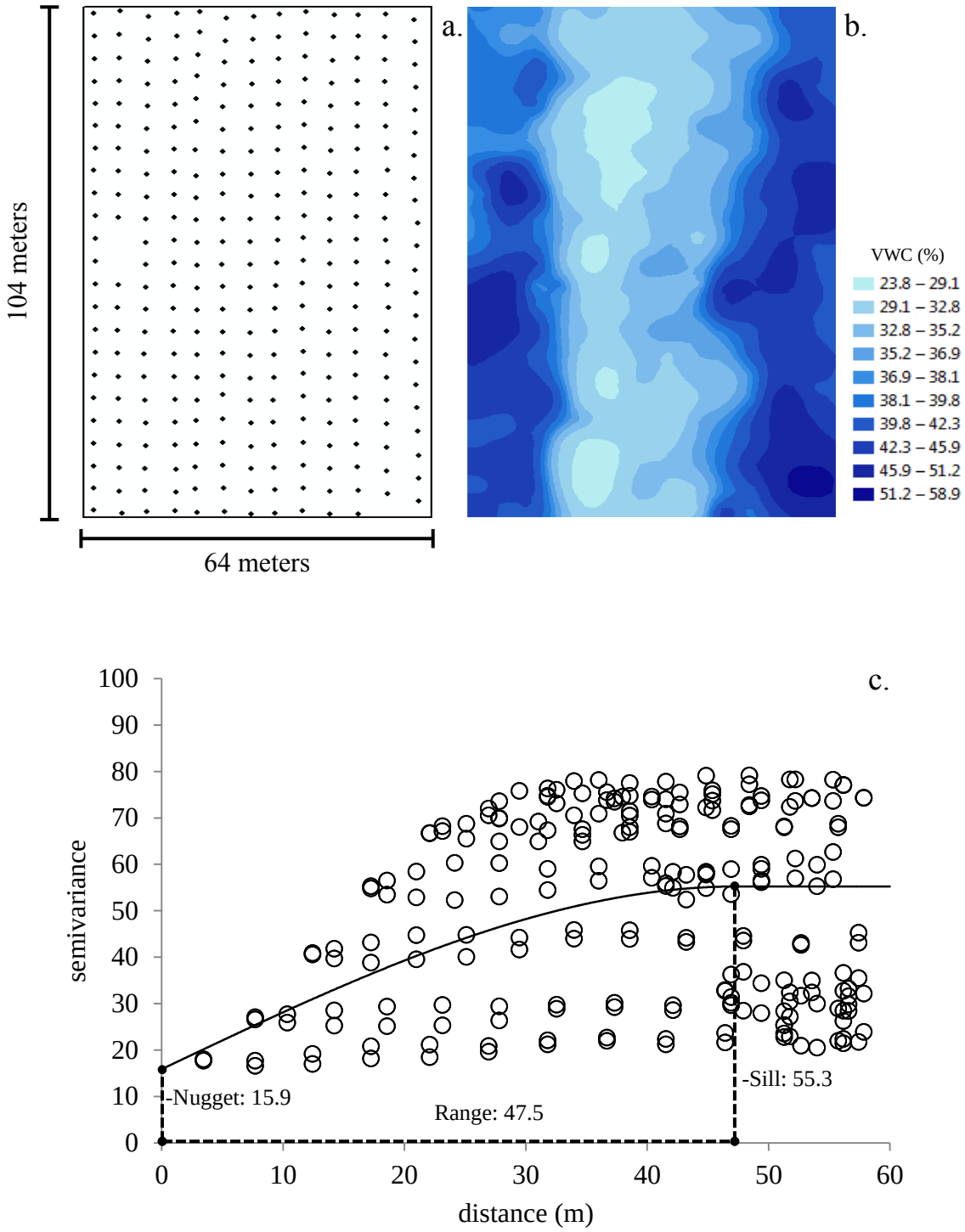


Figure 2.3. (a) Sampling locations (approximately 4.8 m x 4.8 m grid; 295 samples), (b) kriged prediction map and (c) semivariogram including the fitted spherical model of percent volumetric water content (%VWC) on Roswell field 1.

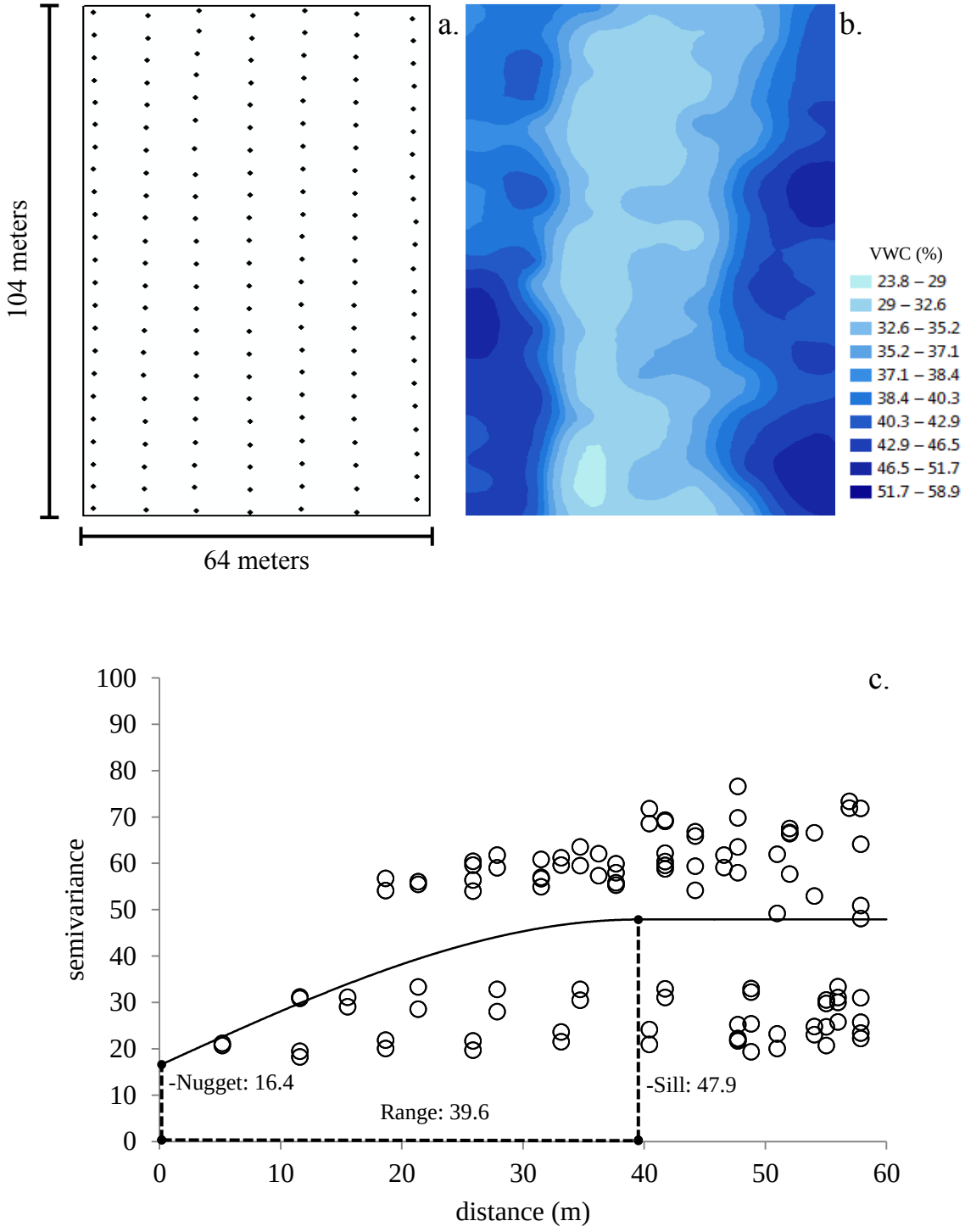


Figure 2.4. (a) Sampling locations (approximately 9.6 m x 4.8 m grid; 160 samples), (b) kriged prediction map and (c) semivariogram including the fitted spherical model of percent volumetric water content (%VWC) on Roswell field 1.

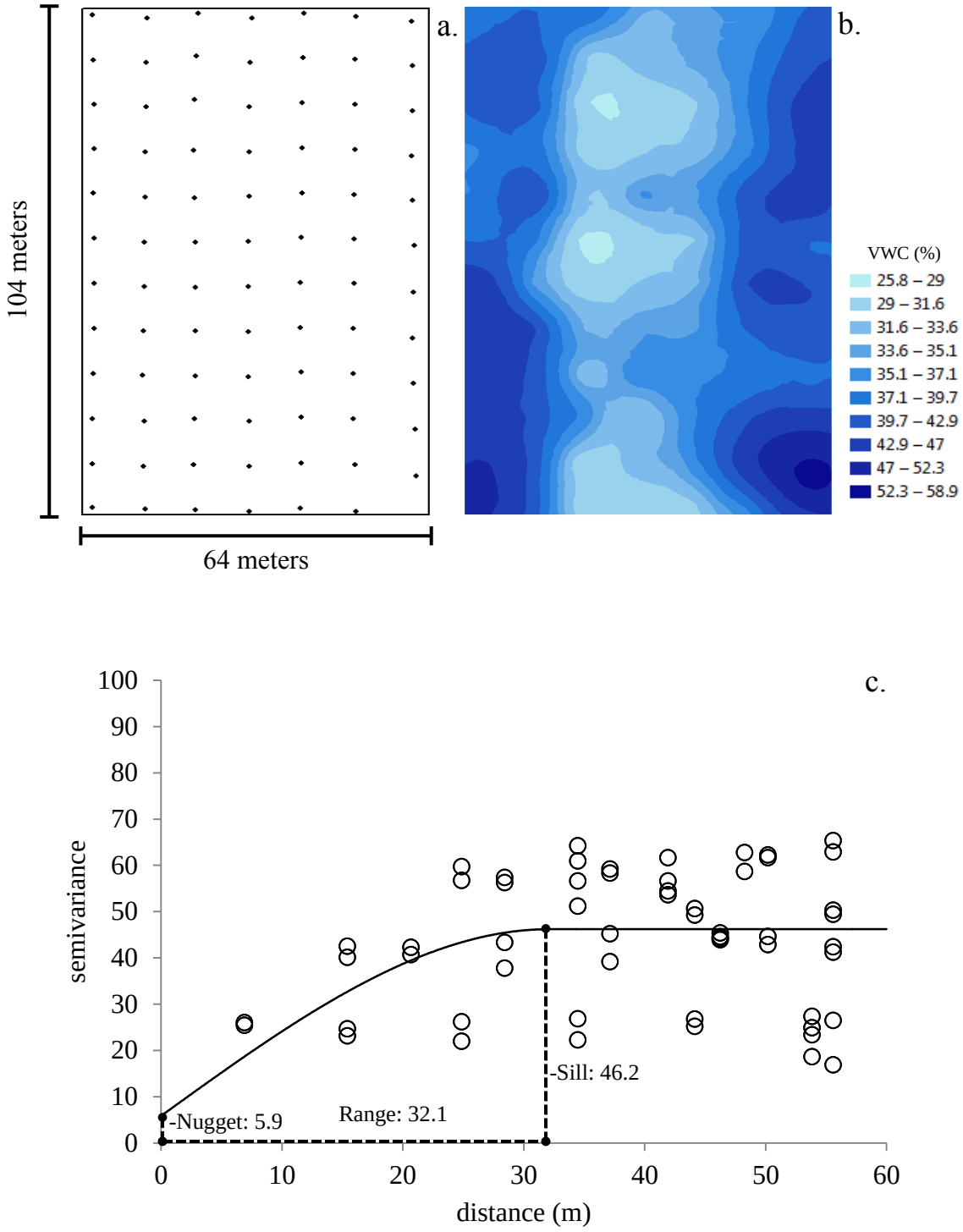


Figure 2.5. (a) Sampling locations (approximately 9.6 m x 9.6 m grid; 83 samples), (b) kriged prediction map and (c) semivariogram including the fitted spherical model of percent volumetric water content (%VWC) on Roswell field 1.

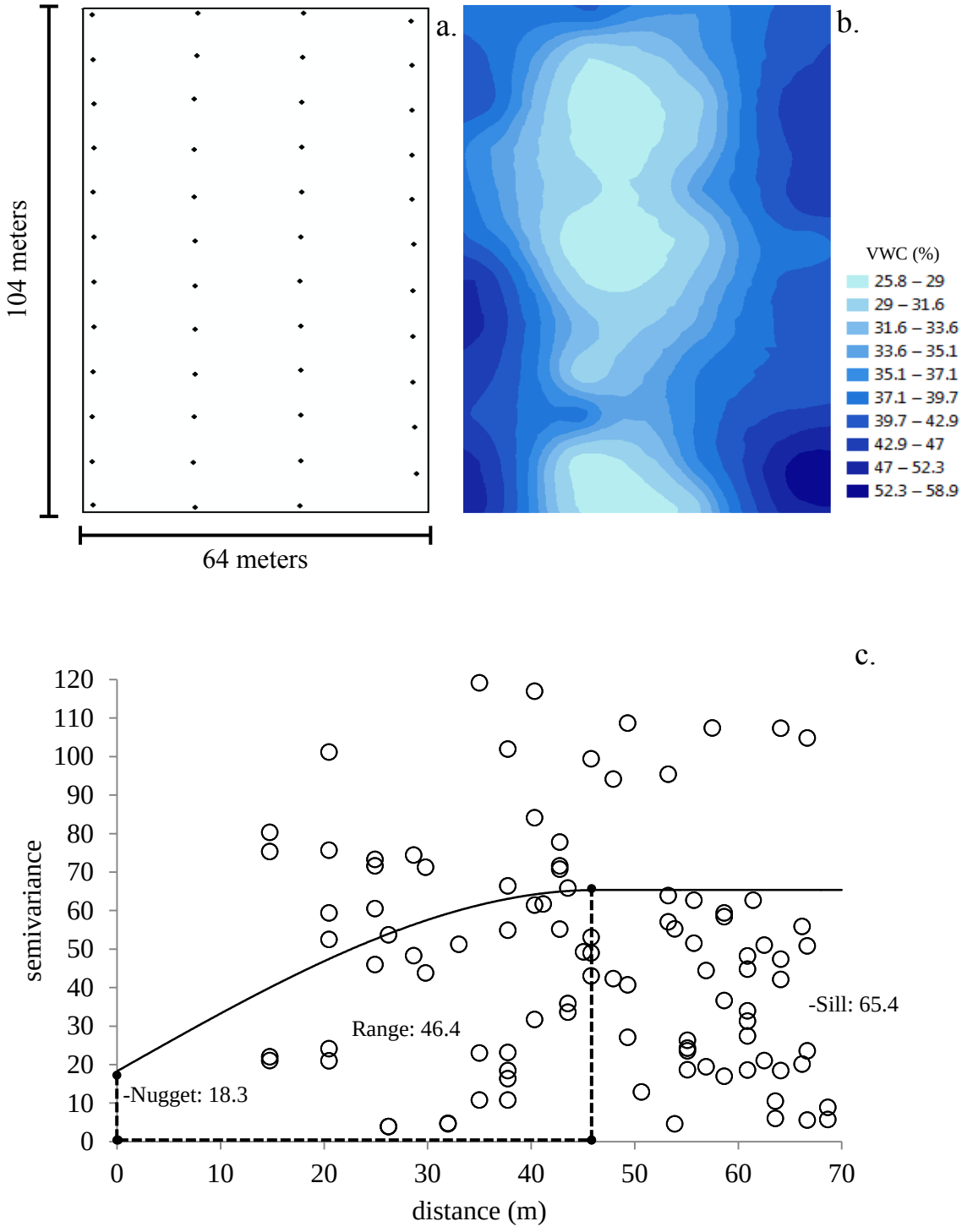


Figure 2.6. (a) Sampling locations (approximately 19.2 m x 9.6 m grid; 47 samples), (b) kriged prediction map and (c) semivariogram including the fitted spherical model of percent volumetric water content (%VWC) on Roswell field 1.

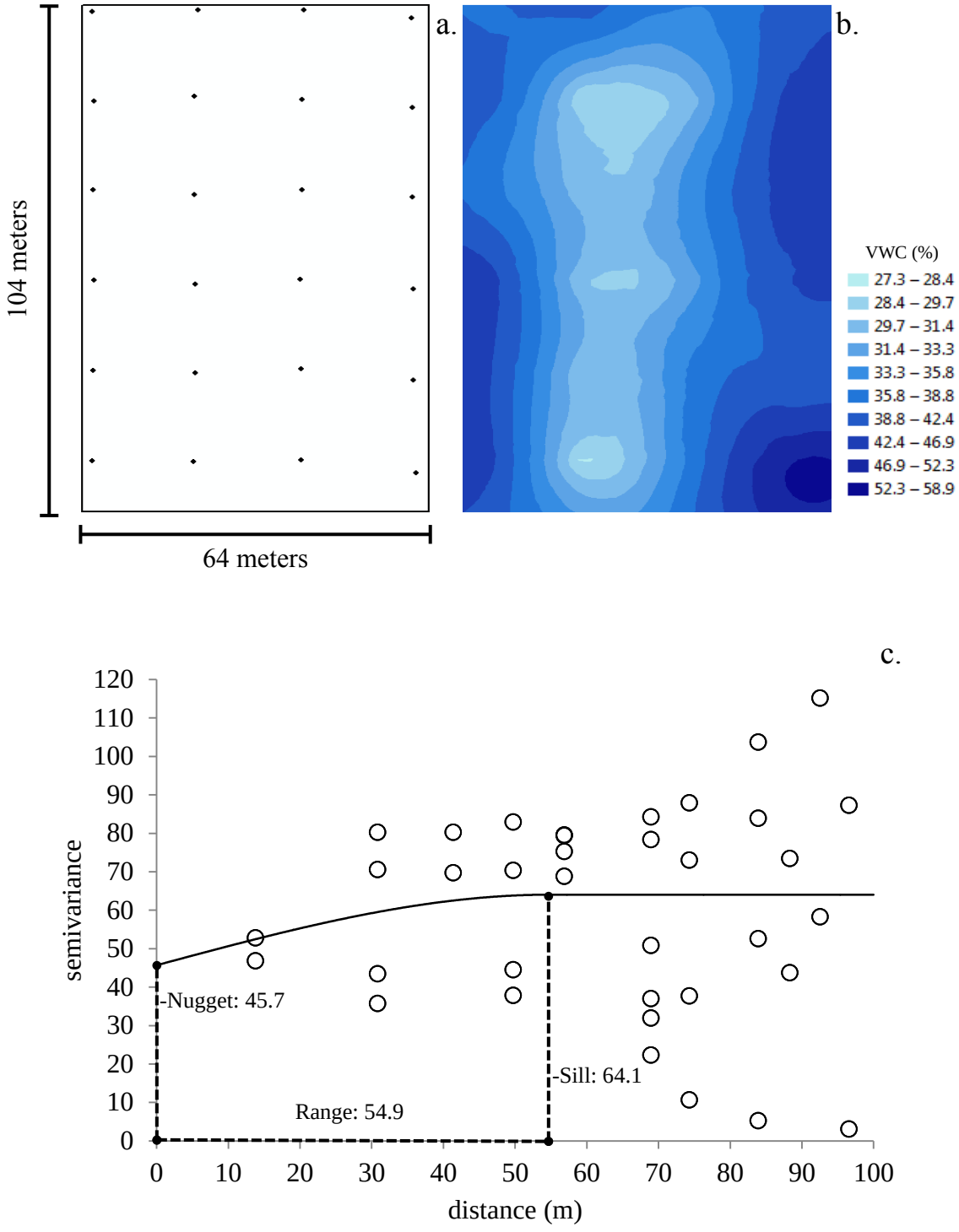


Figure 2.7. (a) Sampling locations (approximately 19.2 m x 19.2 m grid; 24 samples), (b) kriged prediction map and (c) semivariogram including the fitted spherical model of percent volumetric water content (%VWC) on Roswell field 1.

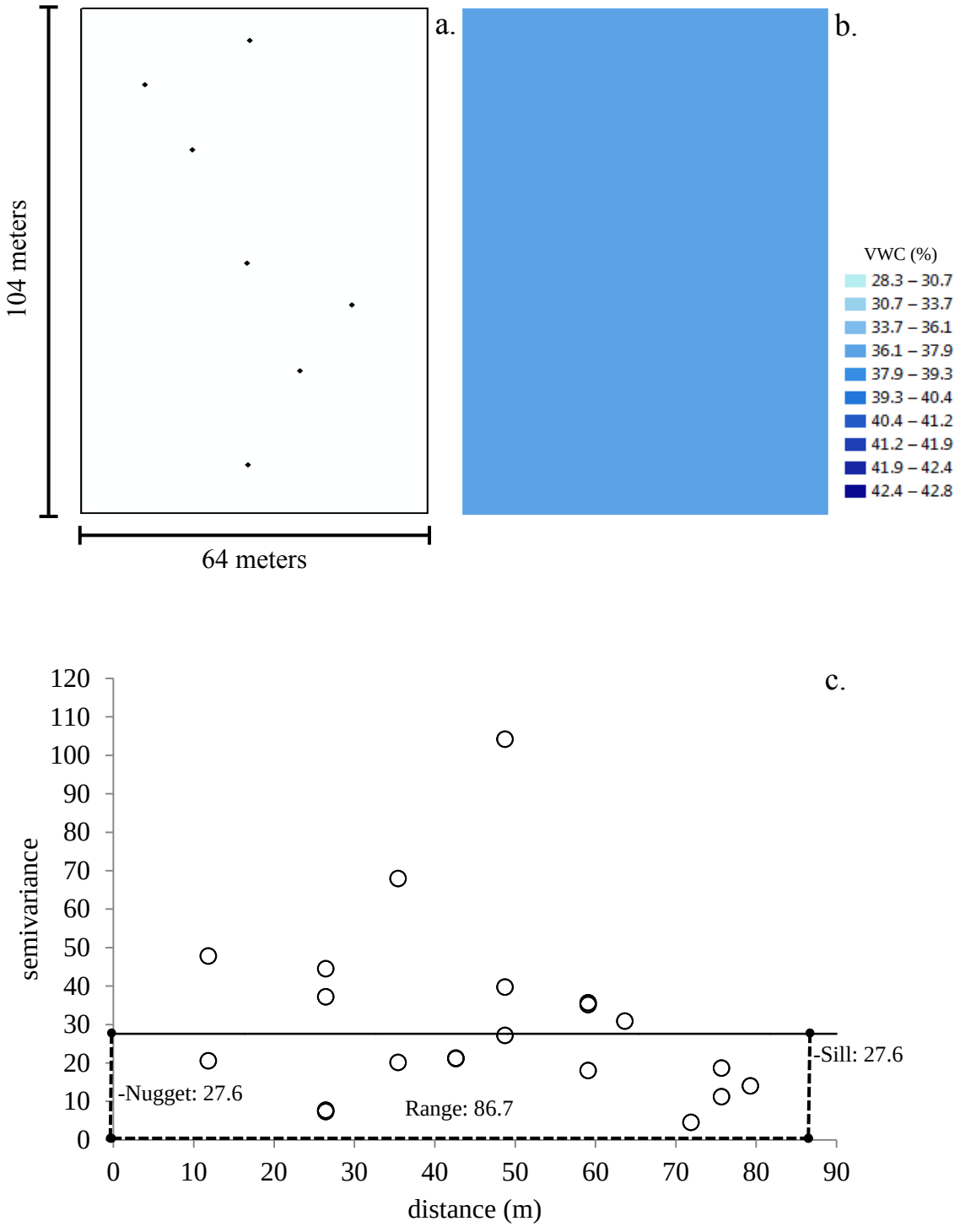


Figure 2.8. (a) Sampling locations (7 samples), (b) kriged prediction map and (c) semivariogram including the fitted spherical model of percent volumetric water content (%VWC) on Roswell field 1.

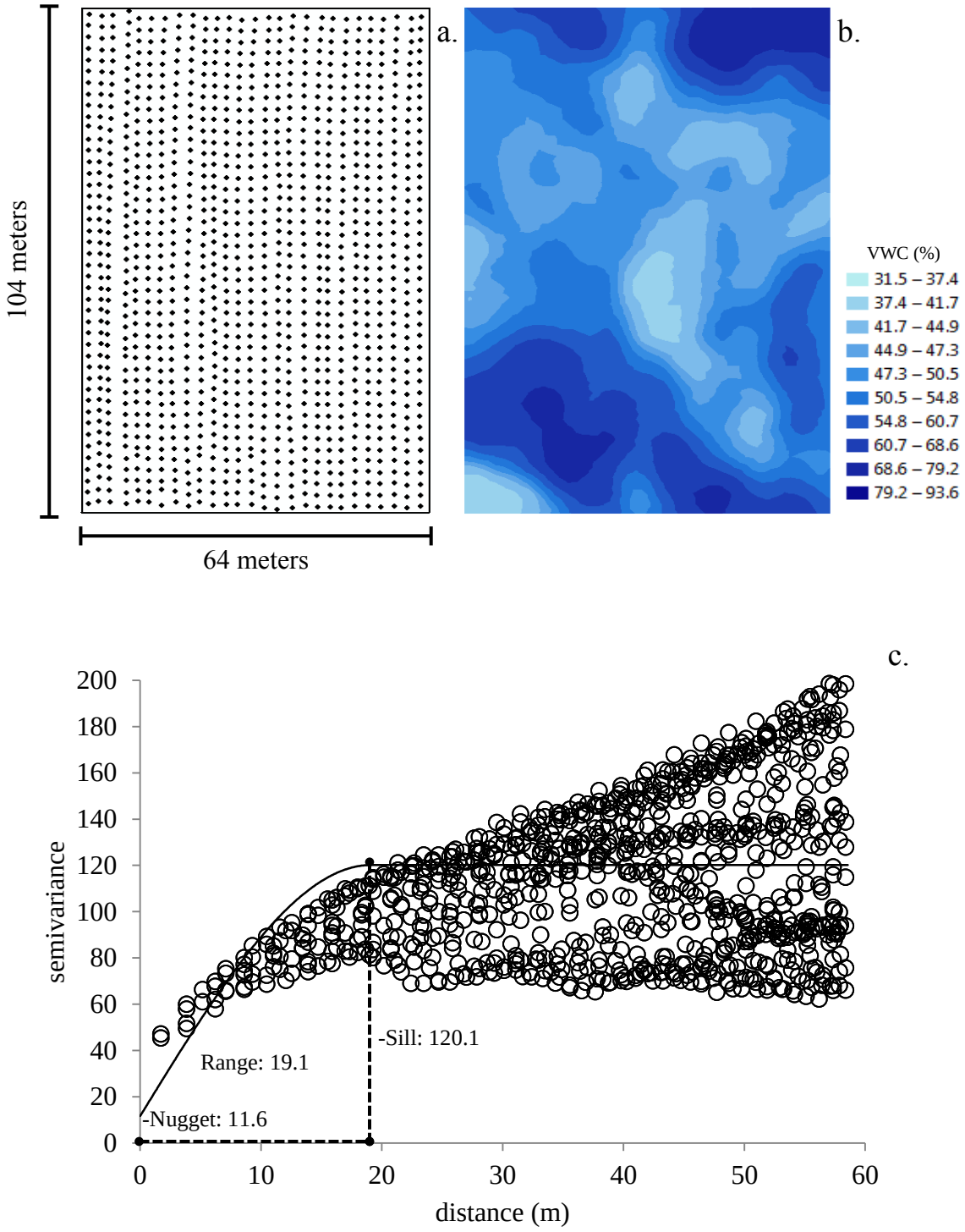


Figure 2.9. (a) Sampling locations (approximately 2.4 m x 2.4 m grid; 1189 samples), (b) kriged prediction map and (c) semivariogram including the fitted spherical model of percent volumetric water content (%VWC) on Roswell field 2.

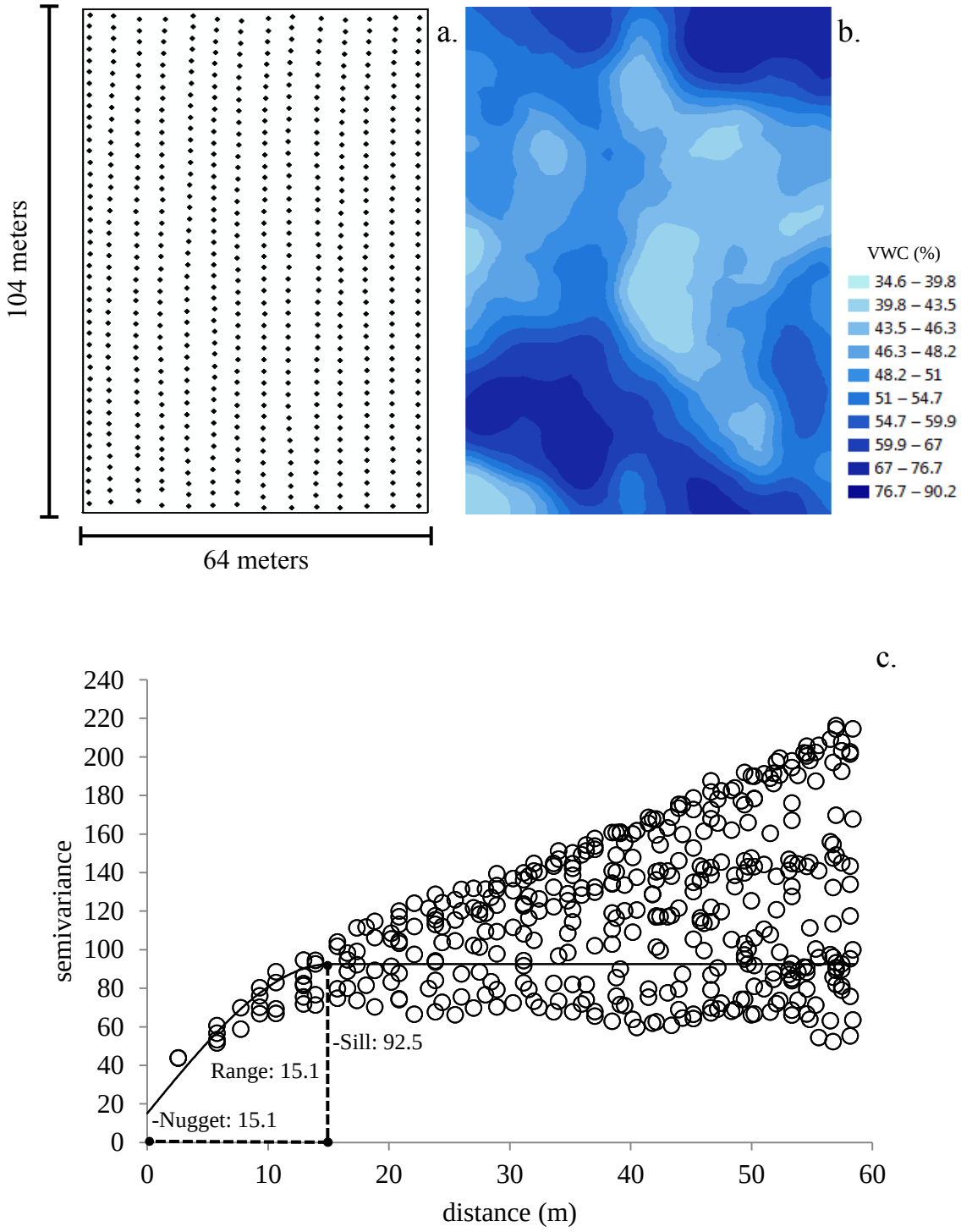


Figure 2.10. (a) Sampling locations (approximately 4.8 m x 2.4 m grid; 616 samples), (b) kriged prediction map and (c) semivariogram including the fitted spherical model of percent volumetric water content (%VWC) on Roswell field 2.

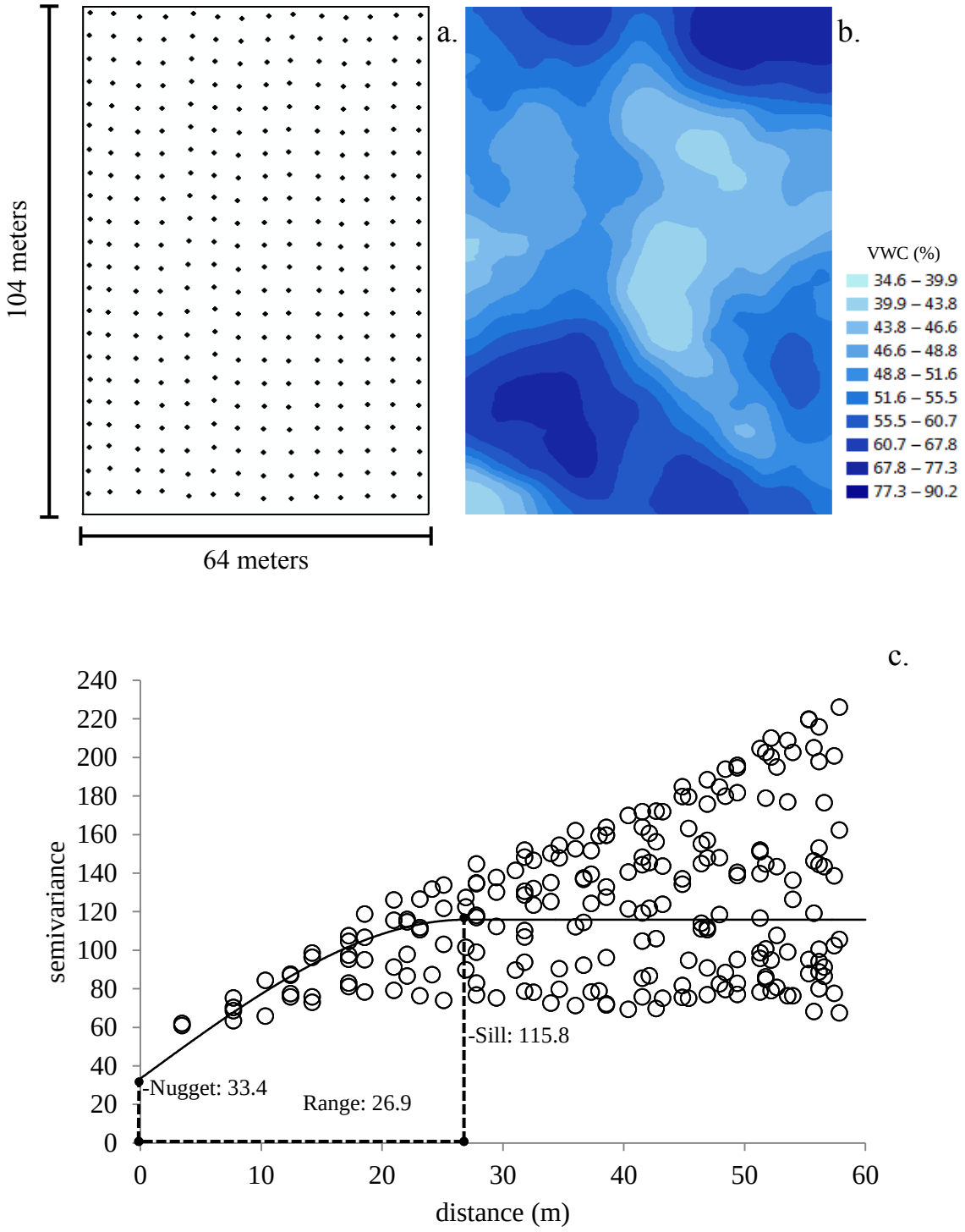


Figure 2.11. (a) Sampling locations (approximately 4.8 m x 4.8 m grid; 308 samples), (b) kriged prediction map and (c) semivariogram including the fitted spherical model of percent volumetric water content (%VWC) on Roswell field 2.

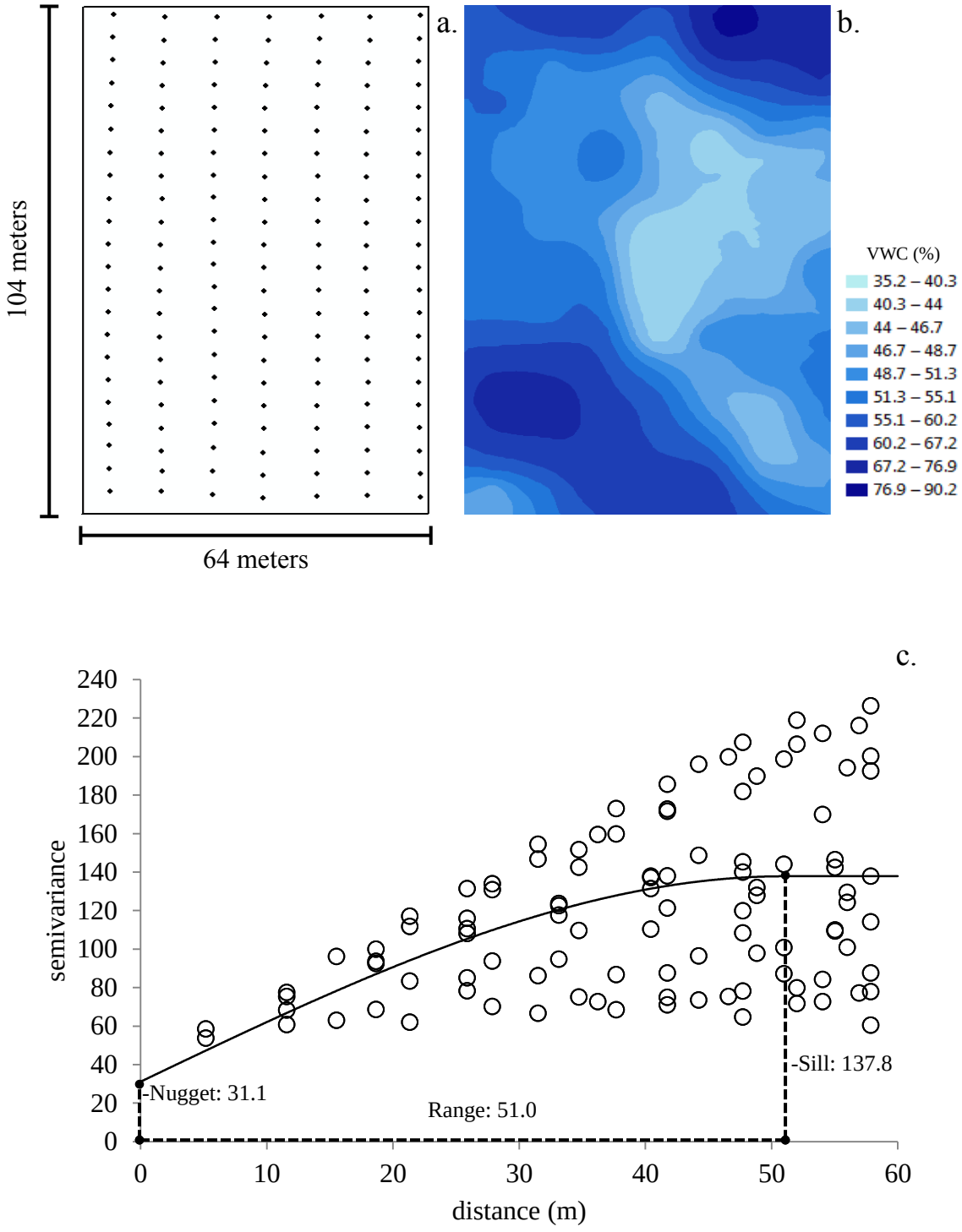


Figure 2.12. (a) Sampling locations (approximately 9.6 m x 4.8 m grid; 154 samples), (b) kriged prediction map and (c) semivariogram including the fitted spherical model of percent volumetric water content (%VWC) on Roswell field 2.

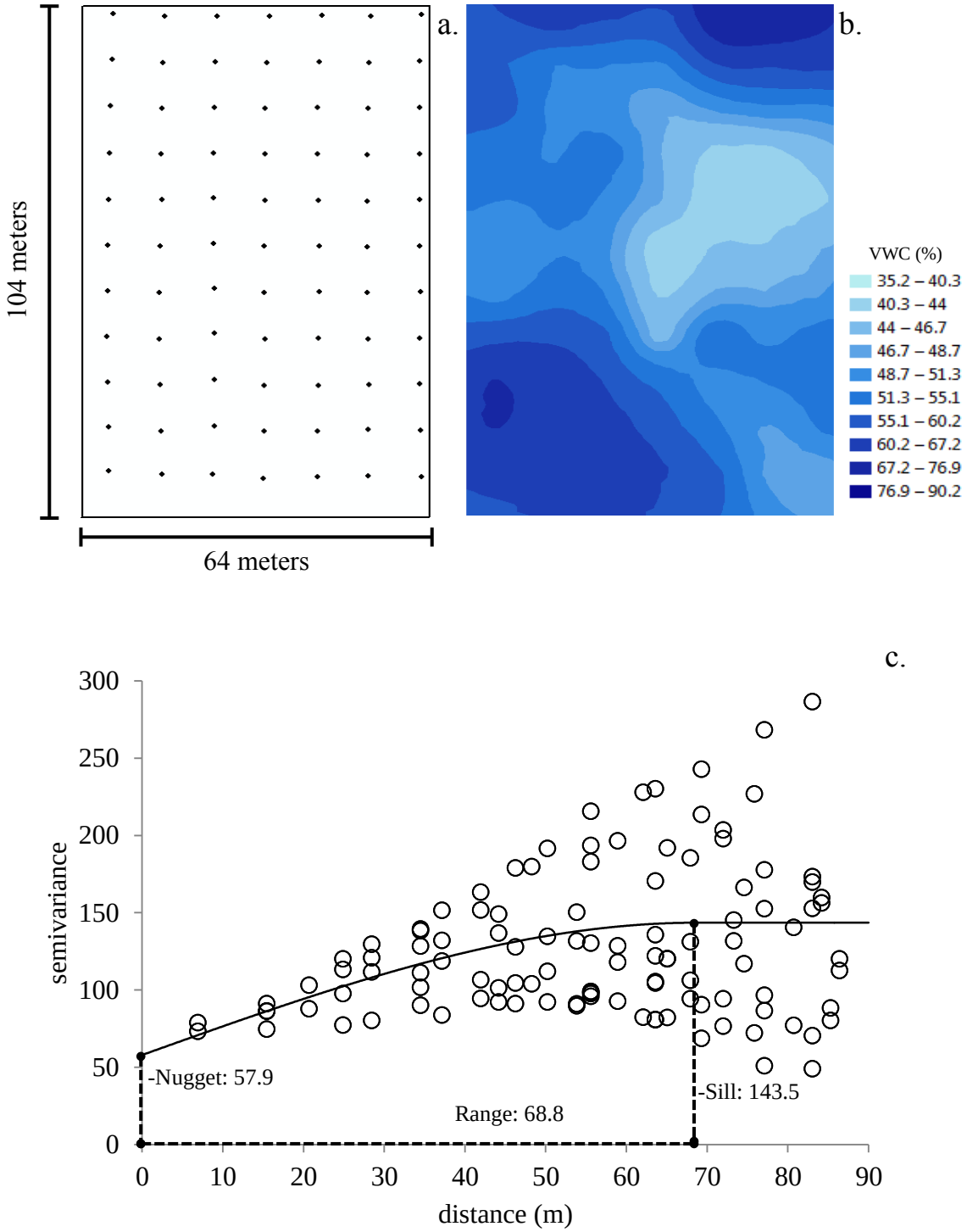


Figure 2.13. (a) Sampling locations (approximately 9.6 m x 9.6 m grid; 77 samples), (b) kriged prediction map and (c) semivariogram including the fitted spherical model of percent volumetric water content (%VWC) on Roswell field 2.

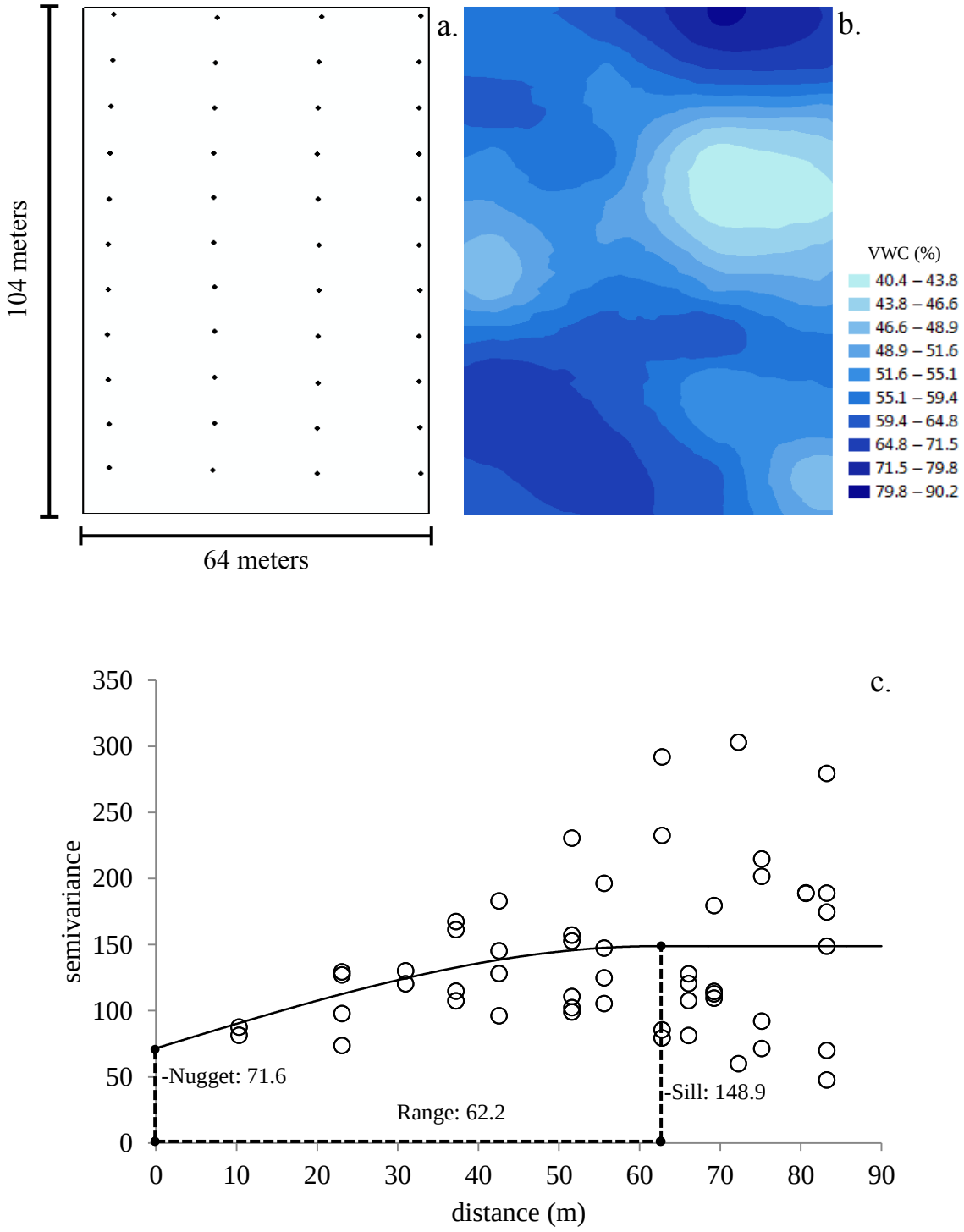


Figure 2.14. (a) Sampling locations (approximately 19.2 m x 9.6 m grid; 44samples), (b) kriged prediction map and (c) semivariogram including the fitted spherical model of percent volumetric water content (%VWC) on Roswell field 2.

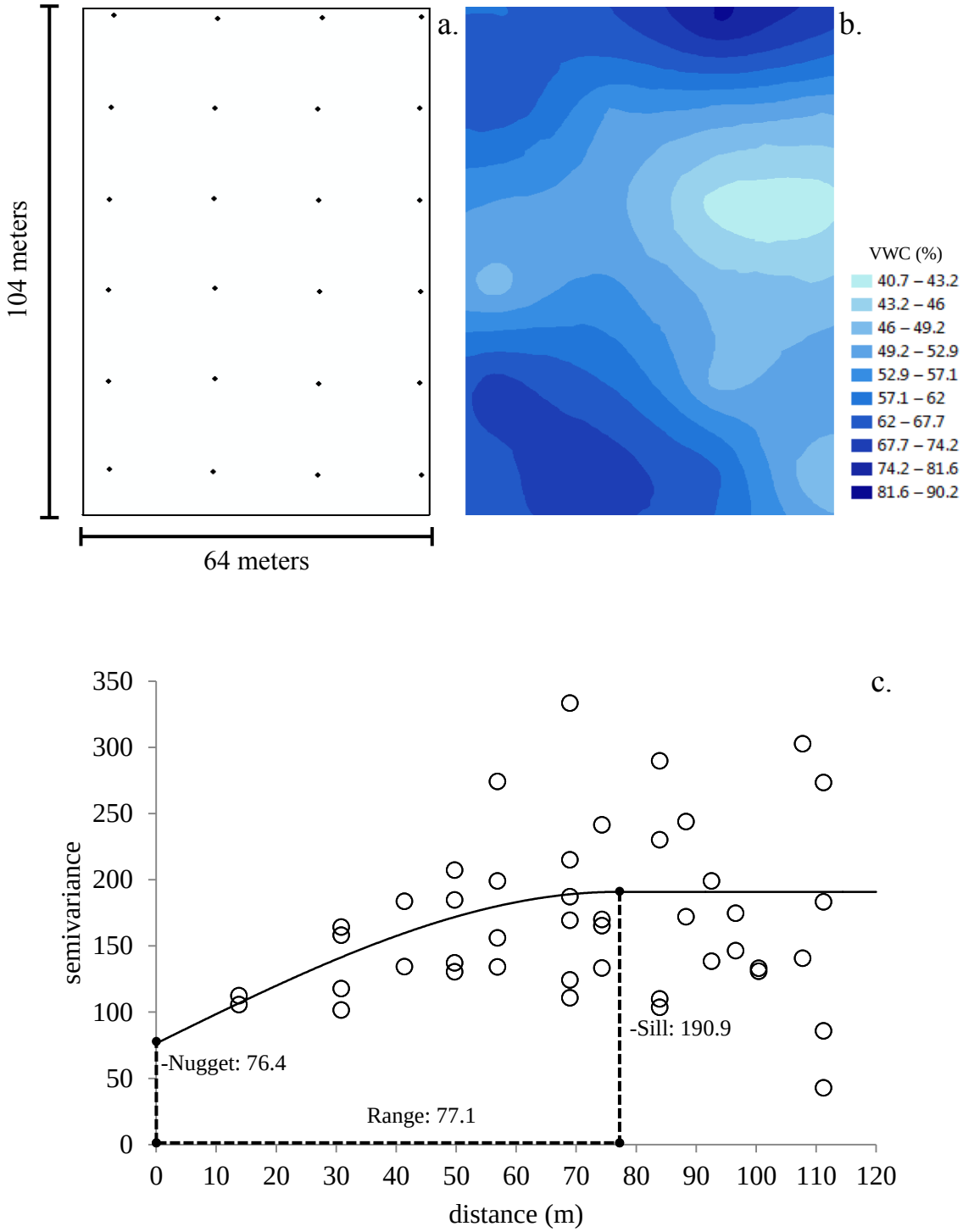


Figure 2.15. (a) Sampling locations (approximately 19.2 m x 19.2 m grid; 24 samples), (b) kriged prediction map and (c) semivariogram including the fitted spherical model of percent volumetric water content (%VWC) on Roswell field 2.

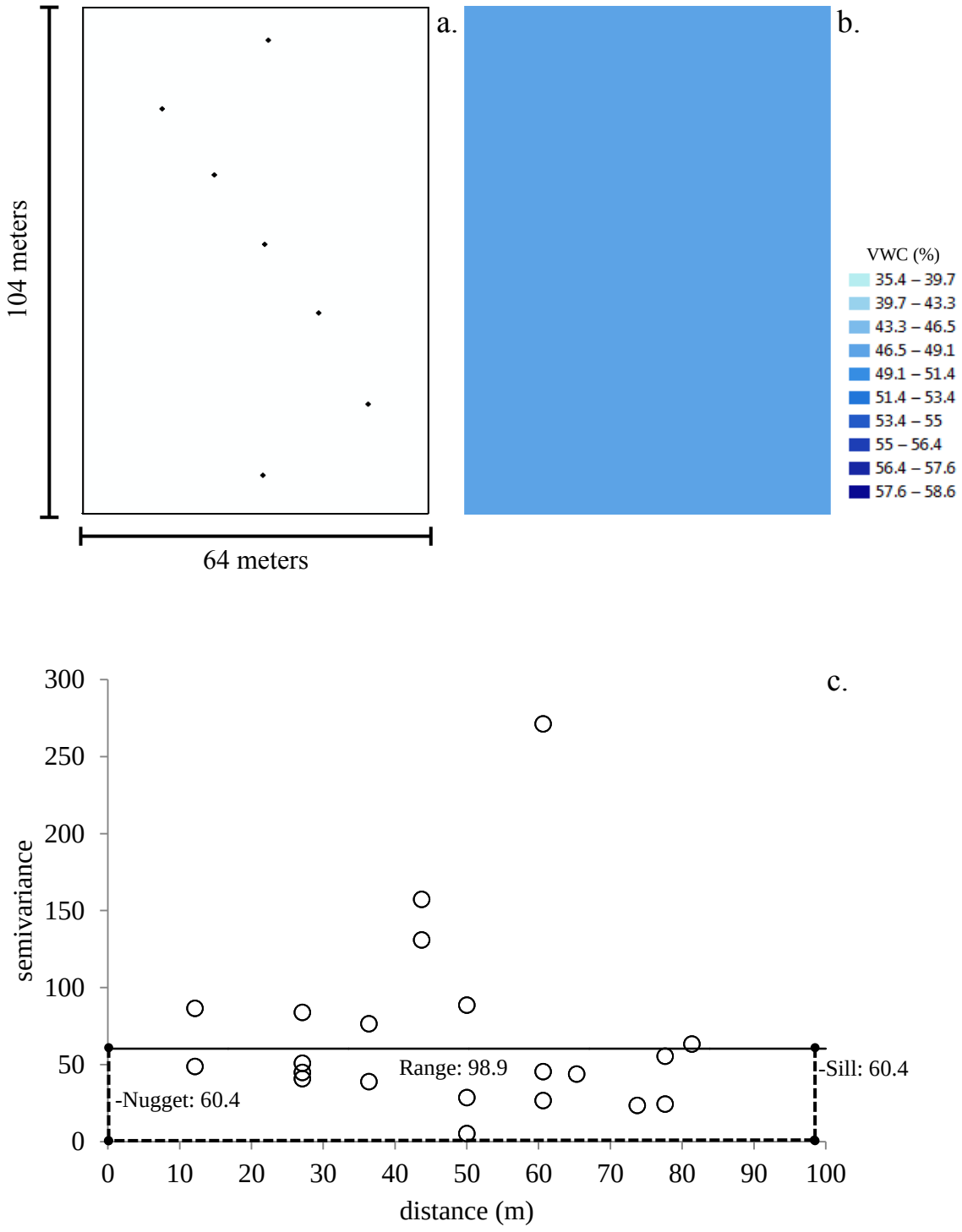


Figure 2.16. (a) Sampling locations (7 samples), (b) kriged prediction map and (c) semivariogram including the fitted spherical model of percent volumetric water content (%VWC) on Roswell field 2.

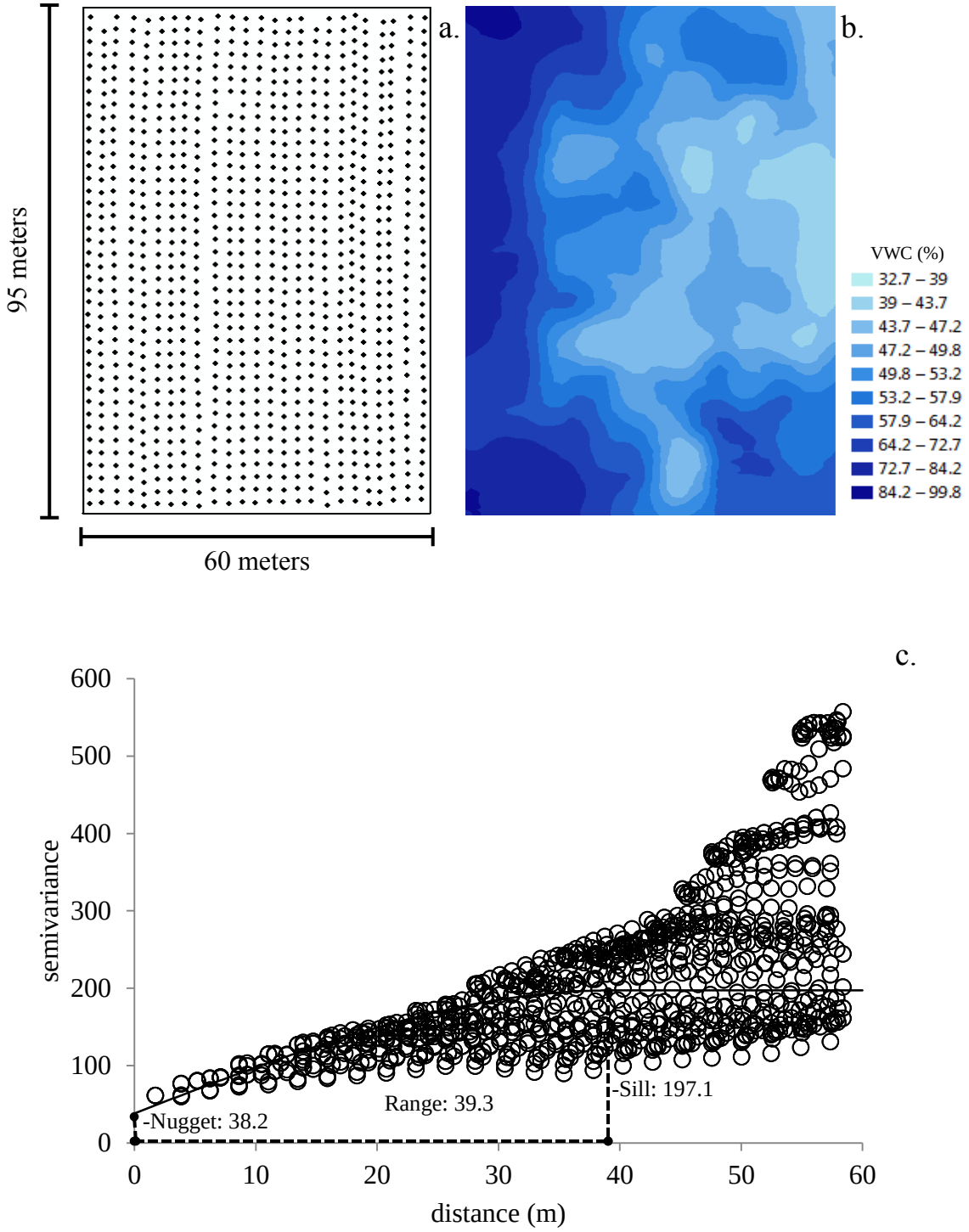


Figure 2.17. (a) Sampling locations (approximately 2.4 m x 2.4 m grid; 997 samples), (b) kriged prediction map and (c) semivariogram including the fitted spherical model of percent volumetric water content (%VWC) on Roswell field 3.

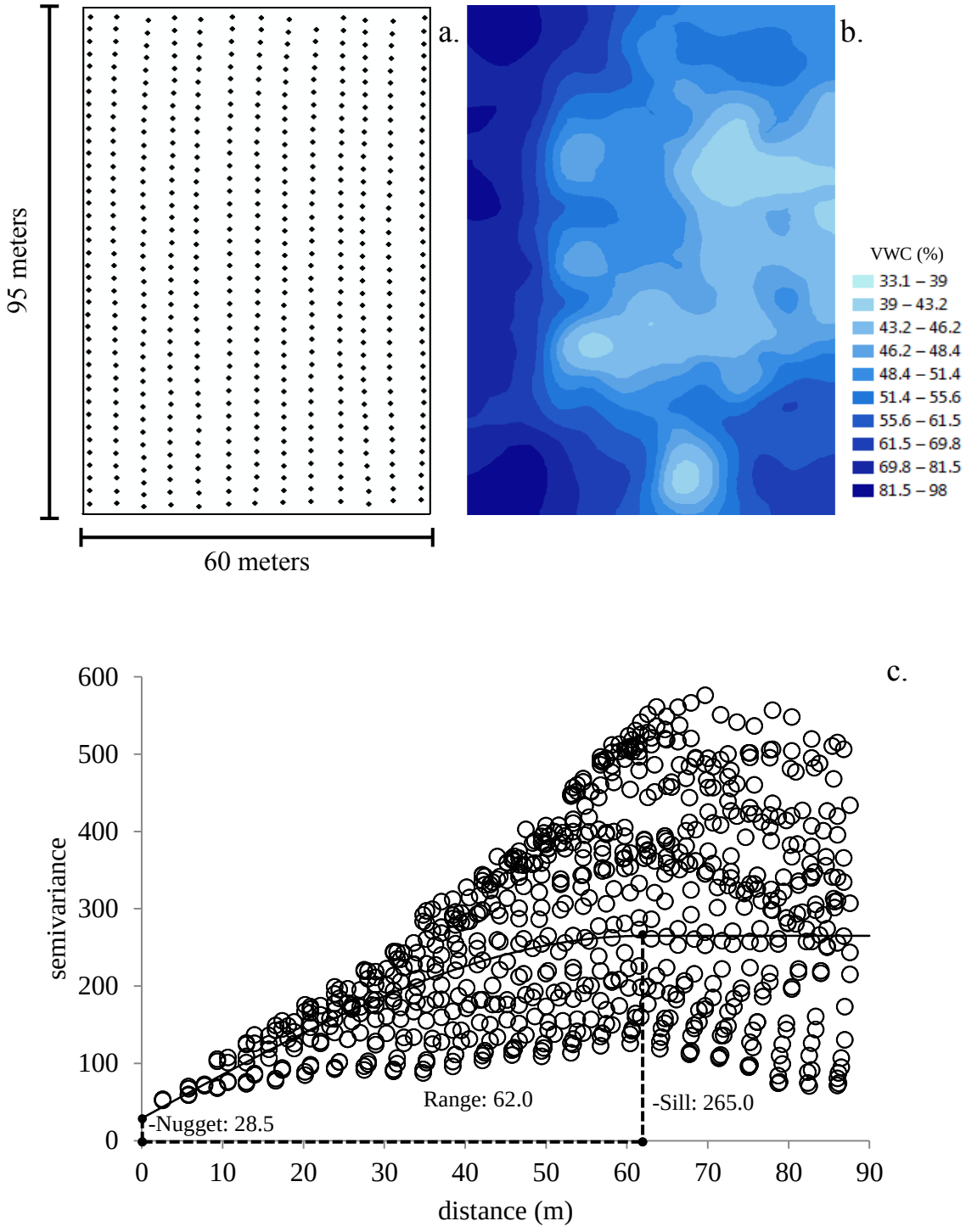


Figure 2.18. (a) Sampling locations (approximately 4.8 m x 2.4 m grid; 519 samples), (b) kriged prediction map and (c) semivariogram including the fitted spherical model of percent volumetric water content (%VWC) on Roswell field 3.

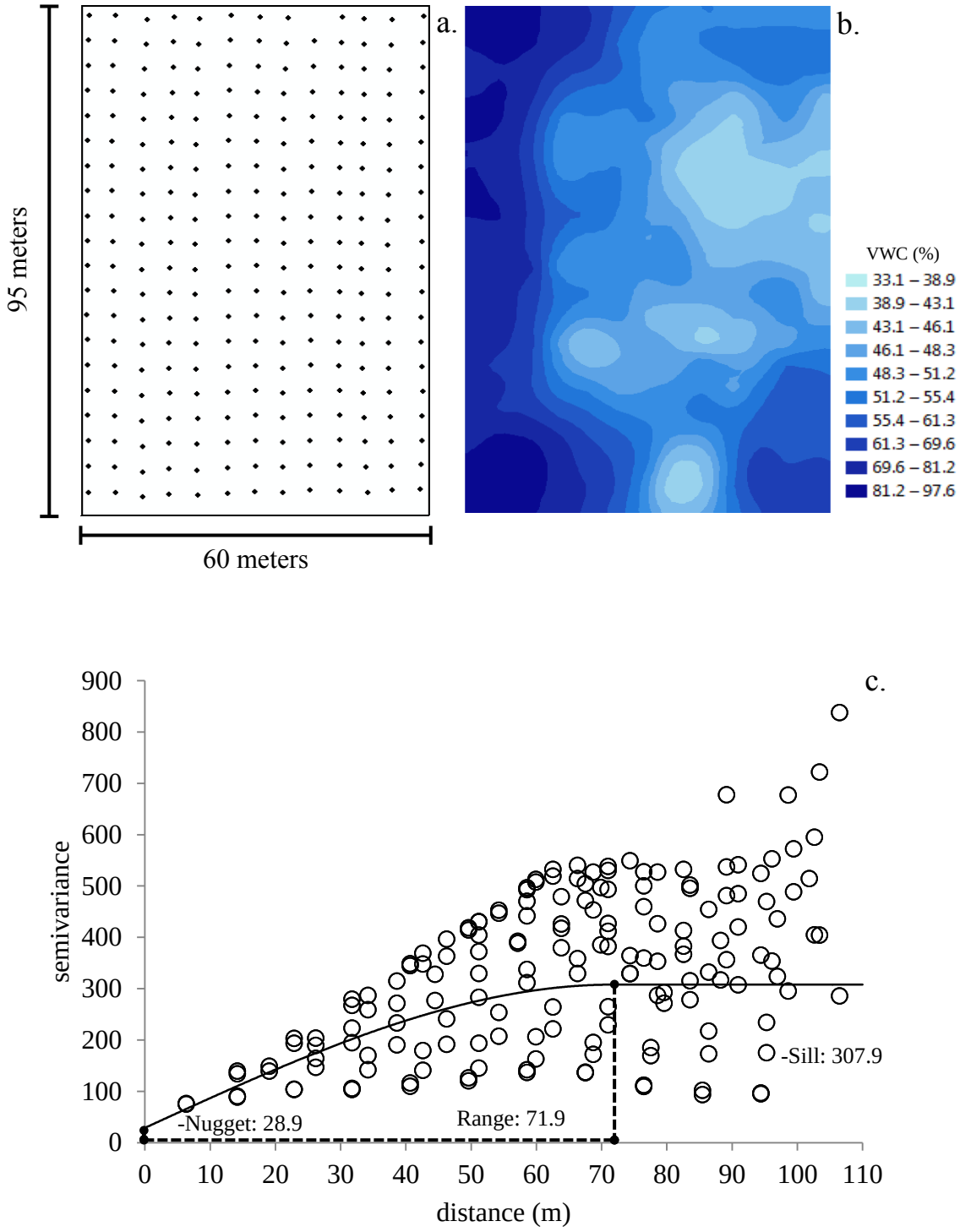


Figure 2.19. (a) Sampling locations (approximately 4.8 m x 4.8 m grid; 259 samples), (b) kriged prediction map and (c) semivariogram including the fitted spherical model of percent volumetric water content (%VWC) on Roswell field 3.

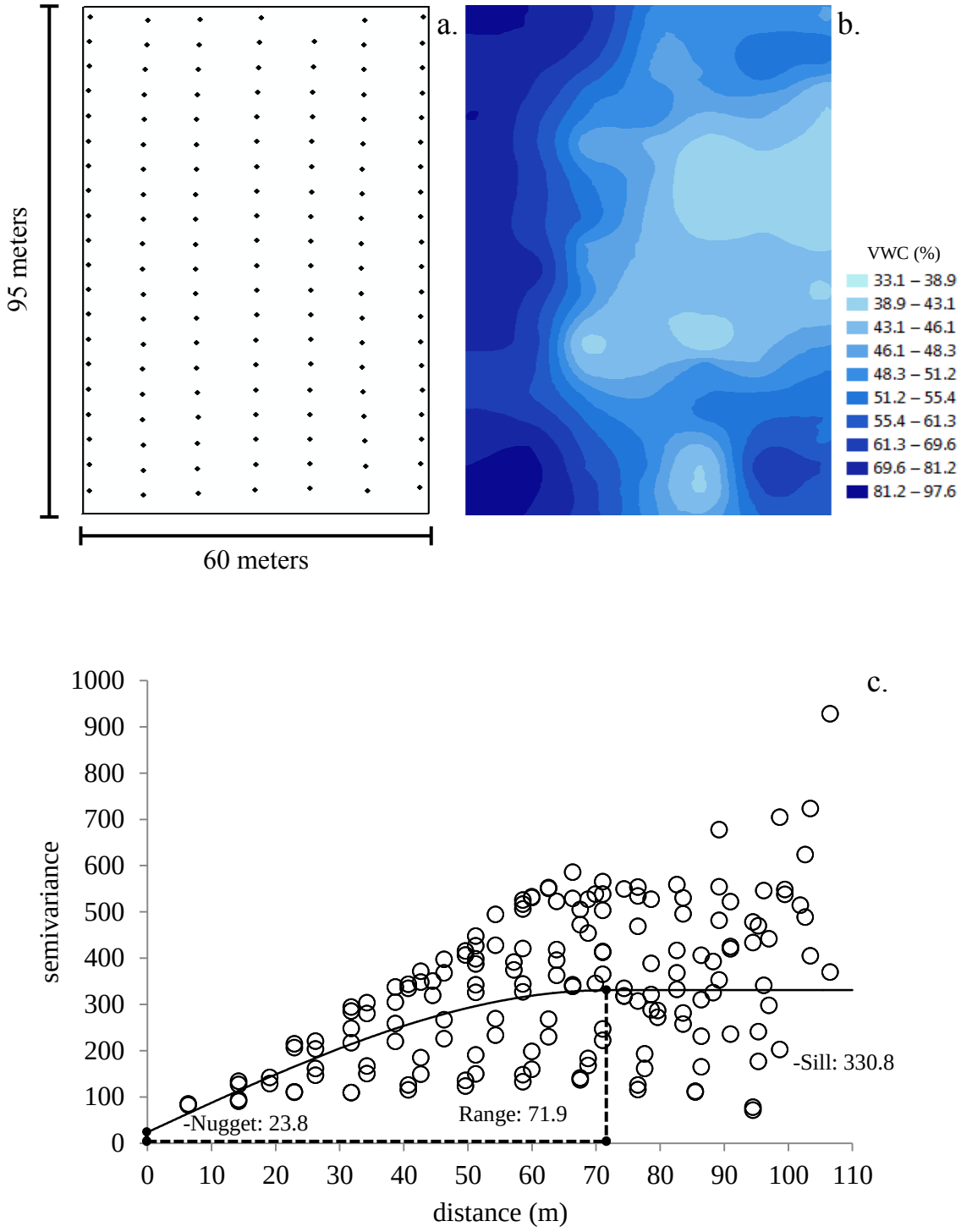


Figure 2.20. (a) Sampling locations (approximately 9.6 m x 4.8 m grid; 139 samples), (b) kriged prediction map and (c) semivariogram including the fitted spherical model of percent volumetric water content (%VWC) on Roswell field 3.

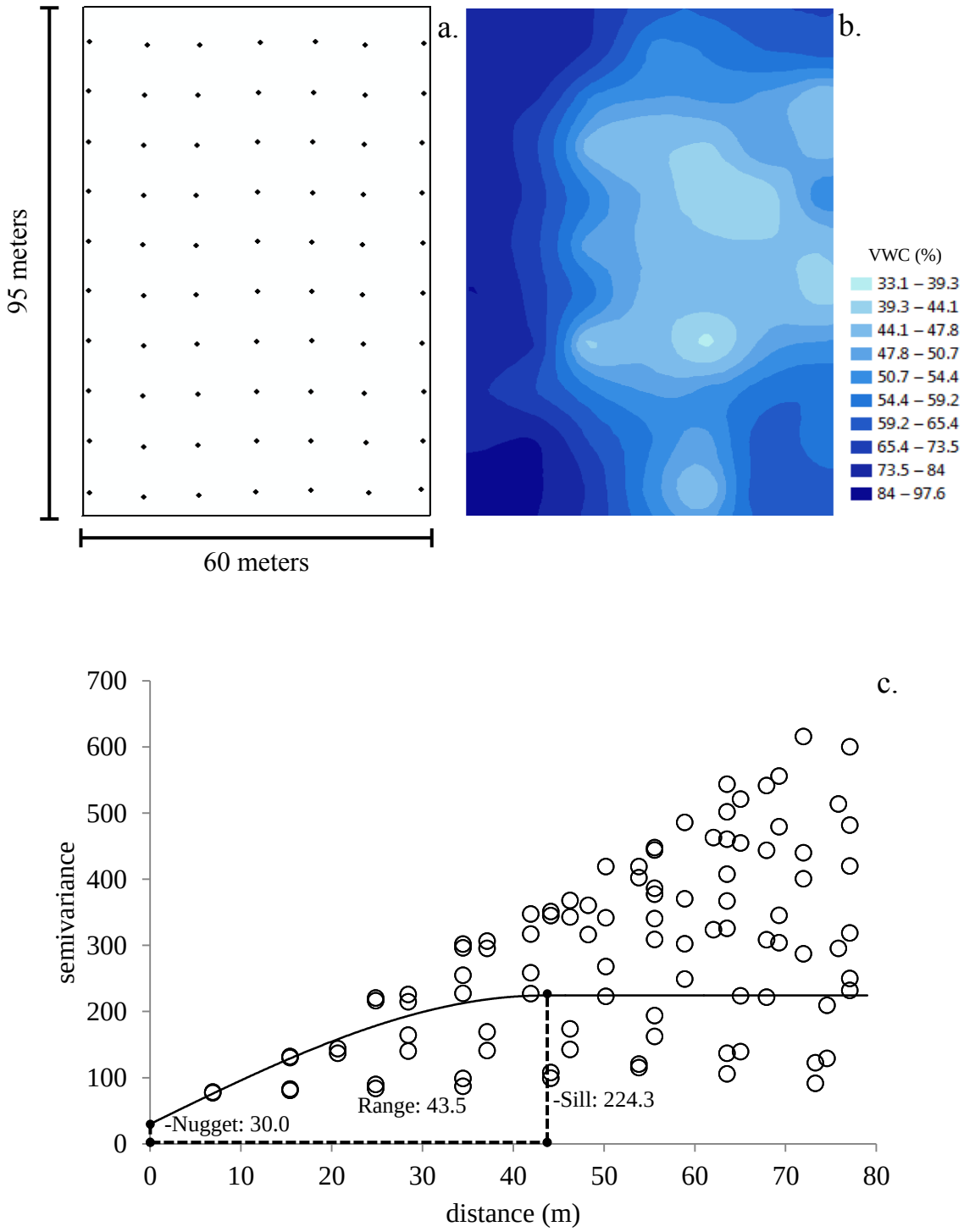


Figure 2.21. (a) Sampling locations (approximately 9.6 m x 9.6 m grid; 70 samples), (b) kriged prediction map and (c) semivariogram including the fitted spherical model of percent volumetric water content (%VWC) on Roswell field 3.

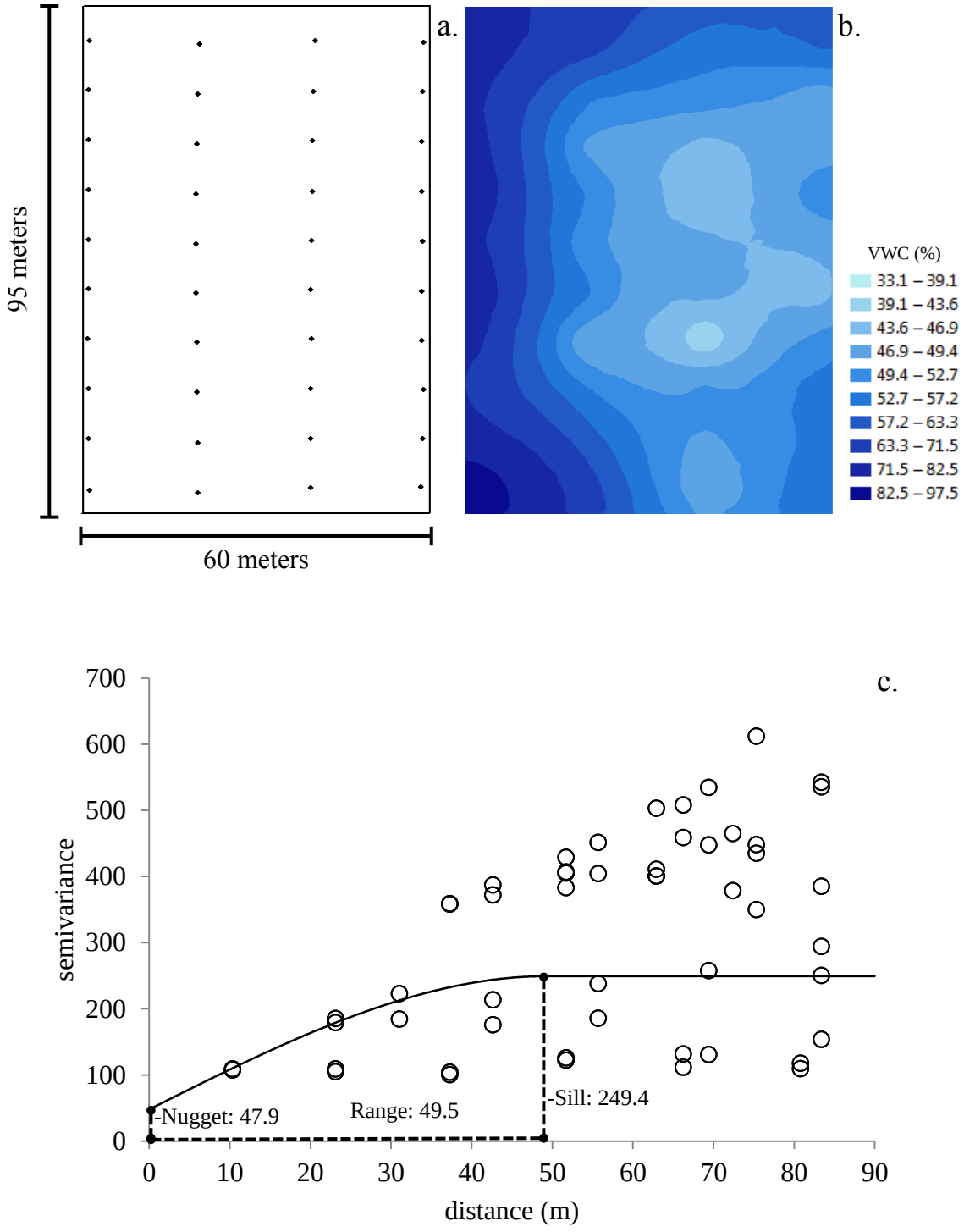


Figure 2.22. (a) Sampling locations (approximately 19.2 m x 9.6 m grid; 40 samples), (b) kriged prediction map and (c) semivariogram including the fitted spherical model of percent volumetric water content (%VWC) on Roswell field 3.

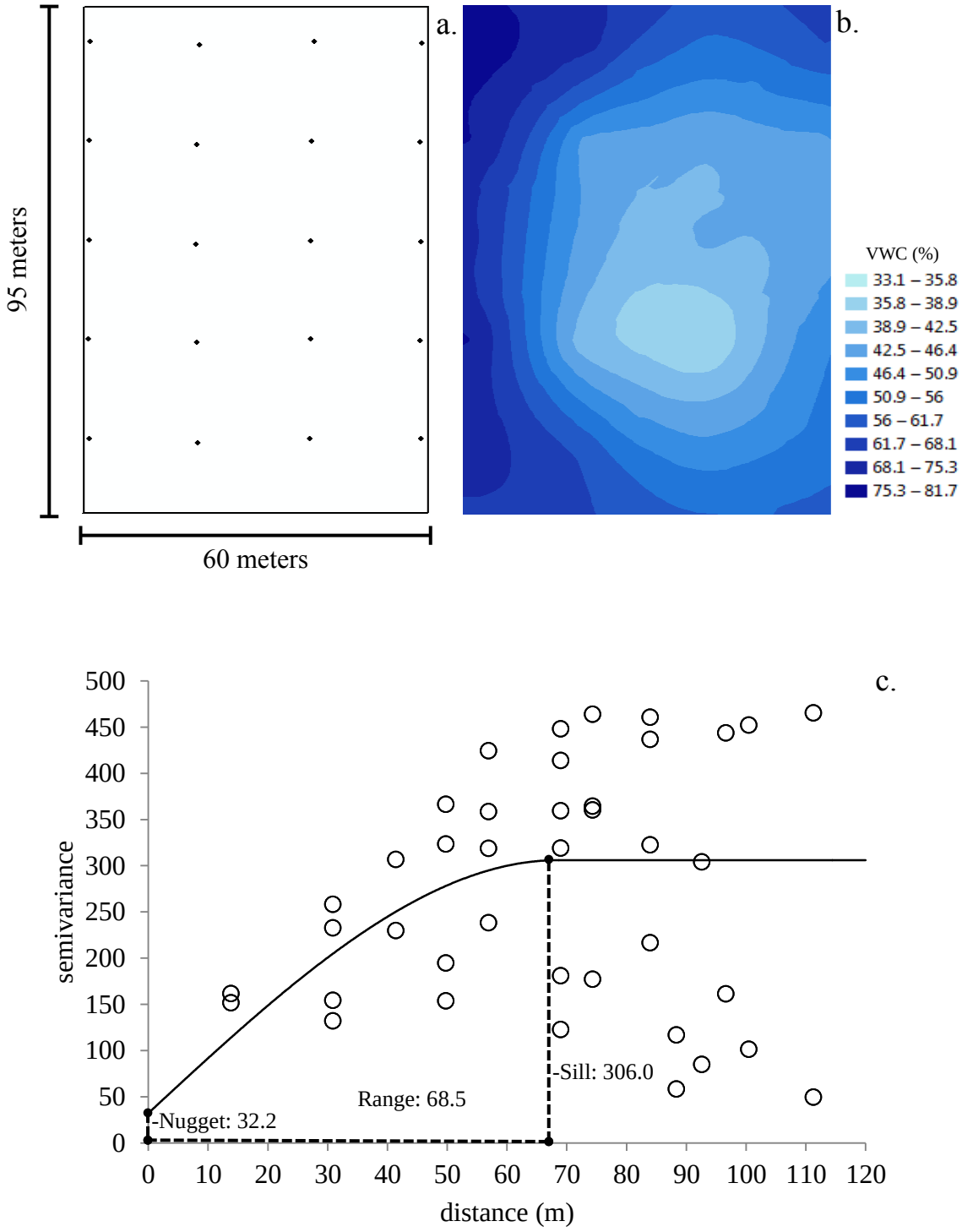


Figure 2.23. (a) Sampling locations (approximately 19.2 m x 19.2 m grid; 20 samples), (b) kriged prediction map and (c) semivariogram including the fitted spherical model of percent volumetric water content (%VWC) on Roswell field 3.

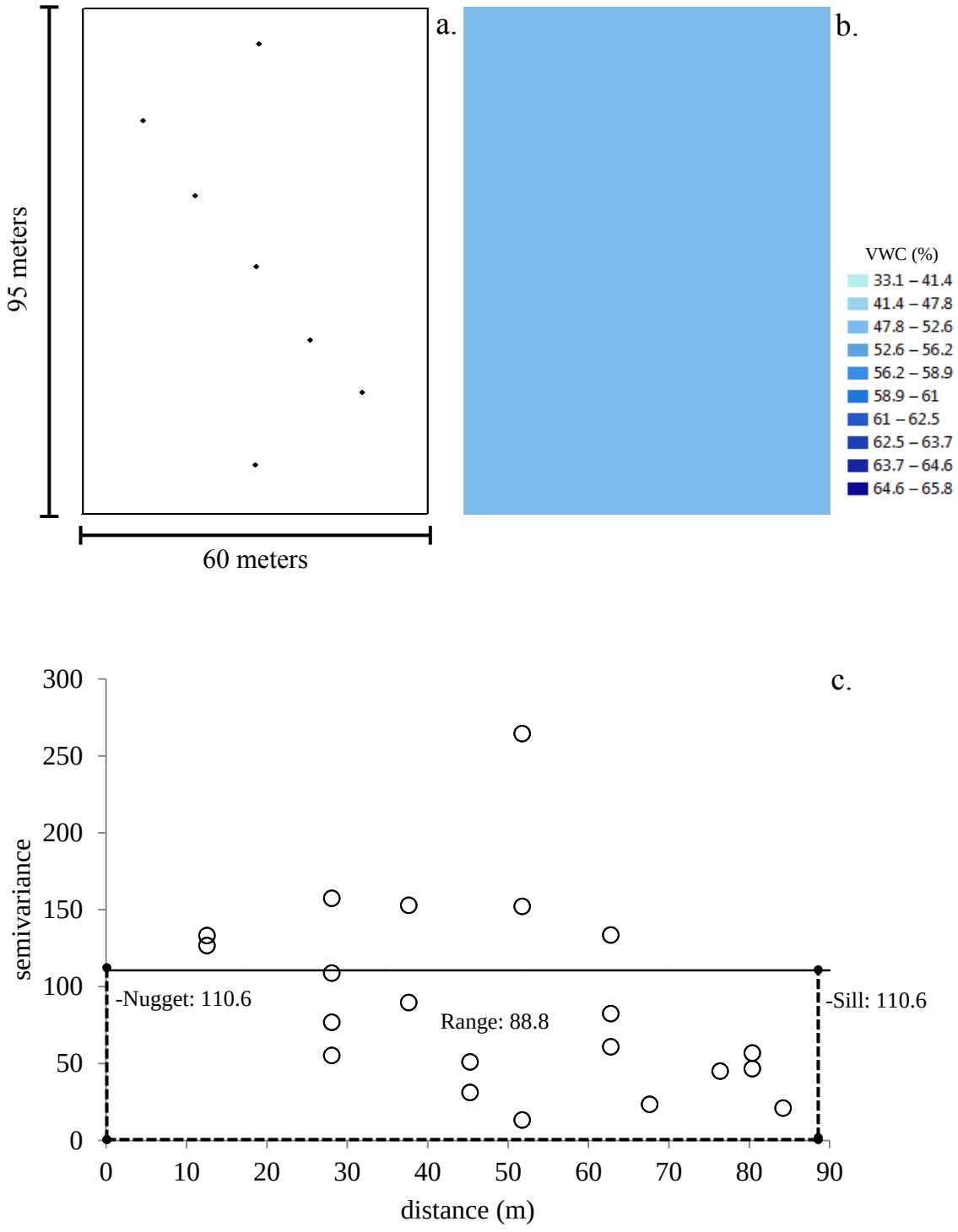


Figure 2.24. (a) Sampling locations (7 samples), (b) kriged prediction map and (c) semivariogram including the fitted spherical model of percent volumetric water content (%VWC) on Roswell field 3.

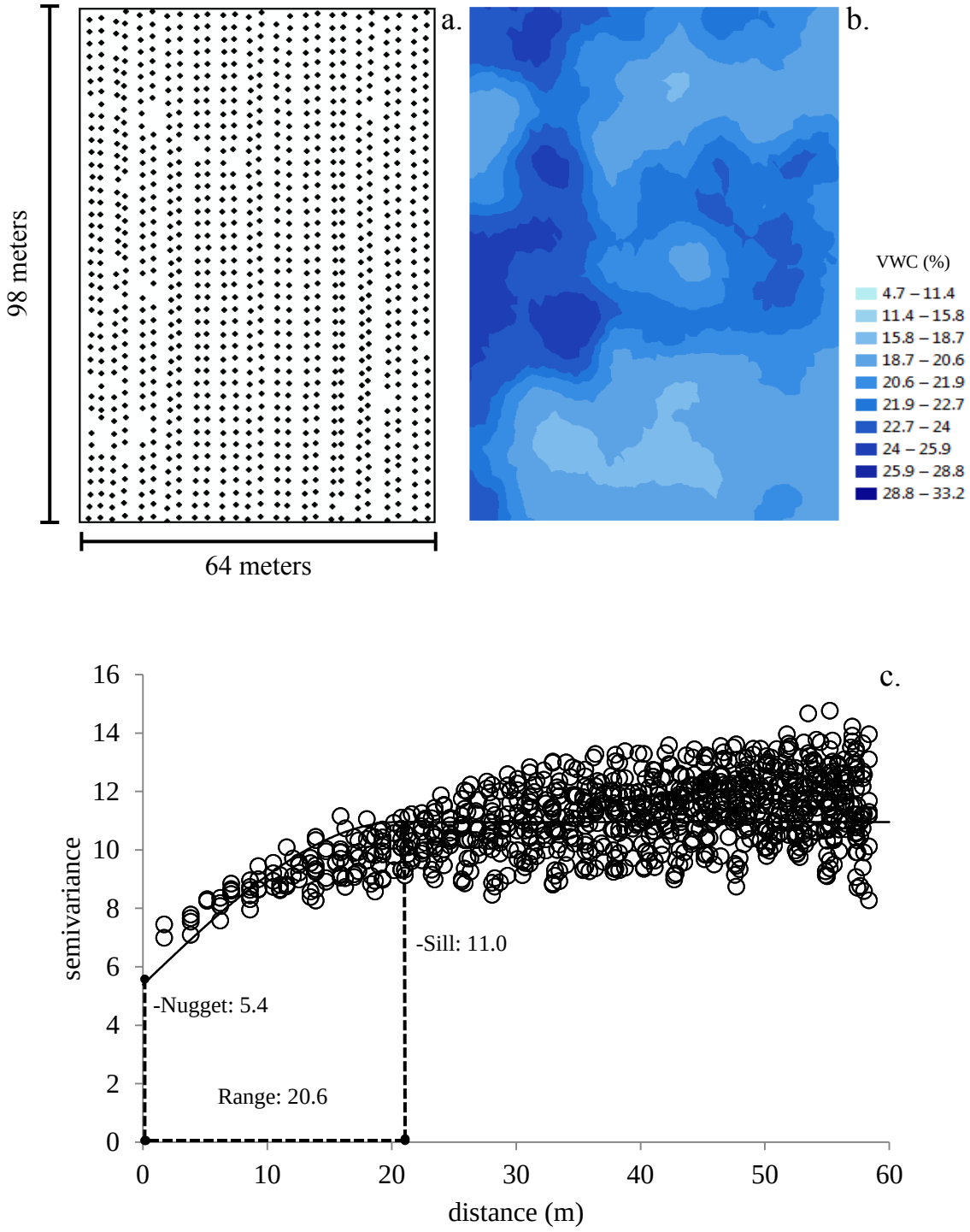


Figure 2.25. (a) Sampling locations (approximately 2.4 m x 2.4 m grid; 1066 samples), (b) kriged prediction map and (c) semivariogram including the fitted spherical model of percent volumetric water content (%VWC) on Watkinsville field 1.

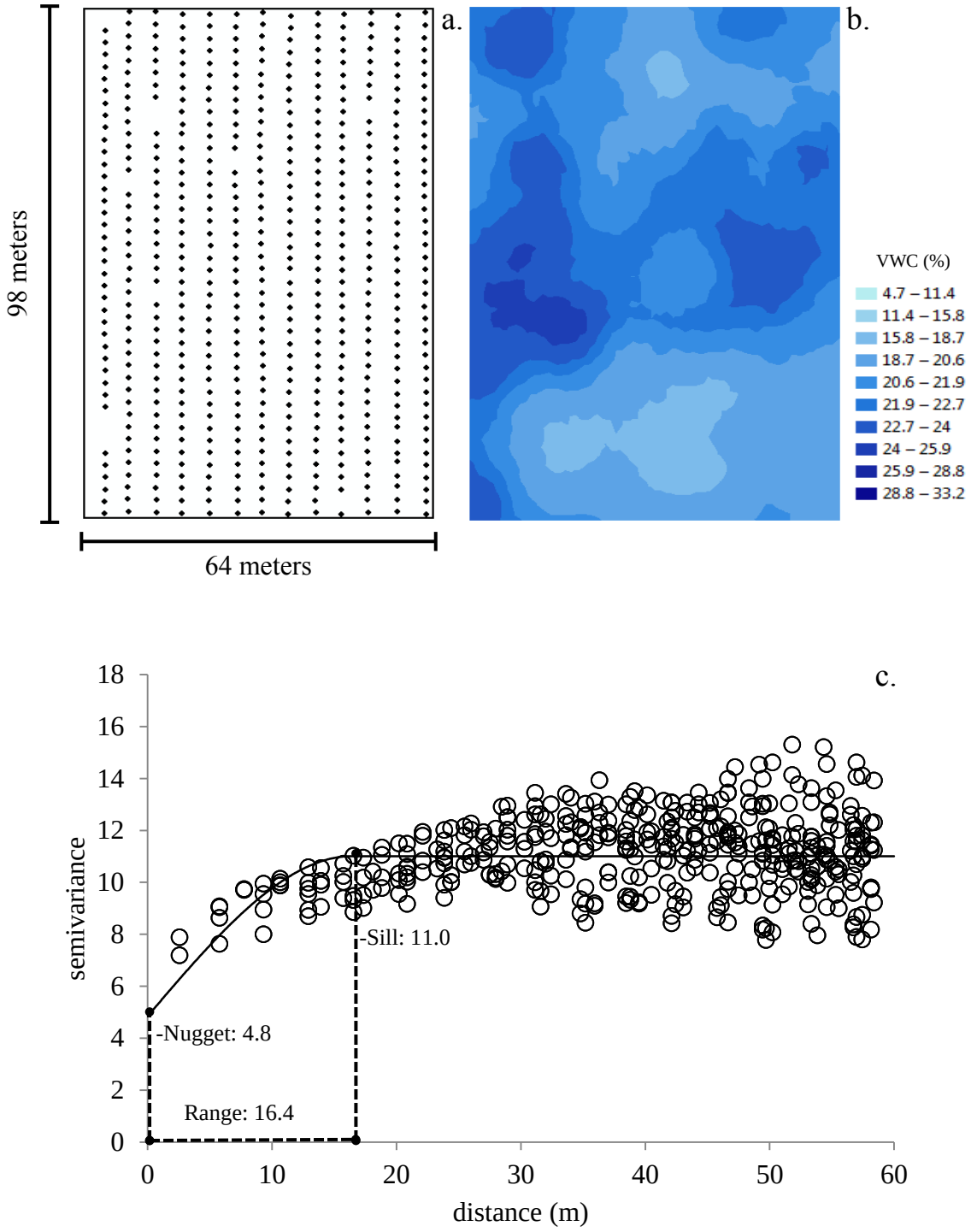


Figure 2.26. (a) Sampling locations (approximately 4.8 m x 2.4 m grid; 535 samples), (b) kriged prediction map and (c) semivariogram including the fitted spherical model of percent volumetric water content (%VWC) on Watkinsville field 1.

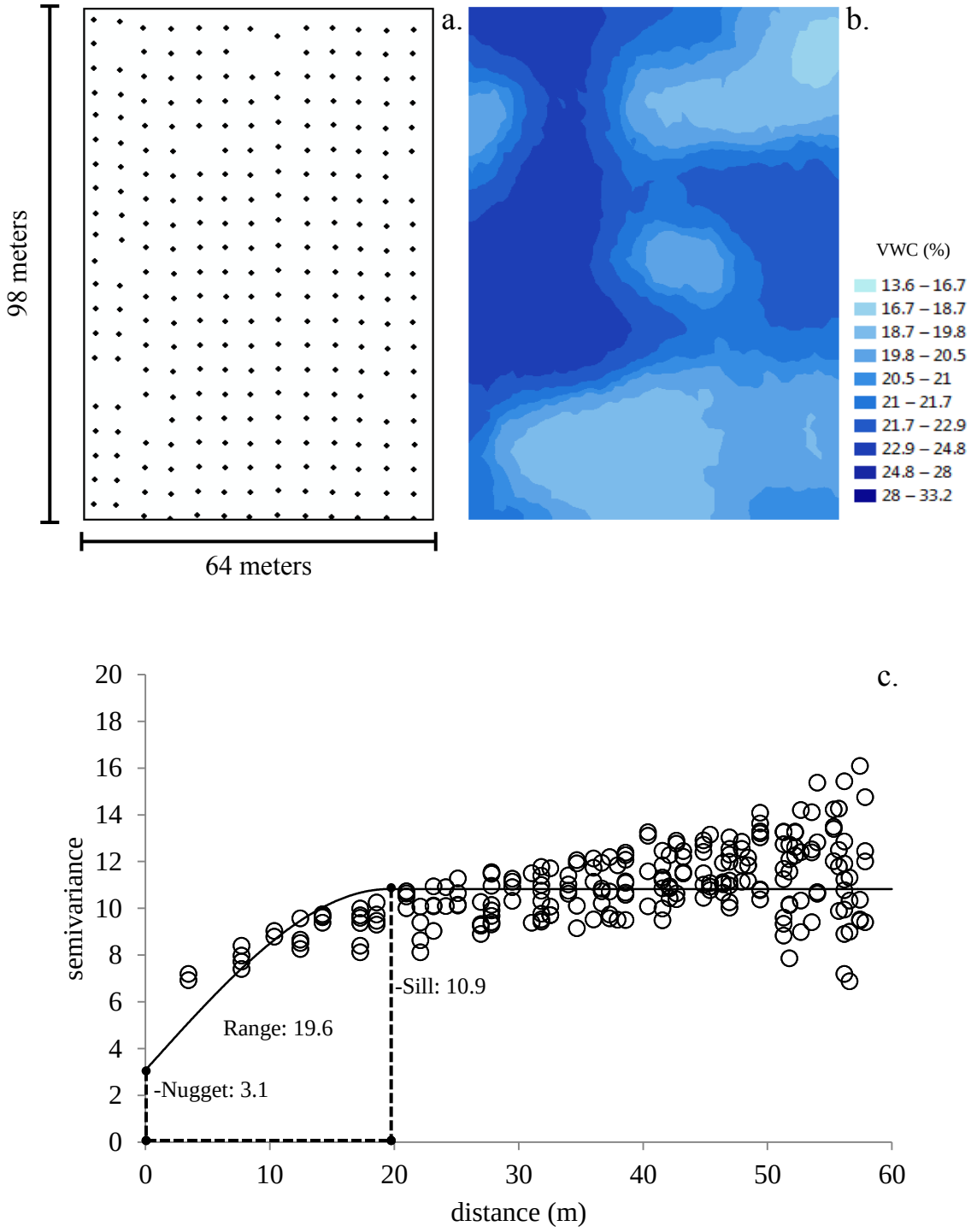


Figure 2.27. (a) Sampling locations (approximately 4.8 m x 4.8 m grid; 263 samples), (b) kriged prediction map and (c) semivariogram including the fitted spherical model of percent volumetric water content (%VWC) on Watkinsville field 1.

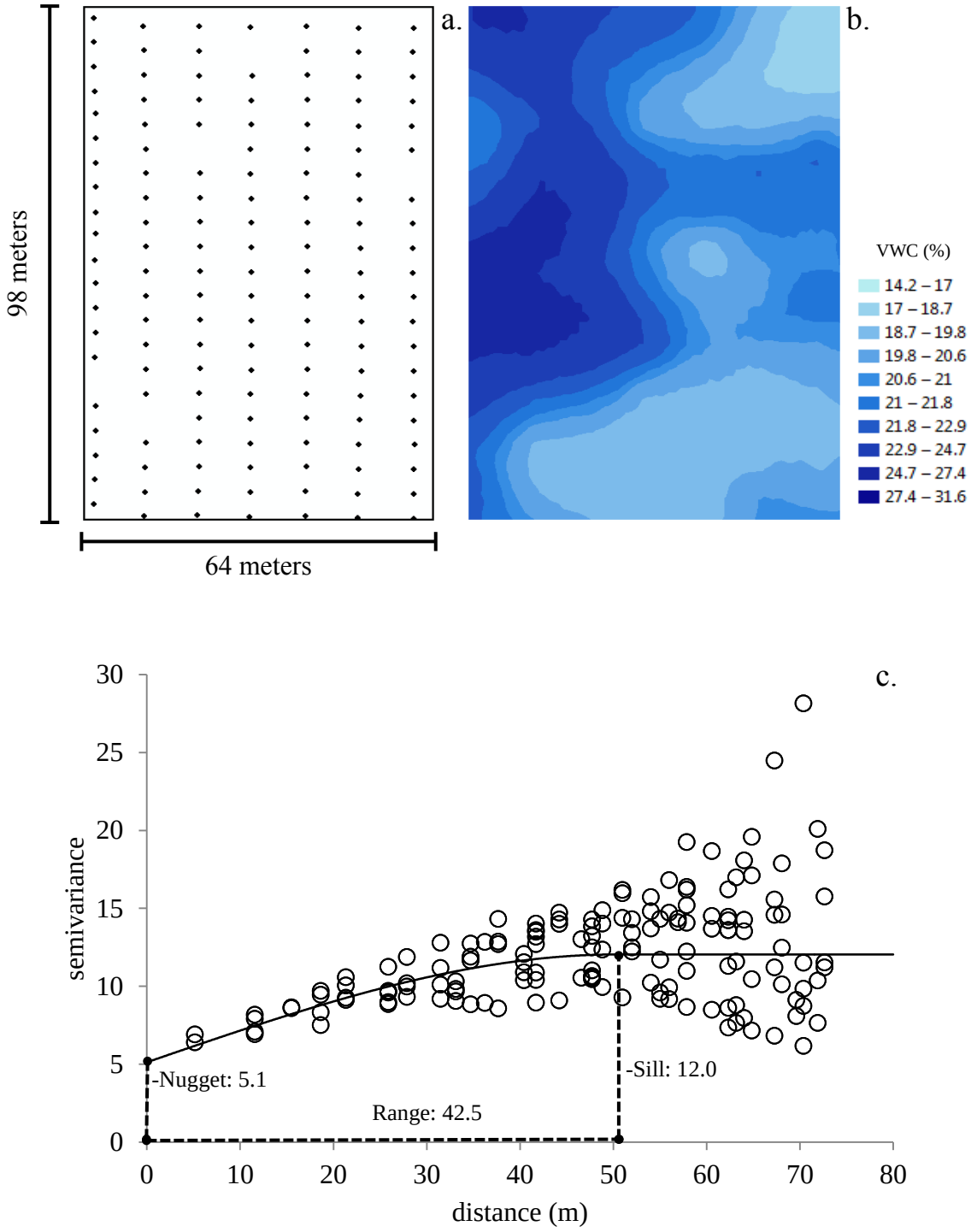


Figure 2.28. (a) Sampling locations (approximately 9.6 m x 4.8 m grid; 142 samples), (b) kriged prediction map and (c) semivariogram including the fitted spherical model of percent volumetric water content (%VWC) on Watkinsville field 1.

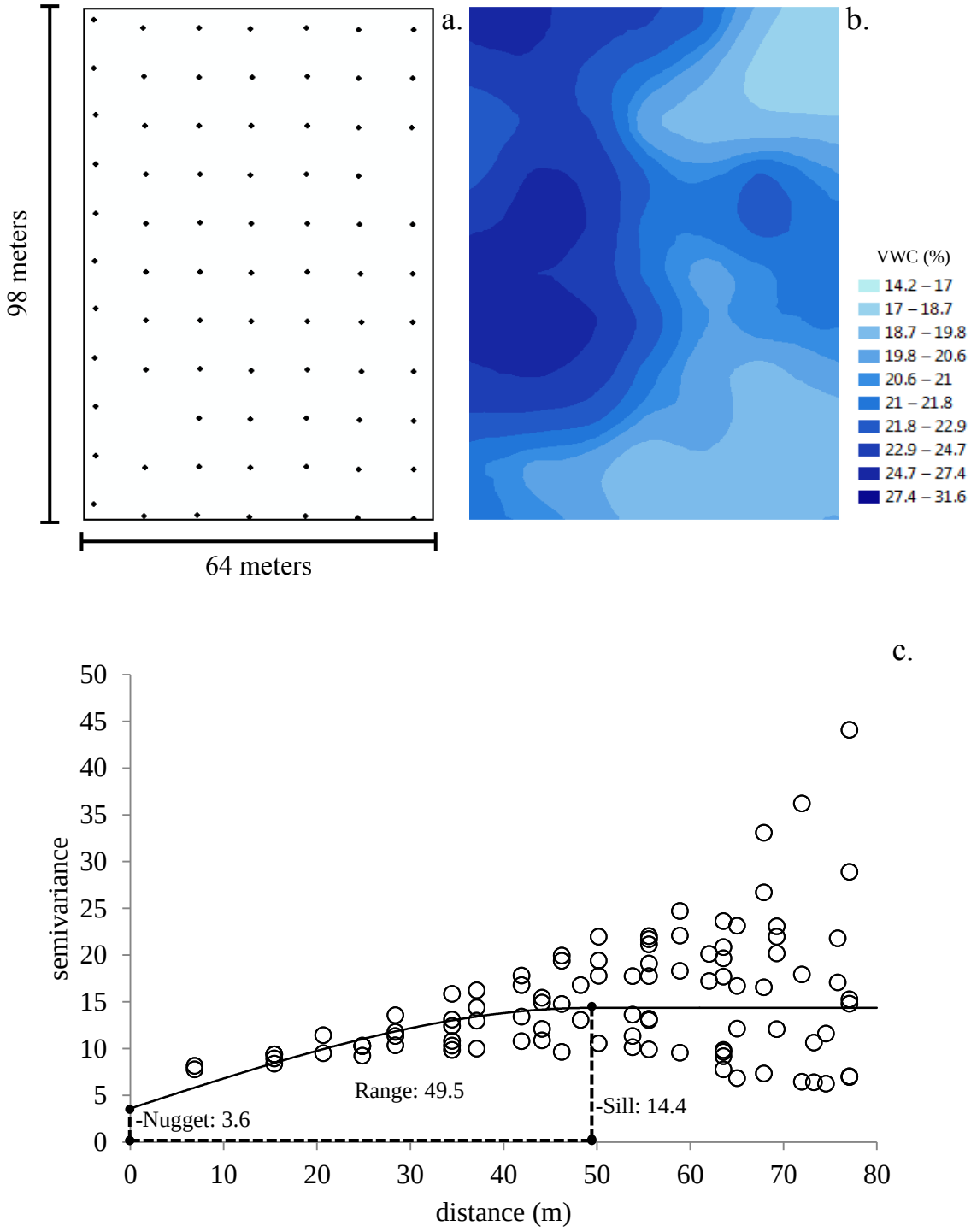


Figure 2.29. (a) Sampling locations (approximately 9.6 m x 9.6 m grid; 75 samples), (b) kriged prediction map and (c) semivariogram including the fitted spherical model of percent volumetric water content (%VWC) on Watkinsville field 1.

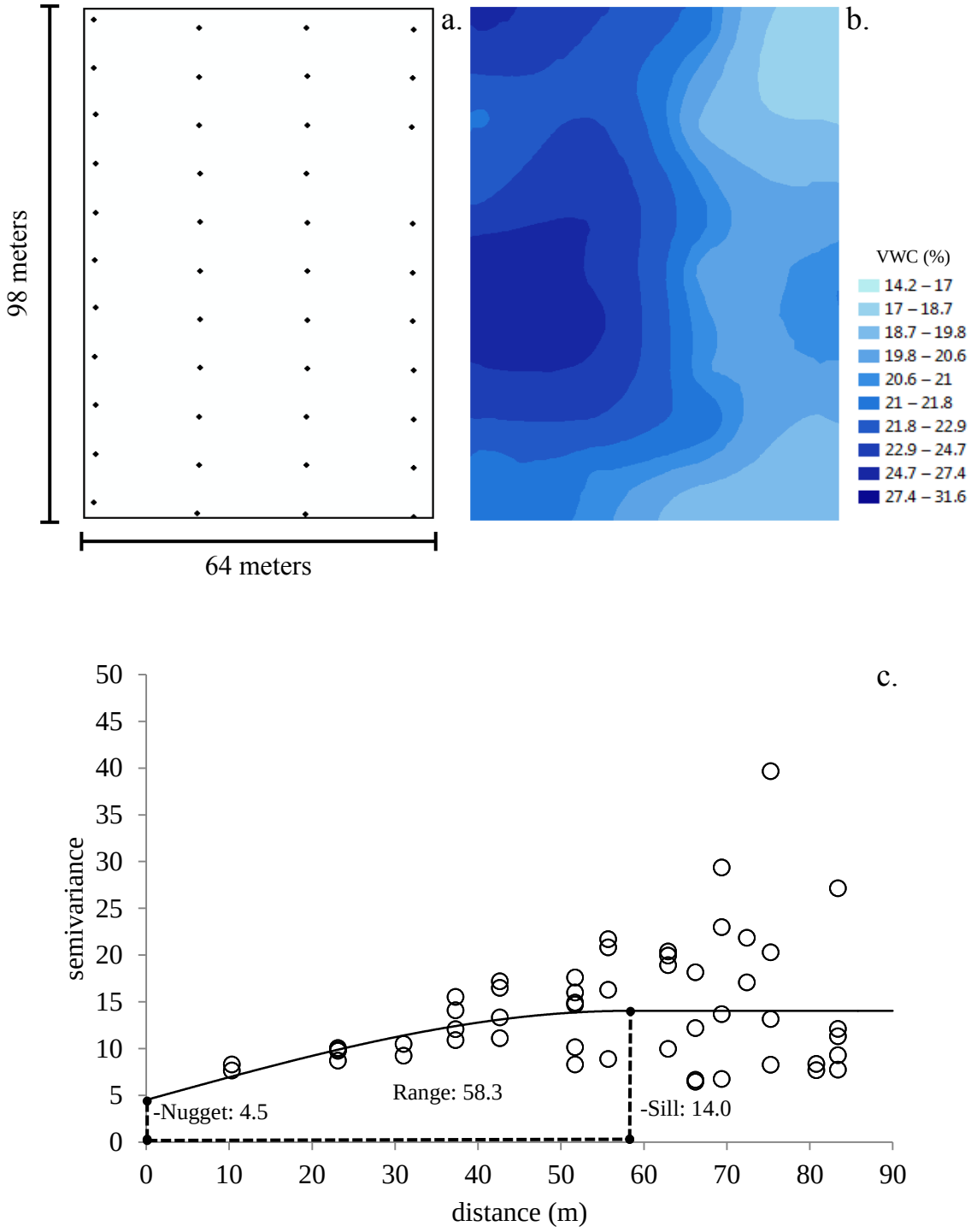


Figure 2.30. (a) Sampling locations (approximately 19.2 m x 9.6 m grid; 43 samples), (b) kriged prediction map and (c) semivariogram including the fitted spherical model of percent volumetric water content (%VWC) on Watkinsville field 1.

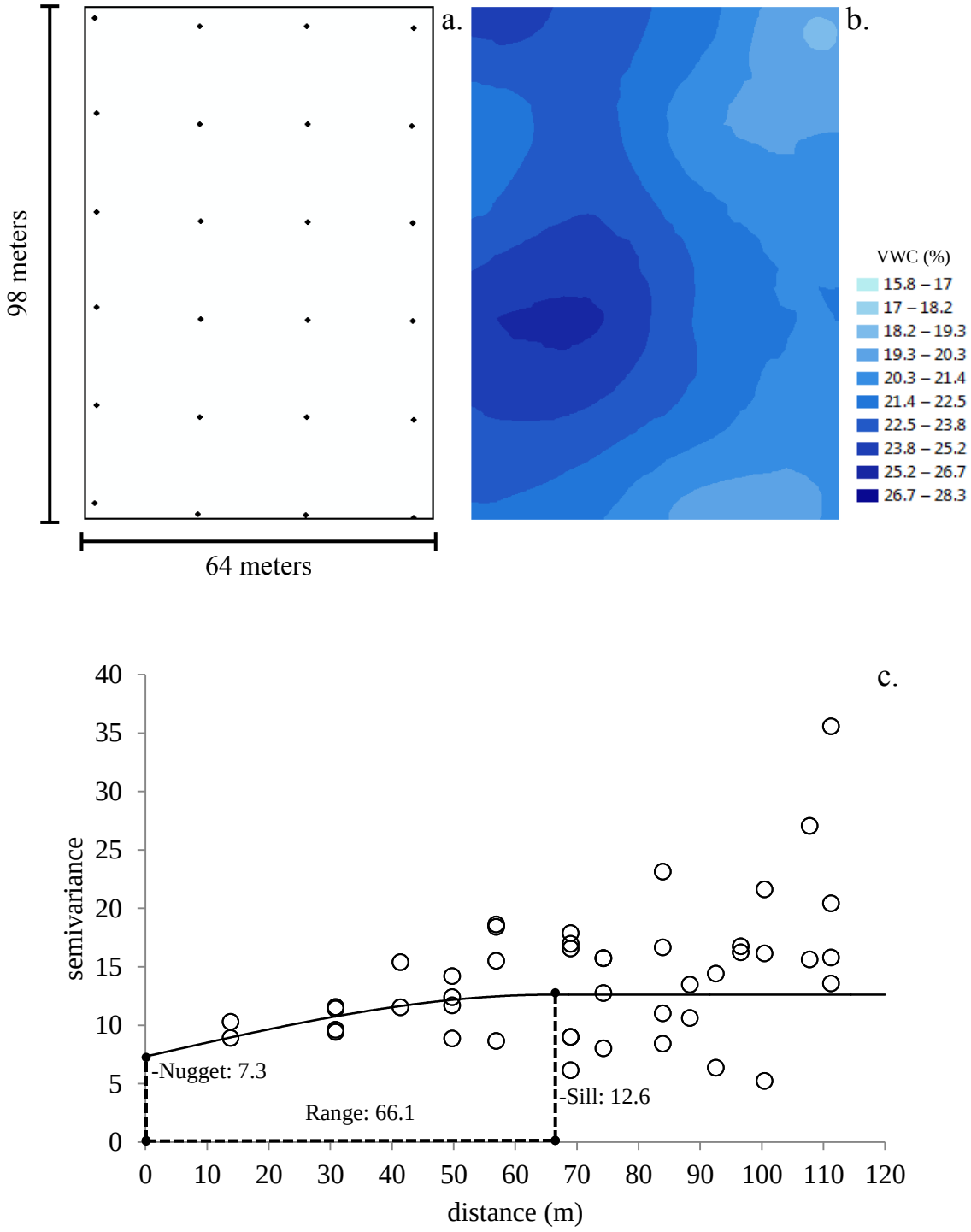


Figure 2.31. (a) Sampling locations (approximately 19.2 m x 19.2 m grid; 24 samples), (b) kriged prediction map and (c) semivariogram including the fitted spherical model of percent volumetric water content (%VWC) on Watkinsville field 1.

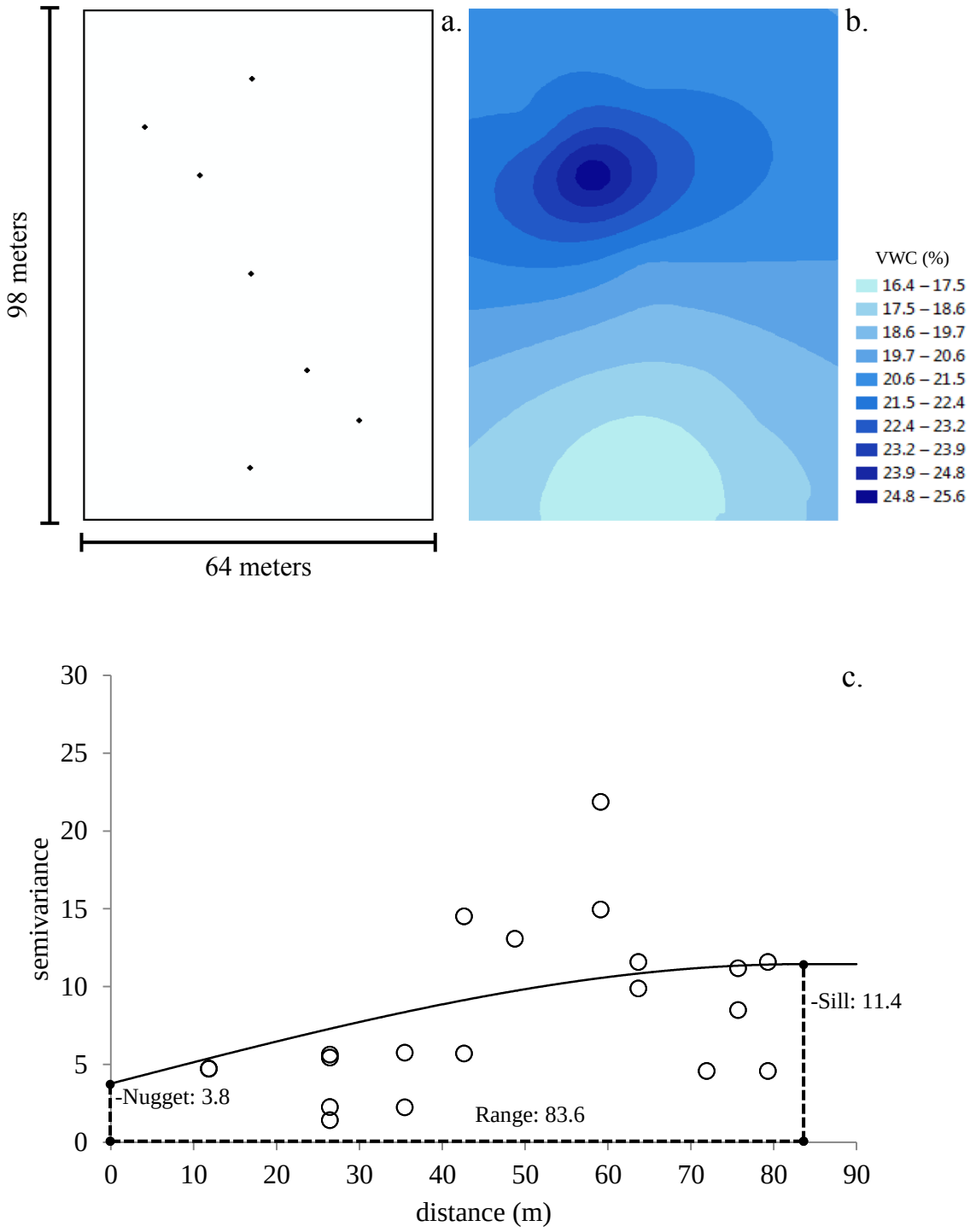


Figure 2.32. (a) Sampling locations (7 samples), (b) kriged prediction map and (c) semivariogram including the fitted spherical model of percent volumetric water content (%VWC) on Watkinsville field 1.

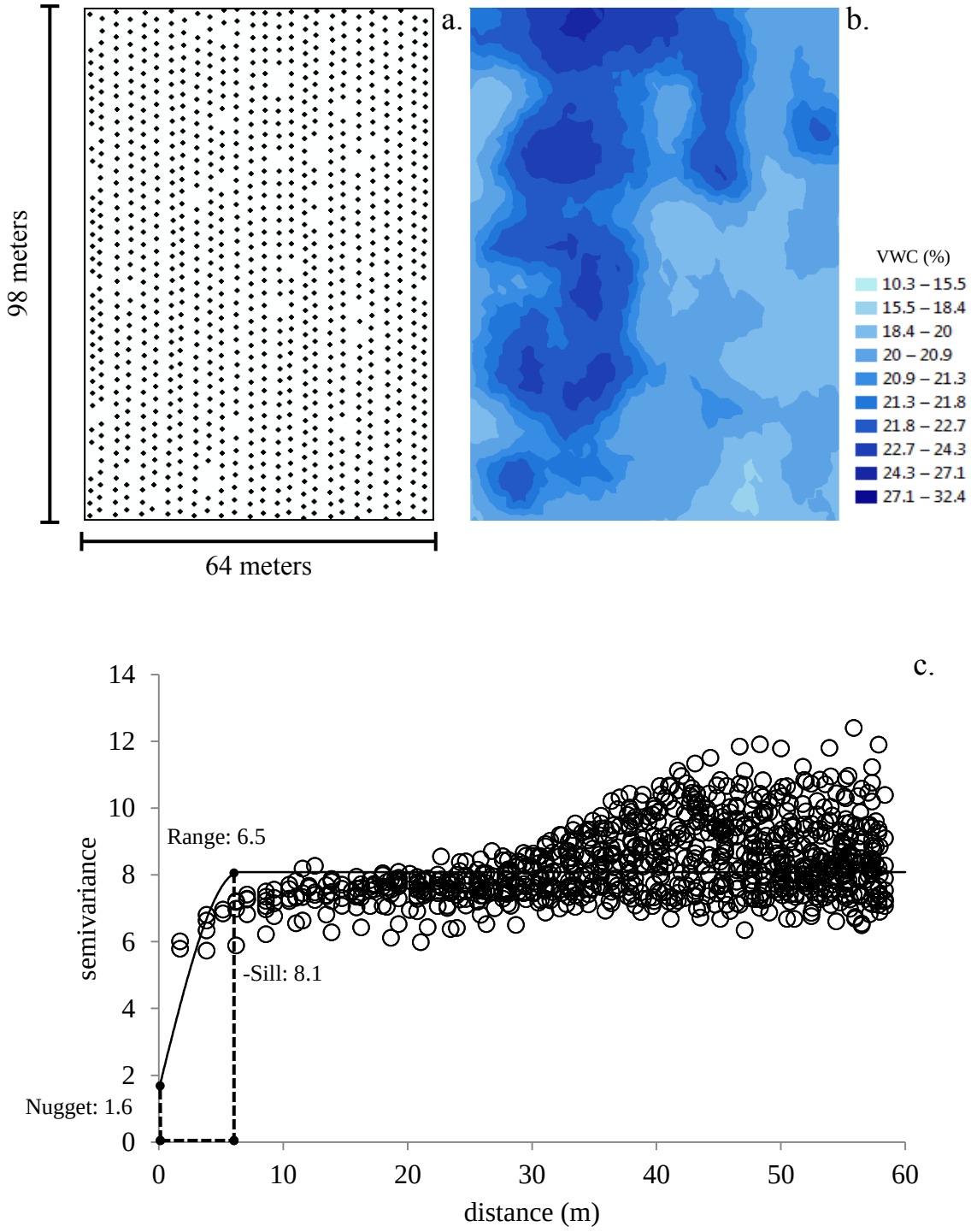


Figure 2.33. (a) Sampling locations (approximately 2.4 m x 2.4 m grid; 1053 samples), (b) kriged prediction map and (c) semivariogram including the fitted spherical model of percent volumetric water content (%VWC) on Watkinsville field 2.

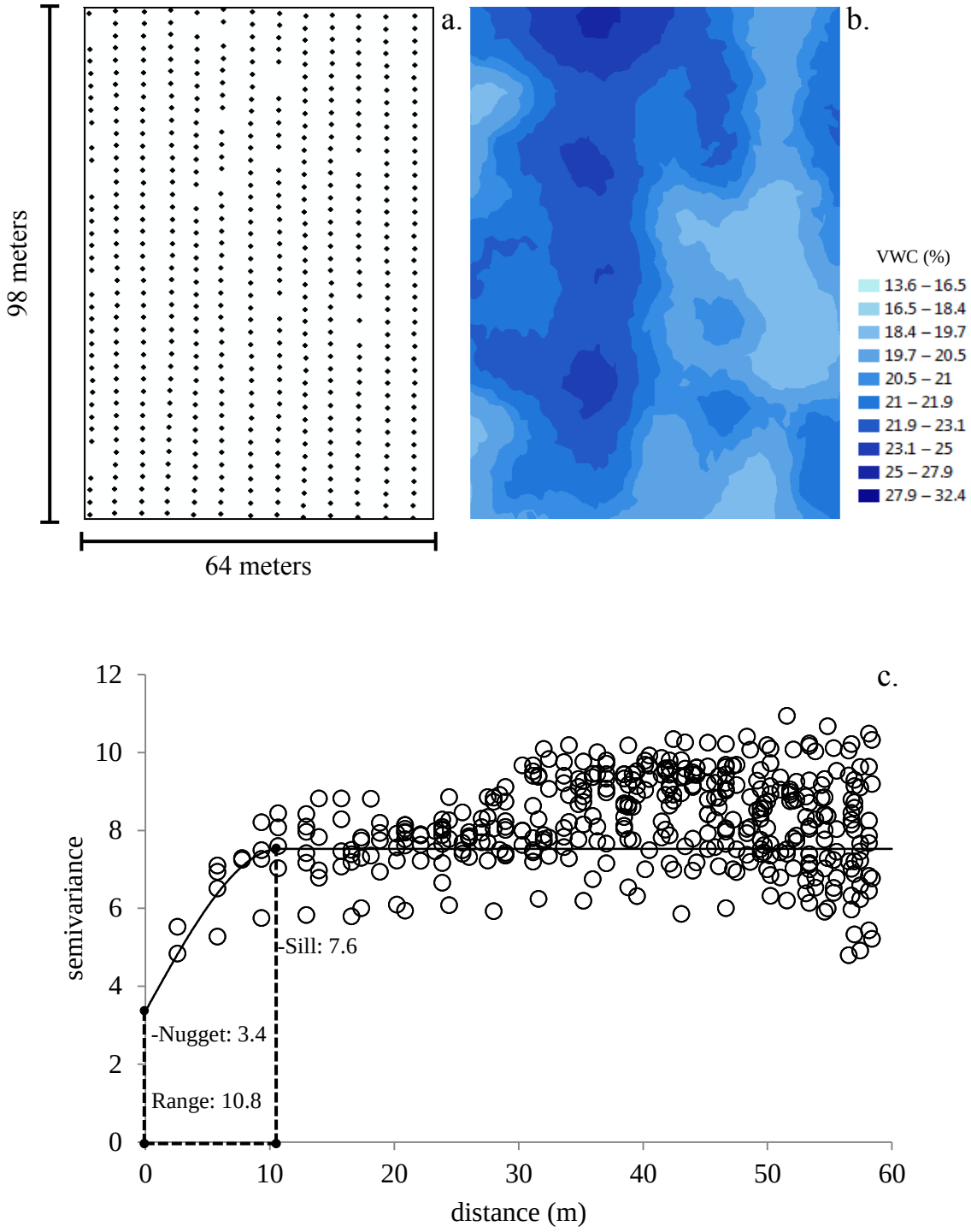


Figure 2.34. (a) Sampling locations (approximately 4.8 m x 2.4 m grid; 526 samples), (b) kriged prediction map and (c) semivariogram including the fitted spherical model of percent volumetric water content (%VWC) on Watkinsville field 2.

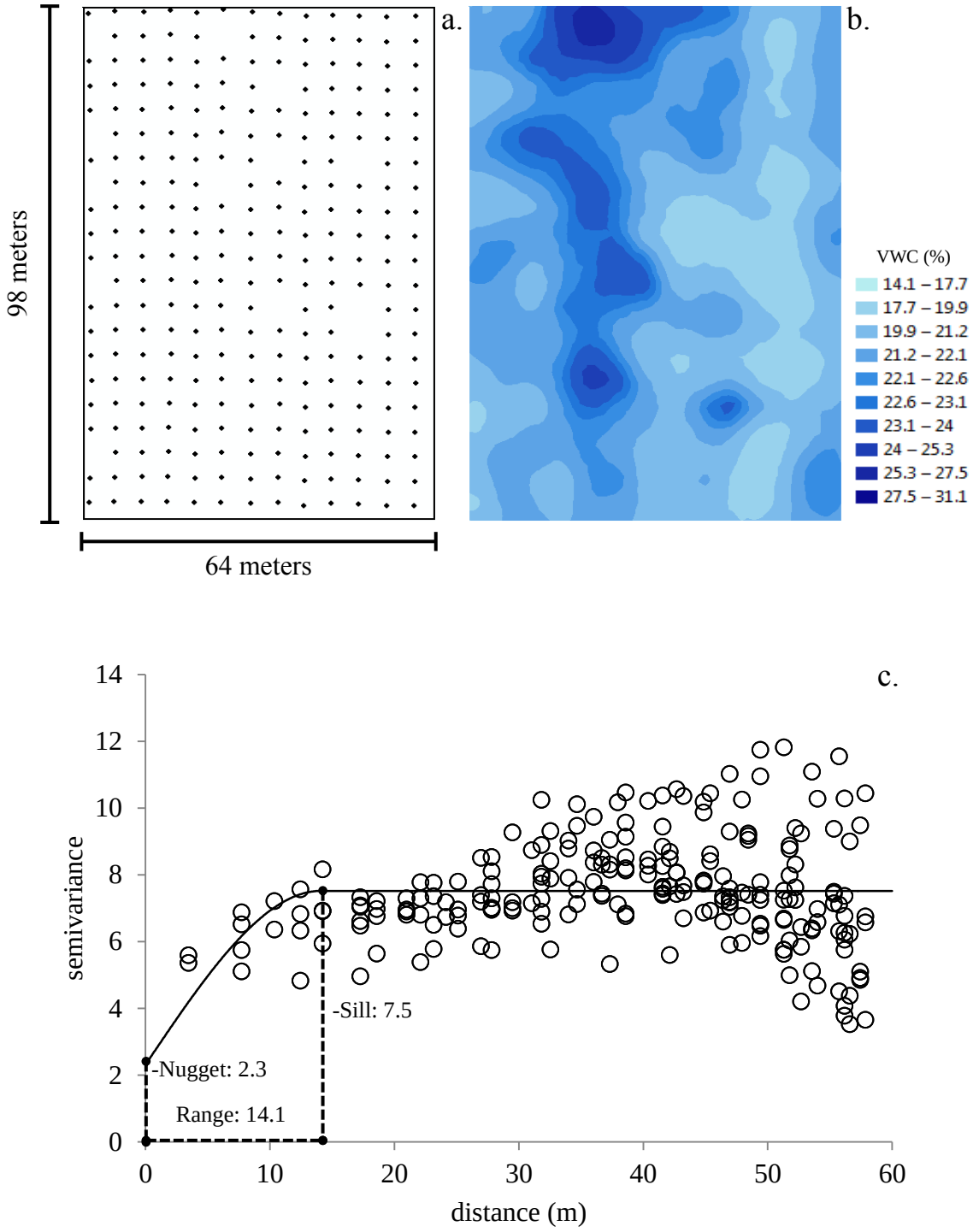


Figure 2.35. (a) Sampling locations (approximately 4.8 m x 4.8 m grid; 260 samples), (b) kriged prediction map and (c) semivariogram including the fitted spherical model of percent volumetric water content (%VWC) on Watkinsville field 2.

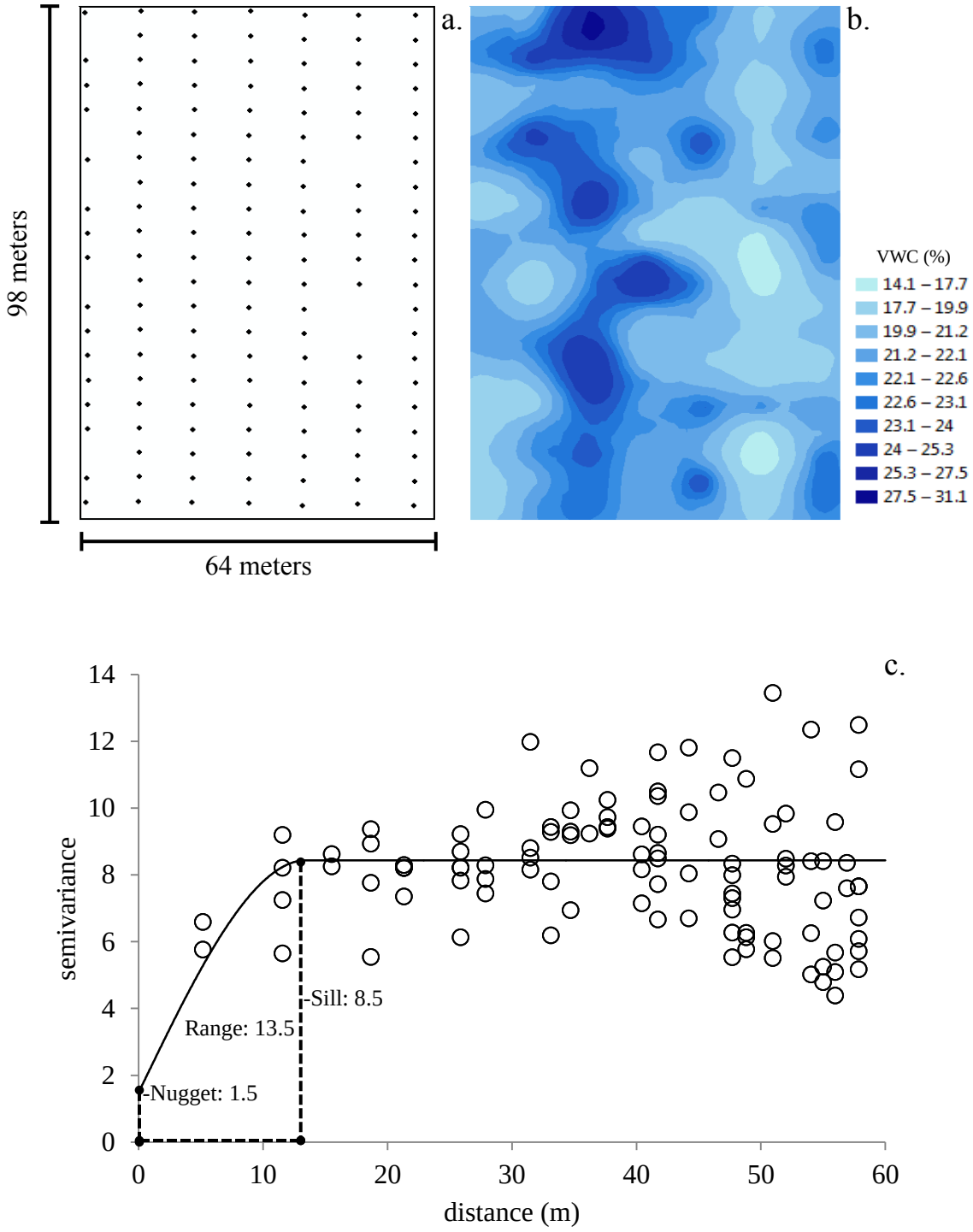


Figure 2.36. (a) Sampling locations (approximately 9.6 m x 4.8 m grid; 139 samples), (b) kriged prediction map and (c) semivariogram including the fitted spherical model of percent volumetric water content (%VWC) on Watkinsville field 2.

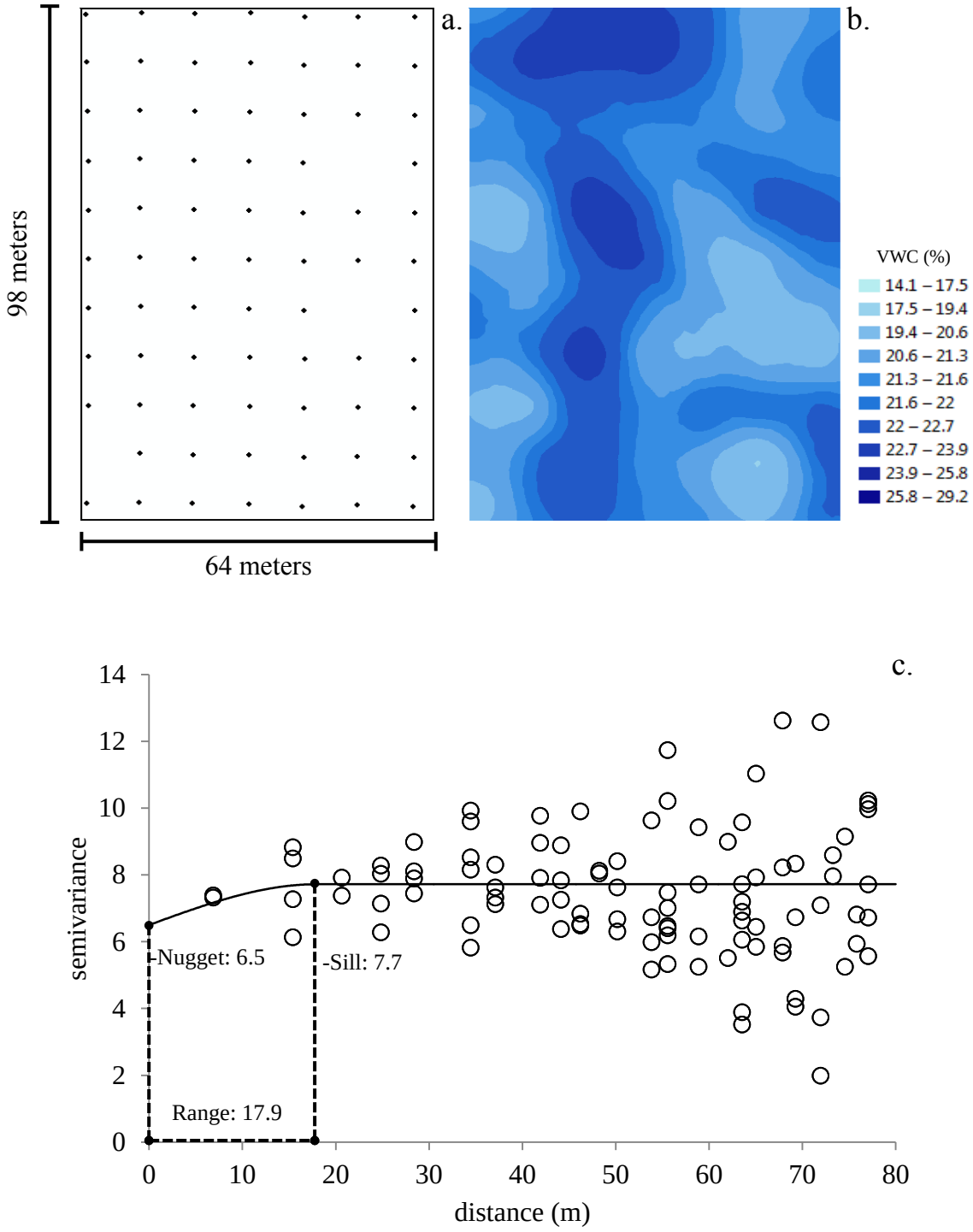


Figure 2.37. (a) Sampling locations (approximately 9.6 m x 9.6 m grid; 74 samples), (b) kriged prediction map and (c) semivariogram including the fitted spherical model of percent volumetric water content (%VWC) on Watkinsville field 2.

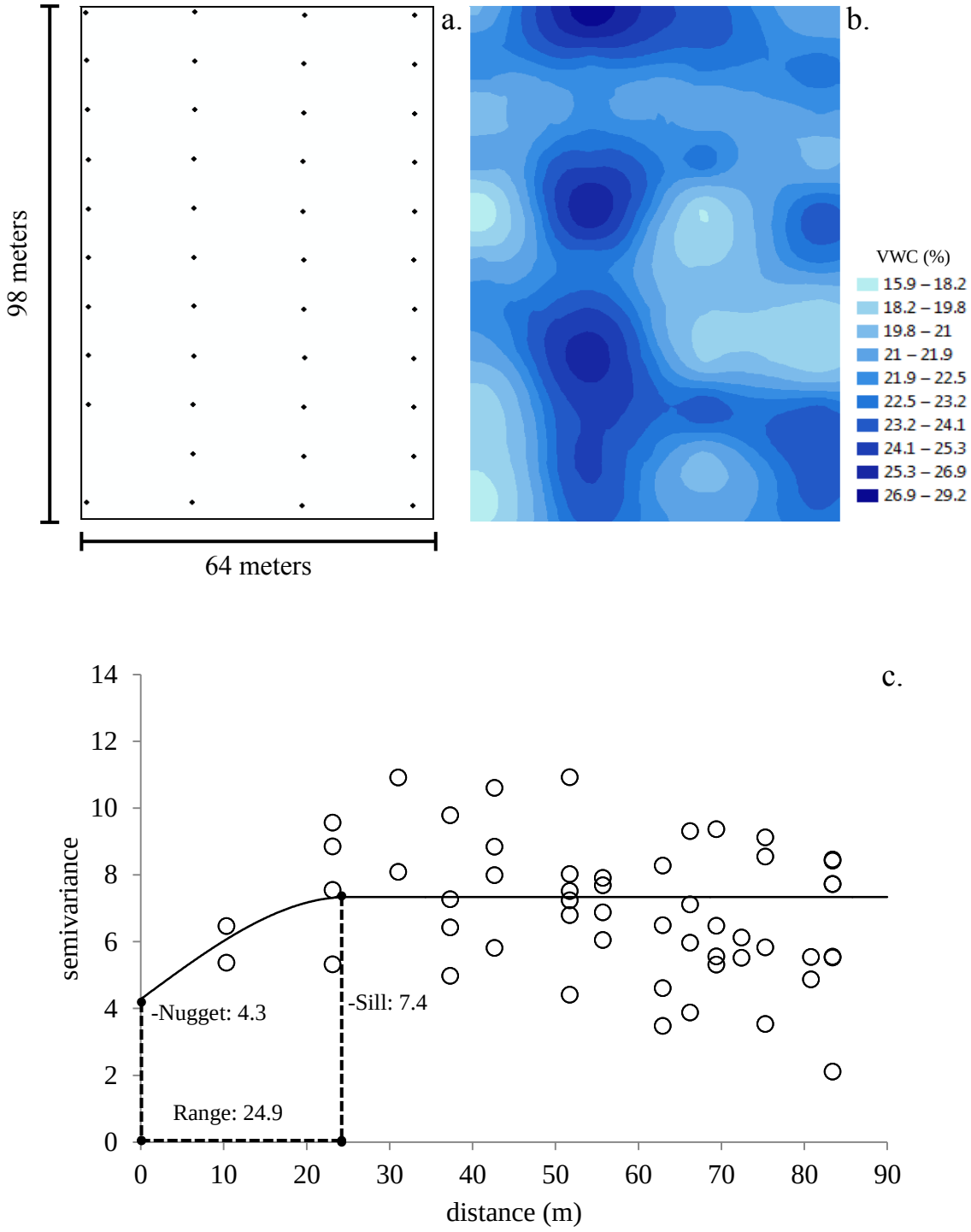


Figure 2.38. (a) Sampling locations (approximately 19.2 m x 9.6 m grid; 43 samples), (b) kriged prediction map and (c) semivariogram including the fitted spherical model of percent volumetric water content (%VWC) on Watkinsville field 2.

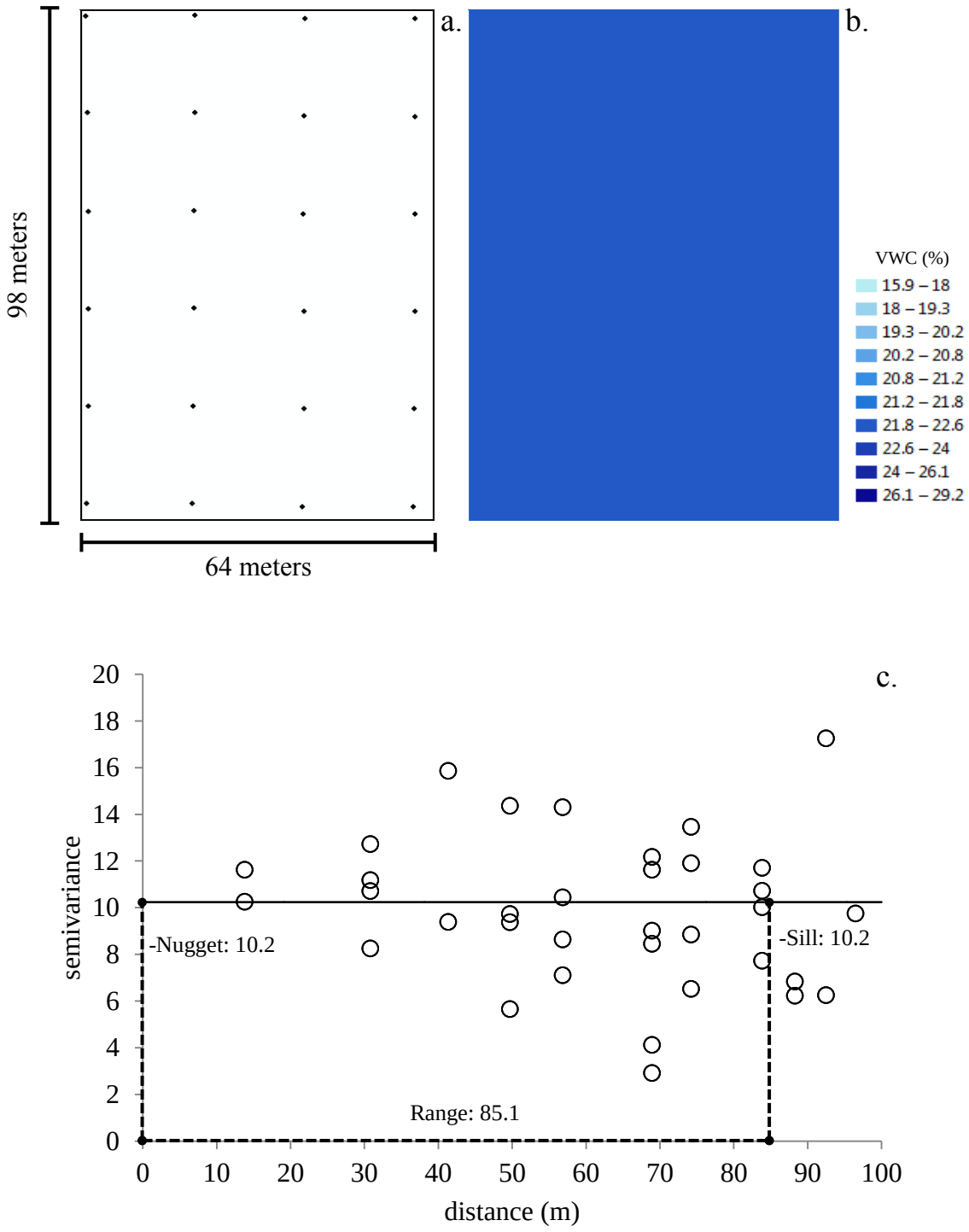


Figure 2.39. (a) Sampling locations (approximately 19.2 m x 19.2 m grid; 24 samples), (b) kriged prediction map and (c) semivariogram including the fitted spherical model of percent volumetric water content (%VWC) on Watkinsville field 2.

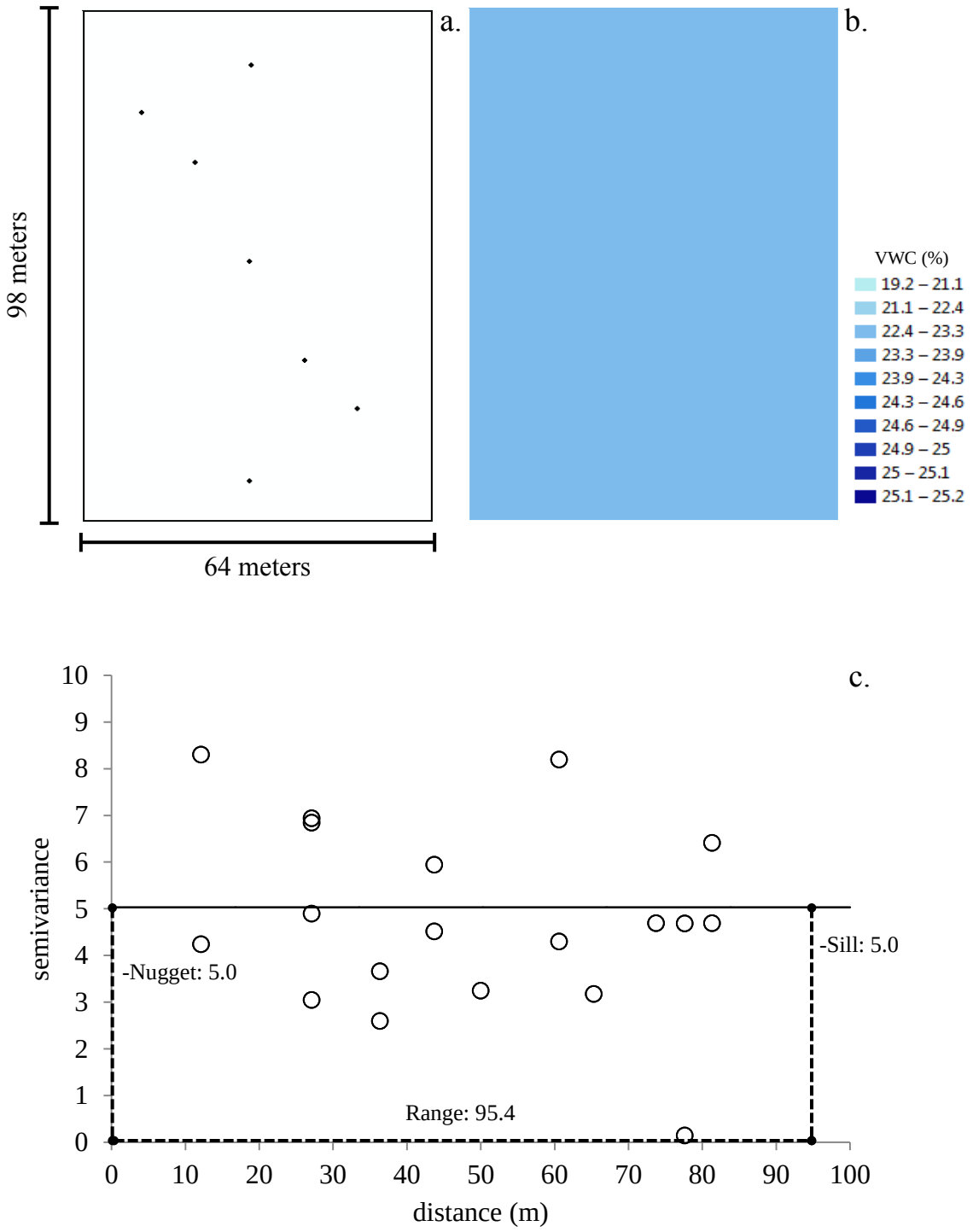


Figure 2.40. (a) Sampling locations (7 samples), (b) kriged prediction map and (c) semivariogram including the fitted spherical model of percent volumetric water content (%VWC) on Watkinsville field 2.

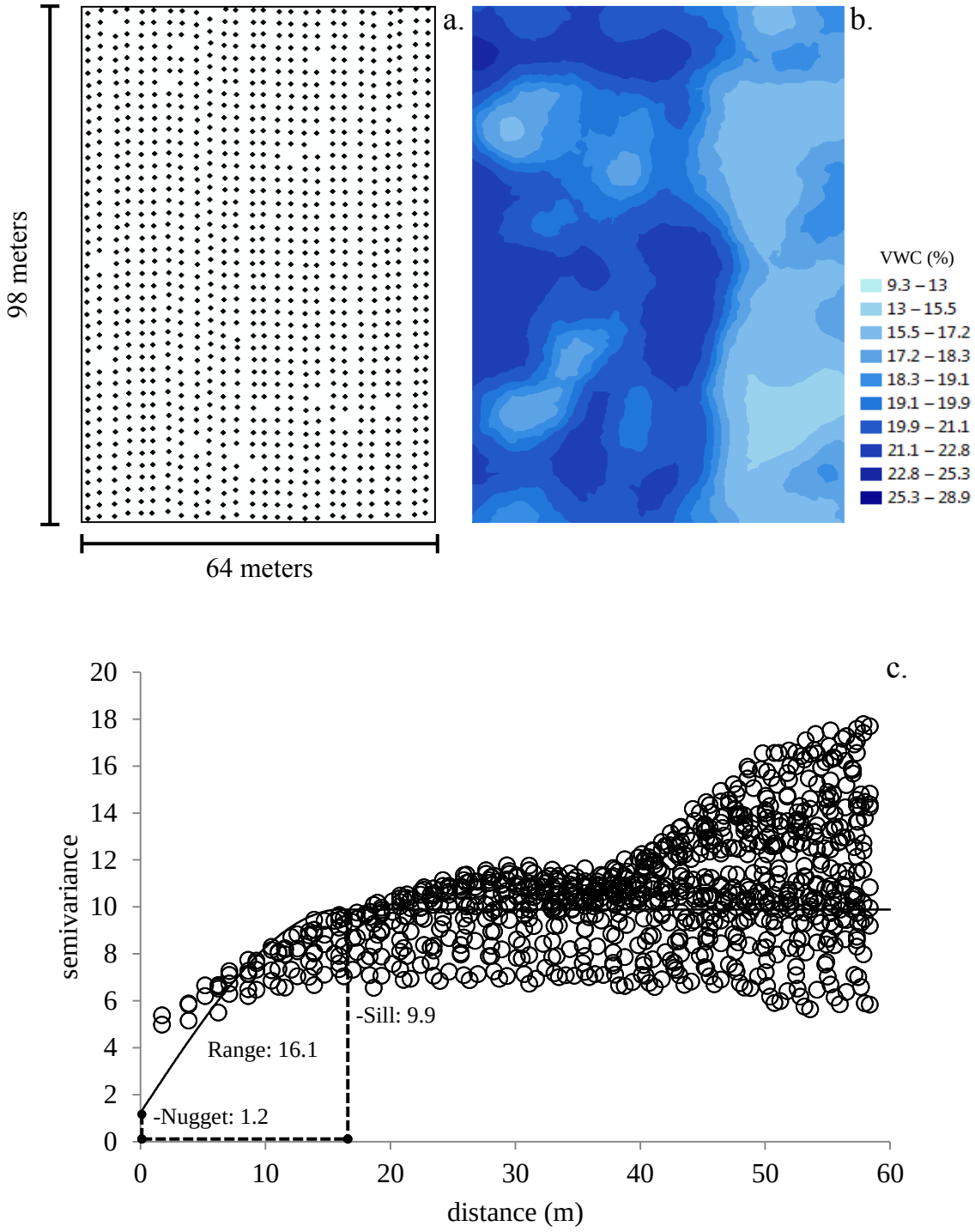


Figure 2.41. (a) Sampling locations (approximately 2.4 m x 2.4 m grid; 1101 samples), (b) kriged prediction map and (c) semivariogram including the fitted spherical model of percent volumetric water content (%VWC) on Watkinsville field 3.

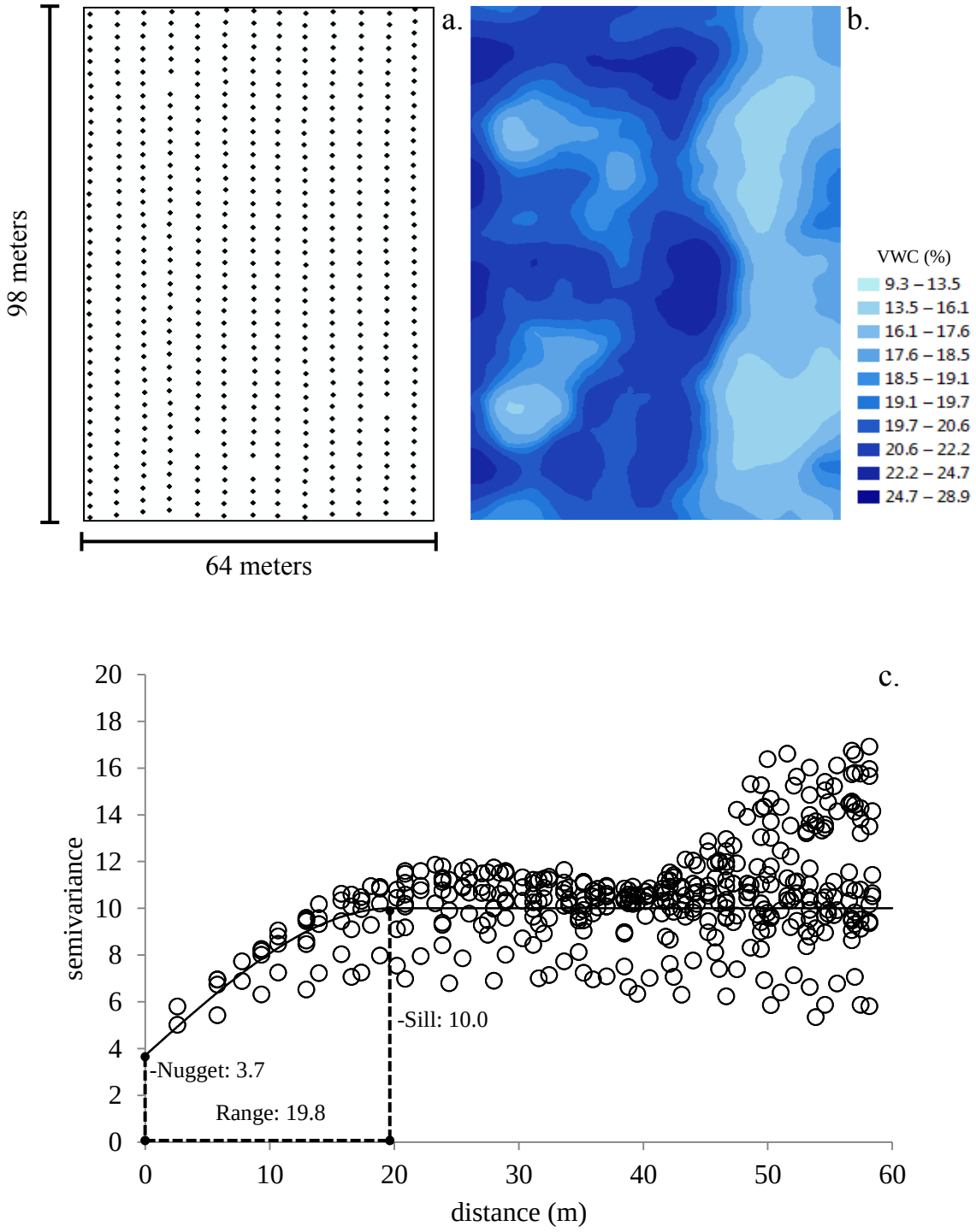


Figure 2.42. (a) Sampling locations (approximately 4.8 m x 2.4 m grid; 555 samples), (b) kriged prediction map and (c) semivariogram including the fitted spherical model of percent volumetric water content (%VWC) on Watkinsville field 3.

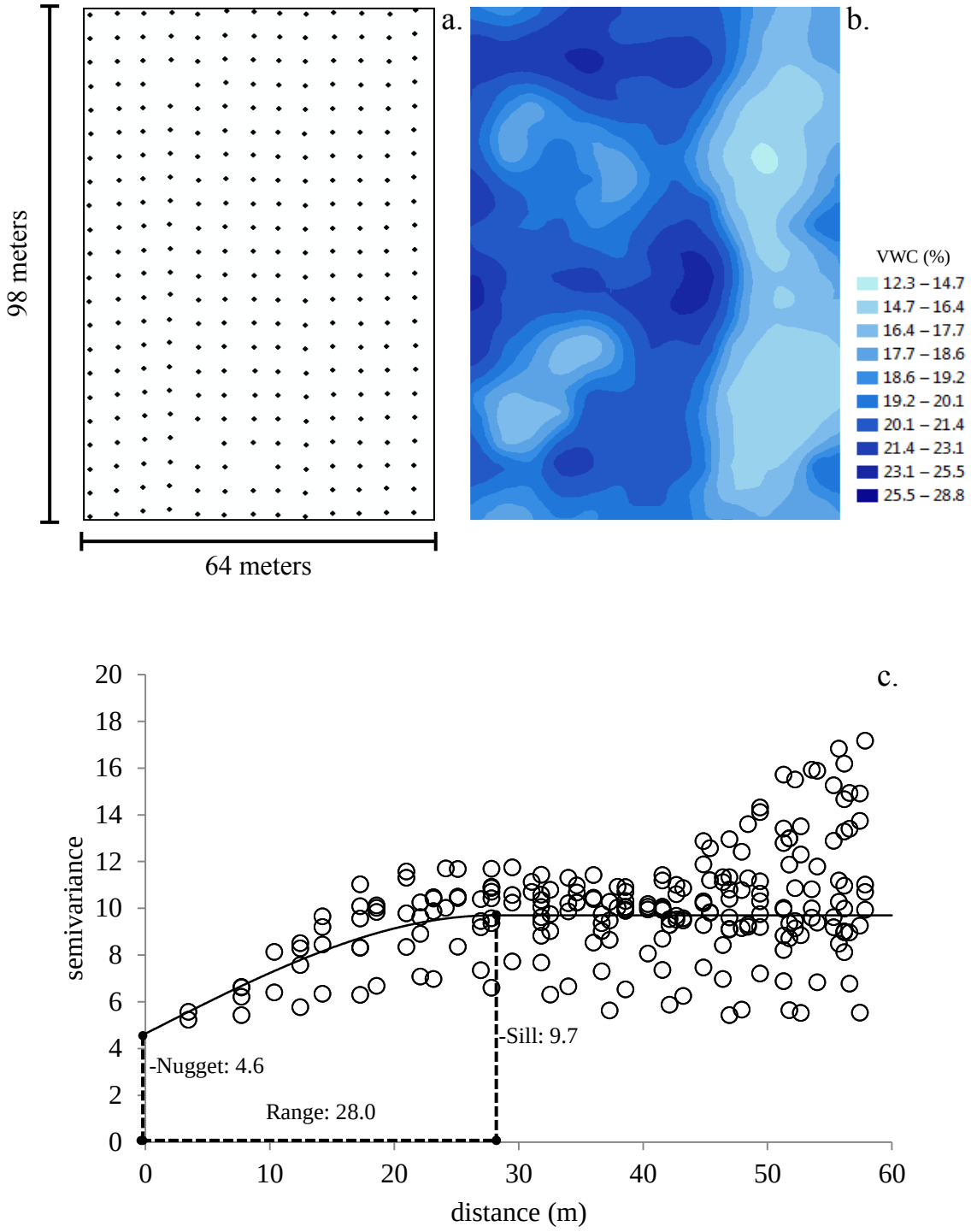


Figure 2.43. (a) Sampling locations (approximately 4.8 m x 4.8 m grid; 282 samples), (b) kriged prediction map and (c) semivariogram including the fitted spherical model of percent volumetric water content (%VWC) on Watkinsville field 3.

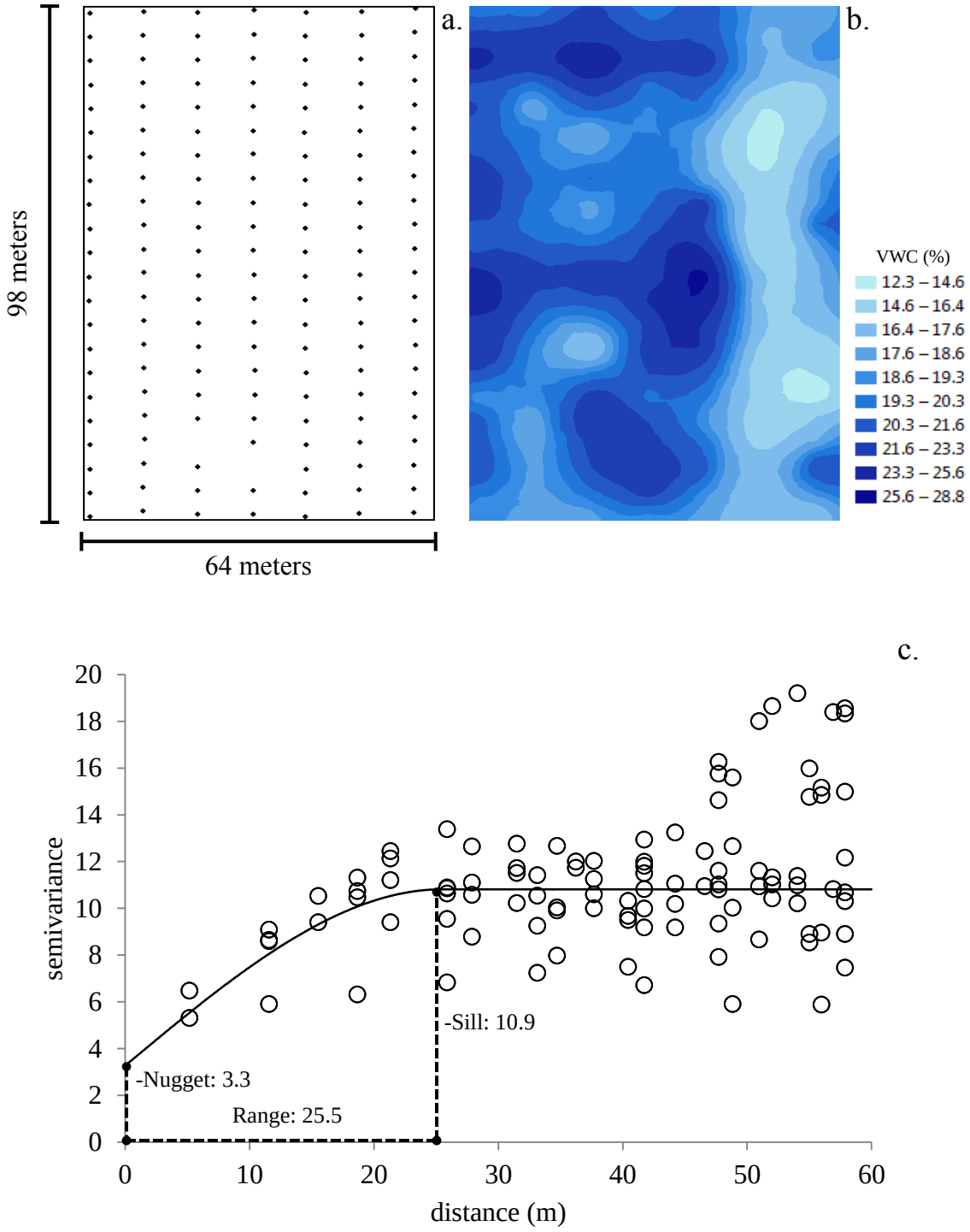


Figure 2.44. (a) Sampling locations (approximately 9.6 m x 4.8 m grid; 152 samples), (b) kriged prediction map and (c) semivariogram including the fitted spherical model of percent volumetric water content (%VWC) on Watkinsville field 3.

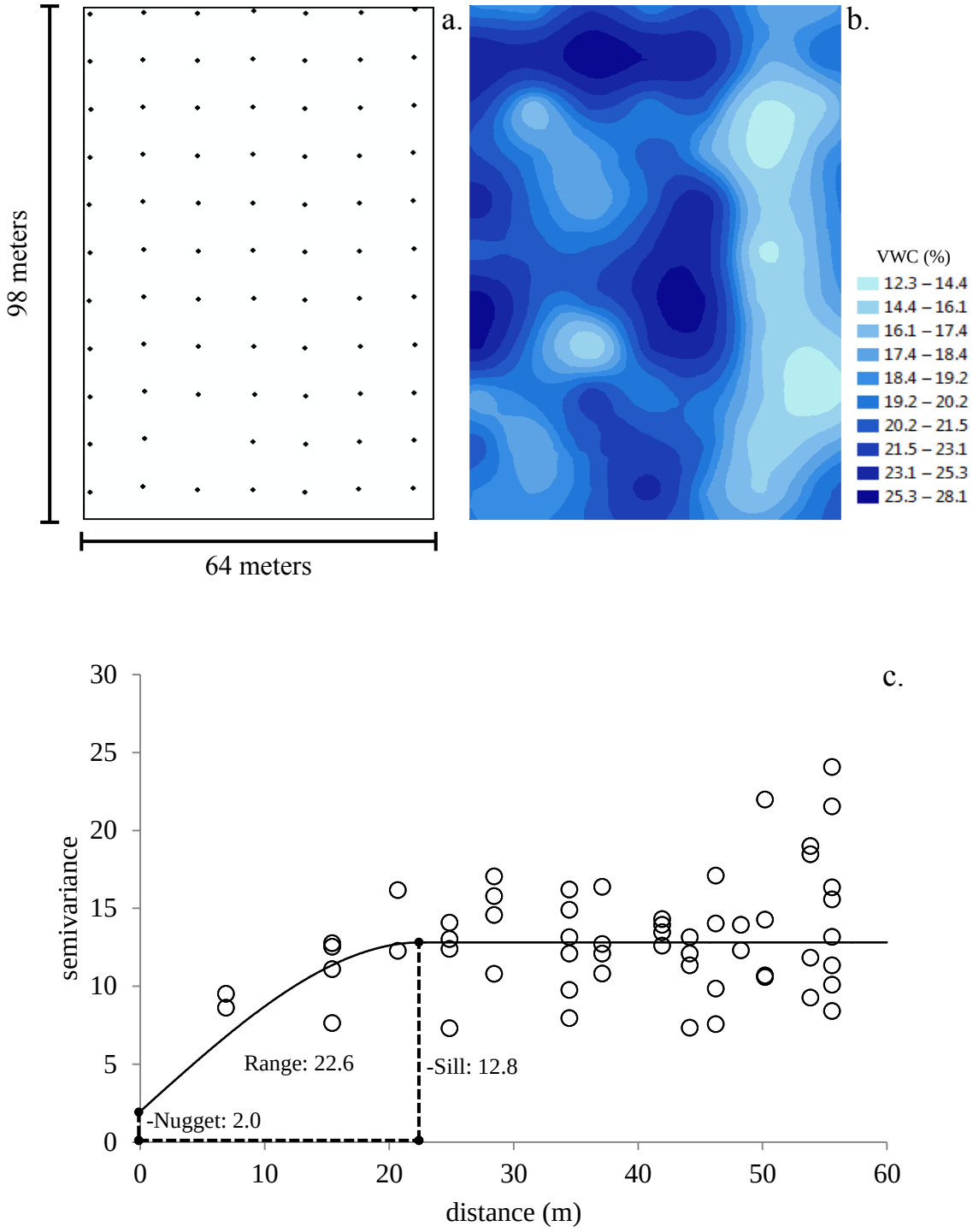


Figure 2.45. (a) Sampling locations (approximately 9.6 m x 9.6 m grid; 76 samples), (b) kriged prediction map and (c) semivariogram including the fitted spherical model of percent volumetric water content (%VWC) on Watkinsville field 3.

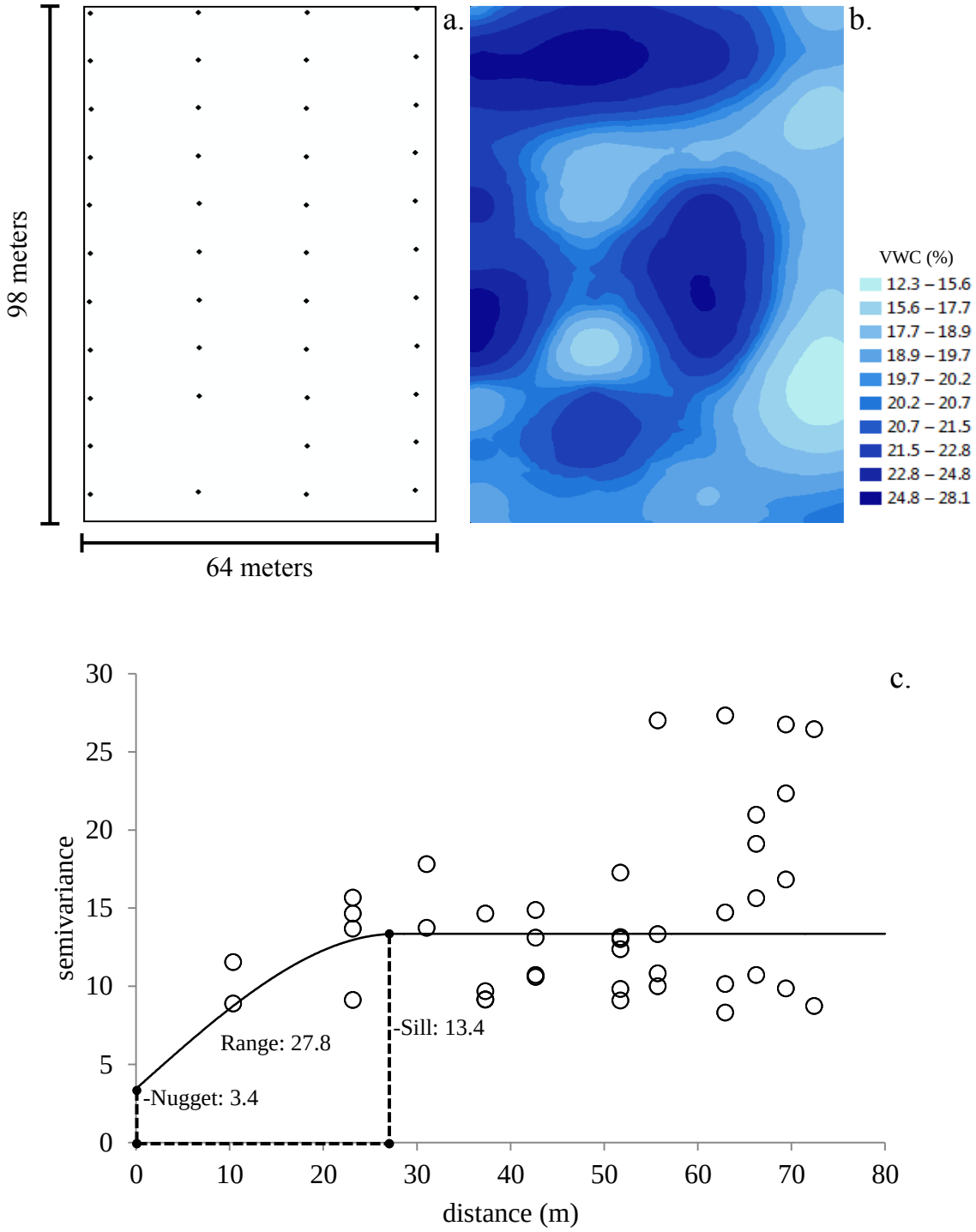


Figure 2.46. (a) Sampling locations (approximately 19.2 m x 9.6 m grid; 43 samples), (b) kriged prediction map and (c) semivariogram including the fitted spherical model of percent volumetric water content (%VWC) on Watkinsville field 3.

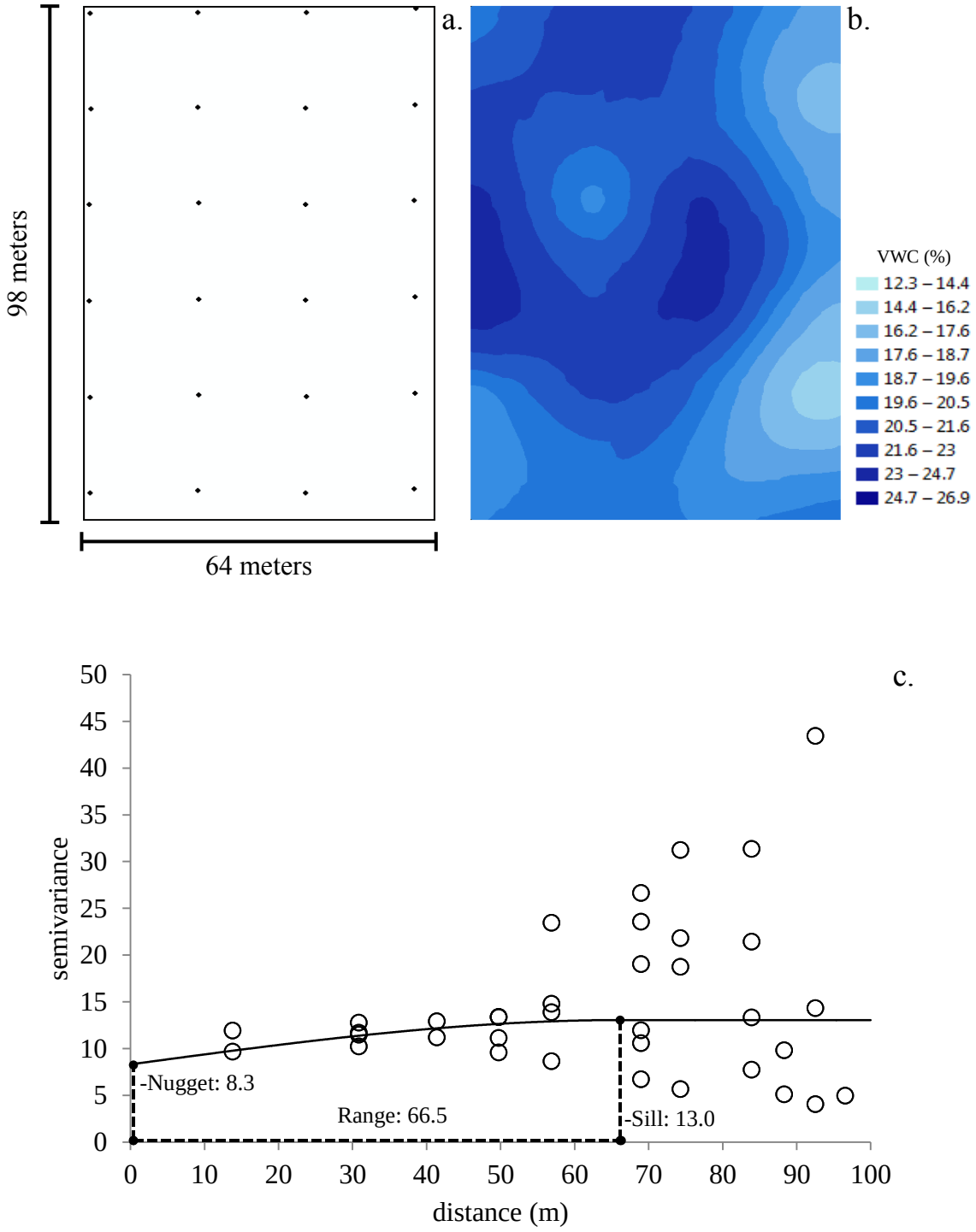


Figure 2.47. (a) Sampling locations (approximately 19.2 m x 19.2 m grid; 24 samples), (b) kriged prediction map and (c) semivariogram including the fitted spherical model of percent volumetric water content (%VWC) on Watkinsville field 3.

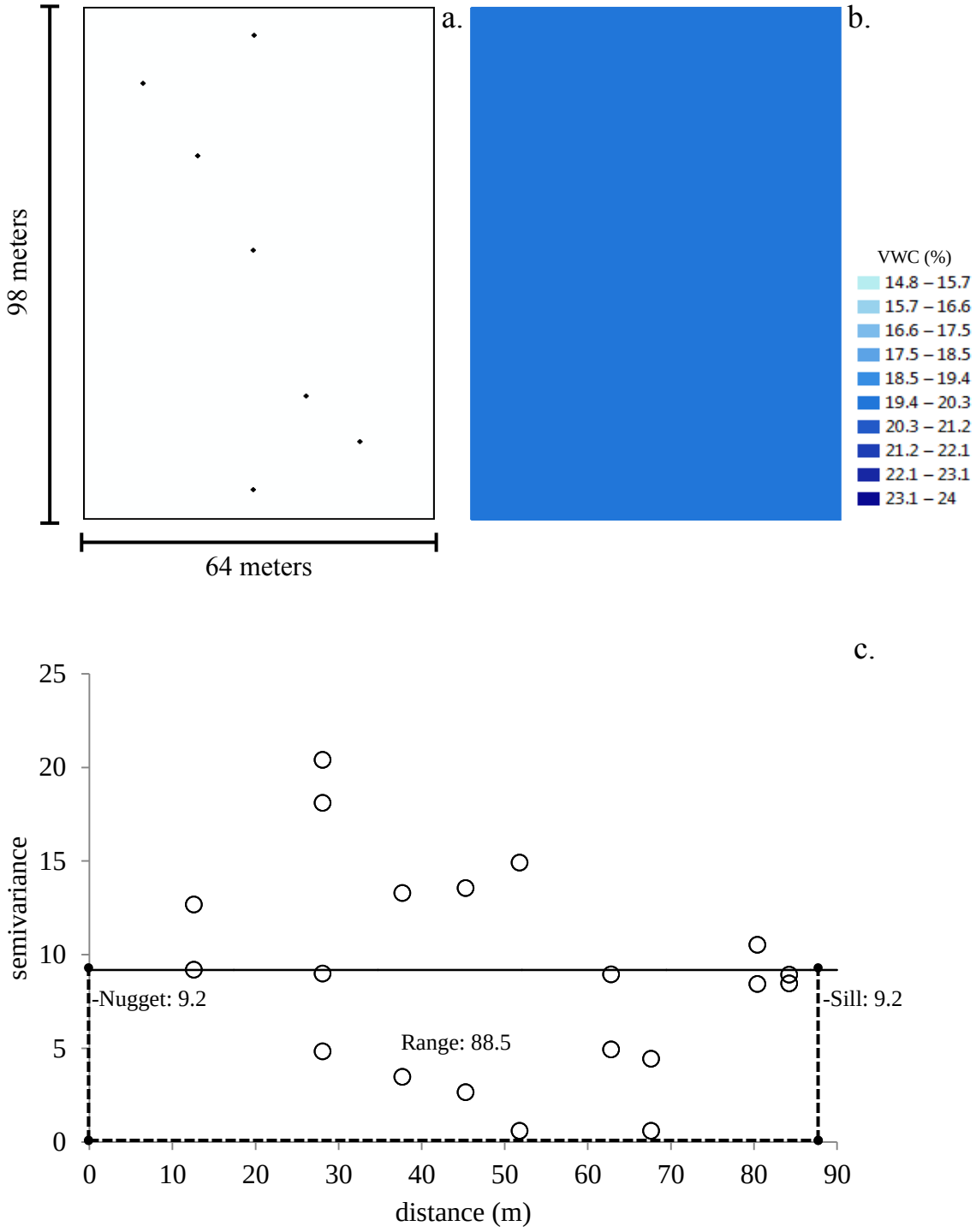


Figure 2.48. (a) Sampling locations (7 samples), (b) kriged prediction map and (c) semivariogram including the fitted spherical model of percent volumetric water content (%VWC) on Watkinsville field 3.

# CHAPTER 3

# EVALUATION OF SAMPLING PROCEDURES FOR SPATIAL ANALYSIS OF SOIL COMPACTION ON SPORTS FIELDS[1]

[1] Straw, C.M., G.M. Henry, R.N. Carrow, V. Cline. To be submitted to *Crop Science.*

Abstract

Foot traffic from game play is the primary cause of soil compaction on natural turf sports fields. Soil compaction causes an overall decline in growth, vigor, quality, and turf persistence and also effects multiple player-surface and ball-surface interactions. The term "performance testing" is a method to quantify the surface and edaphic properties of sports fields, such as soil compaction. Previous procedures have used handheld devices to collect data from minimal locations (6-12). The low number of samples restricts analysis of variability over the entire area. Geostatistics is a branch of statistics that uses semivariograms and interpolation, generated from intense data sampling, for analysis of a given variable in space. The Toro Precision Sense 6000 (PS6000), a mobile multi-sensor device with Global Positioning System (GPS) capability, has recently been introduced for use on turfgrass sites. The PS6000's ability for rapid sampling and geo-referenced data allows for the use of geostatistical methods to conduct spatial analysis. However, there is limited research of sampling procedures or protocols for use on sports fields. The PS6000 was used to measure penetration resistance on three 'Tifway 419' hybrid bermudagrass (*Cynodon dactylon* x *C. transvaalensis*) sports fields in Roswell, Georgia and three 'TifSport' hybrid bermudagrass sports fields in Watkinsville, Georgia during the summer of 2013. Various levels of sample grid sizes were manipulated, using Geographic Information System (GIS) software, from the initial 2.4 m x 2.4 m sample grid. Spatial analysis of penetration resistance was conducted on all sample sizes and compared within each field to evaluate an appropriate sampling procedure. In general, as the sample grid size became larger, the strength of the semivariograms and accuracy of the surface maps minimized. A minimal sample grid size of 9.6 m x 4.8 m was determined, with subsequently decreasing sample grid sizes providing a more accurate and detailed site-specific analysis.

## Introduction

Natural turf sports field managers aspire to produce homogeneous playing conditions with consistent surface and edaphic properties across the entire area (Caple et al., 2012). Foot traffic from game play is considered the major stress of natural turf sports fields (Madison, 1971). The term traffic is general in nature and includes both wear and soil compaction stresses (Carrow and Petrovic, 1992). Wear is the injury to a turf from pressure, scuffing, or tearing on turfgrass tissues (Carrow and Petrovic, 1992). Soil compaction is defined as the pressing together of soil particles, resulting in a more dense soil mass with less pore space (Beard, 1973). Soil compaction causes an overall decline in growth, vigor, quality, and turf persistence by influencing soil aeration, soil strength, and plant and soil moisture relationships (Madison, 1971). Furthermore, a strong correlation has been observed between surface hardness and soil compaction in turf (Baker, 1991), which is particularly important, from a player's perspective, to cover the conditions of player-surface impact that relate to running, falling, and injury prevention (Baker and Canaway, 1993). Additionally, ball-surface interactions, such as ball bounce and ball roll, have been significantly correlated with surface hardness (Holmes and Bell, 1986; Baker, 1991).

An integrated approach comprised of several techniques, including primary cultural practices such as mowing, fertilization, irrigation, and cultivation, is needed to combat stresses from foot traffic. Aerification is one of the more important cultivation practices on a sports field and is the process of making holes in the turfgrass canopy, through removal of soil cores. Although not essential for turf growth, aerification is primarily used to stimulate root growth, increase water infiltration, and relieve soil compaction (Turgeon, 2011). The magnitude and frequency of temporal variations in soil compaction are challenging to control because of

dependency on traffic (Baker, 1991) Therefore, it is necessary to evaluate soil compaction for player safety (i.e. player-surface interactions) and field playability (i.e. ball-surface interactions), as well as assist in management decisions to reduce inputs (such as aerification) (Carrow et al., 2010).

The term "performance testing" (i.e. site assessment) is receiving increasing attention as a procedure to quantify the performance of surface and edaphic properties on sports fields (McAuliffe, 2008; Bartlett et al., 2009; Stiles et al., 2009; Carrow et al., 2010). Performance testing involves collecting data samples at multiple locations across a field to better understand the variability of the property of interest. Soil compaction has been measured using multiple techniques, but the most common and simplest method is the use of a penetrometer device (Holmes and Bell, 1986; Bengough et al., 2000; Flitcroft et al., 2010; Caple et al., 2012). There are various forms of penetrometers available and most allow for data to be obtained in a reasonable time. A penetrometer uses a cylindrical tip (also referred to as a "cone") of a certain length to measure the penetration resistance of the soil at a certain depth (i.e. the force it takes to insert the cone into the soil to a specific depth) (Holmes and Bell, 1986). Higher penetration resistance values would indicate a more compacted soil.

Minimal standards have been established to identify sampling locations to conduct performance tests on sports fields. One procedure is the American Society for Testing and Materials (ASTM) F1936, which identifies 10 test locations to measure surface hardness across a field (ASTM, 2010). The Performance Quality Standards (PQS) provides test procedures for a wide range of parameters; however a direct method for measuring soil compaction in the field is not available (Institute of Groundsmanship (IOG), 2014). Researchers that have evaluated soil compaction on sports fields have collected samples from only 6-12 locations (Holmes and Bell,

1986; Bell and Holmes, 1988; McClements and Baker, 1994). Summary statistics (mean, min, max, standard deviation, etc.) are the primary determinate of central tendency and variability for the data in these procedures. However, performance properties can vary significantly across an area due to dynamic interactions of use, management, climate, plant, and soil factors (Taylor et al., 2007). Thus, the low number of sample locations restricts detailed analysis and may mask variability of the property.

Variability of a property in space is better explained using geostatistics. Geostatistics provides a number of statistical techniques to evaluate spatial data which has been utilized in environmental science fields such as mineral resource mapping and precision agriculture (James and Goodwin, 2003; Taylor et al., 2003; Emery and González, 2007). Global Positioning Systems (GPS) enable the data to be geo-referenced (i.e. record of longitudinal and latitudinal location) and imported into Geographic Information Systems (GIS) where geostatistics can be implemented.

Specifically, two geostatistical techniques, variograms and interpolation, are commonly used. A variogram (also referred to as semivariogram) is a function of the distance and direction separating measured points used to quantify the spatial autocorrelation (also referred to as spatial dependence) of the data set (ESRI, 2004). The semivariogram represents half the difference squared of the values between each pair of points (i.e. semivariance) at different distances then fits a model to the empirically derived data points (Webster and Oliver, 2007).

It is important to note that the most determining factor for an accurate semivariogram, and the one in which we have the most control over, is the sample size that it is based on (Oliver and Webster, 2014). Typically, the more data you have the greater the accuracy. Oliver and Webster (2014) demonstrated, from repeated grid sampling of a large two-dimensional simulated

field, that confidence intervals narrow as the number of data samples increases and the distance between the data samples decreases. They concluded that semivariograms generated from fewer than 100 data samples were unreliable.

Secondly, interpolation creates continuous surface maps of the data for visual assessment. To do so, predictions are made for locations in the study area based on the semivariogram and spatial arrangement of measured values that are nearby (ESRI, 2004). Kriging is a common interpolation method that forms weights from surrounding measured values to predict values at unmeasured locations (ESRI, 2004). With kriging interpolation, the closest measured values have the most influence on weights. Much like the semivariogram, sample size can greatly influence the accuracy and detail of a kriged surface map.

GIS is more common in agriculture to implement the precision agriculture (PA) concept (Rhoades, 1999; Corwin and Lesch, 2005; Thomsen et al., 2007). PA involves applying inputs, such as cultivation, water, and fertilizers, only where, when, and in the amount needed (Bouma et al., 1999; Corwin and Lesch, 2005; Bullock et al., 2007). As a parallel to PA, the concept of precision turfgrass management (PTM) is gaining increasing attention for enhanced input efficiency and management decisions in turfgrass (Stowell and Gelernter, 2008; Carrow et al., 2007; Bell and Xiong, 2008; Krum, 2008; Carrow et al., 2010; Krum et al., 2010). PTM was developed and based on the premise of site-specific management. To a certain degree, complex turf sites already use some degree of PTM. For example, on sports fields, management can differ significantly depending on turf species, soil class, field usage, level of sport, and the sport itself being played. However, the evolution of PTM is based on acquiring detailed site information by intensive data sampling to offer an even more precise and efficient management of inputs, such

as sub-areas within a sports field, than is currently practiced now (Carrow et al., 2010). Performance testing can be viewed as the site assessment referred to in the PTM concept.

To date, only Miller (2004), Freeland et al. (2008), and most recently Caple et al. (2012), have used geostatistical methods to analyze spatial variability of surface and edaphic properties on natural turf sports fields. Research by Miller (2004) evaluated surface hardness of two soccer fields with different soil textures (one sand and one native soil) using a grid pattern to collect 80 samples per field with a Clegg Impact Soil Tester (Jolimont, Western, Australia). Freeland et al. (2008) used ground penetrating radar (GPR) towed behind an electric golf cart to assess a rapid survey method for mapping soil compaction on a collegiate football field. Caple et al. (2012) conducted a more robust spatial analysis on multiple properties using handheld devices. Soil compaction, along with volumetric water content (VWC), traction, surface hardness, and surface energy absorption were evaluated on three sports fields of different soil textures at the beginning, middle, and end of the season using 135 or 150 samples. However, handheld devices have been deemed timely, costly, and labor intensive for such extensive sampling.

In agriculture, mobile platforms, with built in sensors, have been developed for efficient sampling and more precise spatial analysis. These platforms primarily focus on obtaining spatial and temporal soil and plant data, such as soil moisture and plant performance (normalized difference vegetative index; NDVI) rapidly over large areas. In turfgrass, the Toro Precision Sense 6000 (PS6000) (The Toro Company, Bloomington, MN) was recently developed for rapid sampling on complex turfgrass sites. The PS6000 simultaneously measures soil compaction (penetration resistance; N in m kg $s^{-2}$), VWC (%), and NDVI (unit-less with best = 1.0) all while using GPS to geo-reference longitudinal and latitudinal location of samples.

Currently, Flitcroft et al. (2010) are the only researchers to utilize the PS6000 for spatial analysis of penetration resistance in turf. Their study conducted spatial mapping of penetration resistance to implement site-specific cultivation on one golf course fairway. Spatial analysis of soil compaction data on a sports field could also be beneficial for site-specific cultivation practices. Additionally, data could be used for coordinating game and practice schedules to spread out the level of foot traffic between multiple fields or certain areas on one field. Preventing continuous foot traffic in the same locations can decrease compaction levels and increase the quality and longevity of sports fields.

Mobile multi-sensor devices to conduct performance tests with spatial analysis have yet to be utilized on sports fields, but can be fundamental in developing a site-specific, comprehensive sports turf management program. Site-specific information is the first requirement of spatial analysis. To the author's knowledge, the PS6000 is the first and only mobile multi-sensor device, with GPS capability, for use on turfgrass sites. However, there are currently few available for use, thus limiting data collections to handheld devices in most instances. Furthermore, an efficient sampling procedure, using either methodology, has yet to be implemented for an accurate spatial analysis. Therefore, the primary objective of this study was to utilize the PS6000 to evaluate 7 different sample grid sizes, and a sample size of 7 locations resembling previous performance testing methods, to define an effective, science-based grid spacing for an accurate spatial analysis of penetration resistance on natural turf sports fields.

## Materials and Methods

### *Description of sports fields*

Research was conducted at the Grimes Bridge Soccer Complex in the city of Roswell, GA and at Oconee Veterans Park in Watkinsville, GA. A total of six community level sports

fields were used between the two locations. The Roswell location included three 'Tifway 419' hybrid bermudagrass (*Cynodon dactylon* x *C. transvaalensis*) soccer fields mowed two times a week at 2.54 cm with a reel mower. The Watkinsville location included three 'TifSport' bermudagrass soccer fields also mowed two times a week at 2.54 cm with a reel mower. All fields evaluated had sandy loam soils and field size ranged from 60-64 m x 95-104 m (Tables A-1 and A-2, Appendix).

Soccer was the primary sport played on all fields at both locations (Table A-1, Appendix). Fields in Roswell were constructed in tiers, with field 1 being at the top, field 2 in the middle, and field 3 below. Two concrete walls approximately 9.1 m and 3.0 m high separates fields 1 and 2, and fields 2 and 3, respectively. Field 1 is open to the public while fields 2 and 3 remain gated throughout the day and are solely used for scheduled practice and games. Fields in Watkinsville were designed in a flat open area (4.2 ha) and laid in close proximity to one another. Field 1 is directly north of field 3 with the south end zone of 1 being approximately 22.9 m from the north end zone of 3. Field 2 is centered approximately 22.9 m east of 1 and 3. All fields in Watkinsville are open to the public.

*Data collection*

Soil compaction data was collected in Roswell on 9 May, 2013 and in Watkinsville on 10 May, 2013 (Table A-1, Appendix). The PS6000 was used to measure the penetration resistance on all six fields. The PS6000 is a mobile multi-sensor device equipped to attach to the hitch of a utility vehicle. Measurements are made approximately every 2.4 m while traversing the field at a speed of 2.7 to 3.3 km $h^{-1}$. Passes downfield were made 2.4 m apart; therefore measurements were collected using an approximate 2.4 m x 2.4 m sample grid, which resulted in 997-1,189

readings per field. Data was recorded using an on-board computer and displayed in a spreadsheet format.

Penetration resistance was measured by a stainless steel load cell located in the soil sampling head of the PS6000. The sensor measures the maximum penetration force encountered in the top 10 cm of the surface and is reported as pounds of force then was converted to newton (N in m kg $s^{-2}$) To ensure soil penetration at 10 cm, two custom stainless steel probes of 9.53 mm diameter, 3.3 cm spacing, and 10 cm length were installed to the soil sampling head, which is attached to a rotating shaft. Each probe is considered a penetrometer therefore two readings are recorded with each measurement. When the PS6000 is moving forward, the wheel-driven shaft rotates in a circular fashion and the probes are inserted into the ground to collect measurements. A NovAtel GPS (NovAtel Inc., Alberta, Canada), attached to the PS6000, was used to gather latitude and longitude information for the data.

The ArcGIS version 10.1 GIS and mapping software (ArcMap) was used to develop, display, analyze and interpret maps of the PS 6000 penetration resistance data (ESRI, Redlands, CA). Using the editor tool in ArcMap, samples were removed from the initial 2.4 m x 2.4 m sampling grid to create the various sample sizes evaluated in this study. For each field, a total 8 sample sizes were manipulated including 7 sampling grids as well as a sampling pattern that resembles test procedures from previous non-spatial performance testing research (Tables 3.1-3.4; Figures 3.1a-3.48a).

*Statistical analysis*

Analysis of field data was done in three components. First, summary statistics were produced to evaluate central tendency, variability, and frequency distribution of data from each

sample size on all fields. The mean is commonly used to measure central tendency and is calculated by:

$$\bar{x} = \frac{\sum x}{n} \quad \text{[Eq. 3.1]}$$

where $\sum x$ is the sum of all values and *n* is the number of samples taken. Comparison of means between sample sizes within each field was done using one-way ANOVA and Fisher's Protected LSD ($P < 0.05$). Data analysis was performed using the 'agricolae' package (Mendiburu, 2014) in R version 2.15.2 statistical software (R Development Core Team, 2008). Skewness is a measure of degree of symmetry and determines extent of even or uneven data distribution in relation to the mean:

$$\text{Skewness} = \frac{\sum(X_i - \overline{\text{X}})^3}{ns^3} \quad \text{[Eq. 3.2]}$$

Kurtosis measures the degree of flatness or peakness of a data set:

$$\text{Kurtosis} = \frac{\sum(X_i - \overline{\text{X}})^4}{ns^4} \quad \text{[Eq. 3.3]}$$

Histograms (not shown) were also produced to visually assess the central tendency and shape of data distribution.

The range is the simplest measure of data variability and is simply the difference between the highest and the lowest value in the data set. The standard deviation (SD) shows how much variation of the data there is from the mean and can be found using:

$$s = \sqrt{\frac{\sum(\text{X}_i - \overline{\text{X}})^2}{n}} \quad \text{[Eq. 3.4]}$$

where $\text{X}_i$ is the value of observation *i*. The standard error of the mean (SE) is the level of dispersion of the data from the mean and is calculated:

$$\mathrm{SE}_{\bar{X}} = \frac{s}{\sqrt{n}} \qquad \text{[Eq. 3.5]}$$

The coefficient of variability (CV) is different from standard deviation in that it is expressed as a percentage of the mean and consequently allows for analysis between data sets with different absolute values. Therefore, the CV is valuable as a relative index of data dispersion:

$$\mathrm{CV} = \frac{s}{\bar{\mathrm{X}}}(100) \qquad \text{[Eq. 3.6]}$$

Next, semivariograms were created by plotting the semivariance, $\gamma(h)$, between each pair of data. Semivariance is quantified using the equation:

$$\gamma(h) = \frac{1}{2N(h)} \sum_{i=1}^{N(h)} [z(x_i) - z(x_i + h)]^2 \qquad \text{[Eq. 3.7]}$$

where $N(h)$ is the number of pairs of data separated by a lag distance $h$, and $z$ is the value of the given measurement at location $x_i$. The lag distance $h$ is the spatial range between two data points. If a grid survey is used for sampling it is common to use the grid spacing as $h$ (Oliver and Webster, 2014). Therefore, when constructing the semivariograms of the sample grids in this study, the respective grid spacing was used as $h$. For the sample pattern not following a grid survey $h$ was found using the Average Nearest Neighbor tool in the Spatial Statistics toolbox of ArcMap (ESRI, Redlands, CA).

The range ($A_0$), nugget ($C_0$), sill ($C_0 + C$), and partial sill ($C$) are important components of a semivariogram and are used to describe the parameters of spatial structure. The range is the finite lag distance where spatial dependency occurs (i.e. at distances beyond the range there is little to no correlation among variables). The nugget is the value that intercepts the y axis and represents independent error, measurement error, and/or microscale variation at spatial scales that are too small to detect. The sill represents the total variance of the dataset; at large distances

variables become uncorrelated and the sill of the semivariogram is equal to the variance of the random variable. The partial sill is the sill minus the nugget.

There are several models that can be fit to describe semivariograms; the spherical model is considered the most commonly used model for describing spatial data and was used to fit the semivariograms in this study (Jian, 1996). This model has linear behavior at small separation distances near the origin but flattens out at larger distances and reaches the sill at the range (Isaaks, 1989). The spherical model is calculated by:

$$\gamma(h) = \begin{cases} 0, & h = 0 \\ C_0 + (C - C_0)\left\{\frac{3h}{2A_0} - \frac{1}{2}\left(\frac{h}{A_0}\right)^3\right\}, & 0 \le h \le A_0 \\ C_0 + (C - C_0), & h \ge A_0 \end{cases} \qquad \text{[Eq. 3.8]}$$

where $C_0$ is the nugget ($C_0 \geq 0$), $C$ is the sill ($C \geq 0$), $A_0$ is the range ($A_0 \geq 0$), and $h$ is the lag distance as defined in Eq. 3.7 (Jian, 1996).

Lastly, visual assessment of the measured parameters was done using kriging, with the Geostatistical Analyst extension of ArcMap, to create prediction surface maps (ESRI, Redlands, CA). The formula for kriging is:

$$\hat{Z}(x_0) = \sum_{i=1}^{N} \lambda_i z(x_i) \qquad \text{[Eq. 3.9]}$$

where $\hat{Z}(x_0)$ is the predicted value at the prediction location, $N$ is the number of measured values, $\lambda_i$ is an unknown weight for the measured value at the $i$th location, and $z(x_i)$ is the measured value at the $i$th location (ESRI, 2004). There are various models of kriging, for this study simple kriging was used. Simple kriging assumes the model:

$$\hat{Z}(x) = \mu + \varepsilon(x) \qquad \text{[Eq. 3.10]}$$

where $\hat{Z}(x)$ is the variable of interest, $\mu$ is the known mean constant, and $\varepsilon(x)$ is formed from autocorrelated errors.

Following kriging, cross-validation is conducted to provide summary statistics in order to choose the most plausible model. Cross-validation is the process by which each of the *N* data points is omitted in turn from the set of data and it value is predicted using the chosen kriging model (Oliver and Webster, 2014). Three statistics are calculated; the mean error (ME), the root mean squared error (RMSE), and the root mean square standardized error (RMSSE). The ME is the average difference between each measured and predicted value:

$$\frac{1}{N}\sum_{i=1}^{N} z(x_i) - \hat{Z}(x_i) \qquad \text{[Eq. 3.11]}$$

The RMSE indicates how closely the model predicts the measured values:

$$\frac{1}{N}\sum_{i=1}^{N} \{z(x_i) - \hat{Z}(x_i)\}^2 \qquad \text{[Eq. 3.12]}$$

Lastly, the RMSSE is the RMSE divided by the corresponding kriging variance:

$$\frac{1}{N}\sum_{i=1}^{N} \frac{\{z(x_i) - \hat{Z}(x_i)\}^2}{\hat{\sigma}_K^2(x_i)} \qquad \text{[Eq. 3.13]}$$

where $\hat{\sigma}_K^2(x_i)$ is the kriging variance. RMSSE should be close to 1 if the prediction standard errors are valid (ESRI, 2004).

## Results

*Descriptive statistics*

According to Fisher's Protected LSD, significant differences in mean of penetration resistance were only observed between sample sizes at Roswell 1 and Watkinsville 1 (Table 3.1 and 3.2, respectively). At Roswell 1, means of all sample grid sizes were statistically similar (Table 3.1). The 7 sample size was significantly different to all sample grids except for the 9.6 m x 4.8 m and 9.6 m x 9.6 m grid sizes. At Watkinsville 1, sample grid sizes 2.4 m x 2.4 m through 4.8 m x 4.8 m, as well as the 9.6 m x 9.6 m sample grid, all had statistically similar means (Table

3.2). Sample grid sizes 9.6 m x 4.8 m and larger, including the 7 sample size, were all not statistically different.

Positive skewness indicates the mass of the distribution is concentrated on the left side (i.e. lower penetration resistance values). A negative skewness indicates the mass of distribution is concentrated on the right side (i.e. higher penetration resistance values). Both locations exhibited instance of positive and negative skewness. A skewness of 0 would be interpreted as perfect symmetry and data falling within -1 and 1 are said to be normally distributed. Roswell 3 exhibited non-normal distribution with highly positive skewness data for all sample grid sizes (Table 3.1). This indicates that the mass of the distribution is highly concentrated with lower penetration resistance values on this field. The only other sample sizes to exhibit non-normal distribution was the 7 sample size on Watkinsville 1 and the 19.2 m x 19.2 m sample grid on Watkinsville 2 (Table 3.2).

A kurtosis value > 3.0 indicates a leptokurtic (peaked) distribution, a mesokurtic (normal) distribution has a kurtosis of 3.0, and a platykurtic (flat) distribution is < 3.0 (McGrew and Monroe, 2009). Roswell 1 and 2 had fluctuating kurtosis characteristics between sample sizes, with leptokurtic distribution being evident with the smaller sample grid sizes (Tables 3.1). On Roswell 3, all sample grid sizes had leptokurtic distributions and relatively high kurtosis values. The significantly high values, specifically for the 2.4 m x 2.4 m and 4.8 m x 2.4 m sample grids, indicate that the data is not normally distributed and are extremely peaked (centered around the mean). Watkinsville 1 and 2 had leptokurtic distribution for all sample sizes, except for the 7 sample size on Watkinsville 2 (Table 3.2). Watkinsville 3 had leptokurtic distributions for sample grid sizes 2.4 m x 2.4 m to 9.6 m x 9.6 m, with all other sample sizes having platykurtic distribution (Table 3.2).

Although the mean, skewness, and kurtosis can be a useful tool in understanding the data, they provide little information about variability. The range is the simplest method to determine variability, with wide ranges indicating more. From the smallest sample grid size to the largest sample grid size the range often decreased dramatically, indicating far less variability being accounted for with larger spacing between samples (Table 3.1 and 3.2). This result is expected, since low and high values can be omitted from the dataset as more samples are removed to create larger grid sizes. The ranges for the 7 sample sizes were significantly smaller than all grid sizes for all fields, except Roswell 1, indicating that determined variability of the area can be reduced with such a small sample size (Table 3.1 and 3.2).

The SD, SE, and CV are all common measures of data variability. SD and CV tended to not differ dramatically between sample sizes on Roswell fields 2 and 3 and Watkinsville fields 2 and 3, with the exception of the 7 sample size (Table 3.1 and 3.2, respectively). Roswell 1 SD and CV increased from the 2.4 m x 2.4 m sample grid to the 9.6 m x 9.6 m sample grid before decreasing with the larger grid sizes (Table 3.1). Watkinsville 1 SD and CV, in general, increased with increasing sample grid size (Table 3.2). The SD and CV for the 7 sample size were higher than all grid sizes on Roswell 1 and 3 (Table 3.1). For Watkinsville 1, SD and CV tended to be similar to that of the mid-sized sample grids (Table 3.2). SE increased as sample size decreased for all fields (Table 3.1 and 3.2). Smaller SE indicates less sampling error and is primarily influenced by sample size. Therefore, this result was expected.

*Spatial analysis*

Semivariograms were generated for all sample sizes to describe parameters of spatial structure (Figures 3.1c-3.48c). The range represents the distance, at which once beyond, a pair of samples is no longer correlated. Sampling distances should be less than the range if data are to be

spatially correlated for interpolation. The ranges for all sampling grids on each field was greater than the sampling distance used indicating all were sufficient (Tables 3.7-3.12; Figures 3.1c-3.48c).

The nugget and sill provide information to determine error and variability of the models, respectively. A trend in nugget and sill values between sample grid sizes on each field was not observed (Table 3.3 and 3.4). Nugget and sill values also varied from field to field. Sample sizes of 7 indicated a pure nugget for all fields except Roswell 2 (Table 3.3 and 3.4). Pure nugget occur when the nugget equals the sill, which indicates that the distance between sampling intervals is too large and the scale of spatial dependency is determined in ranges less than the shortest sampling distance. It is not recommended to conduct interpolation on a pure nugget (Oliver and Webster, 2014). The sample size of 7 on Roswell 2 exhibited a relatively low nugget value (Table 3.3), however further assessment will indicate this is still a poor model. Furthermore, no trend was observed with the sill on any fields (Table 3.3 and 3.4).

It is common to use the nugget/sill ratio of each dataset to assess the strength of spatial dependence (< 25% indicates strong spatial dependence, 25-75% indicates moderate spatial dependence, and > 75% indicates weak spatial dependence) (Cambardella et al., 1994). A large ratio can indicate that substantial measurement errors are present or the need of a more intense sampling, or both (Oliver and Webster, 2014). At Roswell, the only field to exhibit strong spatial dependence for any sample sizes was field 1 (Table 3.3). Sample grid sizes 2.4 m x 2.4 m through 9.6 m x 4.8 m all had strong spatial dependence, with the 9.6 m x 9.6 m and 19.2 m x 9.6 m sample grids having moderate and the 19.2 m x 19.2 m sample grid and 7 sample size having weak spatial dependence. Additionally, the sample size of 7 indicated a pure nugget (Figure 3.8c). Roswell 2 had moderate spatial dependence for all sample sizes observed (Table 3.3). On

Roswell 3, all sample grid sizes, except 4.8 m x 4.8 m and 19.2 m x 19.2 m, had moderate spatial dependence (Table 3.3). The 4.8 m x 4.8 m and 19.2 m x 19.2 m sample grids and the 7 sample size had weak spatial dependence. Pure nuggets occurred with the 19.2 m x 19.2 m sample grid and the 7 sample size (Figures 3.23c and 3.24c, respectively). At Watkinsville, sample grids on all fields had moderate spatial dependence (Table 3.4). Weak spatial dependence and pure nugget semivariograms occurred for each sample size of 7 (Figures 3.32c, 3.40c, and 3.48c).

*Visual assessment*

At Roswell, the 2.4 m x 2.4 m and 4.8 m x 2.4 m sample grid sizes provided the most detailed visual assessment by map results of penetration resistance variability with only minor alteration between them (Figure 3.1b and 3.2b, 3.9b and 3.10b, and 3.17b and 3.18b). On Roswell 1, although minor differences occurred in patterns between the 2.4 m x 2.4 m and 9.6 m x 9.6 m sample grid sizes, detailed variability did not significantly alter until the 19.2 m x 9. 6 m sample grid and continued to decrease as sample grid size increased (Figures 3.1b-3.7b) Roswell 2 exhibited similar patterns between 2.4 m x 2.4 m and 9.6 m x 4.8 m sample grid sizes (Figure 3.9b-3.12b) then began to decrease at the 9.6 m x 9.6 m grid size until the 7 sample size (Figures 3.13b-3.16b). On Roswell 3, comparable patterns could be observed from sample grids 2.4 m x 2.4 m through 9.6 m x 9.6 m with minor alterations in variability as sample grid size increased (Figures 3.17b-3.21b). The 19.2 m x 9.6 m sample grid did not show an accurate depiction of penetration resistance in comparison to smaller sample grid sizes (Figure 3.22b). No variation was seen with the 7 sample size on Roswell 1, or the 19.2 m x 19.2 m sample grid and the 7 sample size on Roswell 3, due to the occurrence of a pure nugget semivariogram (Figure 3.8b and c, 3.23b and c, and 3.24b and c, respectively).

All fields in Watkinsville also exhibited similar patterns for their sample grid size of 2.4 m x 2.4 m and 4.8 m x 2.4 m (Figures 3.25b and 3.26b, 3.33b and 3.34b, and 3.41b and 3.42b). The 4.8 m x 4.8 m sample grid on Watkinsville 1 indicated high penetration resistance areas not observed with smaller grid sizes (Figure 3.27b). The 9.6 m x 4.8 m and 9.6 m x 9.6 m surface maps had more resemblance to the smaller grid sizes (Figures 3.30b and 3.31b, respectively). The remaining sample grid sizes and the 7 sample size did not exhibit the same patterns as smaller sample grids (Figures 3.30b, 3.31b, and 3.32b). On Watkinsville 2, patterns did not begin to alter until the 9.6 m x 9.6 m sample grid and beyond (Figures 3.33b-3.40b). For Watkinsville 3, variability began to decrease at the 9.6 m x 4.8 m sample grid, and continued to decrease until the 19.2 m x 19.2 sample grid (3.41b-3.48b). All sample sizes of 7 exhibited a pure nugget semivariogram in Watkinsville, indicating no variability of penetration resistance in space (Figures 3.32b, 3.40b, and 3.48b).

Following kriging, cross-validation is conducted to provide prediction errors. The ME should be close to zero if the predicted values are centered around the measurement values (unbiased predictions). The ME varied between sample grids on all fields (Table 3.3 and 3.4). Pure nugget semivariograms exhibited an ME of 0, but these models have already been observed as an unacceptable option.

If predicted values being close to the measurement values would result in a low RMSE value. On Roswell 1 the smallest RMSE was the 19.2 m x 19.2 m sample grid; however, it showed weak spatial dependence so it should not be considered an appropriate model option (Table 3.3). Of the strongly spatial dependent sample grid sizes the smallest RMSE was the 2.4 m x 4.8 m. Roswell 2 RMSE tended to increase with sample grid size (Table 3.3). The 7 sample size RMSE is deceiving, because it is lower than the smallest sample grids RMSE; however, it

exhibited a pure nugget semivariogram, therefore it has already been deemed unacceptable. There were not substantial differences in RMSE on Roswell 3 between sample grid sizes, however, the 4.8 m x 2.4 m sample grid was the smallest (Table 3.3). The 7 sample size was significantly larger than all grid sizes. In Watkinsville, a general trend of RMSE increasing with sample grid size was observed (Tables 3.4). The 7 sample size did not follow this trend due to each being a pure nugget (Tables 3.4).

If RMSSE are greater than 1, the variability in the predictions is underestimated; if the RMSSE are less than 1, the variability in the predictions is overestimated. RMSSE varied between sample sizes on all fields. The 2.4 m x 2.4 m sample grids were the only to continuously show RMSSE 1 or greater, indicating that the smallest sample grid underestimated the variability of the predictions (Table 3.3 and 3.4). No other trend was observed on any field.

## Discussion

Comprehensive insight of the spatial variation of soil compaction on sports fields can be provided with descriptive statistics and geostatistical techniques. Often, as seen with previous methods of performance testing, the mean is the determinate statistic to quantify performance of a given variable on a sports field; although it is highly unpractical to predict the true value. A higher sampling intensity would, in theory, be a better prediction than a low sampling intensity. However, of the six fields evaluated, four showed no significant differences in penetration resistance mean between sample sizes. These results suggest that the central tendency of penetration resistance on a field may be approximated with lower sampling numbers; however variability of penetration resistance in space across the field is masked.

Spatial variability was better defined using geostatistics. Ideally, the best type of model will have a low nugget with a high sill. This would indicate that greater micro-scale variability is

accounted for with less measurement error and also provide a low nugget/sill ratio indicating strong spatial dependence. Furthermore, generated semivariograms are based on Tobler's Law, also known as the first law of geography, which states, "Everything is related to everything else, but near things are more related than distant things" (Tobler, 1970). This indicates semivariance is generally low when two locations are close to each other and increases as the distance between the locations grow until at some point the locations become independent. Therefore, smaller sample grid sizes would be expected to result in a lower nugget and potentially stronger spatial dependence. Although the nugget/sill ratio can warn us of measurement errors and/or micro-scale variability, it tells us nothing about the underlying variation of properties that vary continuously in space (Oliver and Webster, 2014). This phenomenon is better explained with interpolation.

Surface maps generated from kriging interpolation provided better visual indication of penetration resistance in space. Our study showed that, in general, as sample grids increased, variability decreased. Results indicate that larger grid sizes, such as 9.6 m x 9.6 m and 19.2 m x 9.6 m, are capable of showing similar trends of variability as smaller grid sizes. However, these mask detailed variability in certain locations and provide a less accurate surface map. Thus, sampling schemes should be chosen relative to the desired degree of accounted variability, with smaller sampling grids providing the most accuracy and detail. Detailed spatial information is important when identifying why small (or large) areas of extreme (high or low) values are exhibited for a particular property.

The ME, RMSE, and RMSSE, obtained from cross-validation are good indicators of prediction errors and should be used when considering models. However, they depend on the scale of the data and should not be the underlining decision maker. The combination of

descriptive statistics, geostatistics, and general knowledge of the site conditions and use before spatial analysis can aide in interpretation of the interpolated data and selecting the best model (Oliver and Webster, 2014).

As a side note, penetration resistance is primarily influenced by soil type, structure/compaction, and moisture content within the soil (Sudduh et al., 2008). It is important to emphasize that data collection and spatial analysis in this study was conducted after rainfall events when fields were at field capacity. Data collection when the soil is at field capacity reduces the influence of soil drying within a soil type on the penetration resistance value. Henderson et al. (1988) reported that penetration resistance was slightly affected by VWC decreasing from 100 to 70% field capacity, but then exponentially increasing with further drying. Thus, within a soil type, as the soil dries below field capacity, penetration resistance increases, especially at below 70% field capacity (Henderson et al., 1988; Unger and Kasper, 1994). Therefore, mapping at field capacity appears to reflect inherent penetration resistance of existing soil types.

Comparison of these results to previous research is difficult since, to the author's knowledge, Straw et al. (Chapter 2) have been the only researchers to use mobile devices to evaluate sampling procedures for spatial analyses on sports fields, but only for VWC. However, similar results were observed regarding measuring central tendency with smaller sample sizes and general trends of variability decreasing with increasing sample size.

Caple et al. (2012) are the only researchers to spatially analyze penetration resistance on sports fields. However, the purpose of their study was not to compare sampling procedures. The 135 or 150 samples used in that study exhibited random variation of penetration resistance across each field. Semivariogram data was not shown; therefore, comparison of spatial dependency at

that sample size in their study cannot be made with our results. Furthermore, handheld devices that were used for data collection may be time, cost, and labor intensive for certain facilities. The PS6000 was capable of sampling a soccer field using the 2.4 m x 2.4 m grid (~1000-1100 samples) in approximately 1 h and would be more practical for use of mapping multiple sports fields.

Handheld devices, however, should not be completely disregarded due to the development of mobile devices. Data collection for spatial analysis of a small number of fields could be feasible using handheld devices with the sample grids evaluated in this study. Our results found a minimum sampling procedure of 9.6 m x 4.8 m (~140-160 samples) can provide an acceptably accurate spatial analysis. However, the sample grids used in this study were manipulated in GIS from data collected with the PS6000. Future research should consider using handheld devices, at these sampling grids, to determine if they correlate with analyses conducted in this study.

Moreover, spatial analysis of sports fields by Miller (2004) and Caple et al. (2012) evaluated variability of surface and edaphic properties for various soil classes. Miller (2004) observed higher uniformity of surface hardness on sand-based fields than that of native soil. Caple et al. (2012) detected greater spatial and temporal uniformity of sand rootzone fields compared to clay loam and loamy sand for all observed properties. These results are likely due to the effects of compaction on course textured soils (sand) are less evident than that of fine textured soils (clay), because of bridging between the hard sand particles prevents elimination of most large pores (Beard, 1973). Due to the observed uniformity of properties on sand-based sports fields, a smaller sampling grid may be required to account for short-range variability between samples. Our study only evaluated fields with sandy loam soils; therefore, further

research with varying sampling schemes on fields with different soil classes should be conducted for comparisons.

## Conclusion

Performance tests to spatially analyze surface and edaphic properties, such as soil compaction, on sports fields can be fundamental in determining a site-specific sports turf management program. As a result, an increase in player safety and field playability, and the reduction of inputs can be achieved. Performance testing on sports fields in the past have used minimal amount of samples across a field. However, to better assess the variability of a property, as well as the relationship between properties, spatial analysis using geostatistics is more appropriate. This would involve implementing a more intense sampling procedure and the use of geostatistical techniques, such as semivariograms and interpolation.

The most important factor in determining the reliability, or accuracy, of a semivariogram is the sample size on which it is based (Oliver and Webster, 2014). In general, the more data you have for spatial analysis, the greater the accuracy. It is for this reason that mobile sensor platforms are the most practical means of data collection over larger areas, because of the ability to sample more intensely and the addition of an equipped GPS. With a mobile platform, like the PS6000, the user may sample as intense as desired. Our results suggest that at minimum a 9.6 m x 4.8 m sample grid size (~140-160 samples) be utilized for spatial analysis of soil compaction on sports fields using geostatistical techniques. For the PS6000, this exact sample grid size is not achievable in the field because samples are collected every ~2.4 m. We suggest distances between passes downfield be 4.8 m (an approximate 4.8 m x 2.4 m sample grid) or at most 9.6 m (an approximate 9.6 m x 2.4 m sample grid). However, due to the relatively short time for data collection with the PS6000 (~1 h per field), an intense sample grid such as 2.4 m x 2.4 m would

be most beneficial and give the most detail. Small area differences in penetration resistance could be of great influence on player safety and field playability.

Furthermore, to date, mobile sensors are not abundantly available for commercial use. Sports fields differ from agriculture and golf courses with respect to the area managed. Use of the more commonly available handheld devices to spatially analyze sports field properties could be feasible if a standard procedure or protocol is implemented. However, the sample grids used in this study were manipulated in GIS from data collected with the PS6000. Future research should consider a comparison of spatial analyses, using sample grids from this study, between handheld and mobile devices.

## References

American Society for Testing and Matrials (ASTM). 2010. F1936–10, Standard specification of impact attenuation of turf playing systems as measured in the field. Annual book of ASTM standards. American Society for Testing Materials, West Conshohocken, PA.

Baker, S.W. 1991. Temporal variation of selected mechanical properties of natural turf football pitches. J. Sports Turf Res. Inst. 67:83-92.

Baker, S.W., and P.M Canaway. 1993. Concepts of playing quality: criteria and management. Int. Turfgrass Soc. Res. J. 7:172-181.

Bartlett, M.D., I.T. James, M. Ford, and M. Jennings-Temple. 2009. Testing natural turf sports surfaces: the value of performance quality standards. Proceedings of the Institution of Mechanical Engineers, Part P. J. Sports Eng. and Technol. 223:21-29.

Beard, J.B. 1973. Turfgrass: Science and culture. Prentice Hall Inc., Englewood Cliffs, NJ.

Bell, M.J., and G. Holmes. 1988. The playing quality of association football pitches. J. Sports Turf Res. Inst. 61:19-47.

Bell, G.E., and X. Xiong. 2008. The history, role, and potential of optical sensing for practical turf management. p. 641-660. *In* M. Pessarakli (Ed.), Handbook of turfgrass management and physiology. CRC Press, NY.

Bengough, A.G., D.J. Campbell, and M.F. O'Sullivan. 2000. Penetrometer techniques in relation to soil compaction and root growth. p. 377-403. *In* Smith, K.A., and C.E Mullins (Eds.), Soil and Environmental Analysis. 2nd ed. Marcel Dekker, NY.

Bouma, J., J. Stoorvogel, B.J. van Alphen, and H.W.G. Booltink. 1999. Pedology, precision agriculture, and the changing paradigm of agricultural research. Soil Sci. 63.6:1763-1768.

Bullock, D.S., N. Kitchen, and D.G., Bullock. 2007. Multidisciplinary teams: a necessity for research in precision agriculture systems. Crop Sci. 47:1765-1769.

Cambardella, C.A., T.B. Moorman, T.B. Parkin, D.L. Karlen, J.M. Novak, R.F. Turco, and A.E. Konopka. 1994. Field-scale variability of soil properties in central Iowa soils. Soil Sci. Soc. Am. J. 58:1501-1511.

Caple, M., I. James, and M. Bartlett. 2012. Spatial analysis of the mechanical behaviour of natural turf sports pitches. Sports Eng. 15:143-157.

Carrow, R.N., and A.M. Petrovic. 1992. Effects of traffic on turfgrasses. p. 285-330. *In* Carrow, R.N and R.C. Shearman (Eds.), Turfgrass. ASA, Madison, WI.

Carrow, R.N., V. Cline, and J. Krum. 2007. Monitoring spatial variability in soil properties and turfgrass stress: applications and protocols. Proc. of 28th Int. Irrigation Show, 9-11 Dec. 2007, San Diego, CA.

Carrow, R.N., J.M Krum, I. Flitcroft, and V. Cline. 2010. Precision turfgrass management: challenges and field applications for mapping turfgrass soil and stress. Precis. Agric, 11:115-134.

Corwin, D.L., and S.M. Lesch. 2005. Apparent soil electrical conductivity measurements in agriculture. Comput. Electron. Agric. 46:103-133.

Emery, X., and K. González. 2007. Incorporating the uncertainty in geological boundaries into mineral resources evaluation. J. Geol. Soc. India. 69:29–38.

ESRI. 2004. ArcGIS 9: Using ArcGIS Geostatistical Analyst. ESRI, Redlands, CA.

Flitcroft, I., J. Krum, R. Carrow, K. Rice, T. Carson, and V. Cline. 2010. Spatial mapping of penetrometer resistance on turfgrass soils for site-specific cultivation. Proceedings CD of the 10th Int. Conf. on Prec. Ag., Denver, CO. 18-21 July, 2010. ISPA, Monticello, IL.

Freeland, R.S., J.C. Sorochan, M.J. Goddard, and J.S. McElroy. 2008. Using ground-penetrating radar to evaluate soil compaction of athletic turfgrass fields. Appl. Eng. Agric. 24:509-514.

Henderson, C., A. Levett, and D. Lisle. 1988. The effects of soil water content and bulk density on the compactibility and soil penetration resistance of some Western Australian sandy soils. Soil Research 26:391-400.

Holmes, G., and M.J. Bell. 1986. A pilot study of the playing quality of football pitches. J. Sports Turf Res. Inst. 62:74-91.

Institute of Groundsmanship (IOG). 2014. Performance Quality Test (PQS) Methods. http://www.iog.org/train-education/Technical-Library/Performance+Quality+Standards/PQS+Methods+of+Test (accessed 25 Feb 2014).

Isaaks, E.H., and R.M Srivastava. 1989. Applied geostatistics. Oxford University Press. New York, NY.

James, I.T., and R.J. Godwin. 2003. Soil, water and yield relationships in developing strategies for the precision application of nitrogen fertiliser to winter barley. Biosyst. Eng. 84:467-480.

Jian, X., R.A. Olea, and Y.S. Yu. 1996. Semivariogram modeling by weighted least squares. Comput. Geosci. 22:387-397.

Krum, J.M. 2008. Spatial site assessment of soil moisture and plant status on golf courses. M.S. thesis. Univ. of Georgia, Athens, GA.

Krum, J.M., R.N. Carrow, and K. Karnok. 2010. Spatial mapping of complex turfgrass sites: Site-specific management units and protocols. Crop Sci. 50:301-315.

Madison, L.H. 1971. Principle of turfgrass culture. Van Nostrand Reinhold Co., NY.

McAuliffe, K.W. 2008. The role of performance testing and standards in the sports turf industry: A case study approach. *In* J.C. Stier, L. Han, and D. Li (Eds.). Proceedings of 2nd international conference on turfgrass management and sports fields (pp. 391-398). Int. Soc. Hort. Sci. Belgium.

McClements, I., and S.W. Baker. 1994. The playing quality of rugby pitches. J. Sports Turf Res. Inst. 70:29-43.

McGrew Jr, J.C., and C.B. Monroe. 2009. An introduction to statistical problem solving in geography. Waveland Press, Long Grove, IL.

Mendiburu, F. (2014). agricolae: Statistical Procedures for Agricultural Research. R package version 1.1-7. http://CRAN.R-project.org/package=agricolae (accessed 1 April 2014).

Miller, G.L. 2004. Analysis of soccer field surface hardness. *In* P.A. Nektarios (Ed.), Proceedings of the first International Conference on Turfgrass Management and Science for Sports Fields. ISHS, Leuven, pp. 287-294.

Oliver, M.A., and R. Webster. 2014. A tutorial guide to geostatistics: Computing and modelling variograms and kriging. Catena. 113:56-69.

R Development Core Team. 2008. R: A language and environment for statistical computing. R Foundation for Statistical Computing, Vienna, Austria. http://www.R-project.org (accessed 1 April 2014).

Rhoades, J.D., F. Chanduvi, and S.M. Lesch. 1999. Soil salinity assessment: Methods and interpretation of electrical conductivity measurements. FAO Irrigation and Drainage Paper 57. Food and Agric. Organ. of the United Nations. Rome, Italy.

Stiles, V.H., I.T. James, S.J. Dixon, and I.N. Guisasola. 2009. Natural turf surfaces. Sports Med. 39(1):65-84.

Stowell, L., and W. Gelernter. 2008. Evaluation of a Geonics EM38 and NTech GreenSeeker sensor array for use in precision turfgrass management. *In* Abstracts, GSA-SSSA-ASACSSA-GCAGS Int. Annu. Meet., Houston, TX, 5-9 Oct. 2008. ASA-CSSA-SSSA, Madison, WI.

Sudduth, K.A., S. Chung, P. Andrade-Sanchez, and S.K. Upadhyaya. 2008. Field comparison of two prototype soil strength profile sensors. Computers and Electronics in Agric. 61:20-31.

Taylor, J.C., G.A. Wood, R. Earl, and R.J. Godwin. 2003. Soil factors and their influence on within-field crop variability, part II: spatial analysis and determination of management zones. Biosyst. Eng. 84:441-453.

Taylor, J.A., A.B. McBratney, and B.M. Whelan. 2007. Establishing management classes for broadacre agricultural production. Agron. J. 99:1366-1376.

Thomsen, A., K. Schelde, P. Drøscher, and F. Steffensen. 2007. Mobile TDR for geo-referenced measurement of soil water content and electrical conductivity. Precis. Agric. 8:213-223.

Tobler W.R. 1970. A computer movie simulating urban growth in the Detroit region. Econ. Geogr. 46:234–240.

Turgeon, A.J. 2011. Turfgrass Management. Ninth Edition. Prentice Hall Inc., Englewood Cliffs, NJ.

Unger, P.W. and T.C. Kaspar. 1994. Soil compaction and root growth: a review. Agron. J. 86:759-766.

Webster, R., and Oliver, M.A. 2007. Geostatistics for environmental scientists. John Wiley & Sons, Hoboken, NJ.

**Table 3.1.** Descriptive statistics of penetration resistance (N in m kg $s^{-2}$) on fields at Roswell for evaluated sample sizes on 9 May, 2013.

| Sample size | Sample Grid | Mean (±SE)[†‡] | Min[§] | Max[¶] | Range | SD[#] | CV[††] (%) | Skewness | Kurtosis |
|---|---|---|---|---|---|---|---|---|---|
| Roswell 1 | | | | | | | | | |
| | | Newton | | | | | | | |
| 1121 | 2.4 m x 2.4 m | 1278 ± 17a | 98 | 3640 | 3542 | 554 | 43.4 | 0.64 | 3.23 |
| 584 | 4.8 m x 2.4 m | 1268 ± 22a | 98 | 3253 | 3155 | 543 | 42.8 | 0.51 | 3.03 |
| 295 | 4.8 m x 4.8 m | 1279 ± 32a | 98 | 3253 | 3155 | 557 | 43.5 | 0.60 | 3.29 |
| 160 | 9.6 m x 4.8 m | 1314 ± 46ab | 252 | 3253 | 3002 | 582 | 44.3 | 0.70 | 3.59 |
| 83 | 9.6 m x 9.6 m | 1289 ± 68ab | 311 | 3253 | 2942 | 617 | 47.9 | 0.74 | 3.63 |
| 47 | 19.2 m x 9.6 m | 1221 ± 60a | 328 | 1859 | 1531 | 411 | 33.6 | -0.65 | 2.64 |
| 24 | 19.2 m x 19.2 m | 1251 ± 62a | 592 | 1757 | 1165 | 305 | 31.5 | -0.36 | 2.47 |
| 7 | N/A | 1698 ± 350b | 592 | 2774 | 2183 | 927 | 54.6 | 0.12 | 1.29 |
| Roswell 2 | | | | | | | | | |
| | | Newton | | | | | | | |
| 1189 | 2.4 m x 2.4 m | 832 ± 9a | 182 | 2862 | 2680 | 324 | 39.0 | 0.92 | 5.22 |
| 616 | 4.8 m x 2.4 m | 836 ± 13a | 233 | 2862 | 2629 | 322 | 38.5 | 0.99 | 5.69 |
| 308 | 4.8 m x 4.8 m | 846 ± 18a | 233 | 2135 | 1902 | 318 | 37.6 | 0.83 | 3.97 |
| 154 | 9.6 m x 4.8 m | 826 ± 25a | 233 | 1822 | 1589 | 313 | 37.9 | 0.58 | 2.77 |
| 77 | 9.6 m x 9.6 m | 841 ± 37a | 317 | 1822 | 1505 | 324 | 38.6 | 0.47 | 2.78 |
| 44 | 19.2 m x 9.6 m | 916 ± 48a | 317 | 1822 | 1505 | 319 | 34.9 | 0.31 | 3.37 |
| 24 | 19.2 m x 19.2 m | 915 ± 65a | 317 | 1642 | 1325 | 321 | 35.1 | -0.09 | 2.56 |
| 7 | N/A | 803 ± 99a | 491 | 1134 | 643 | 262 | 32.6 | -0.08 | 1.33 |
| Roswell 3 | | | | | | | | | |
| | | Newton | | | | | | | |
| 997 | 2.4 m x 2.4 m | 617 ± 7a | 192 | 2367 | 2175 | 233 | 37.8 | 1.89 | 10.22 |
| 519 | 4.8 m x 2.4 m | 617 ± 10a | 192 | 2277 | 2084 | 226 | 36.6 | 2.01 | 11.38 |
| 259 | 4.8 m x 4.8 m | 615 ± 13a | 201 | 1486 | 1286 | 212 | 34.5 | 1.12 | 4.98 |
| 139 | 9.6 m x 4.8 m | 625 ± 18a | 297 | 1486 | 1190 | 213 | 34.1 | 1.33 | 5.56 |
| 70 | 9.6 m x 9.6 m | 619 ± 25a | 297 | 1341 | 1044 | 210 | 33.9 | 1.22 | 5.03 |
| 40 | 19.2 m x 9.6 m | 621 ± 37a | 297 | 1341 | 1044 | 235 | 37.9 | 1.36 | 4.99 |
| 20 | 19.2 m x 19.2 m | 605 ± 52a | 330 | 1341 | 1011 | 234 | 38.6 | 1.55 | 5.90 |
| 7 | N/A | 711 ± 131a | 416 | 1341 | 925 | 347 | 48.8 | 0.97 | 2.46 |

[†] Within columns, means followed by the same letter are not significantly different at $p \leq 0.05$ according to Fisher's Protected LSD test.
[‡] SE, standard error
[§] Min, minimum
[¶] Max, maximum
[#] SD, standard deviation
[††] CV, coefficient of variability

**Table 3.2.** Descriptive statistics of penetration resistance (N in m kg $s^{-2}$) on fields at Watkinsville for evaluated sample sizes on 10 May, 2013.

| Sample size | Sample Grid | Mean (±SE)[†‡] | Min[§] | Max[¶] | Range | SD[#] | CV[††] (%) | Skewness | Kurtosis |
|---|---|---|---|---|---|---|---|---|---|
| Watkinsville 1 | | | | | | | | | |
| | | Newton | | | | | | | |
| 1066 | 2.4 m x 2.4 m | 2419 ± 18a | 47 | 4666 | 4619 | 578 | 23.9 | -0.02 | 5.26 |
| 535 | 4.8 m x 2.4 m | 2434 ± 23a | 61 | 4666 | 4605 | 553 | 22.7 | 0.46 | 5.46 |
| 263 | 4.8 m x 4.8 m | 2425 ± 36a | 106 | 4246 | 4140 | 591 | 24.4 | -0.38 | 4.67 |
| 142 | 9.6 m x 4.8 m | 2289 ± 52b | 106 | 3761 | 3655 | 623 | 27.2 | -0.59 | 4.62 |
| 75 | 9.6 m x 9.6 m | 2320 ± 73ab | 289 | 3761 | 3472 | 635 | 27.4 | -0.61 | 4.41 |
| 43 | 19.2 m x 9.6 m | 2277 ± 109b | 289 | 3499 | 3210 | 716 | 31.5 | -0.77 | 3.98 |
| 24 | 19.2 m x 19.2 m | 2255 ± 144b | 315 | 3499 | 3184 | 705 | 31.3 | -0.47 | 3.89 |
| 7 | N/A | 2249 ± 224b | 968 | 2766 | 1798 | 593 | 26.4 | -1.64 | 4.38 |
| Watkinsville 2 | | | | | | | | | |
| | | Newton | | | | | | | |
| 1053 | 2.4 m x 2.4 m | 1677 ± 16a | 111 | 4684 | 4573 | 528 | 31.5 | 0.17 | 4.33 |
| 526 | 4.8 m x 2.4 m | 1696 ± 23a | 143 | 3704 | 3560 | 540 | 31.9 | 0.10 | 3.66 |
| 260 | 4.8 m x 4.8 m | 1688 ± 34a | 143 | 3327 | 3184 | 540 | 32.0 | -0.04 | 3.39 |
| 139 | 9.6 m x 4.8 m | 1717 ± 45a | 270 | 3327 | 3057 | 528 | 30.7 | 0.21 | 3.32 |
| 74 | 9.6 m x 9.6 m | 1742 ± 63a | 270 | 3327 | 3057 | 545 | 31.3 | 0.45 | 3.70 |
| 43 | 19.2 m x 9.6 m | 1719 ± 87a | 270 | 3327 | 3057 | 571 | 33.2 | 0.47 | 3.88 |
| 24 | 19.2 m x 19.2 m | 1758 ± 103a | 1003 | 3327 | 2324 | 505 | 28.7 | 1.29 | 5.07 |
| 7 | N/A | 1915 ± 145a | 1374 | 2393 | 1020 | 383 | 20.0 | -0.13 | 1.56 |
| Watkinsville 3 | | | | | | | | | |
| | | Newton | | | | | | | |
| 1101 | 2.4 m x 2.4 m | 2387 ± 13a | 1110 | 4404 | 3294 | 444 | 18.6 | 0.50 | 3.73 |
| 555 | 4.8 m x 2.4 m | 2374 ± 19a | 1110 | 4250 | 3141 | 446 | 18.8 | 0.40 | 3.55 |
| 283 | 4.8 m x 4.8 m | 2369 ± 27a | 1110 | 3743 | 2633 | 448 | 18.9 | 0.15 | 3.03 |
| 152 | 9.6 m x 4.8 m | 2320 ± 38a | 1110 | 3599 | 2490 | 465 | 20.1 | 0.17 | 3.11 |
| 76 | 9.6 m x 9.6 m | 2323 ± 54a | 1110 | 3599 | 2490 | 467 | 20.1 | -0.07 | 3.43 |
| 43 | 19.2 m x 9.6 m | 2180 ± 69a | 1110 | 2952 | 1843 | 449 | 20.6 | -0.48 | 2.65 |
| 24 | 19.2 m x 19.2 m | 2162 ± 95a | 1190 | 2952 | 1763 | 467 | 21.6 | -0.28 | 2.47 |
| 7 | N/A | 2521 ± 105a | 2197 | 2897 | 700 | 277 | 11.0 | 0.03 | 1.54 |

[†] Within columns, means followed by the same letter are not significantly different at $p \leq 0.05$ according to Fisher's Protected LSD test.
[‡] SE, standard error
[§] Min, minimum
[¶] Max, maximum
[#] SD, standard deviation
[††] CV, coefficient of variability

**Table 3.3.** Geostatistical model parameters for penetration resistance (N in m kg $s^{-2}$) on fields at Roswell for evaluated sample sizes on 9 May, 2013.

| Sample size | Sample Grid | Model | Nugget ($C_0$) | Sill ($C_0 + C$) | Nugget/Sill (%) | Spatial dependence[†] | Range (m) | ME[‡] | RMSE[§] | RMSSE[¶] |
|---|---|---|---|---|---|---|---|---|---|---|
| Roswell 1 | | | | | | | | | | |
| 1121 | 2.4 m x 2.4 m | Spherical | 56751 | 321954 | 17.6 | Strong | 20.8 | 1.0 | 327.2 | 1.02 |
| 584 | 4.8 m x 2.4 m | Spherical | 47732 | 306866 | 15.6 | Strong | 20.3 | 1.3 | 315.4 | 0.97 |
| 295 | 4.8 m x 4.8 m | Spherical | 52340 | 359339 | 14.6 | Strong | 25.6 | 1.4 | 345.6 | 0.94 |
| 160 | 9.6 m x 4.8 m | Spherical | 78871 | 353984 | 22.3 | Strong | 22.4 | 0.4 | 372.8 | 0.85 |
| 83 | 9.6 m x 9.6 m | Spherical | 165050 | 393757 | 41.9 | Moderate | 22.6 | -1.7 | 530.0 | 0.93 |
| 47 | 19.2 m x 9.6 m | Spherical | 51242 | 174573 | 29.4 | Moderate | 27.0 | 2.2 | 362.1 | 0.99 |
| 24 | 19.2 m x 19.2 m | Spherical | 71102 | 88958 | 79.9 | Weak | 37.1 | 0.4 | 295.2 | 1.00 |
| 7 | N/A | Spherical | 859878 | 859878 | 100 | Weak | 86.7 | 0 | 858.5 | 0.93 |
| Roswell 2 | | | | | | | | | | |
| 1189 | 2.4 m x 2.4 m | Spherical | 57714 | 123695 | 46.7 | Moderate | 65.2 | 0.0 | 257.2 | 1.01 |
| 616 | 4.8 m x 2.4 m | Spherical | 59471 | 120312 | 49.4 | Moderate | 68.4 | -1.4 | 258.8 | 0.99 |
| 308 | 4.8 m x 4.8 m | Spherical | 60142 | 114591 | 52.5 | Moderate | 60.6 | -0.7 | 265.6 | 0.99 |
| 154 | 9.6 m x 4.8 m | Spherical | 50785 | 115235 | 44.1 | Moderate | 70.1 | -0.3 | 258.1 | 1.01 |
| 77 | 9.6 m x 9.6 m | Spherical | 60625 | 125183 | 48.4 | Moderate | 80.4 | -1.2 | 297.0 | 1.05 |
| 44 | 19.2 m x 9.6 m | Spherical | 72881 | 113637 | 64.1 | Moderate | 87.8 | 4.0 | 311.6 | 1.06 |
| 24 | 19.2 m x 19.2 m | Spherical | 68365 | 121426 | 56.3 | Moderate | 97.6 | 4.5 | 328.0 | 1.07 |
| 7 | N/A | Spherical | 58589 | 83721 | 70.0 | Moderate | 85.8 | 22.8 | 251.3 | 0.90 |
| Roswell 3 | | | | | | | | | | |
| 997 | 2.4 m x 2.4 m | Spherical | 28866 | 50410 | 57.3 | Moderate | 8.1 | 1.5 | 202.1 | 1.00 |
| 519 | 4.8 m x 2.4 m | Spherical | 22962 | 50961 | 45.1 | Moderate | 13.6 | 1.9 | 193.7 | 1.04 |
| 259 | 4.8 m x 4.8 m | Spherical | 33975 | 44780 | 75.9 | Weak | 34.4 | 2.5 | 193.8 | 0.99 |
| 139 | 9.6 m x 4.8 m | Spherical | 26709 | 49077 | 54.4 | Moderate | 23.4 | 2.5 | 201.2 | 1.02 |
| 70 | 9.6 m x 9.6 m | Spherical | 26097 | 44663 | 58.4 | Moderate | 18.8 | 5.3 | 194.9 | 0.95 |
| 40 | 19.2 m x 9.6 m | Spherical | 26447 | 57095 | 46.3 | Moderate | 27.1 | 7.5 | 206.2 | 0.93 |
| 20 | 19.2 m x 19.2 m | Spherical | 54637 | 54637 | 100 | Weak | 74.5 | 0 | 227.8 | 0.97 |
| 7 | N/A | Spherical | 120576 | 120576 | 100 | Weak | 88.8 | 0 | 321.5 | 0.93 |

[†] Spatial dependence is described as strong, moderate, or weak for nugget/sill ratios <25%, 25-75%, or >75%, respectively.
[‡] ME, mean prediction error.
[§] RMSE, root-mean square prediction error.
[¶] RMSSE, root-mean square standardized prediction error.

**Table 3.4.** Geostatistical model parameters for penetration resistance (N in m kg $s^{-2}$) on fields at Watkinsville for evaluated sample sizes on 10 May, 2013.

| Sample size | Sample Grid | Model | Nugget ($C_0$) | Sill ($C_0 + C$) | Nugget/Sill (%) | Spatial dependence[†] | Range (m) | ME[‡] | RMSE[§] | RMSSE[¶] |
|---|---|---|---|---|---|---|---|---|---|---|
| ----------Watkinsville 1---------- | | | | | | | | | | |
| 1066 | 2.4 m x 2.4 m | Spherical | 178149 | 315995 | 56.4 | Moderate | 26.6 | 5.2 | 491.4 | 1.07 |
| 535 | 4.8 m x 2.4 m | Spherical | 154206 | 305483 | 50.5 | Moderate | 15.1 | 4.2 | 473.9 | 1.02 |
| 263 | 4.8 m x 4.8 m | Spherical | 222946 | 346790 | 64.3 | Moderate | 46.3 | 7.2 | 517.6 | 1.01 |
| 142 | 9.6 m x 4.8 m | Spherical | 265872 | 384877 | 69.1 | Moderate | 41.4 | 6.8 | 557.0 | 0.99 |
| 75 | 9.6 m x 9.6 m | Spherical | 251589 | 431846 | 58.3 | Moderate | 68.3 | 6.4 | 584.1 | 1.04 |
| 43 | 19.2 m x 9.6 m | Spherical | 344828 | 557095 | 61.9 | Moderate | 76.0 | 0.8 | 676.1 | 1.02 |
| 24 | 19.2 m x 19.2 m | Spherical | 262627 | 599859 | 43.8 | Moderate | 97.6 | 4.6 | 710.5 | 1.11 |
| 7 | N/A | Spherical | 351459 | 351459 | 100 | Weak | 82.6 | 0 | 548.9 | 0.93 |
| ----------Watkinsville 2---------- | | | | | | | | | | |
| 1053 | 2.4 m x 2.4 m | Spherical | 127110 | 278939 | 45.6 | Moderate | 47.3 | 0.2 | 390.3 | 1.02 |
| 526 | 4.8 m x 2.4 m | Spherical | 106563 | 292737 | 36.4 | Moderate | 37.5 | 0.1 | 403.1 | 1.08 |
| 260 | 4.8 m x 4.8 m | Spherical | 148770 | 372112 | 40.0 | Moderate | 85.1 | -0.9 | 440.4 | 1.04 |
| 139 | 9.6 m x 4.8 m | Spherical | 182796 | 328491 | 55.6 | Moderate | 78.7 | -1.3 | 418.3 | 0.90 |
| 74 | 9.6 m x 9.6 m | Spherical | 169828 | 329894 | 51.5 | Moderate | 58.3 | 1.1 | 501.8 | 1.05 |
| 43 | 19.2 m x 9.6 m | Spherical | 215246 | 362373 | 59.4 | Moderate | 73.0 | -1.9 | 555.1 | 1.05 |
| 24 | 19.2 m x 19.2 m | Spherical | 109696 | 298562 | 36.7 | Moderate | 76.4 | -0.2 | 459.1 | 1.03 |
| 7 | N/A | Spherical | 125921 | 125921 | 100 | Weak | 95.4 | 0 | 354.9 | 1.00 |
| ----------Watkinsville 3---------- | | | | | | | | | | |
| 1101 | 2.4 m x 2.4 m | Spherical | 110344 | 178825 | 61.7 | Moderate | 13.1 | 5.7 | 378.8 | 1.02 |
| 555 | 4.8 m x 2.4 m | Spherical | 116523 | 186313 | 62.5 | Moderate | 16.6 | 9.9 | 380.3 | 0.99 |
| 283 | 4.8 m x 4.8 m | Spherical | 118363 | 196109 | 60.4 | Moderate | 25.0 | 12.6 | 391.4 | 1.01 |
| 152 | 9.6 m x 4.8 m | Spherical | 114225 | 200729 | 56.9 | Moderate | 19.2 | 11.8 | 407.7 | 0.99 |
| 76 | 9.6 m x 9.6 m | Spherical | 157926 | 248079 | 63.7 | Moderate | 84.5 | 21.6 | 452.6 | 1.04 |
| 43 | 19.2 m x 9.6 m | Spherical | 129884 | 230310 | 56.4 | Moderate | 87.8 | 21.5 | 435.8 | 1.06 |
| 24 | 19.2 m x 19.2 m | Spherical | 164670 | 244034 | 67.5 | Moderate | 97.6 | 29.0 | 493.9 | 1.08 |
| 7 | N/A | Spherical | 76718 | 76718 | 100 | Weak | 88.5 | 0 | 256.4 | 0.93 |

[†] Spatial dependence is described as strong, moderate, or weak for nugget/sill ratios <25%, 25-75%, or >75%, respectively.
[‡] ME, mean prediction error.
[§] RMSE, root-mean square prediction error.
[¶] RMSSE, root-mean square standardized prediction error.

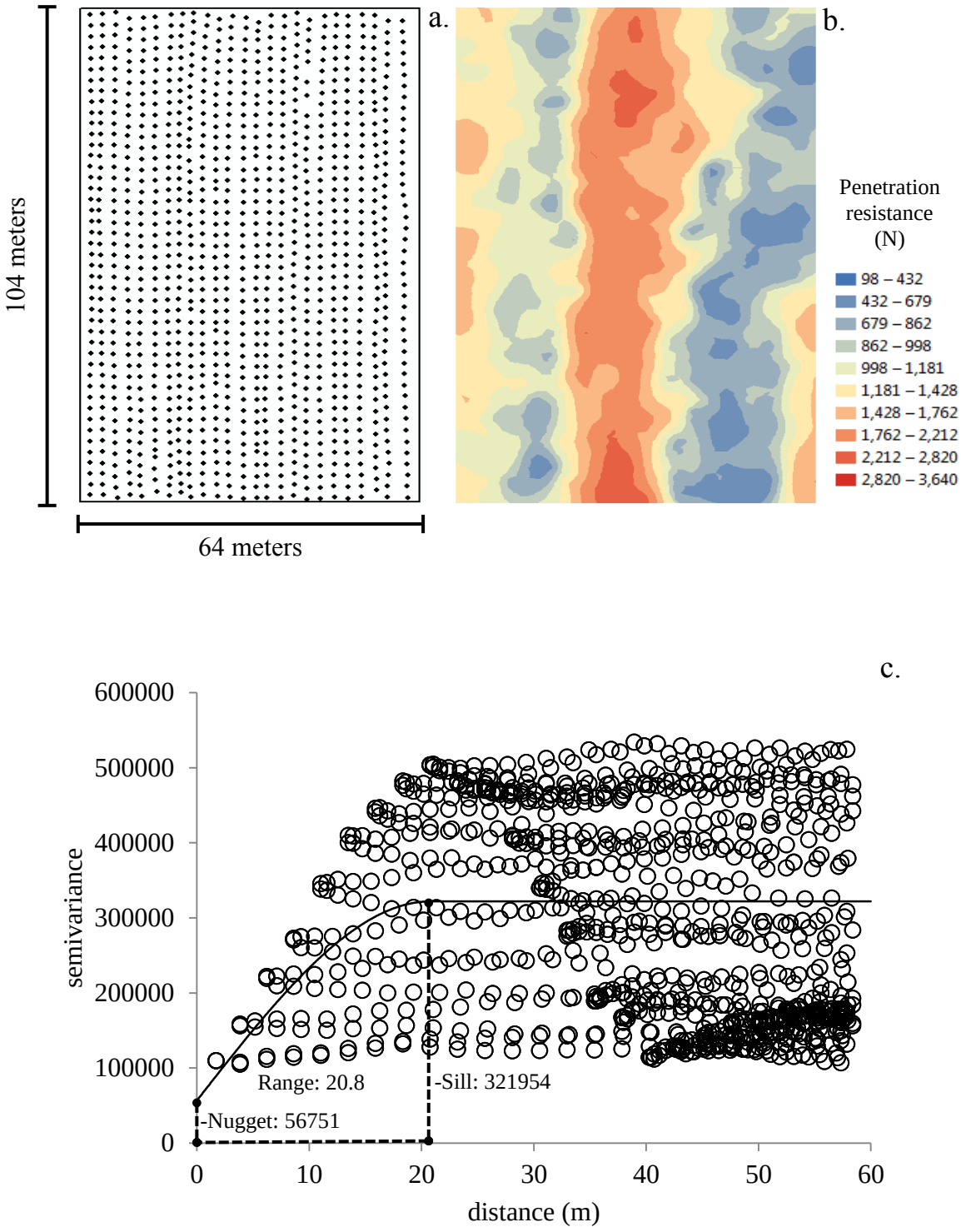


Figure 3.1. (a) Sampling locations (approximately 2.4 m x 2.4 m grid; 1121 samples), (b) kriged prediction map and (c) semivariogram including the fitted spherical model of penetration resistance on Roswell field 1.

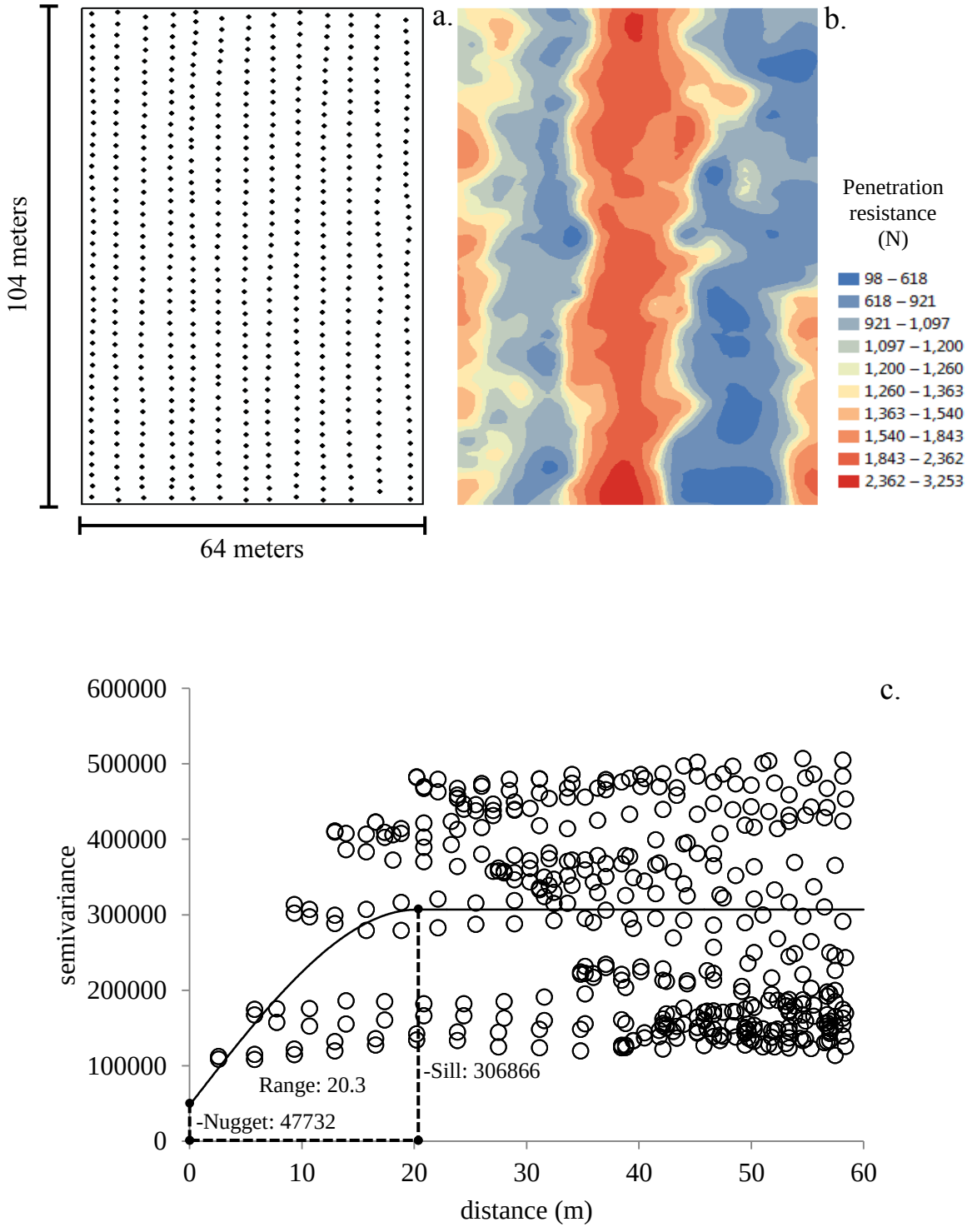


Figure 3.2. (a) Sampling locations (approximately 4.8 m x 2.4 m grid; 584 samples), (b) kriged prediction map and (c) semivariogram including the fitted spherical model of penetration resistance on Roswell field 1.

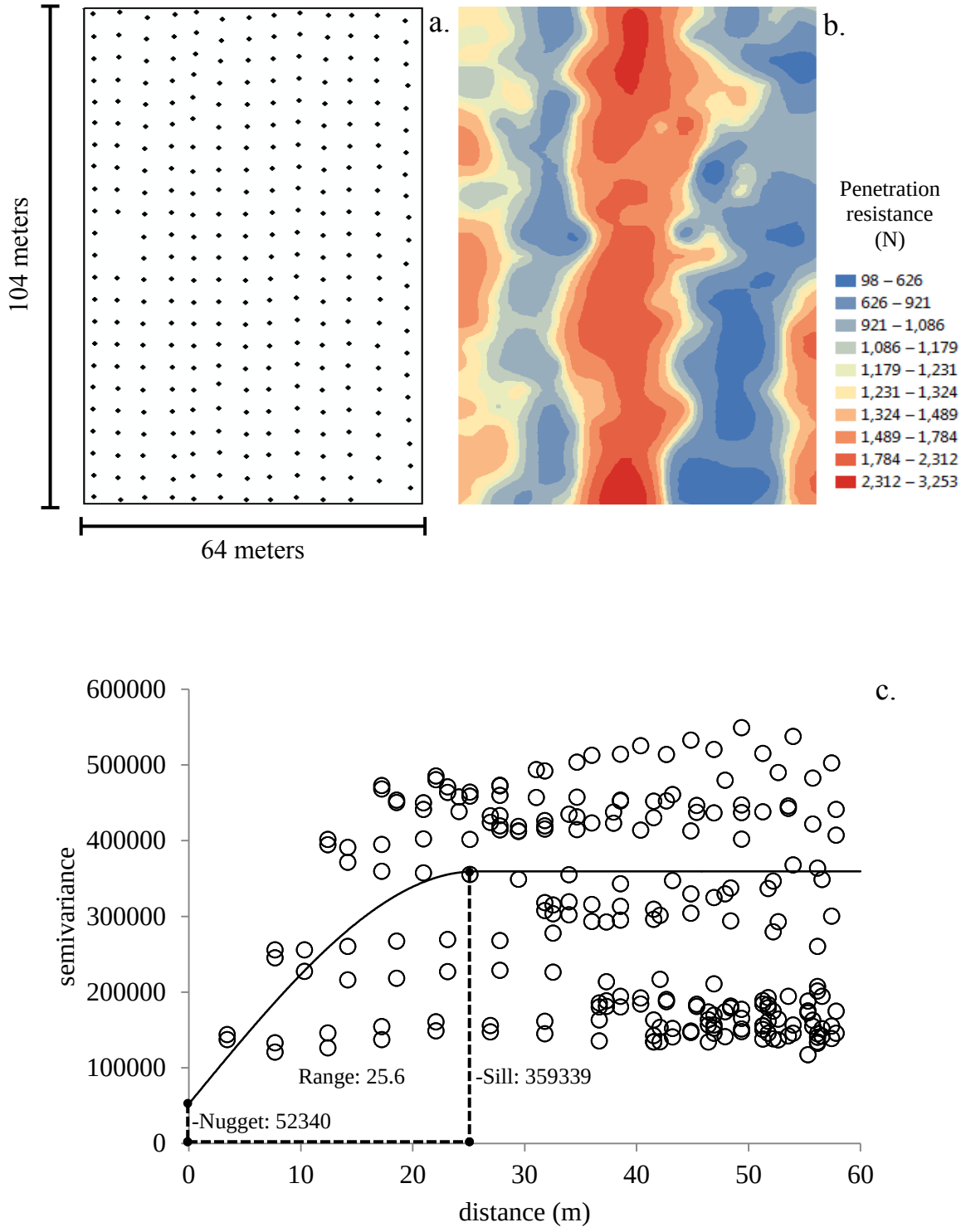


Figure 3.3. (a) Sampling locations (approximately 4.8 m x 4.8 m grid; 295 samples), (b) kriged prediction map and (c) semivariogram including the fitted spherical model of penetration resistance on Roswell field 1.

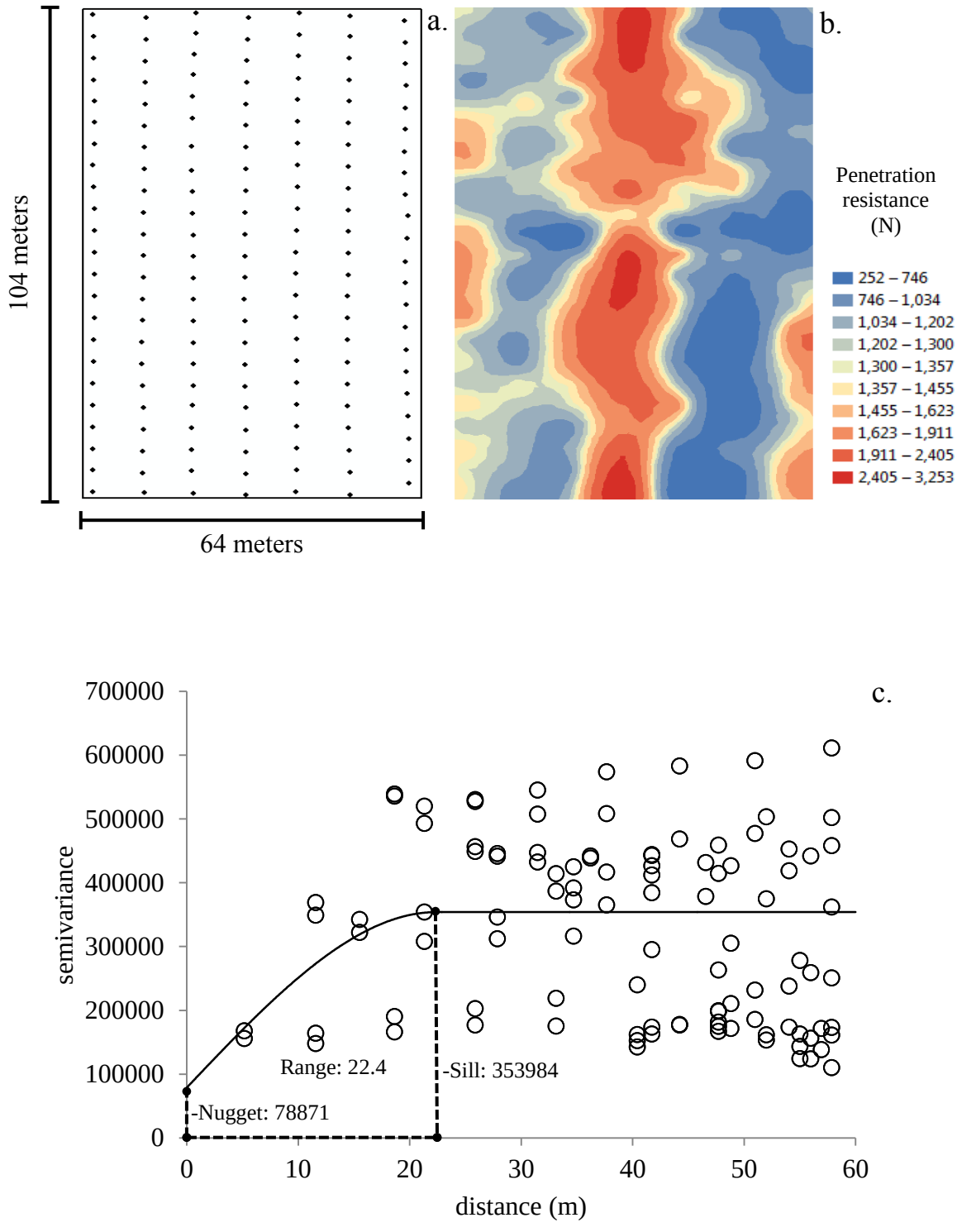


Figure 3.4. (a) Sampling locations (approximately 9.6 m x 4.8 m grid; 160 samples), (b) kriged prediction map and (c) semivariogram including the fitted spherical model of penetration resistance on Roswell field 1.

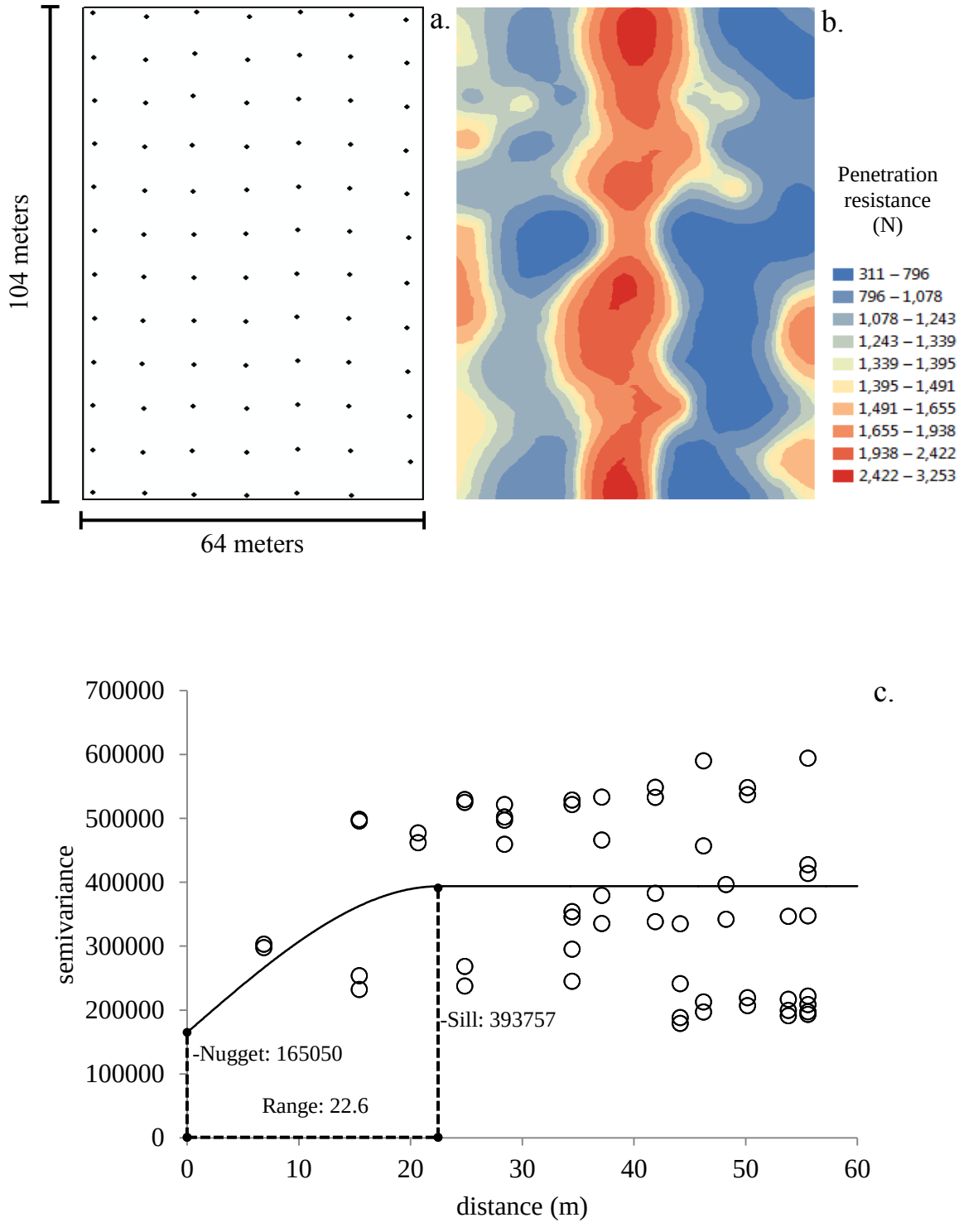


Figure 3.5. (a) Sampling locations (approximately 9.6 m x 9.6 m grid; 83 samples), (b) kriged prediction map and (c) semivariogram including the fitted spherical model of penetration resistance on Roswell field 1.

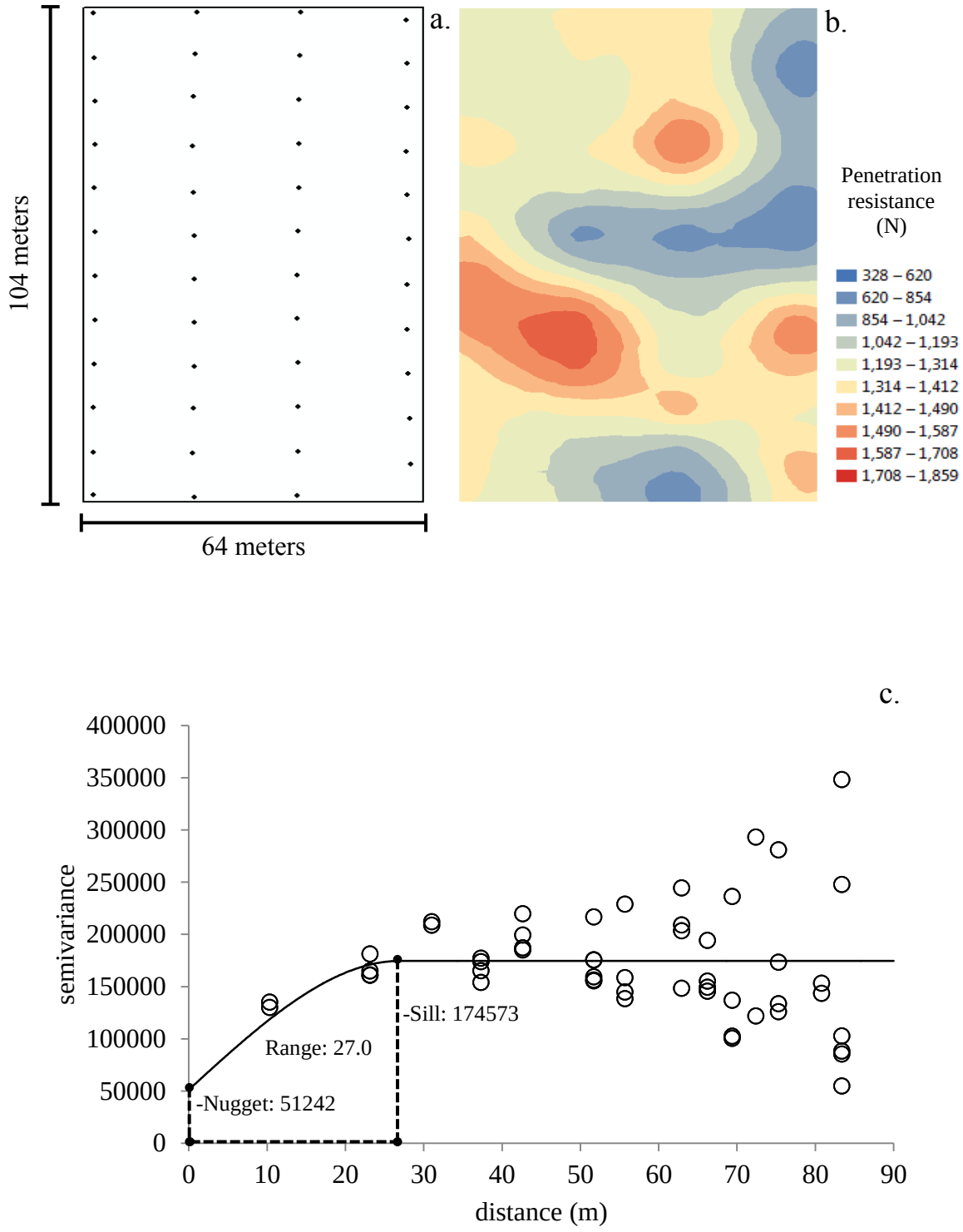


Figure 3.6. (a) Sampling locations (approximately 19.2 m x 9.6 m grid; 47 samples), (b) kriged prediction map and (c) semivariogram including the fitted spherical model of penetration resistance on Roswell field 1.

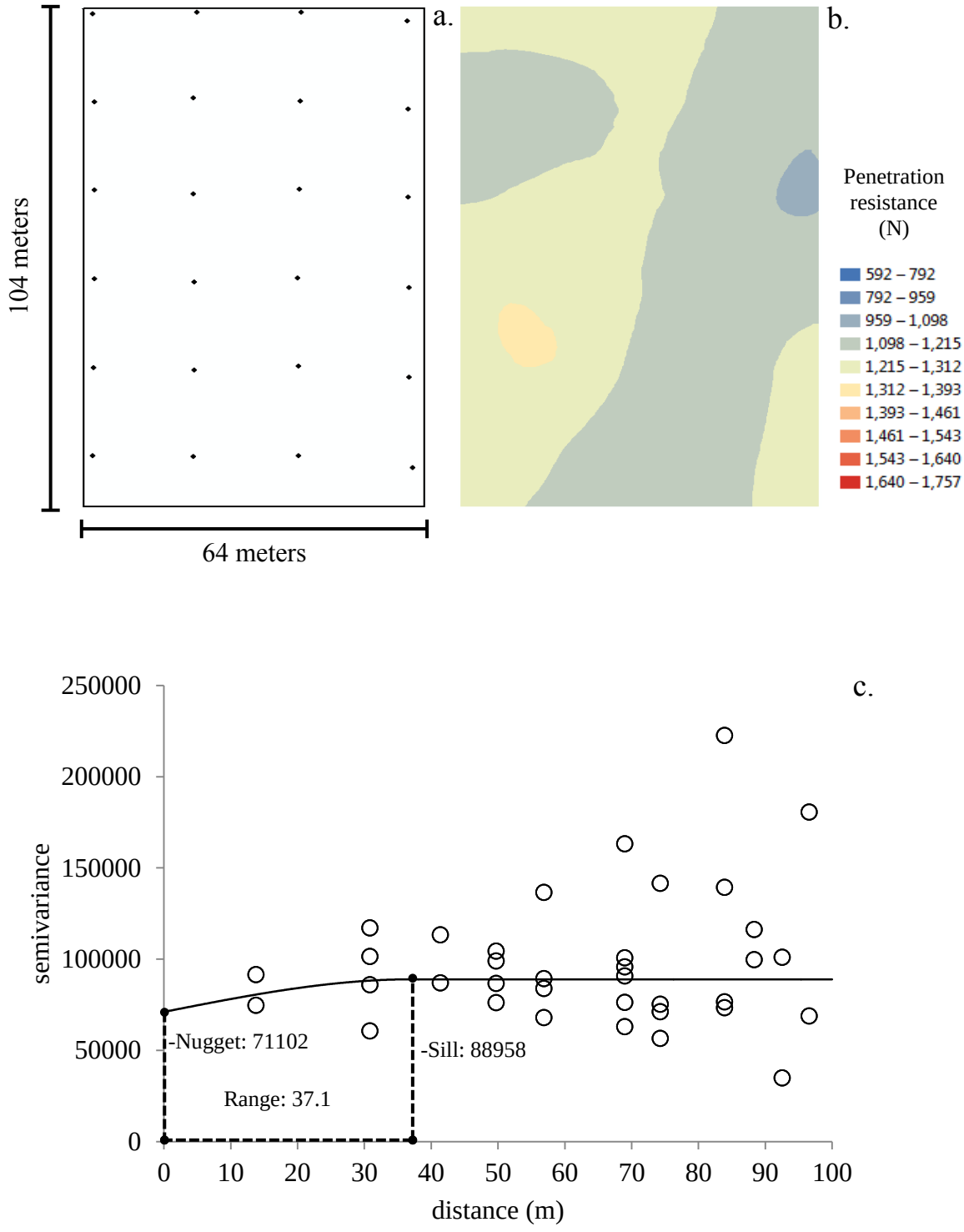


Figure 3.7. (a) Sampling locations (approximately 19.2 m x 19.2 m grid; 24 samples), (b) kriged prediction map and (c) semivariogram including the fitted spherical model of penetration resistance on Roswell field 1.

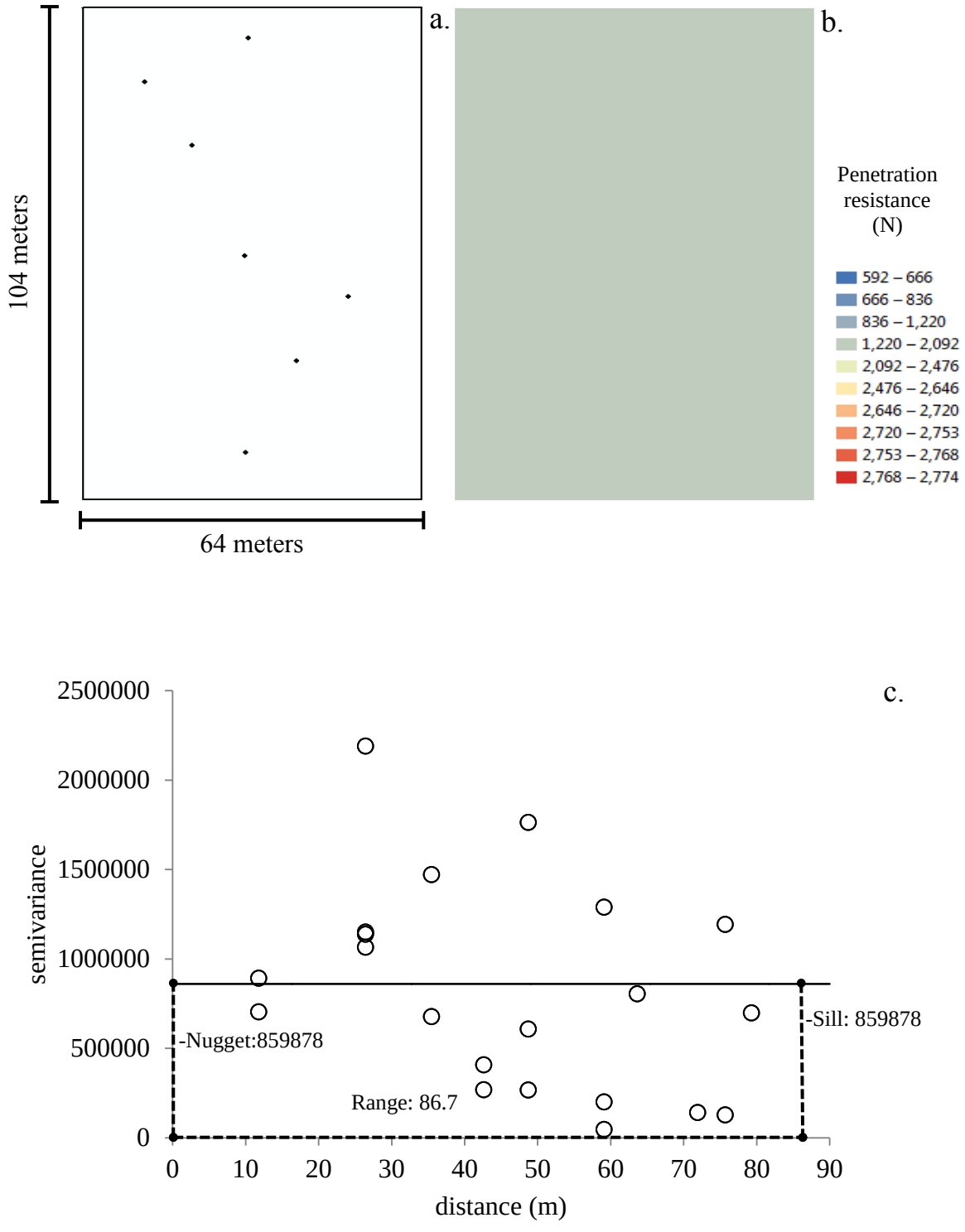


Figure 3.8. (a) Sampling locations (7 samples), (b) kriged prediction map and (c) semivariogram including the fitted spherical model of penetration resistance on Roswell field 1.

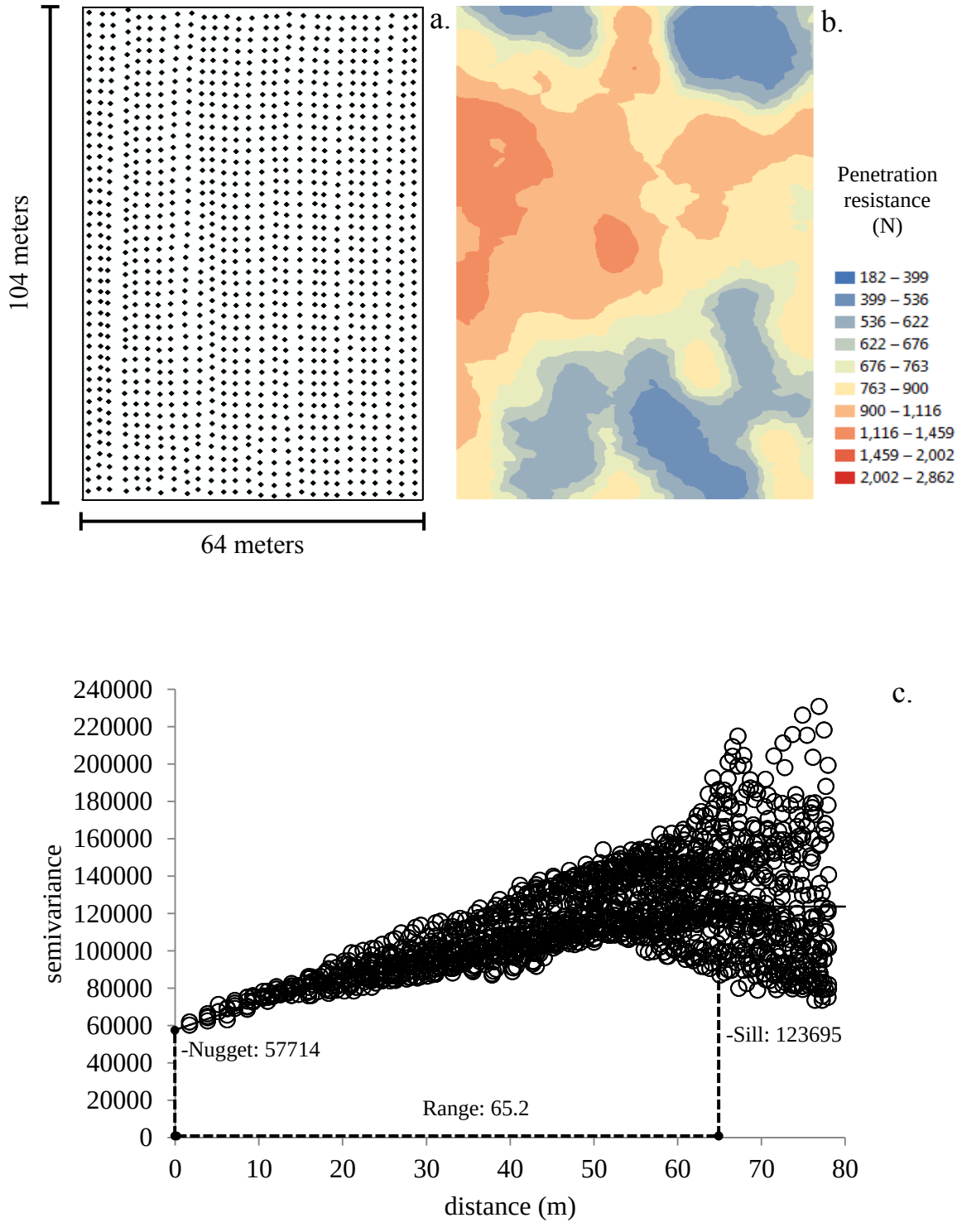


Figure 3.9. (a) Sampling locations (approximately 2.4 m x 2.4 m grid; 1189 samples), (b) kriged prediction map and (c) semivariogram including the fitted spherical model of penetration resistance on Roswell field 2.

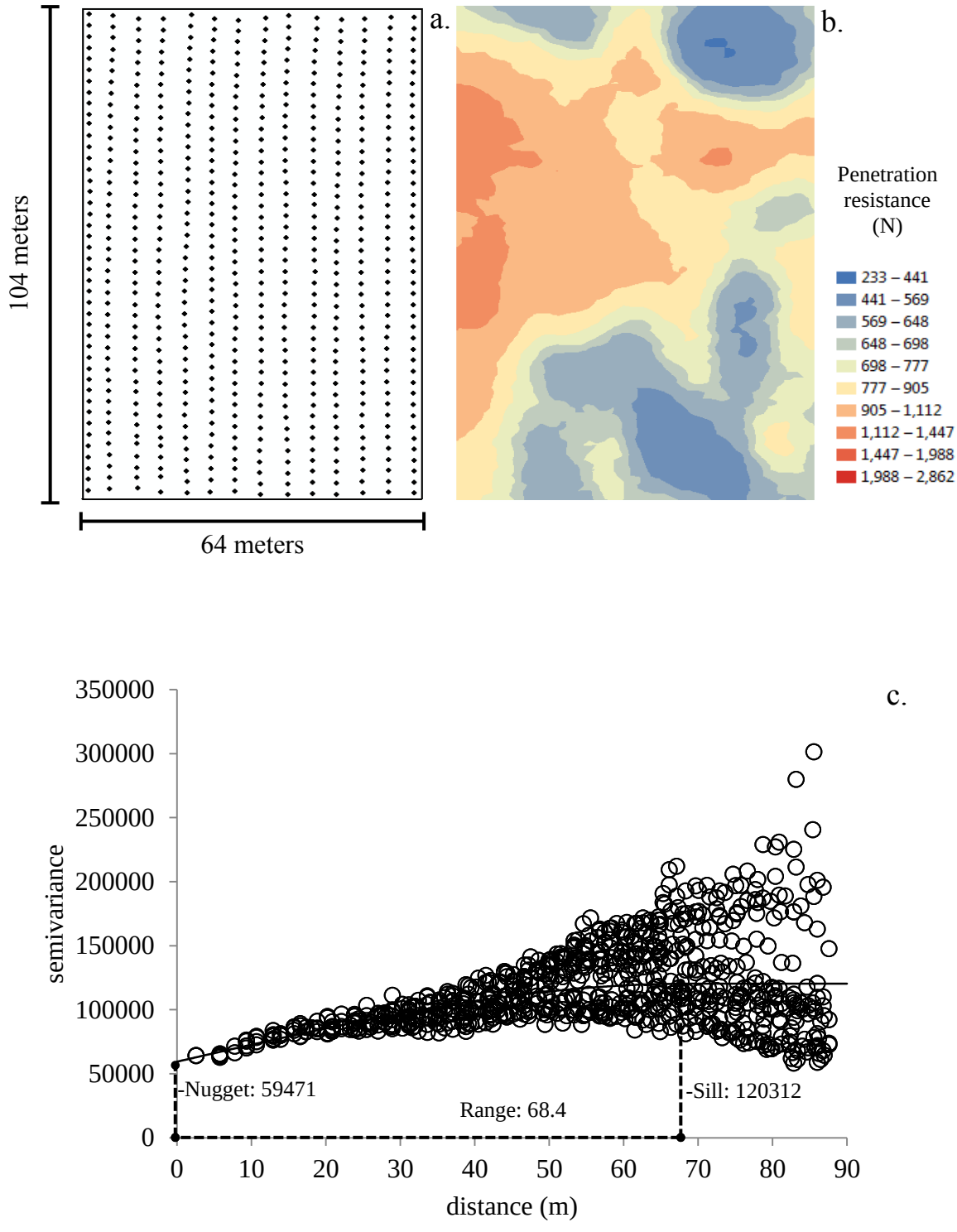


Figure 3.10. (a) Sampling locations (approximately 4.8 m x 2.4 m grid; 616 samples), (b) kriged prediction map and (c) semivariogram including the fitted spherical model of penetration resistance on Roswell field 2.

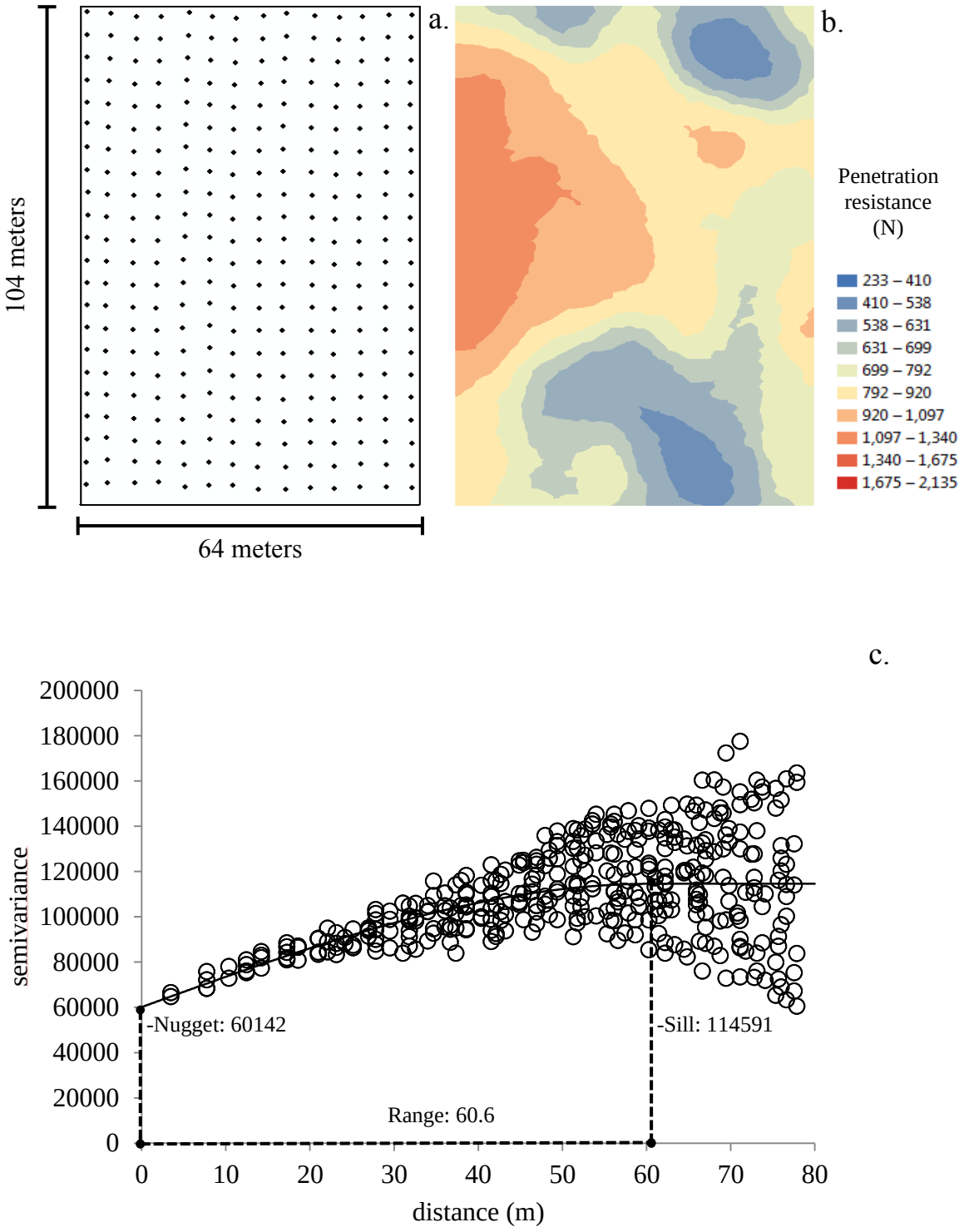


Figure 3.11. (a) Sampling locations (approximately 4.8 m x 4.8 m grid; 308 samples), (b) kriged prediction map and (c) semivariogram including the fitted spherical model of penetration resistance on Roswell field 2.

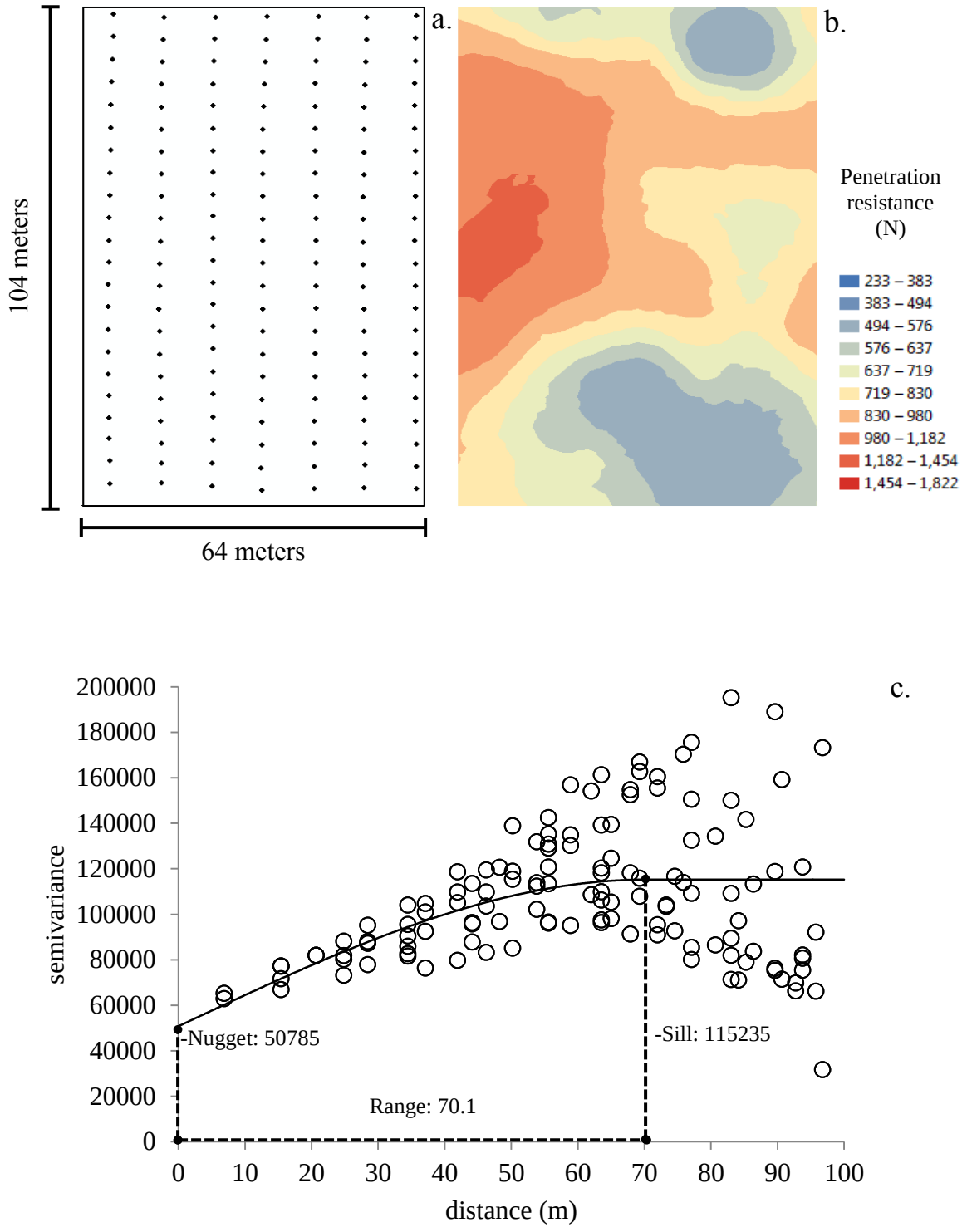


Figure 3.12. (a) Sampling locations (approximately 9.6 m x 4.8 m grid; 154 samples), (b) kriged prediction map and (c) semivariogram including the fitted spherical model of penetration resistance on Roswell field 2.

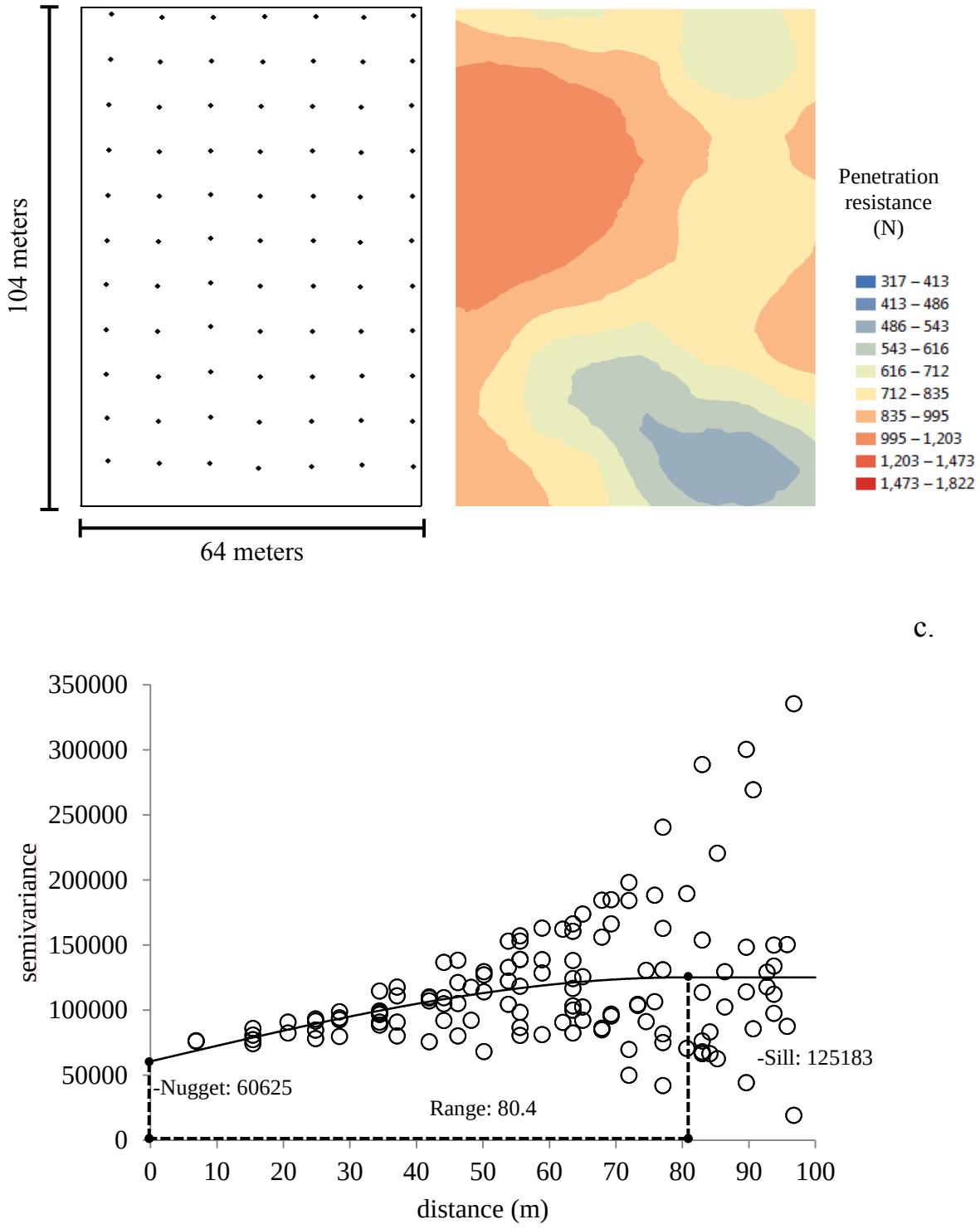


Figure 3.13. (a) Sampling locations (approximately 9.6 m x 9.6 m grid; 77 samples), (b) kriged prediction map and (c) semivariogram including the fitted spherical model of penetration resistance on Roswell field 2.

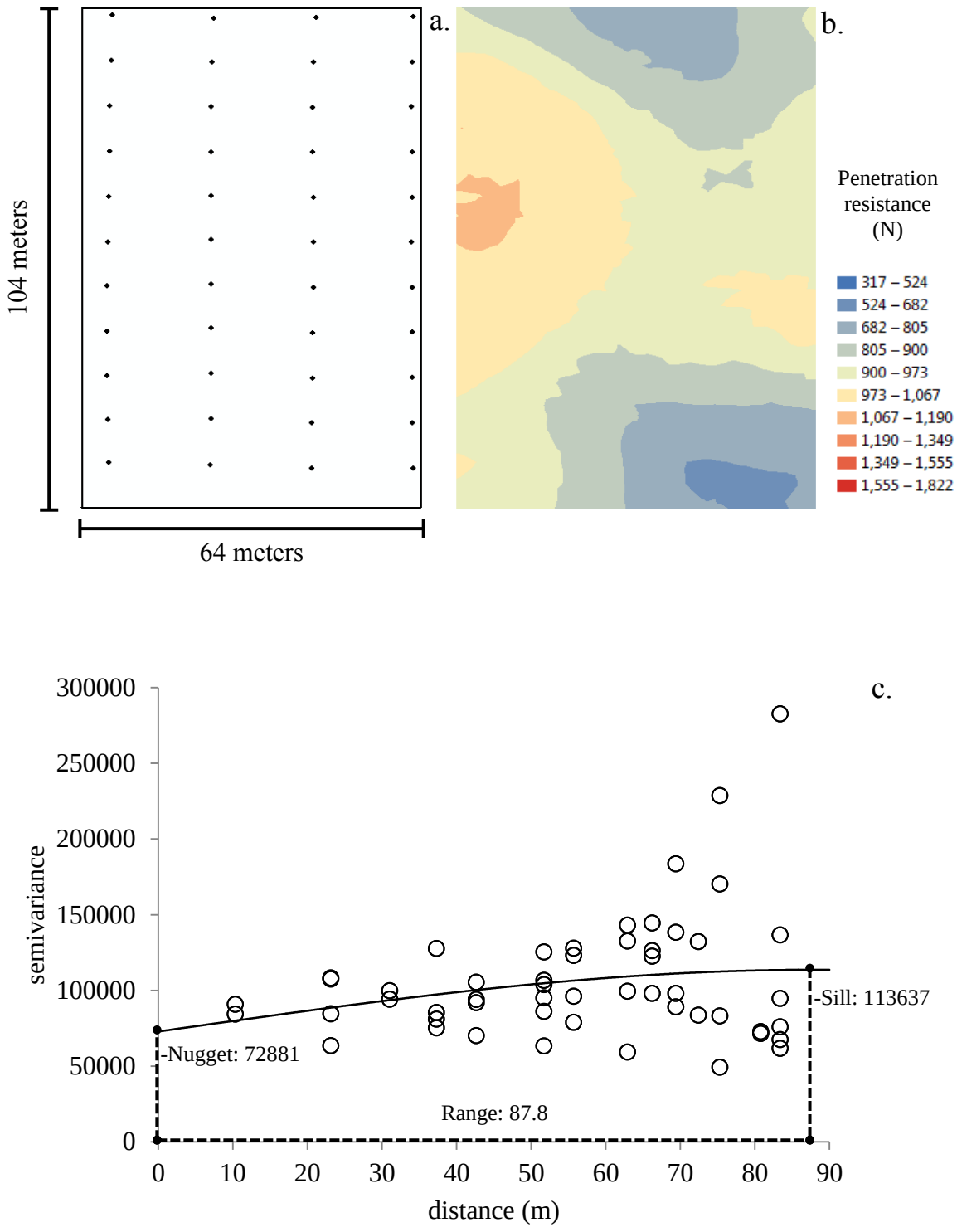


Figure 3.14. (a) Sampling locations (approximately 19.2 m x 9.6 m grid; 44 samples), (b) kriged prediction map and (c) semivariogram including the fitted spherical model of penetration resistance on Roswell field 2.

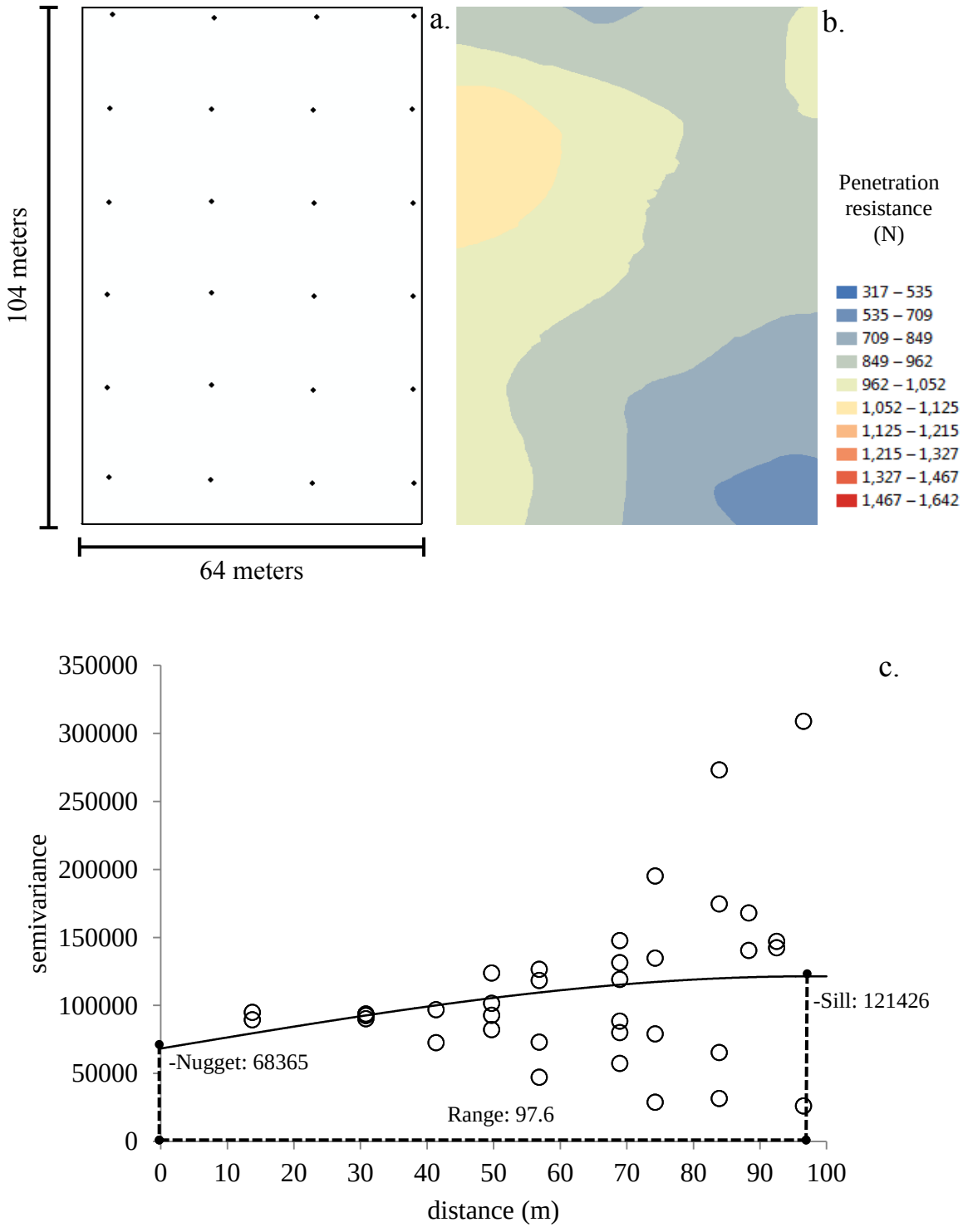


Figure 3.15. (a) Sampling locations (approximately 19.2 m x 19.2 m grid; 24 samples), (b) kriged prediction map and (c) semivariogram including the fitted spherical model of penetration resistance on Roswell field 2.

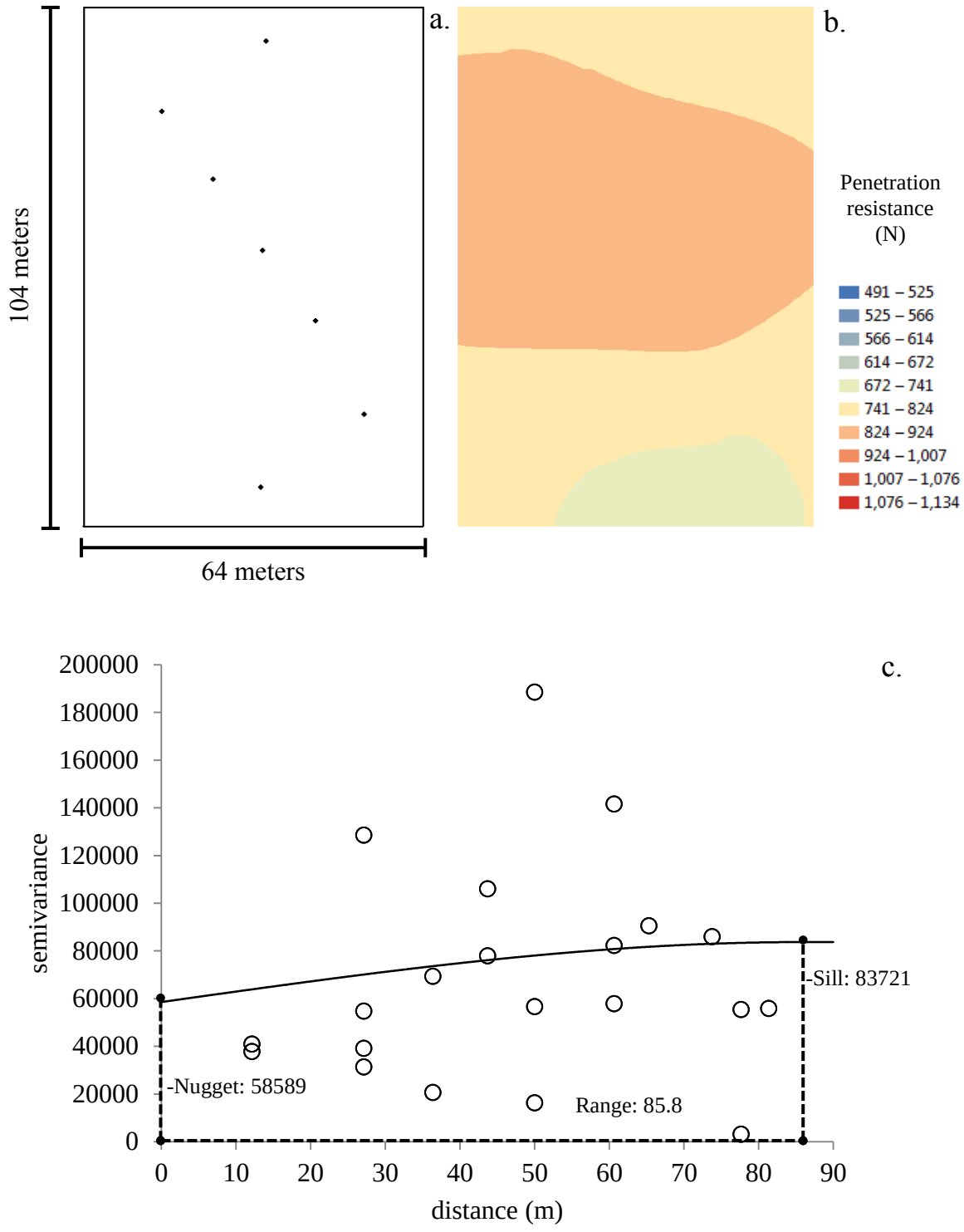


Figure 3.16. (a) Sampling locations (7 samples), (b) kriged prediction map and (c) semivariogram including the fitted spherical model of penetration resistance on Roswell field 2.

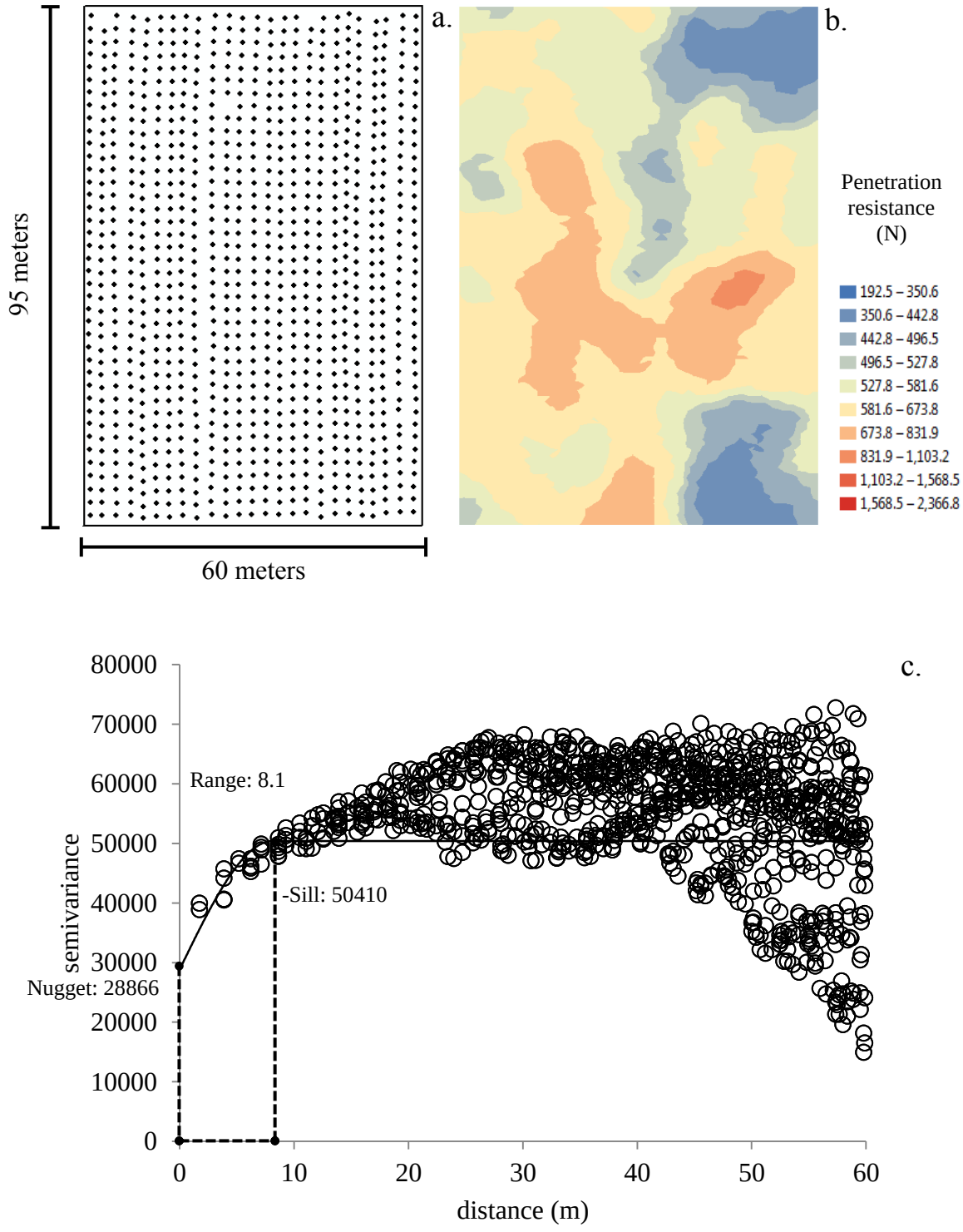


Figure 3.17. (a) Sampling locations (approximately 2.4 m x 2.4 m grid; 997 samples), (b) kriged prediction map and (c) semivariogram including the fitted spherical model of penetration resistance on Roswell field 3.

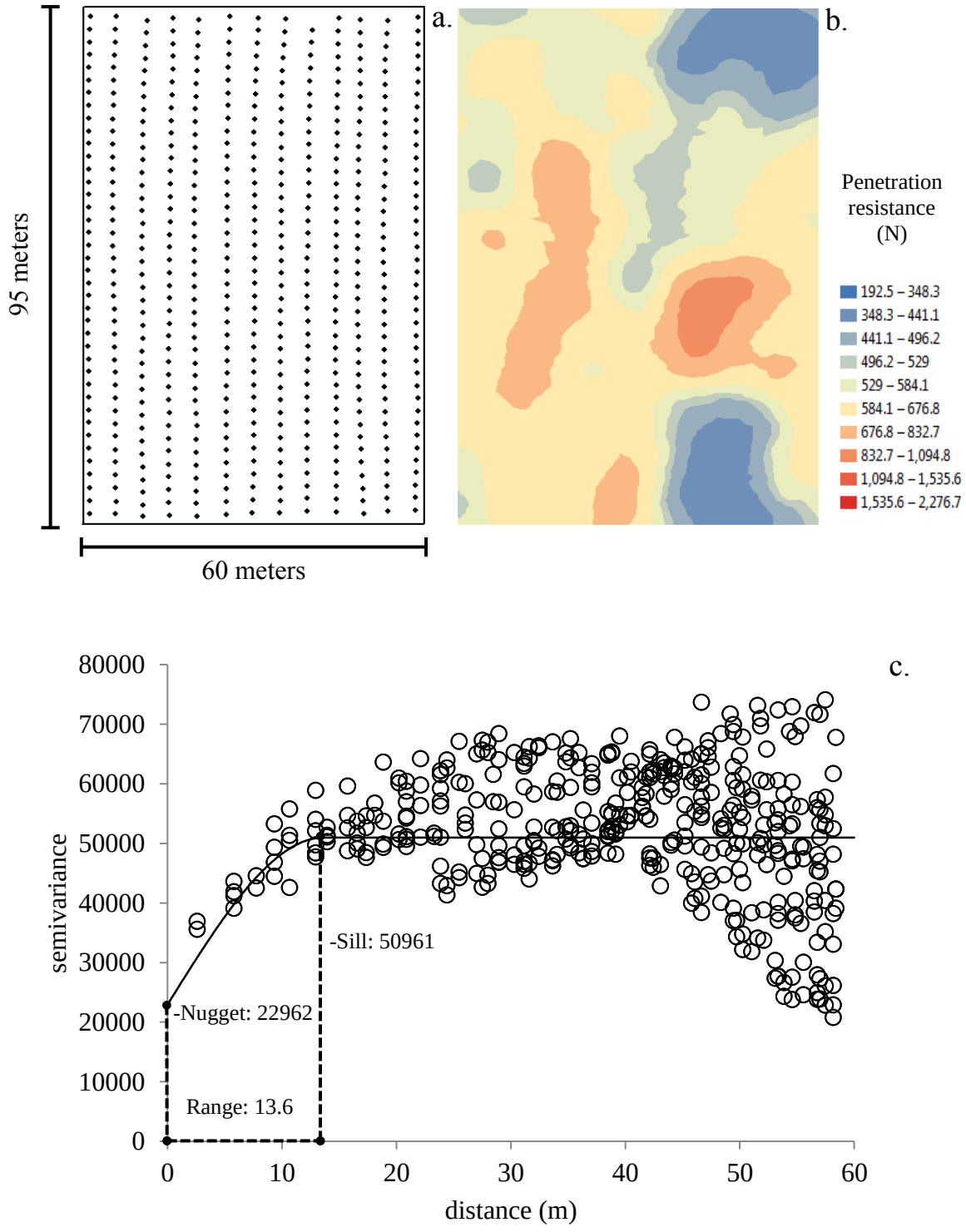


Figure 3.18. (a) Sampling locations (approximately 4.8 m x 2.4 m grid; 519 samples), (b) kriged prediction map and (c) semivariogram including the fitted spherical model of penetration resistance on Roswell field 3.

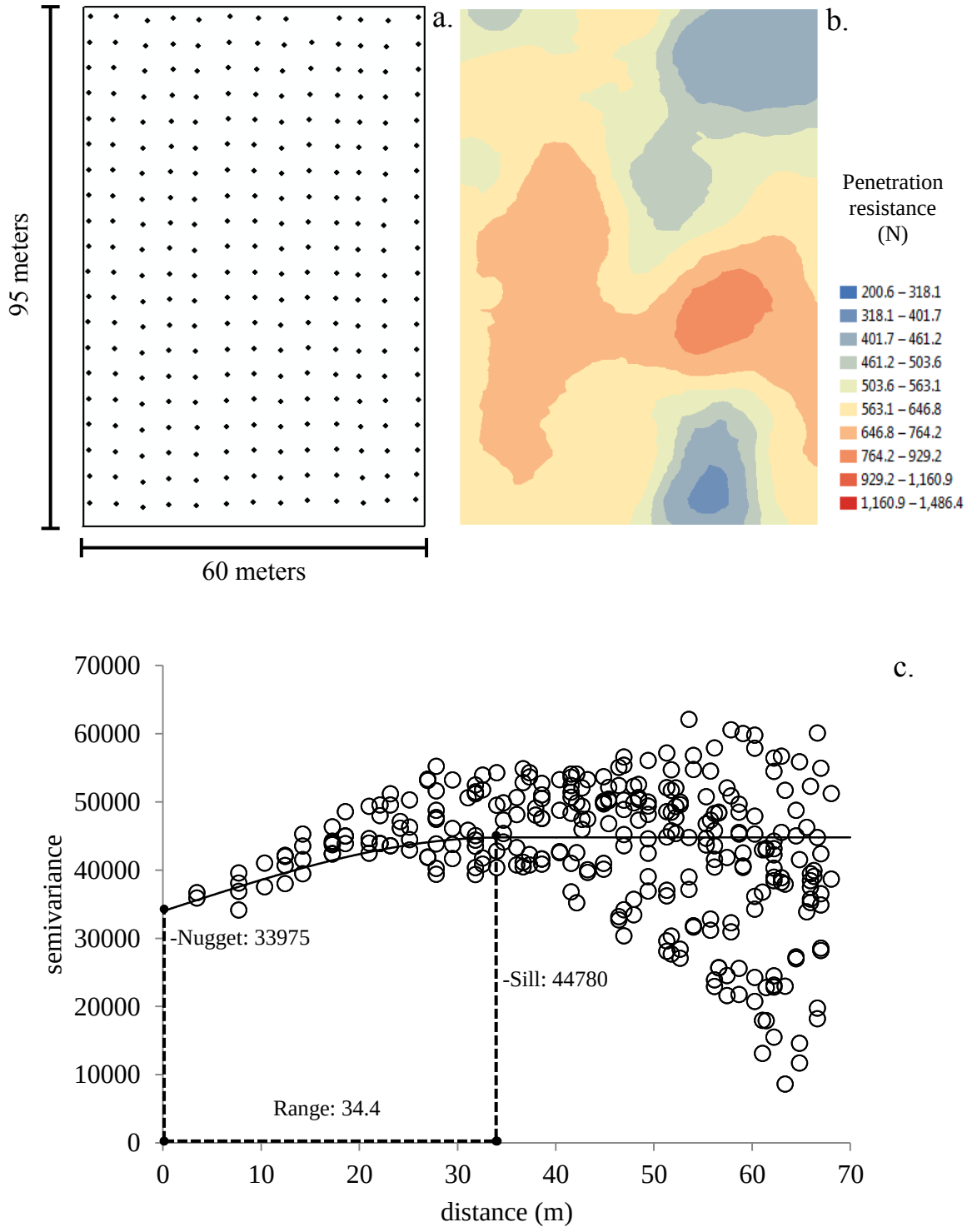


Figure 3.19. (a) Sampling locations (approximately 4.8 m x 4.8 m grid; 259 samples), (b) kriged prediction map and (c) semivariogram including the fitted spherical model of penetration resistance on Roswell field 3.

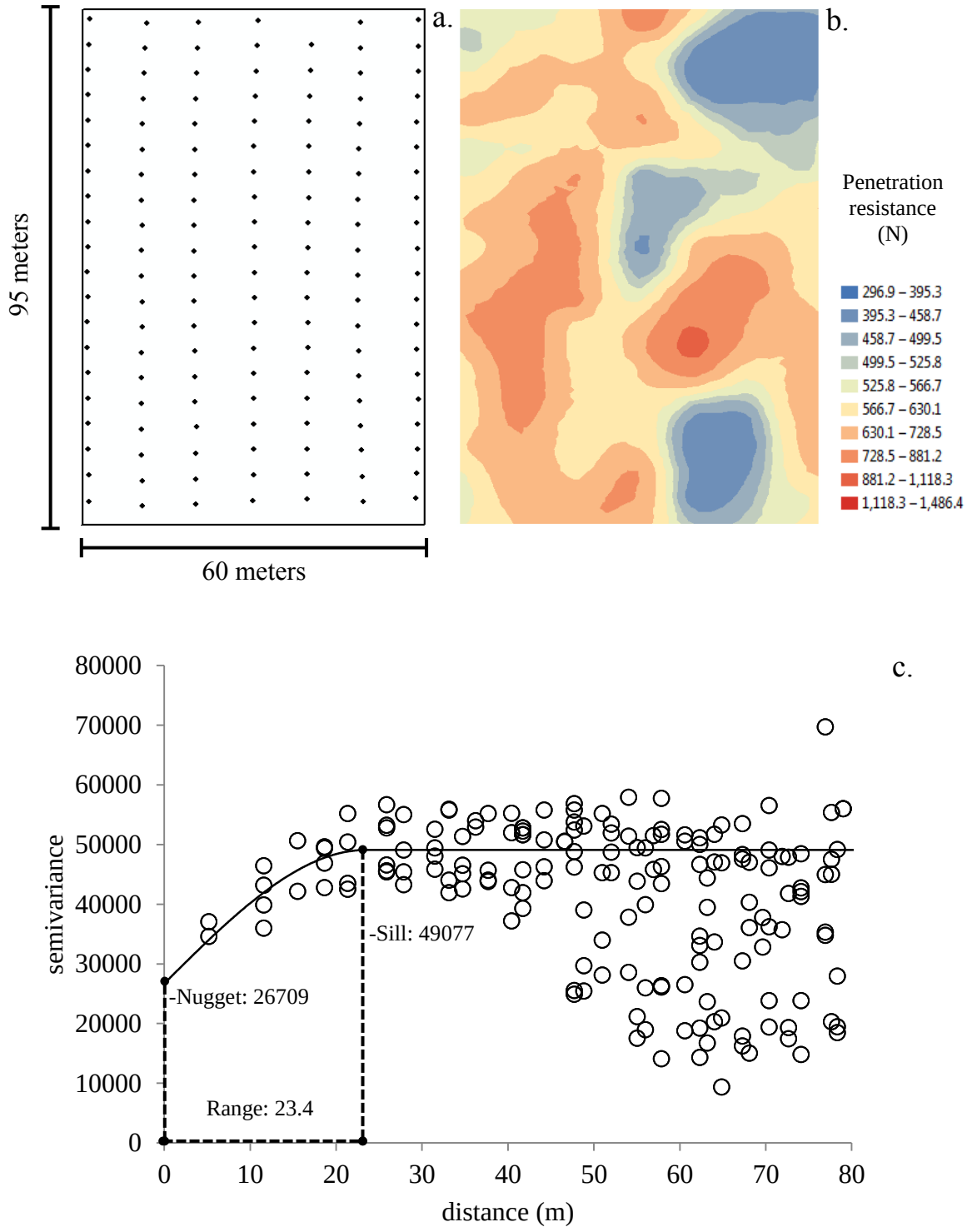


Figure 3.20. (a) Sampling locations (approximately 9.6 m x 4.8 m grid; 139 samples), (b) kriged prediction map and (c) semivariogram including the fitted spherical model of penetration resistance on Roswell field 3.

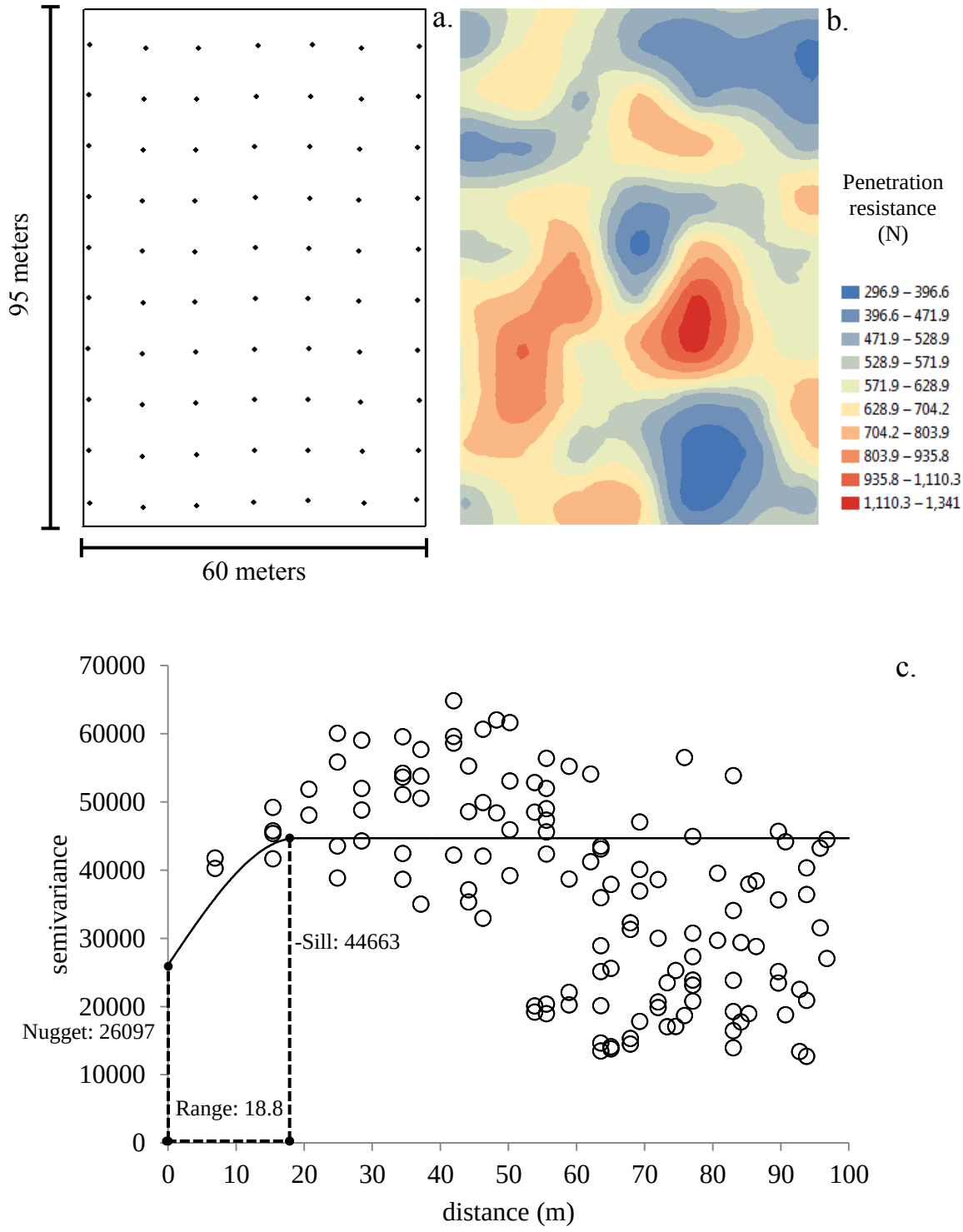


Figure 3.21. (a) Sampling locations (approximately 9.6 m x 9.6 m grid; 70 samples), (b) kriged prediction map and (c) semivariogram including the fitted spherical model of penetration resistance on Roswell field 3.

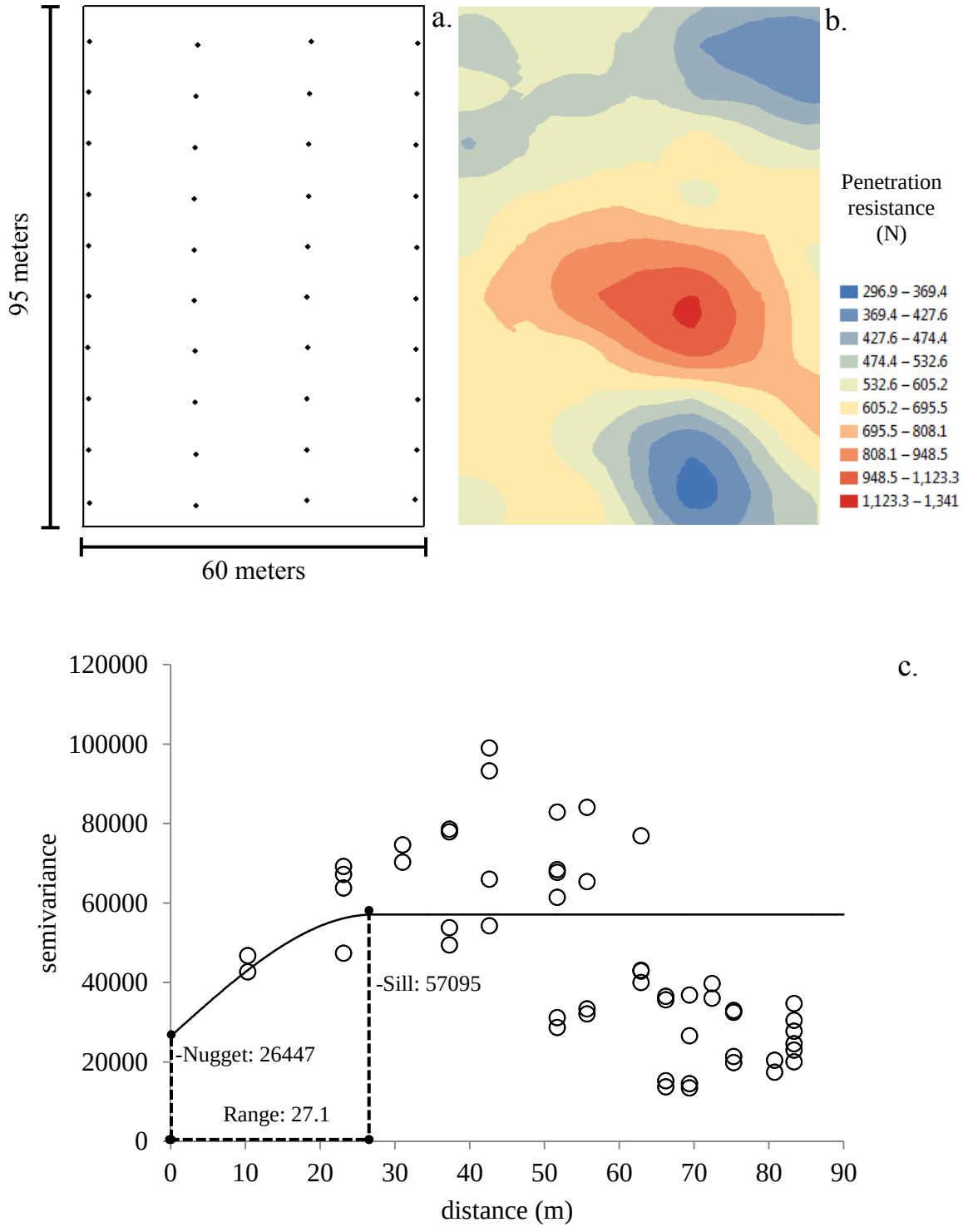


Figure 3.22. (a) Sampling locations (approximately 19.2 m x 9.6 m grid; 40 samples), (b) kriged prediction map and (c) semivariogram including the fitted spherical model of penetration resistance on Roswell field 3.

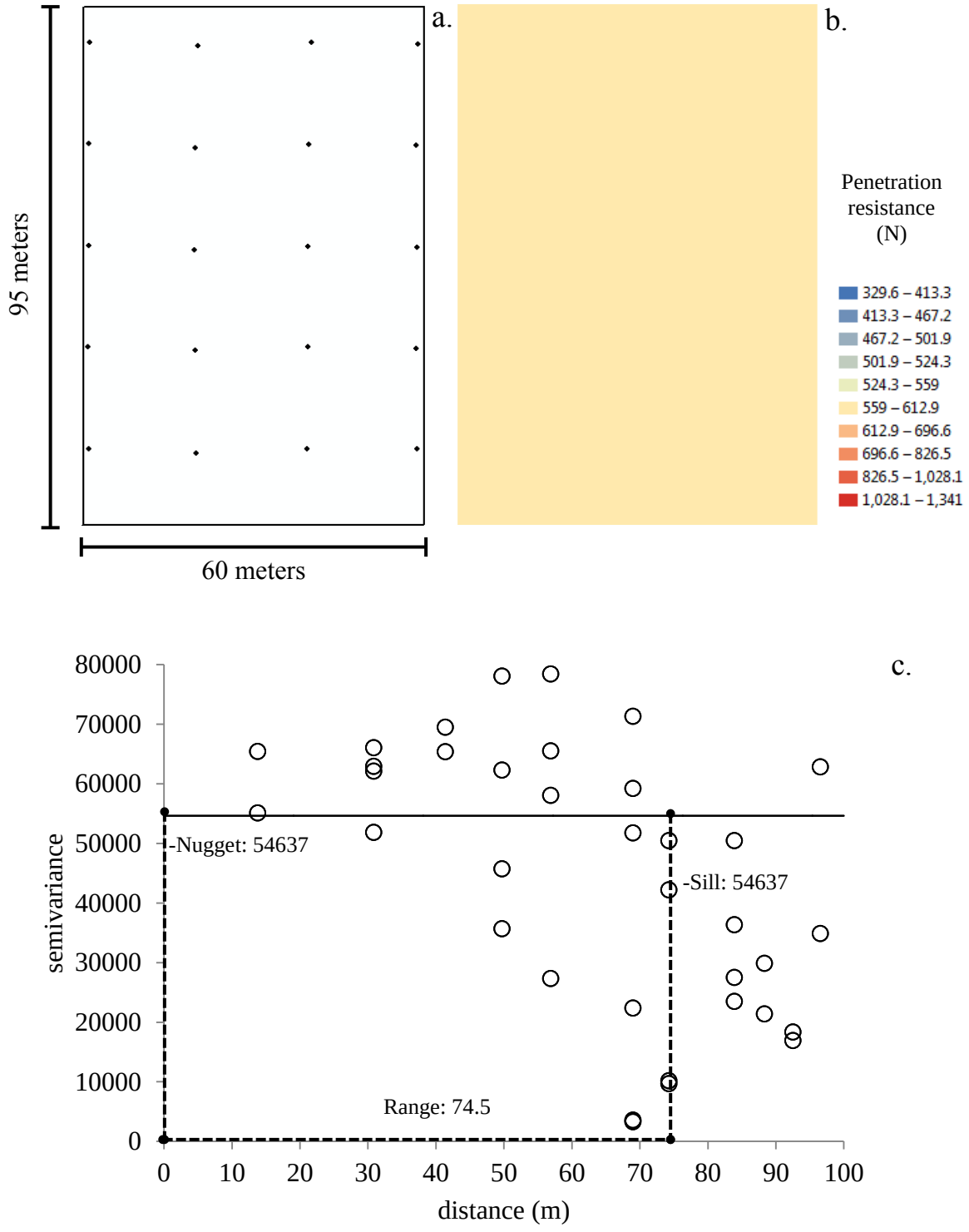


Figure 3.23. (a) Sampling locations (approximately 19.2 m x 19.2 m grid; 20 samples), (b) kriged prediction map and (c) semivariogram including the fitted spherical model of penetration resistance on Roswell field 3.

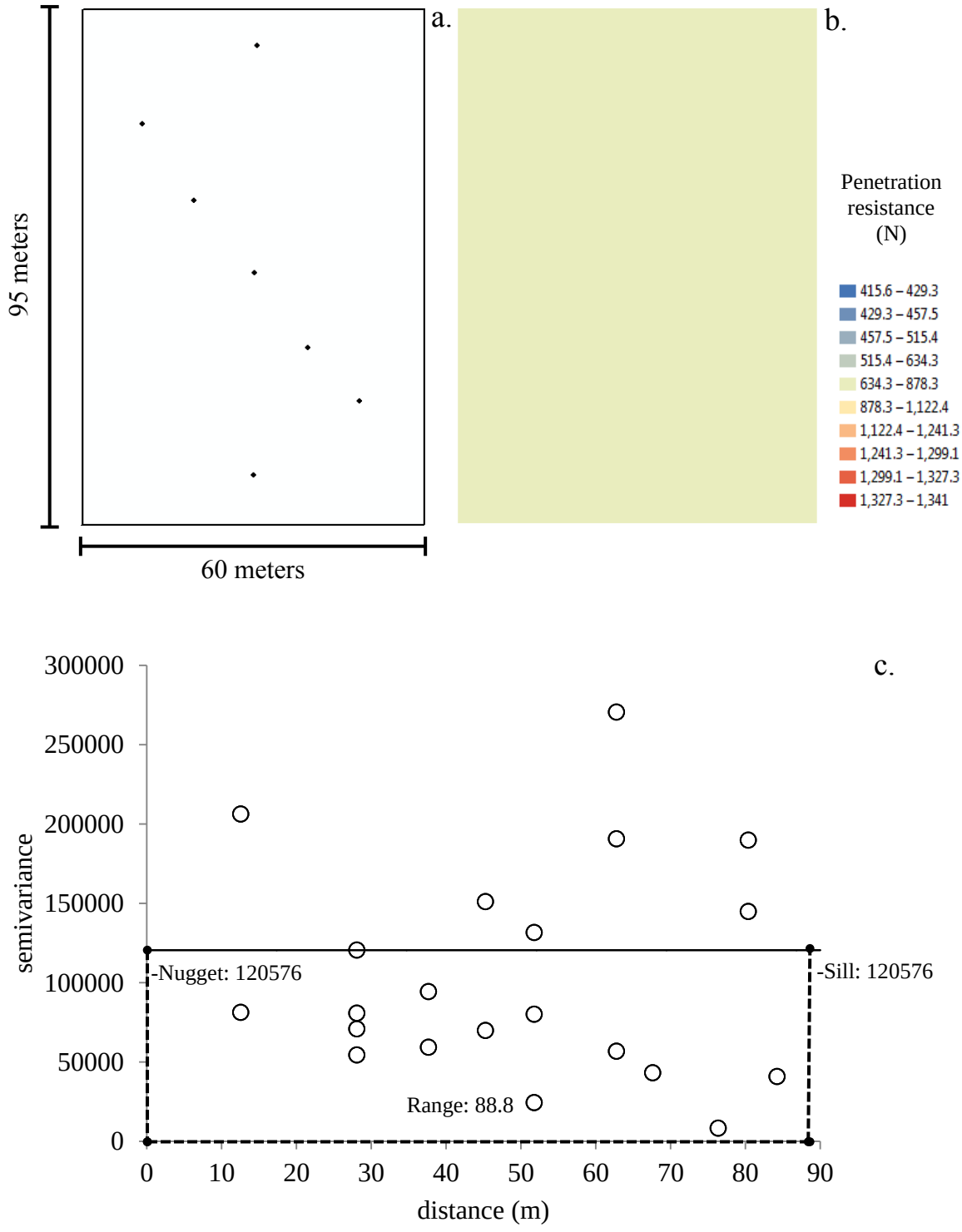


Figure 3.24. (a) Sampling locations (7 samples), (b) kriged prediction map and (c) semivariogram including the fitted spherical model of penetration resistance on Roswell field 3.

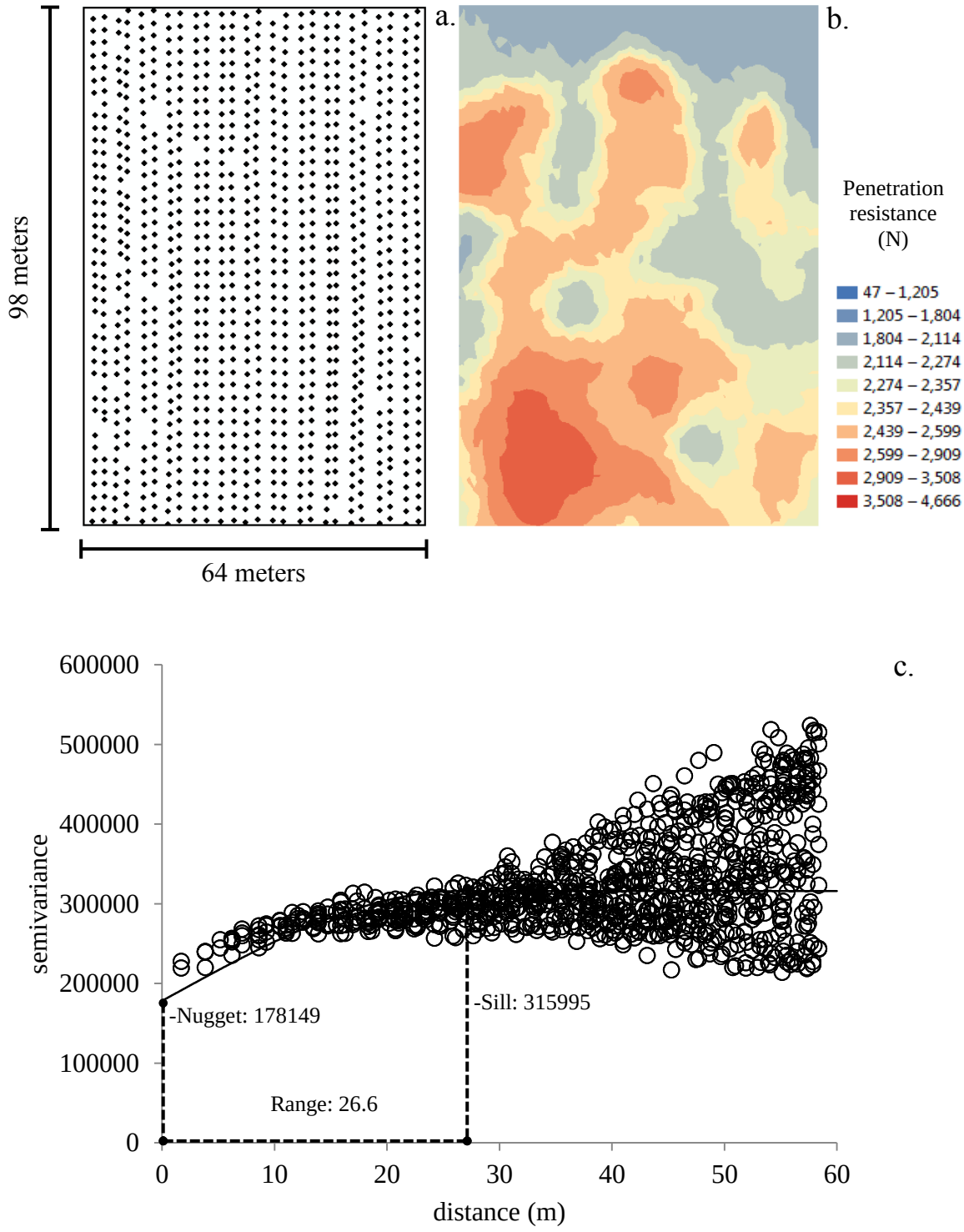


Figure 3.25. (a) Sampling locations (approximately 2.4 m x 2.4 m grid; 1066 samples), (b) kriged prediction map and (c) semivariogram including the fitted spherical model of penetration resistance on Watkinsville field 1.

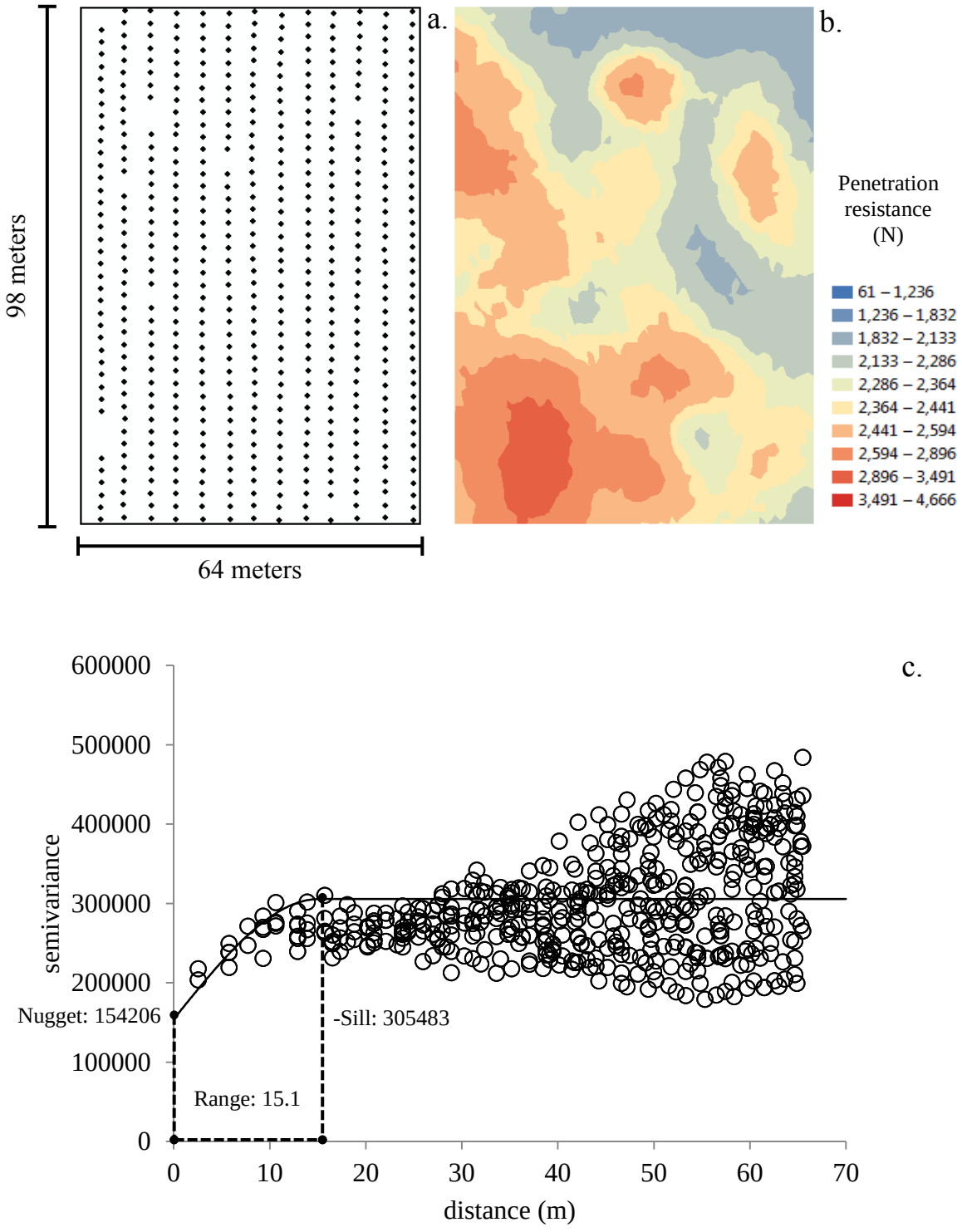


Figure 3.26. (a) Sampling locations (approximately 4.8 m x 2.4 m grid; 535 samples), (b) kriged prediction map and (c) semivariogram including the fitted spherical model of penetration resistance on Watkinsville field 1.

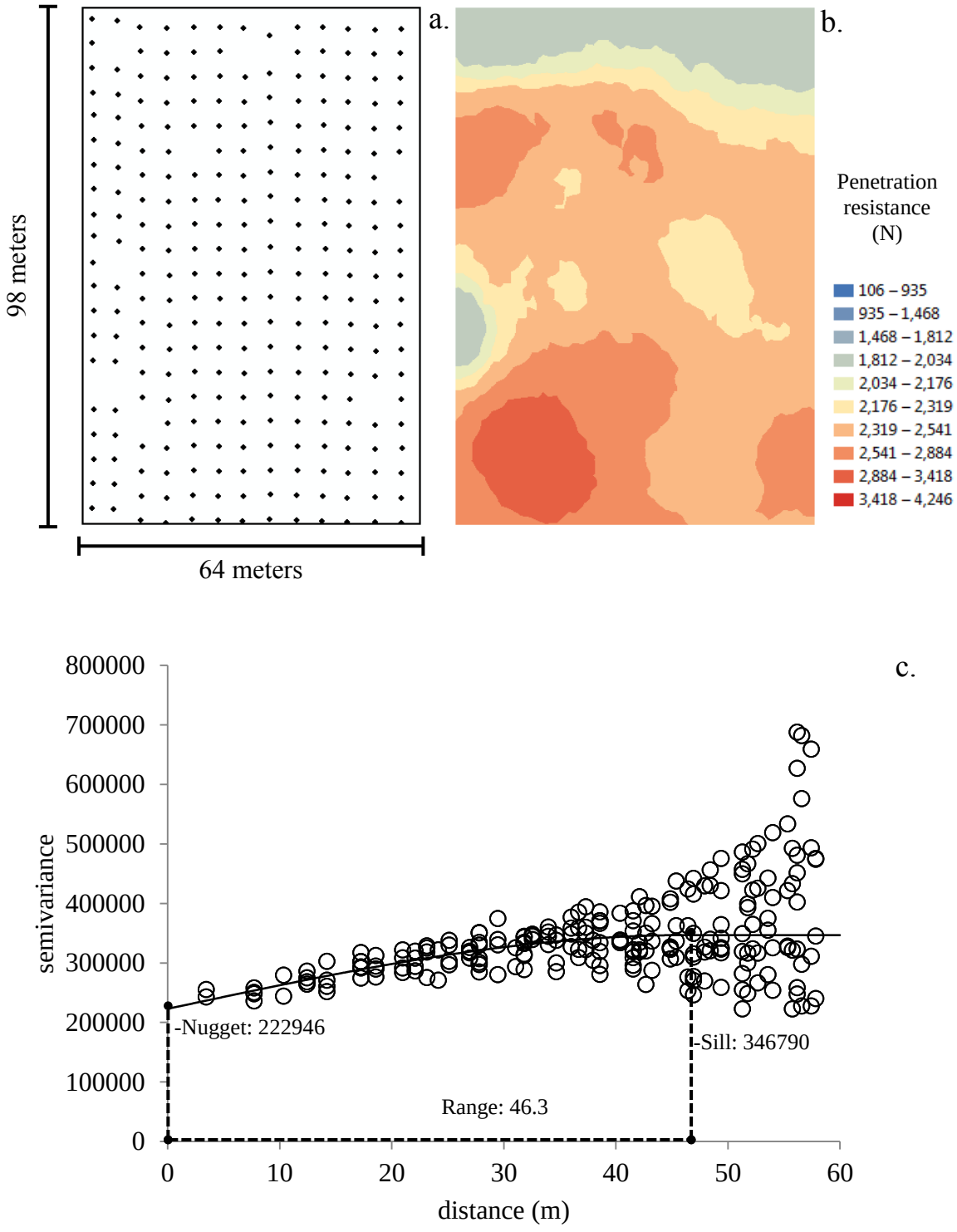


Figure 3.27. (a) Sampling locations (approximately 4.8 m x 4.8 m grid; 263 samples), (b) kriged prediction map and (c) semivariogram including the fitted spherical model of penetration resistance on Watkinsville field 1.

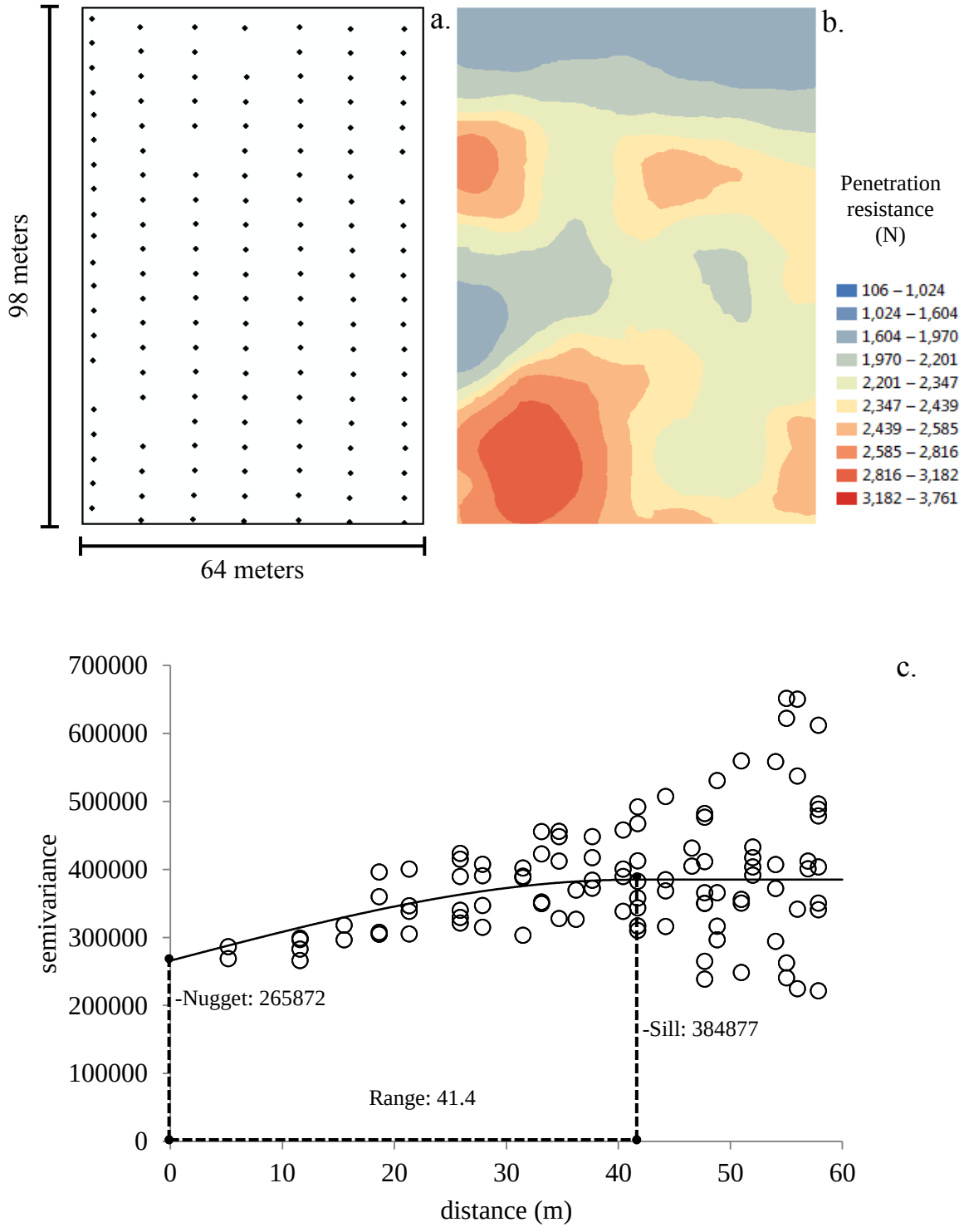


Figure 3.28. (a) Sampling locations (approximately 9.6 m x 4.8 m grid; 142 samples), (b) kriged prediction map and (c) semivariogram including the fitted spherical model of penetration resistance on Watkinsville field 1.

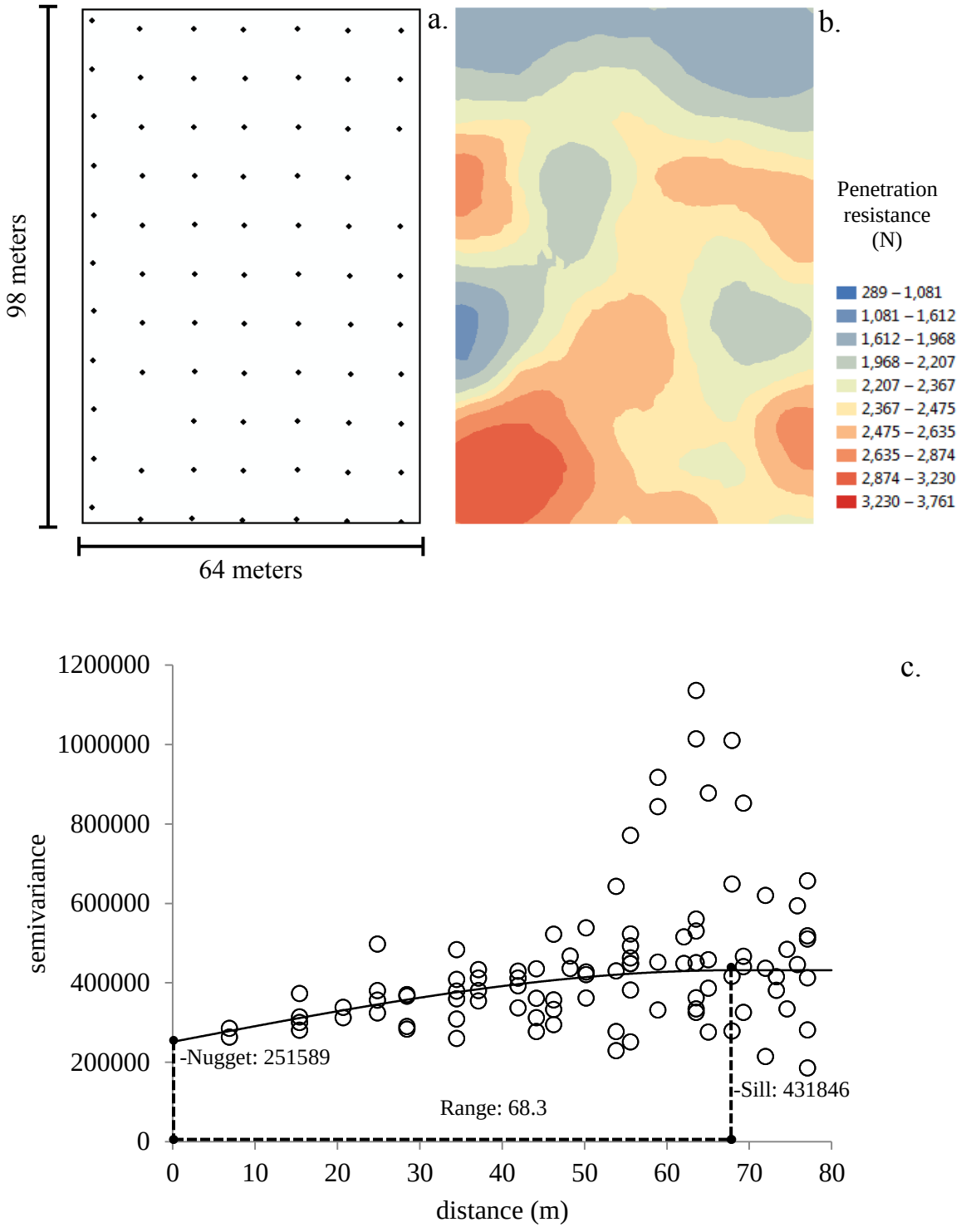


Figure 3.29. (a) Sampling locations (approximately 9.6 m x 9.6 m grid; 75 samples), (b) kriged prediction map and (c) semivariogram including the fitted spherical model of penetration resistance on Watkinsville field 1.

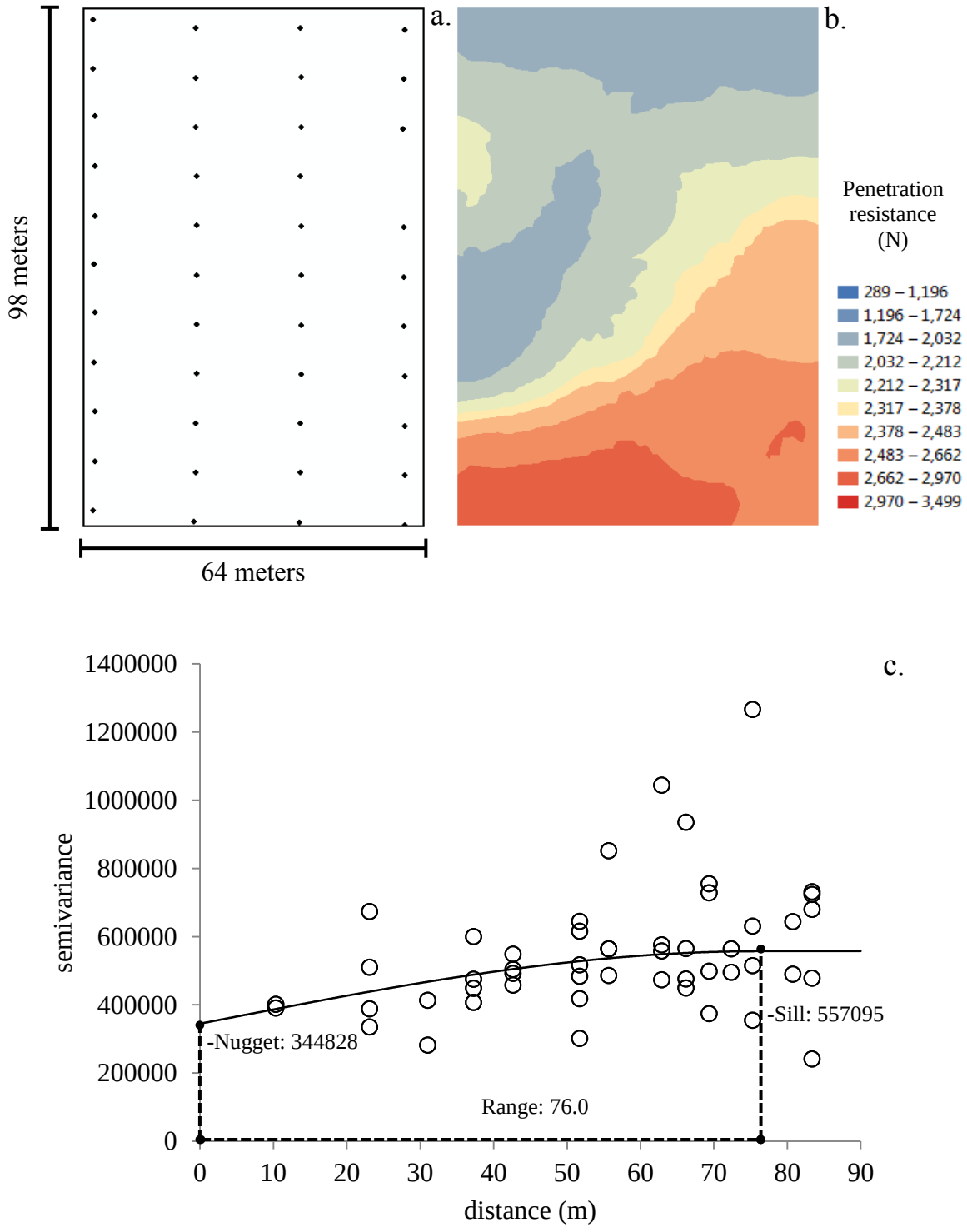


Figure 3.30. (a) Sampling locations (approximately 19.2 m x 9.6 m grid; 43 samples), (b) kriged prediction map and (c) semivariogram including the fitted spherical model of penetration resistance on Watkinsville field 1.

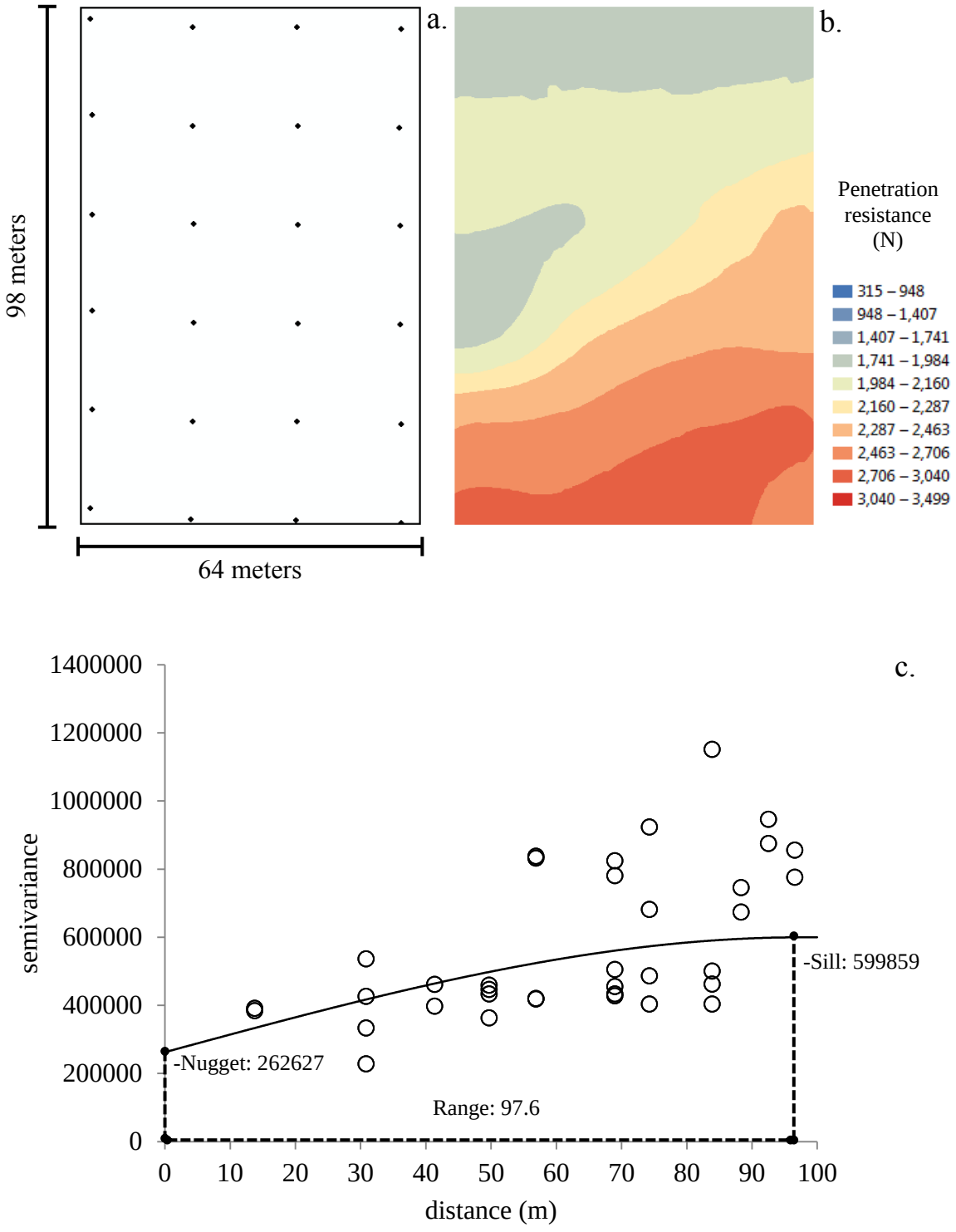


Figure 3.31. (a) Sampling locations (approximately 19.2 m x 19.2 m grid; 24 samples), (b) kriged prediction map and (c) semivariogram including the fitted spherical model of penetration resistance on Watkinsville field 1.

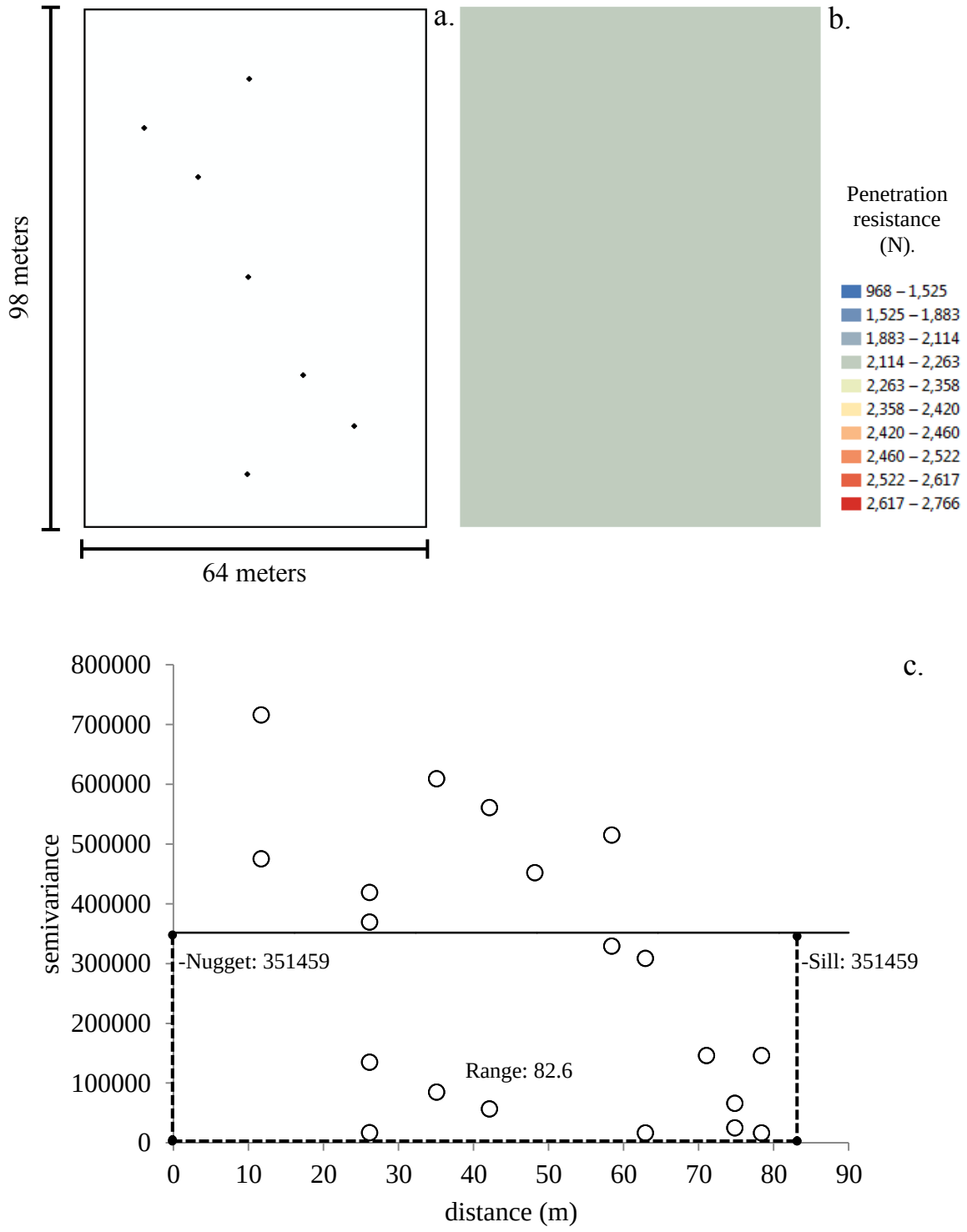


Figure 3.32. (a) Sampling locations (7 samples), (b) kriged prediction map and (c) semivariogram including the fitted spherical model of penetration resistance on Watkinsville field 1.

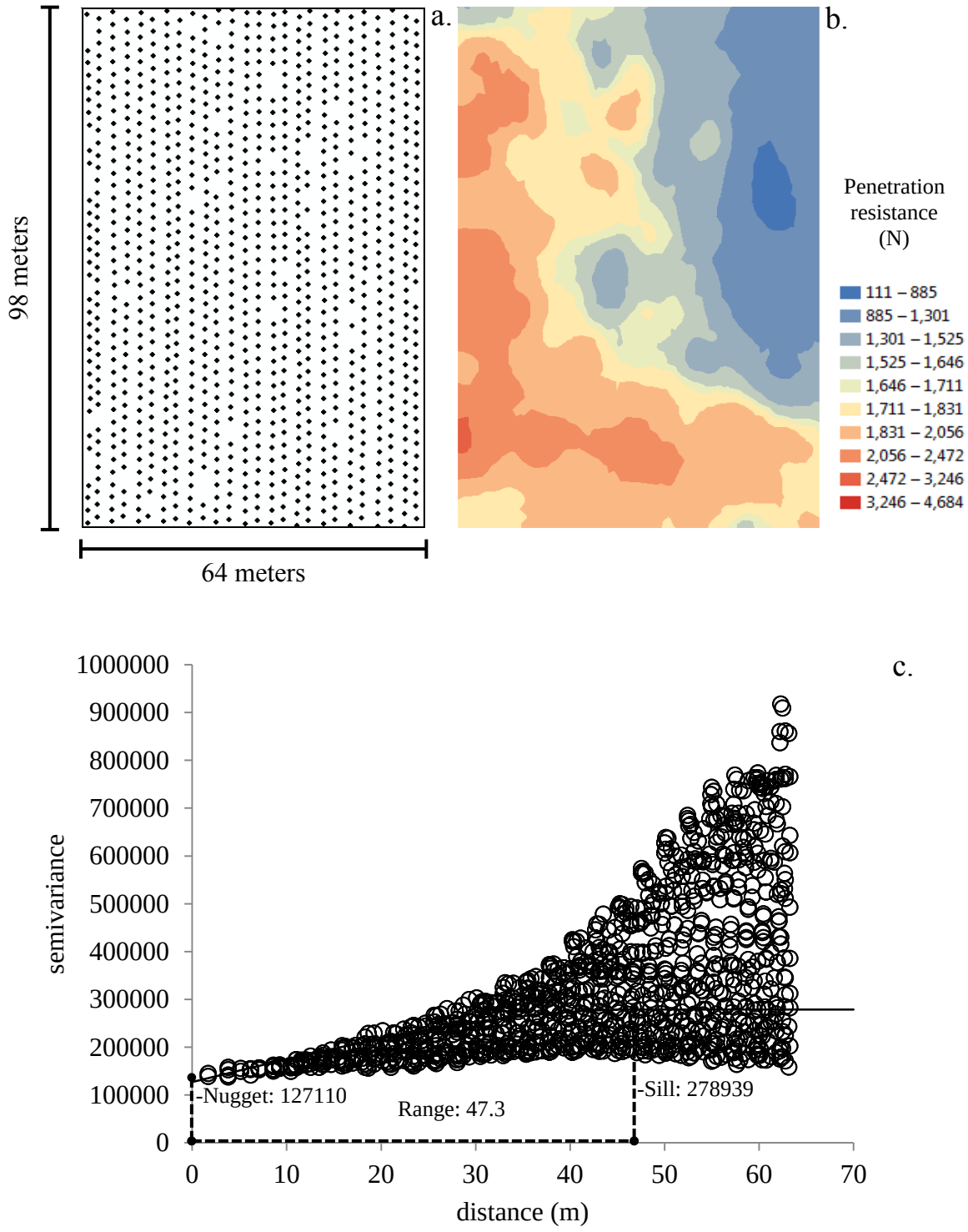


Figure 3.33. (a) Sampling locations (approximately 2.4 m x 2.4 m grid; 1053 samples), (b) kriged prediction map and (c) semivariogram including the fitted spherical model of penetration resistance on Watkinsville field 2.

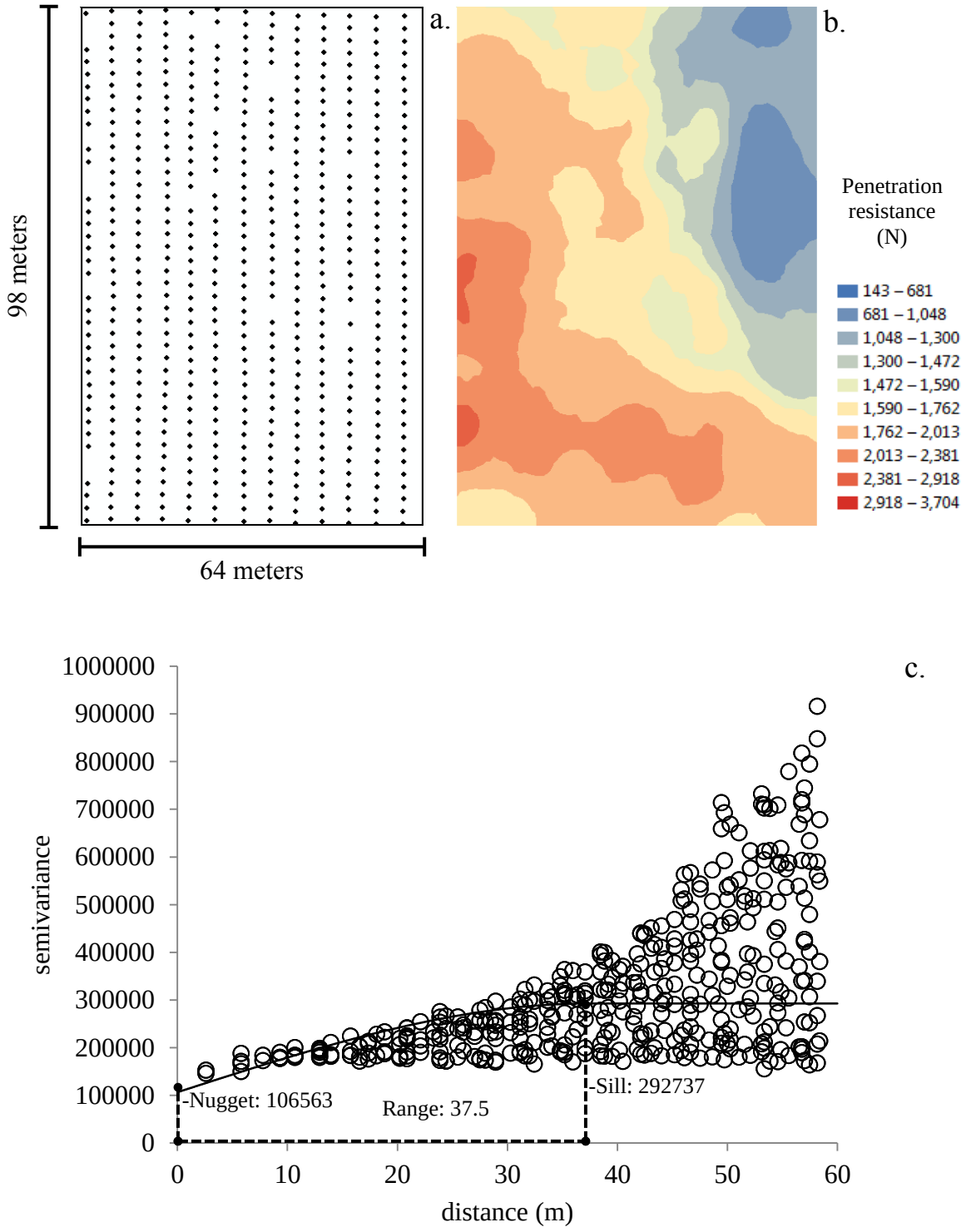


Figure 3.34. (a) Sampling locations (approximately 4.8 m x 2.4 m grid; 526 samples), (b) kriged prediction map and (c) semivariogram including the fitted spherical model of penetration resistance on Watkinsville field 2.

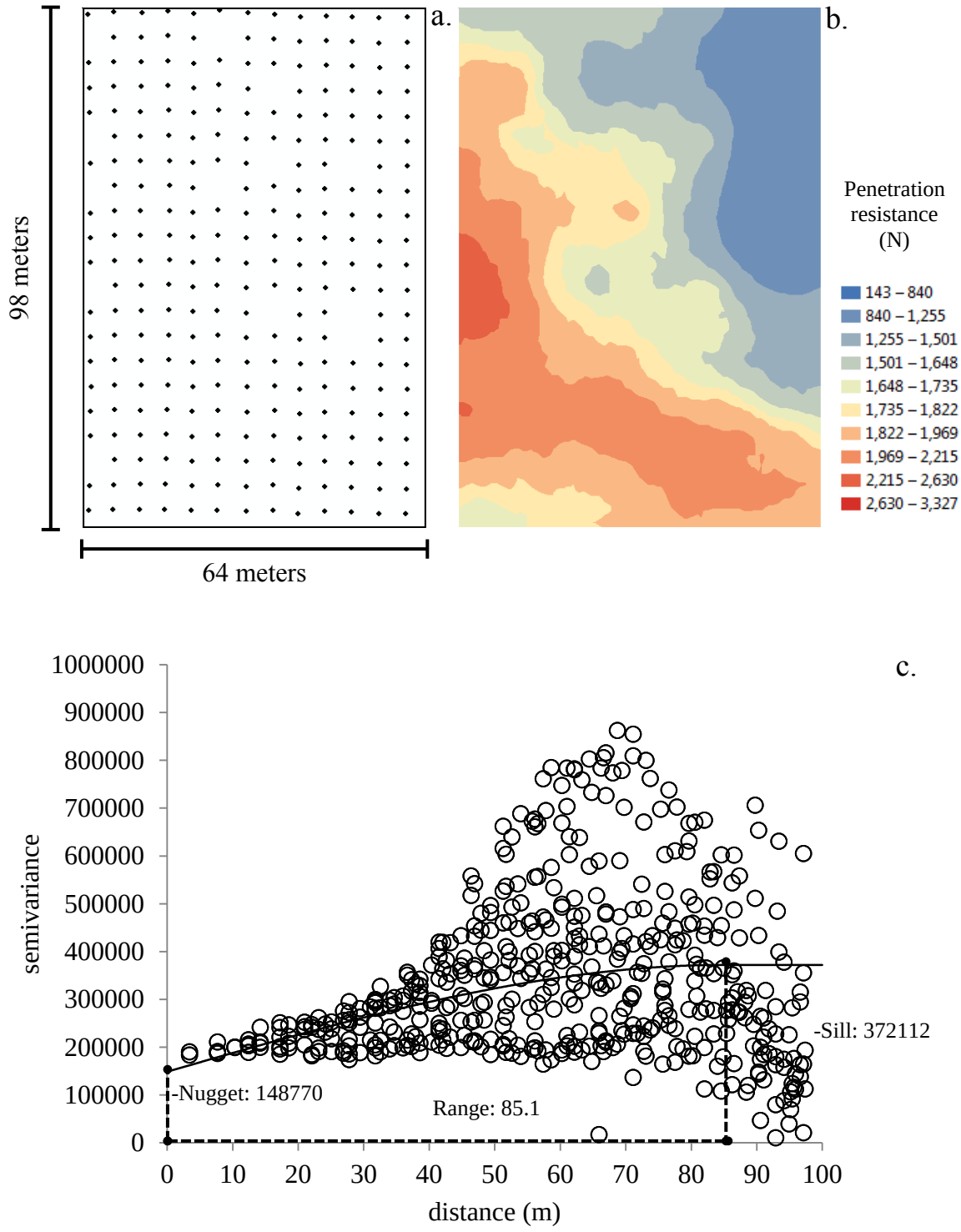


Figure 3.35. (a) Sampling locations (approximately 4.8 m x 4.8 m grid; 260 samples), (b) kriged prediction map and (c) semivariogram including the fitted spherical model of penetration resistance on Watkinsville field 2.

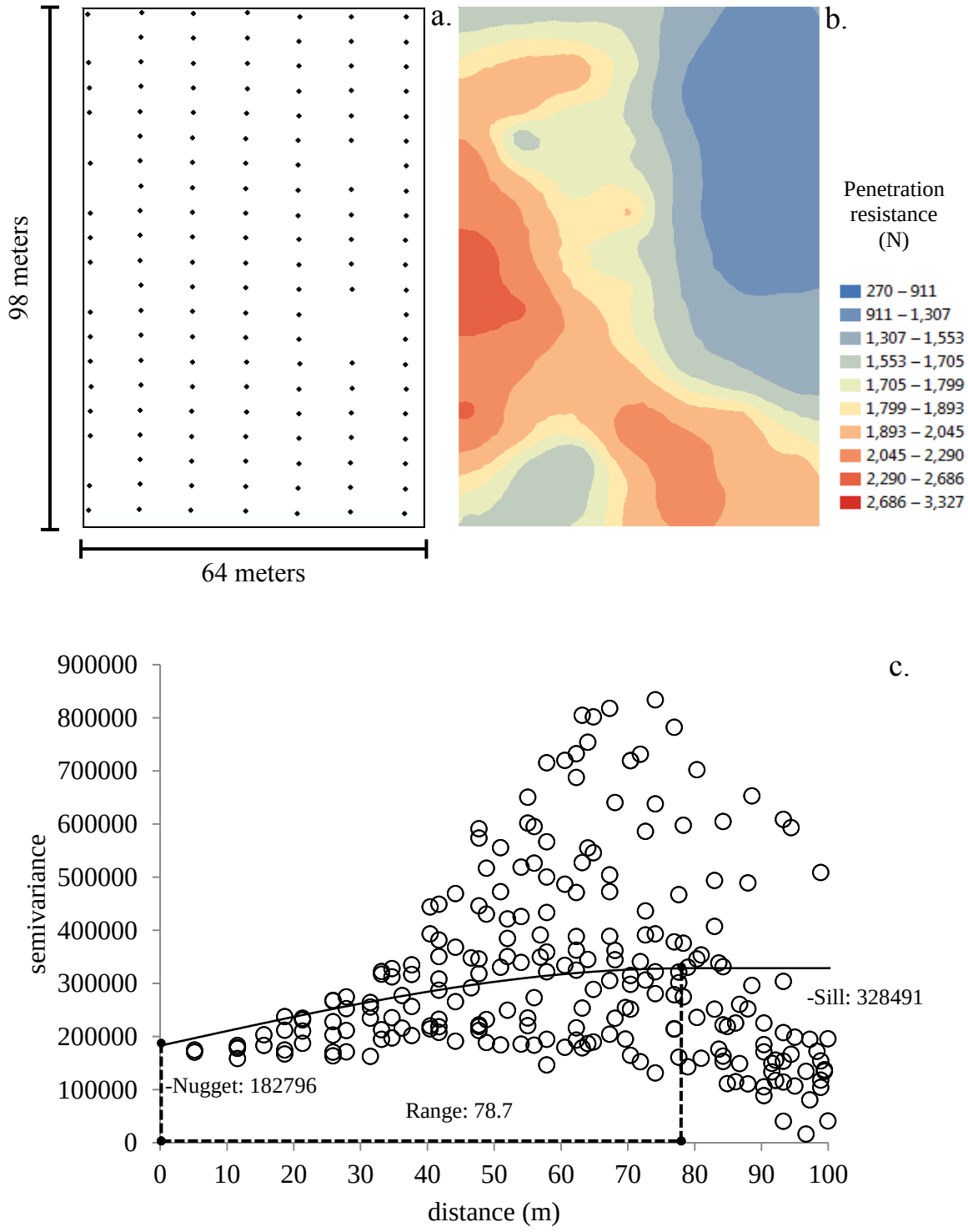


Figure 3.36. (a) Sampling locations (approximately 9.6 m x 4.8 m grid; 139 samples), (b) kriged prediction map and (c) semivariogram including the fitted spherical model of penetration resistance on Watkinsville field 2.

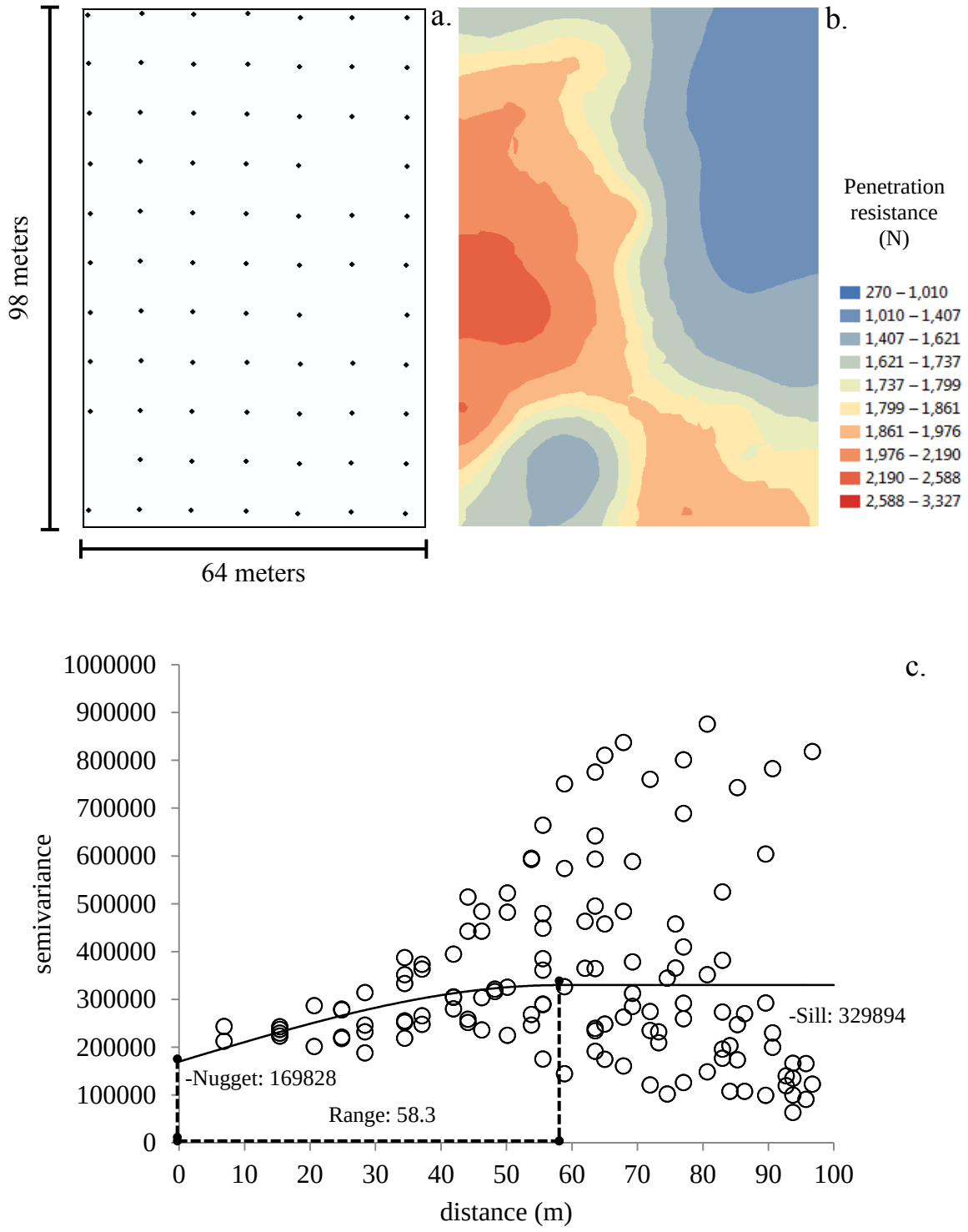


Figure 3.37. (a) Sampling locations (approximately 9.6 m x 9.6 m grid; 74 samples), (b) kriged prediction map and (c) semivariogram including the fitted spherical model of penetration resistance on Watkinsville field 2.

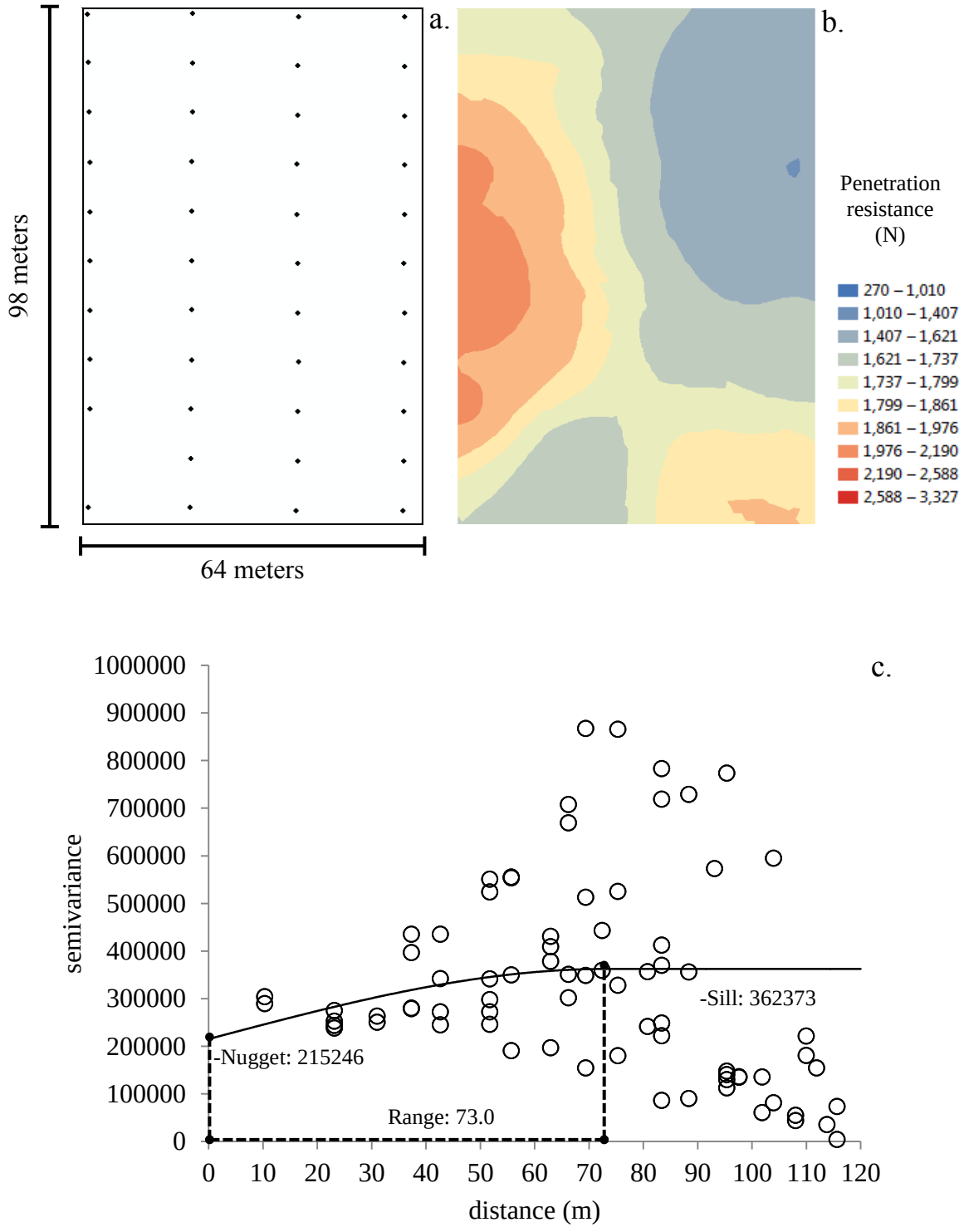


Figure 3.38. (a) Sampling locations (approximately 19.2 m x 9.6 m grid; 43 samples), (b) kriged prediction map and (c) semivariogram including the fitted spherical model of penetration resistance on Watkinsville field 2.

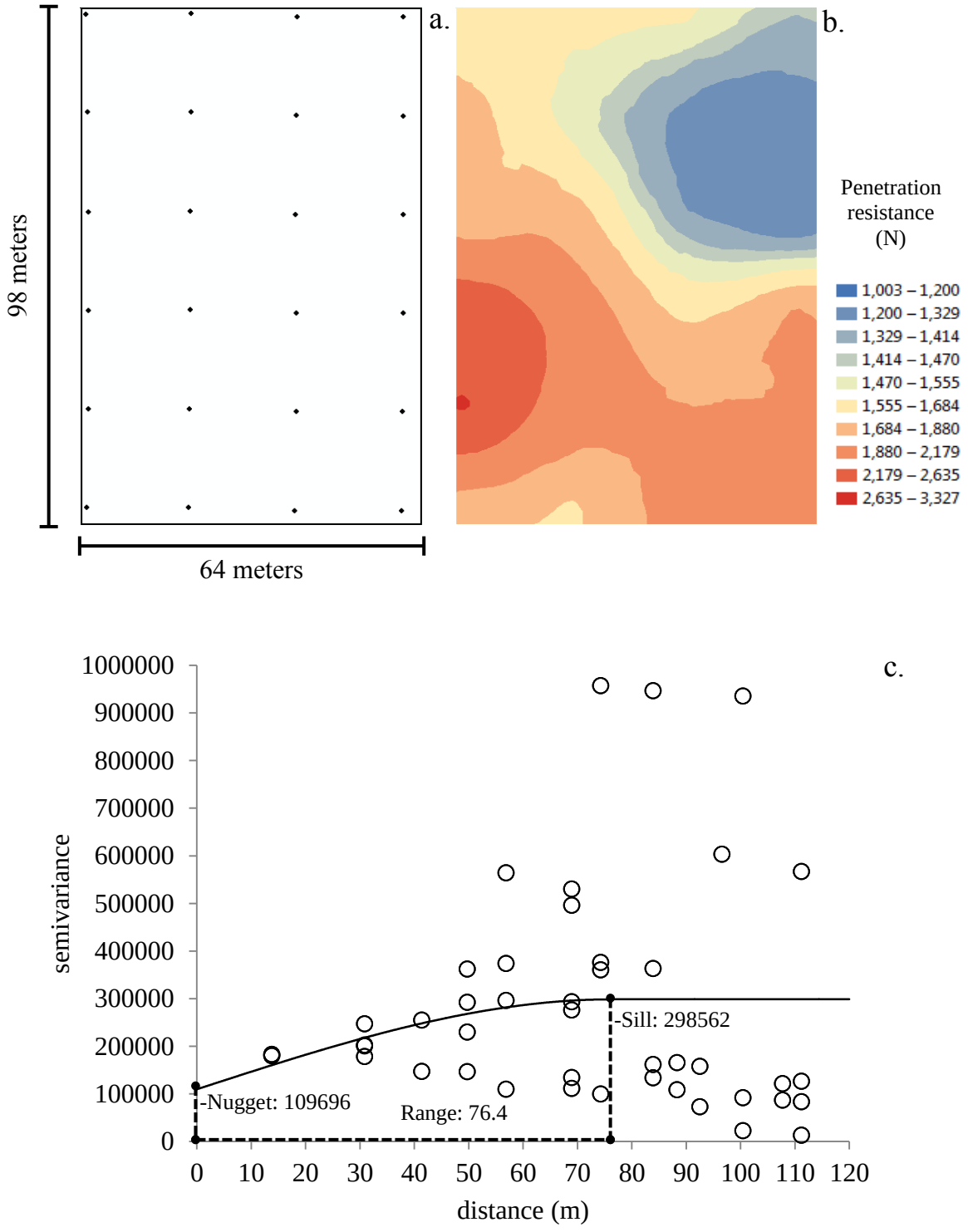


Figure 3.39. (a) Sampling locations (approximately 19.2 m x 19.2 m grid; 24 samples), (b) kriged prediction map and (c) semivariogram including the fitted spherical model of penetration resistance on Watkinsville field 2.

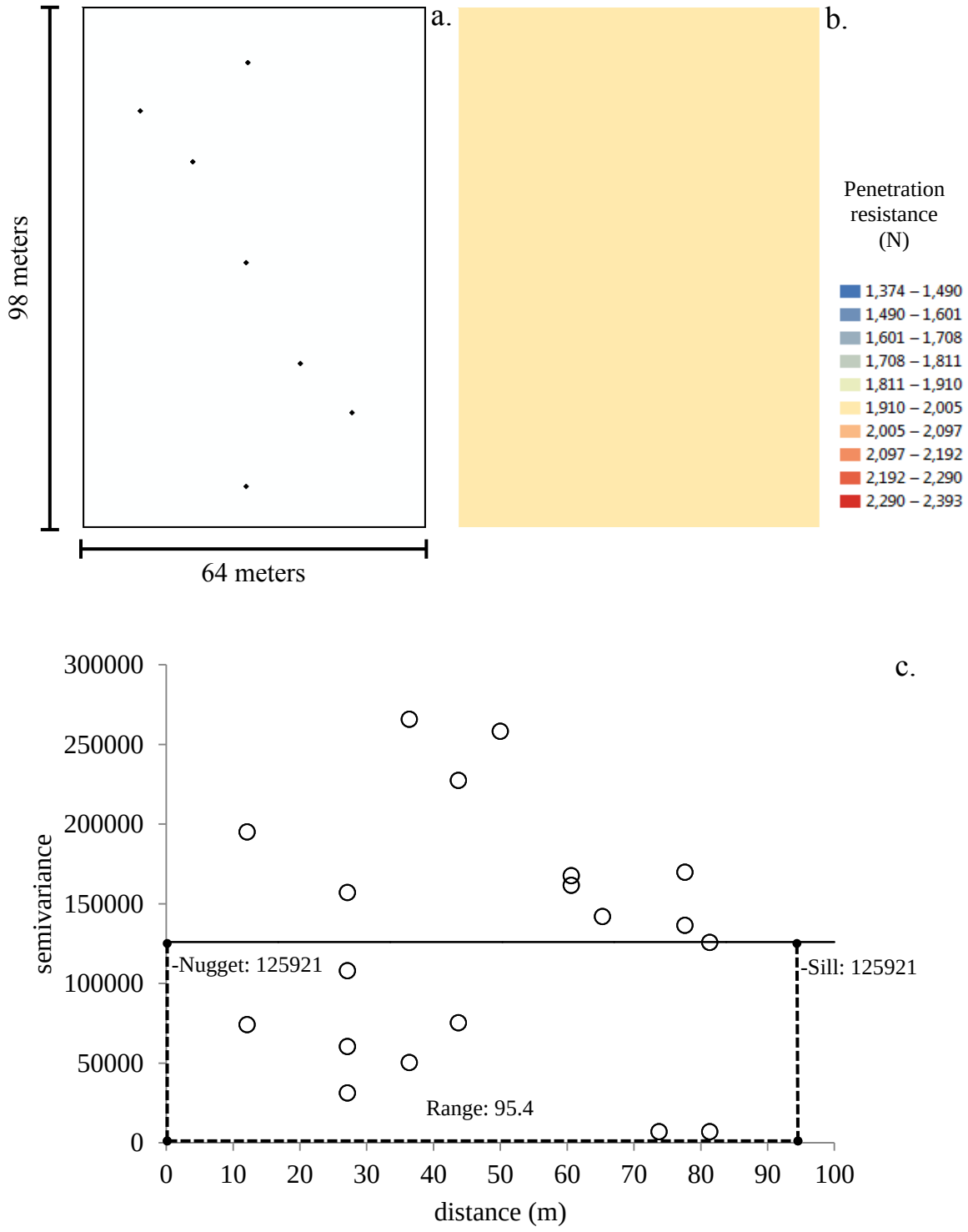


Figure 3.40. (a) Sampling locations (7 samples), (b) kriged prediction map and (c) semivariogram including the fitted spherical model of penetration resistance on Watkinsville field 2.

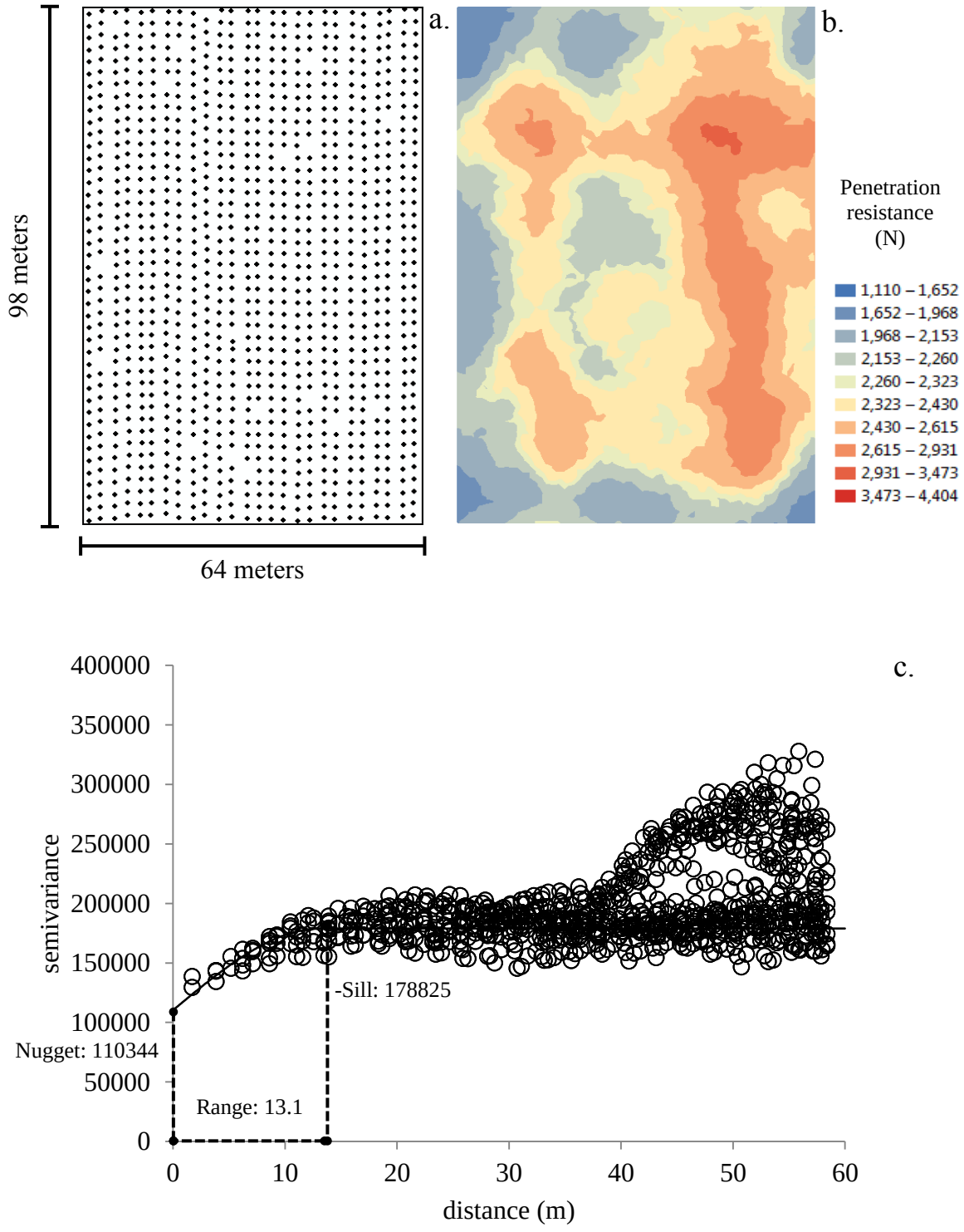


Figure 3.41. (a) Sampling locations (approximately 2.4 m x 2.4 m grid; 1101 samples), (b) kriged prediction map and (c) semivariogram including the fitted spherical model of penetration resistance on Watkinsville field 3.

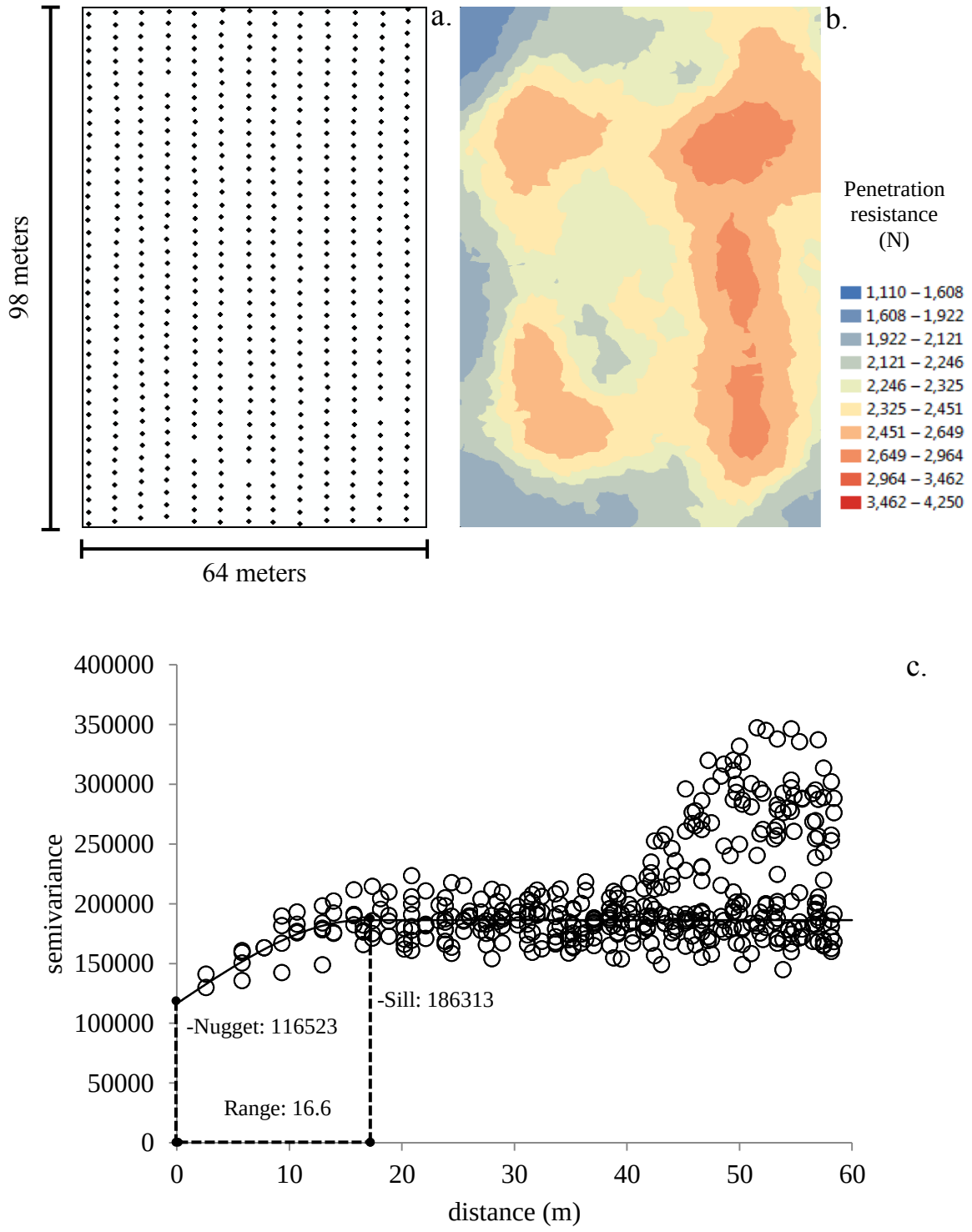


Figure 3.42. (a) Sampling locations (approximately 4.8 m x 2.4 m grid; 555 samples), (b) kriged prediction map and (c) semivariogram including the fitted spherical model of penetration resistance on Watkinsville field 3.

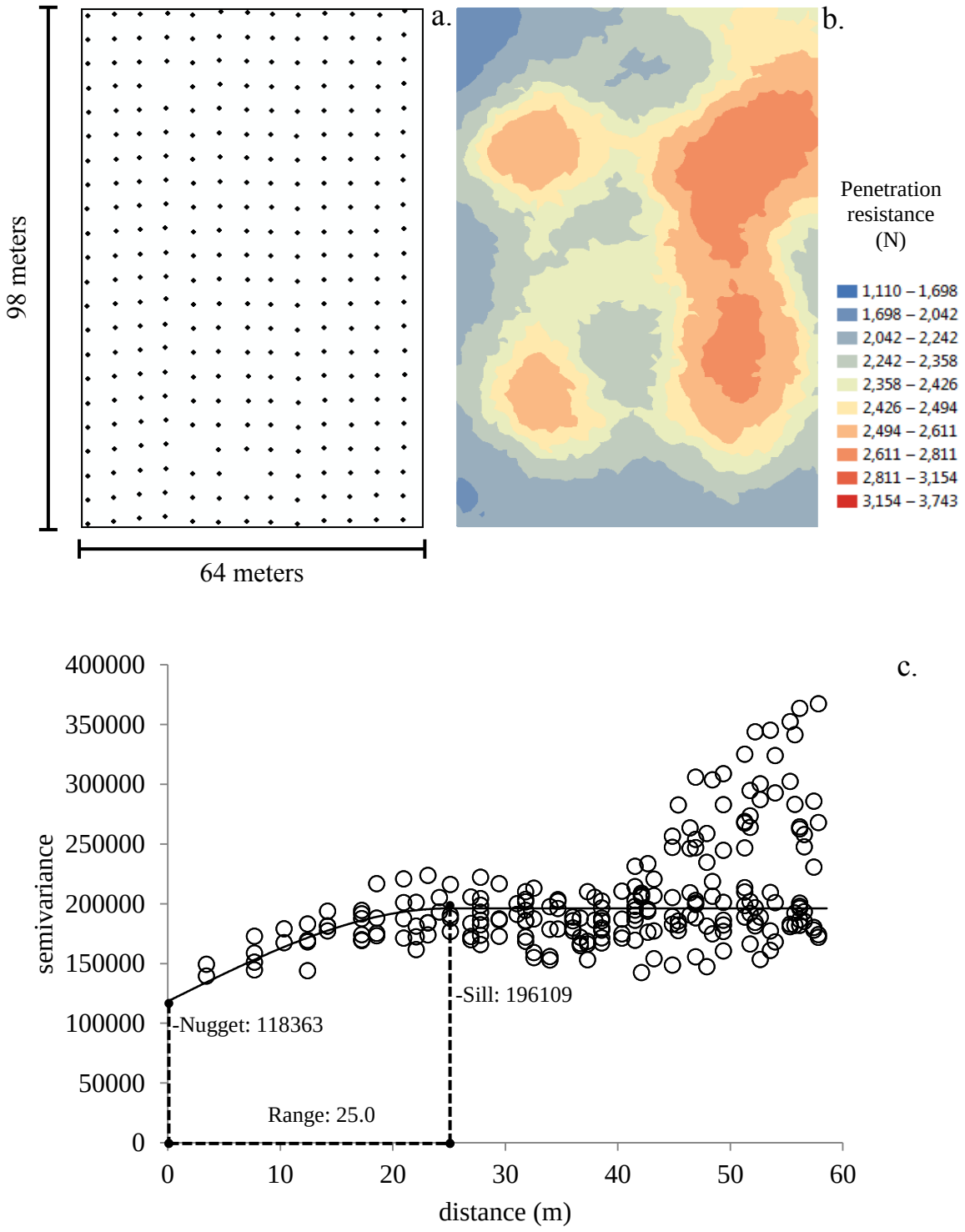


Figure 3.43. (a) Sampling locations (approximately 4.8 m x 4.8 m grid; 282 samples), (b) kriged prediction map and (c) semivariogram including the fitted spherical model of penetration resistance on Watkinsville field 3.

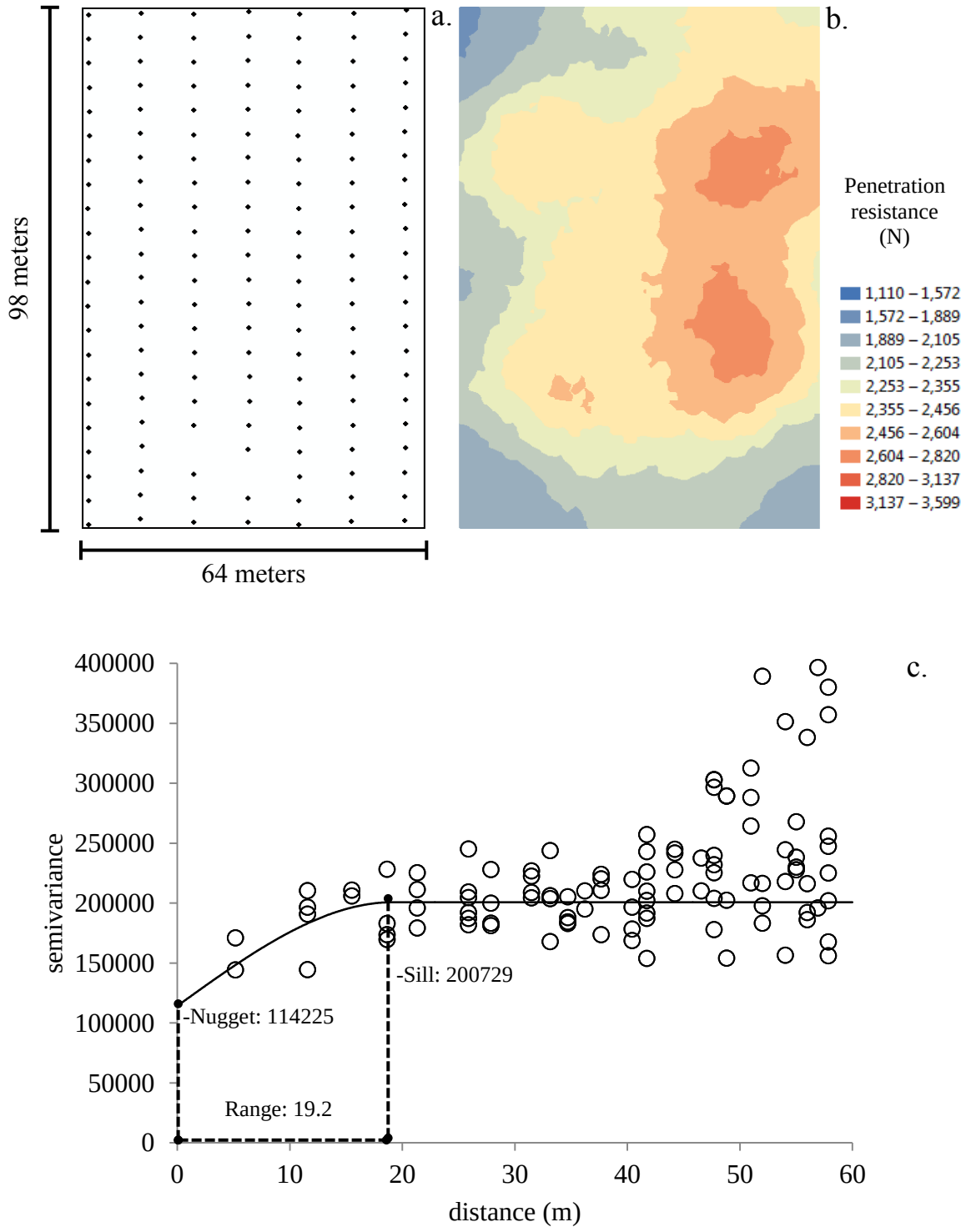


Figure 3.44. (a) Sampling locations (approximately 9.6 m x 4.8 m grid; 152 samples), (b) kriged prediction map and (c) semivariogram including the fitted spherical model of penetration resistance on Watkinsville field 3.

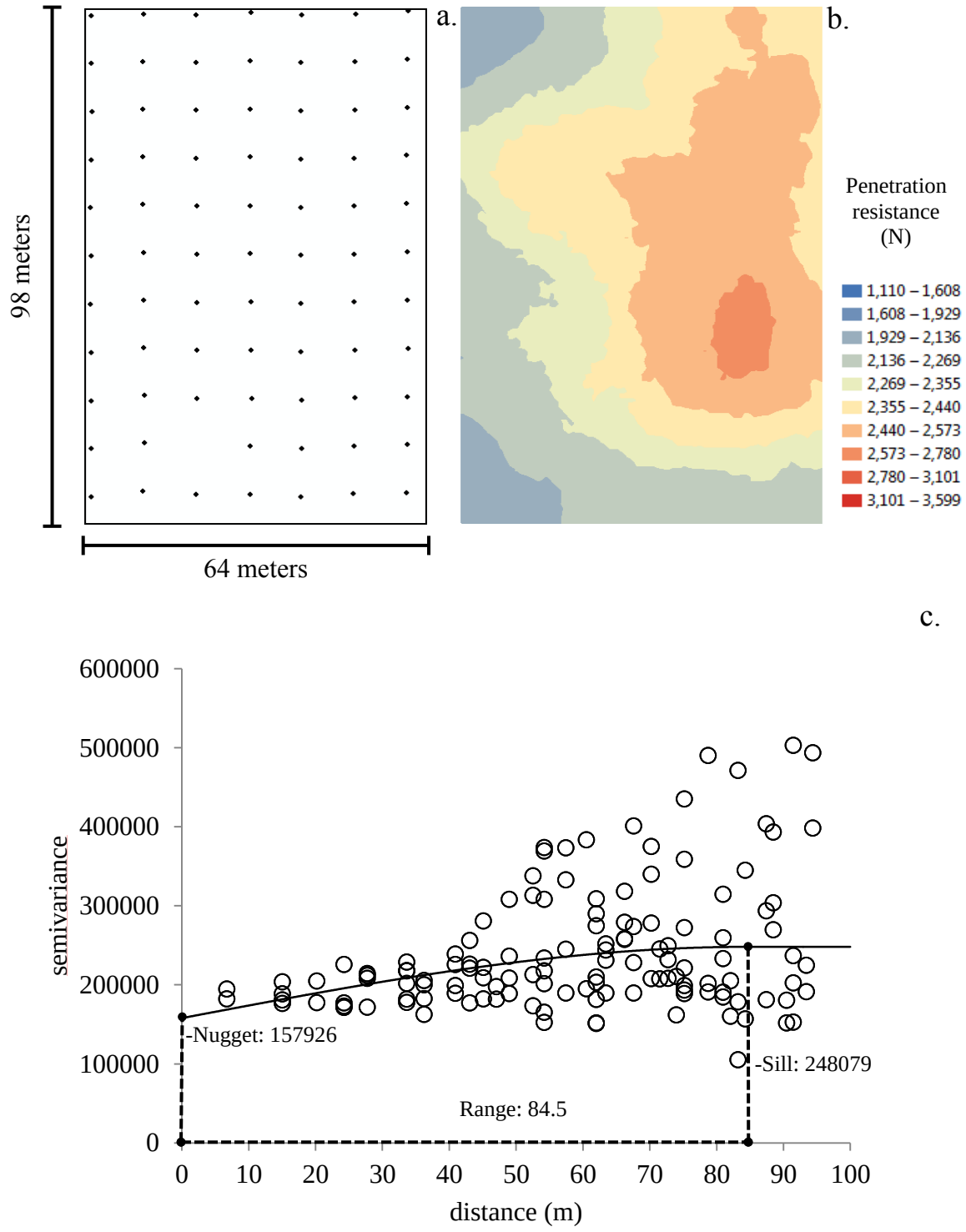


Figure 3.45. (a) Sampling locations (approximately 9.6 m x 9.6 m grid; 76 samples), (b) kriged prediction map and (c) semivariogram including the fitted spherical model of penetration resistance on Watkinsville field 3.

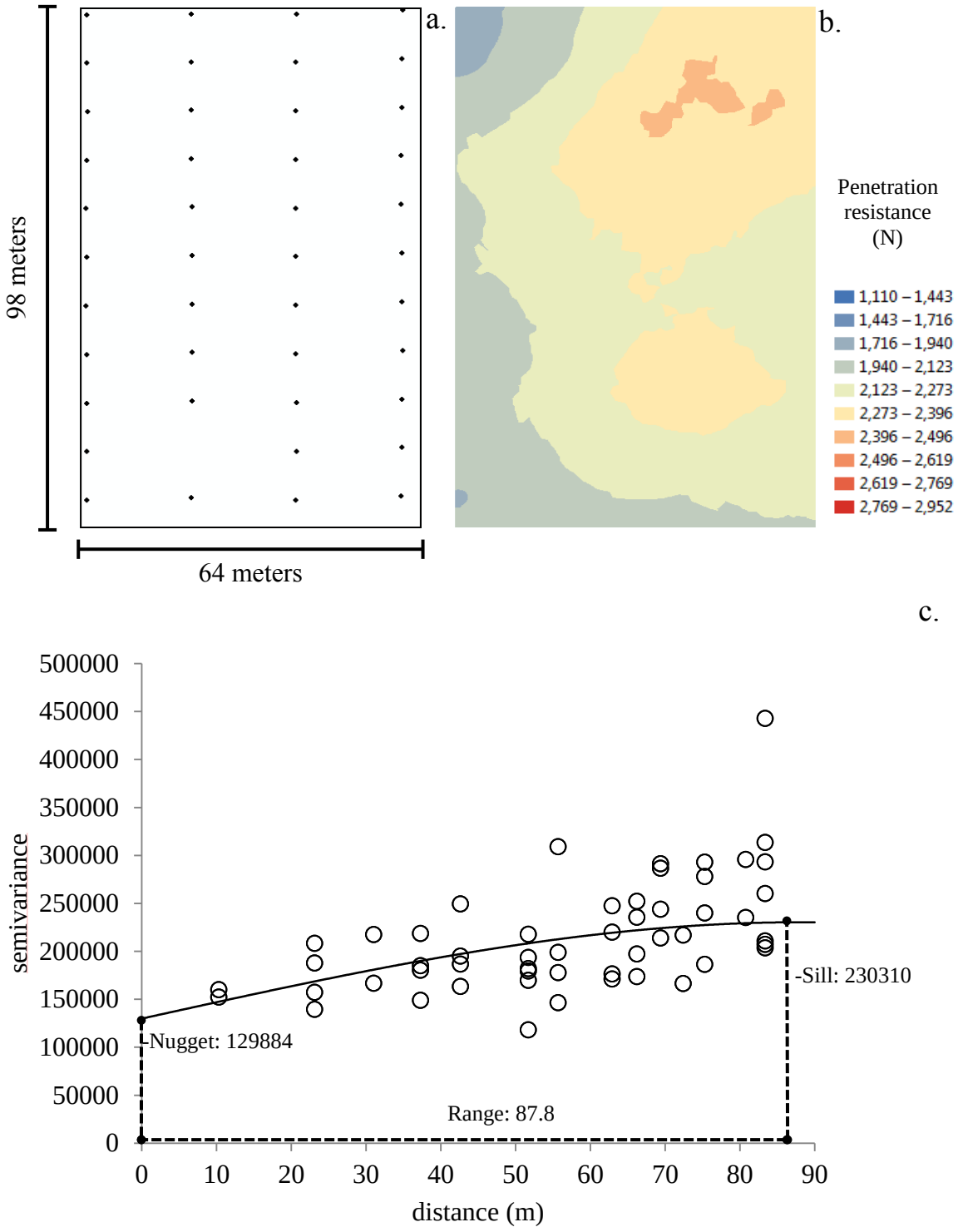


Figure 3.46. (a) Sampling locations (approximately 19.2 m x 9.6 m grid; 43 samples), (b) kriged prediction map and (c) semivariogram including the fitted spherical model of penetration resistance on Watkinsville field 3.

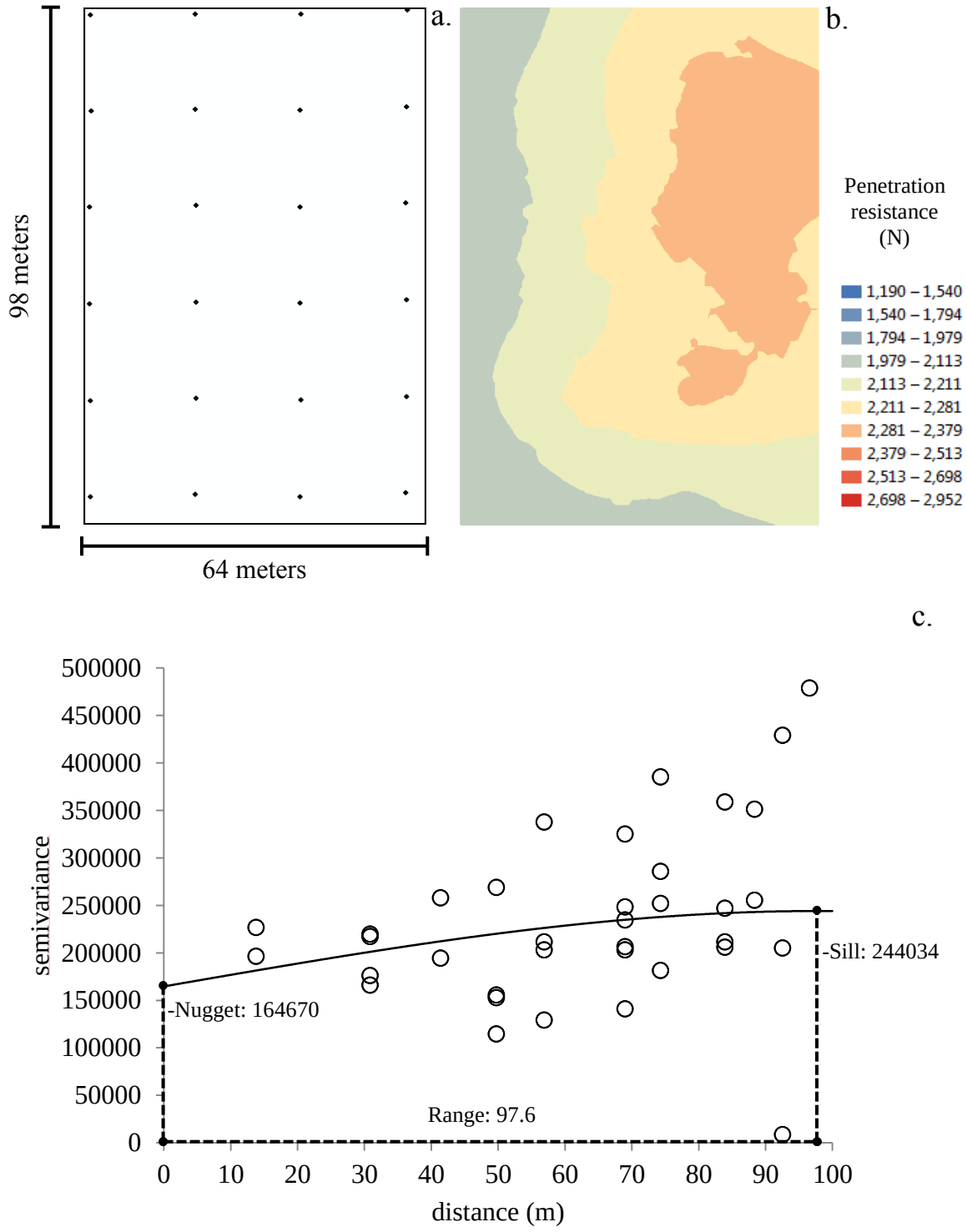


Figure 3.47. (a) Sampling locations (approximately 19.2 m x 19.2 m grid; 24 samples), (b) kriged prediction map and (c) semivariogram including the fitted spherical model of penetration resistance on Watkinsville field 3.

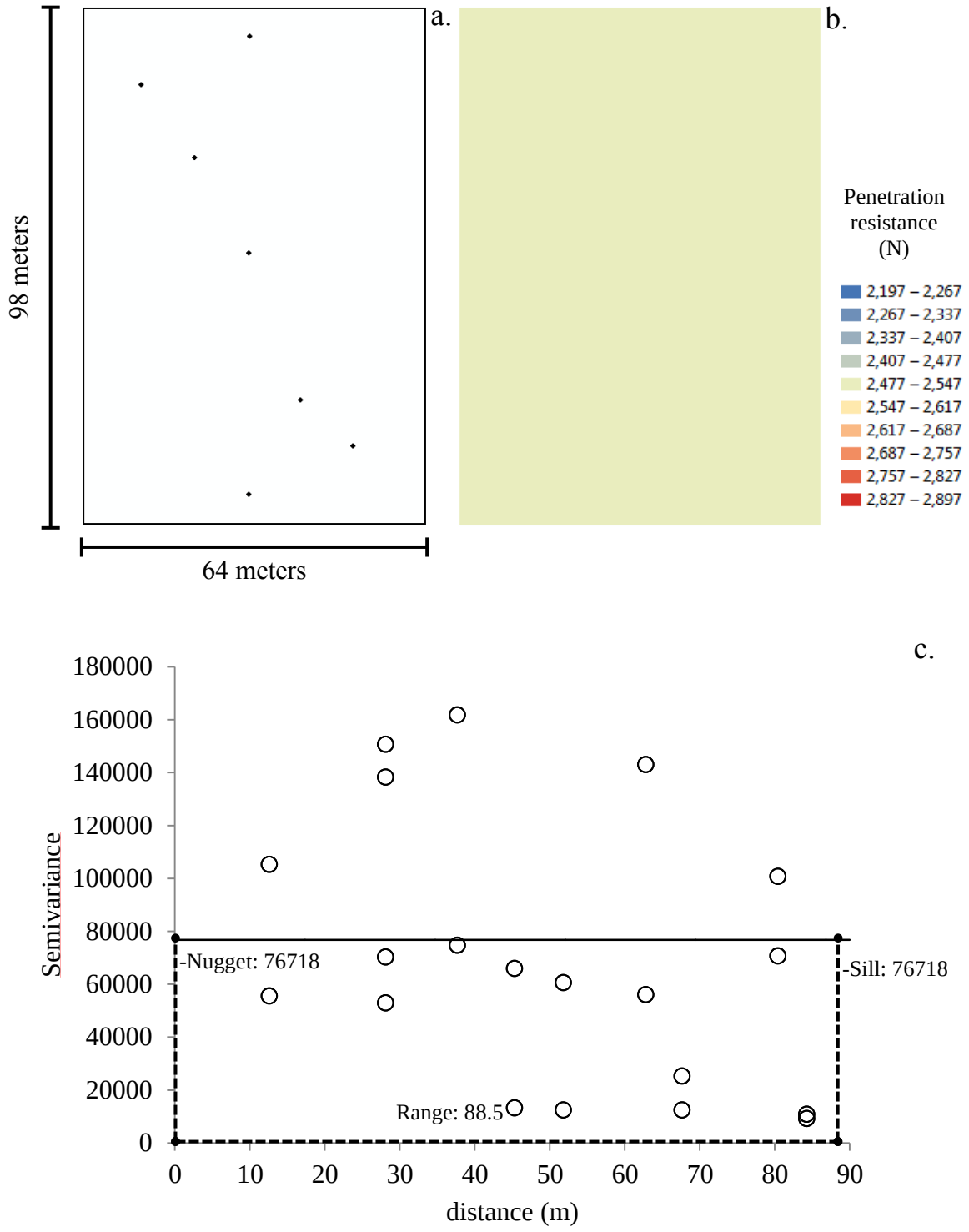


Figure 3.48. (a) Sampling locations (7 samples), (b) kriged prediction map and (c) semivariogram including the fitted spherical model of penetration resistance on Watkinsville field 3.

# CHAPTER 4

# EVALUATION OF SAMPLING PROCEDURES FOR SPATIAL ANALYSIS OF PLANT PERFORMANCE ON SPORTS FIELDS[1]

[1] Straw, C.M., G.M. Henry, R.N. Carrow, V. Cline. To be submitted to *Crop Science.*

Abstract

Plant performance qualities (coverage, uniformity, and density) on natural turf sports fields are highly dependent on the level of foot traffic from game play and are critical in terms of player and ball surface interactions. Whole-field evaluation of these qualities is necessary to ensure player safety and field playability, as well as potentially reduce inputs necessary for optimal turf growth. The term "performance testing" is a method to quantify surface and edaphic properties on sports fields, such as normalized difference vegetative index (NDVI) (i.e. plant performance). Previous procedures have used handheld devices to collect data from minimal locations (6-12). The low number of samples restricts analysis of variability over the entire area. Geostatistics is a branch of statistics that uses semivariograms and interpolation, generated from intense data sampling, for analysis of a given variable in space. The Toro Precision Sense 6000 (PS6000), a mobile multi-sensor device with Global Positioning System (GPS) capability, has recently been introduced for use on turfgrass sites. The PS6000's ability for rapid sampling and geo-referenced data allows for the use of geostatistical methods to conduct spatial analysis. However, there is limited research of sampling procedures or protocols for use on sports fields. The PS6000 was used to measure penetration resistance on three 'Tifway 419' hybrid bermudagrass (*Cynodon dactylon* x *C. transvaalensis*) sports fields in Roswell, GA and three 'TifSport' hybrid bermudagrass sports fields in Watkinsville, GA during the summer of 2013. Various levels of sample sizes were manipulated, using Geographic Information System (GIS) software, from the initial 2.4 m x 2.4 m sample grid. Spatial analysis of NDVI was conducted on all sample sizes and compared within each field to evaluate an appropriate sampling procedure. In general, as the sample grids became larger, the strength of the semivariograms and accuracy of the surface maps

minimized. A minimal sample grid size of 9.6 m x 4.8 m was determined, with subsequently decreasing sample grid sizes providing a more accurate and detailed site-specific analysis.

## Introduction

The two most important components of managing a sports field is player safety and field playability (Baker, 1991; Caple et al., 2012). Player safety is related to player-surface interactions such as surface hardness (the hardness of the playing surface), soil compaction, traction (the amount of grip footwear has on the turf and soil), and soil moisture (amount of moisture in the soil profile) (Holmes and Bell, 1986; Baker and Canaway, 1993). Field playability is related to ball-surface interactions such as rebound height (how well the ball rebounds from the surface), smoothness (evenness of the surface), and speed of the surface (speed of ball movement across the surface) (Holmes and Bell 1986; Baker and Canaway, 1993).

For natural turf sports fields, plant performance qualities (coverage, uniformity, and density) are critical in terms of both interactions; for example, unexpected changes in the surface can cause a player to stumble, slip, or fall and also can effect ball bounce and ball roll (Baker, 1991). Turf performance is highly dependent on the level of foot traffic during game play. Foot traffic is a general term and includes both wear and soil compaction stresses (Carrow and Petrovic, 1992). Wear occurs from pressure, scuffing, or tearing of the turfgrass tissues (Carrow and Petrovic, 1992). Soil compaction is the pressing together of soil particles resulting in a more dense soil mass with less pore space (Beard, 1973). These stresses are alleviated with an integrated approach of several techniques, including primary cultural practices such as mowing, fertilization, irrigation, and cultivation. Being that plant performance is ever changing in time and space, whole-field evaluation is necessary to ensure player safety and field playability, as well as potentially reduce inputs necessary for optimal turf growth (water, fertilizer, etc.) (Carrow et al., 2010).

The term “performance testing” (i.e. site assessment) is receiving increasing attention as a method to quantify the performance of surface and edaphic properties on sports fields (McAuliffe, 2008; Bartlett et al., 2009; Stiles et al., 2009; Carrow et al., 2010). Performance testing involves collecting data samples at multiple locations across a field to better understand the variability of the property of interest. In respect to turf performance qualities, multiple methods of testing have been used. Turf coverage has been assessed visually using quadrat frames to find percent coverage within each quadrat (Bartlett et al., 2009; Institute of Groundsmanship (IOG), 2014). A method by Haggar et al. (1983) has been used by researchers to evaluate ground cover using spectral reflectance sensors. The operation of the sensor depends on measuring the radiance ratio of red (R) and near-infrared (IR) of the form [(R + IR)/IR]. This ratio is higher for green canopies than for soil. Recently, a more broad spectrum assessment has been reported by Trenholm et al. (1999) using a spectral reflectance methodology referred to as normalized difference vegetative index (NDVI). NDVI has been shown to be significantly associated with visual turf quality, density, and shoot tissue injury (Trenholm et al., 1999). NDVI sensors are equipped with internal light emitting diodes and a photodiode optical detector that measures the reflectance of red (R = 660 nm) and near-infrared (NIR = 770 nm) spectra used to calculate a vegetative index {NDVI = $[(R_{770} - R_{660})/(R_{770} + R_{660})]$} (Krum, 2010). Healthy plants have greater NIR and lower R reflectance than plants under stress.

Minimal standards have been established to identify sampling locations for performance testing. One procedure is the American Society for Testing and Materials (ASTM) F1936, which identifies test locations to measure only surface hardness (ASTM, 2010). The Performance Quality Standards (PQS) provides a test procedure for a wide range of parameters, with a method available to estimate turf coverage using small quadrat frames from 5 to 20 locations (IOG,

2014). Methods to measure turf height and evenness are also available; however uniformity and density are not. Researchers that have evaluated turf performance qualities on sports fields have used the spectral reflectance method by Haggar et al. (1983) or the quadrat method from only six to twelve locations (Holmes and Bell, 1986; Baker, 1991; Jennings-Temple et al., 2006; Bartlett et al., 2009). In these procedures, descriptive statistics (mean, min, max, standard deviation, etc.) are the primary determinate of central tendency and variability of plant performance across a field. However, plant performance can vary significantly across an area due to dynamic interactions of use, management, climate, plant, and soil factors (Taylor et al., 2007). Thus the low number of sampling locations restricts detailed analysis and may mask variability.

Variability of a property in space is better explained using geostatistics. Geostatistics provides a number of statistical techniques to evaluate spatial data which has been utilized in environmental science fields such as mineral resource mapping and precision agriculture (James and Goodwin, 2003; Taylor et al., 2003; Emery and González, 2007). Global Positioning Systems (GPS) enable the data to be geo-referenced (i.e. record of longitudinal and latitudinal location) and imported into Geographic Information Systems (GIS) where geostatistics can be implemented.

Specifically, two geostatistical techniques, variograms and interpolation, are commonly used. A variogram (also referred to as semivariogram) is a function of the distance and direction separating measured points used to quantify the spatial autocorrelation (also referred to as spatial dependence) of the data set (ESRI, 2004). The semivariogram represents half the difference squared of the values between each pair of points (i.e. semivariance) at different distances then fits a model to the empirically derived data points (Webster and Oliver, 2007).

It is important to note that the most determining factor for an accurate semivariogram, and the one in which we have the most control over, is the sample size that it is based on (Oliver and Webster, 2014). Typically, the more data you have the greater the accuracy. Oliver and Webster (2014) demonstrated, from repeated grid sampling of a large two-dimensional simulated field, that confidence intervals narrow as the number of data samples increases and the distance between the data samples decreases. They concluded that semivariograms generated from fewer than 100 data samples were unreliable.

Secondly, interpolation creates continuous surface maps of the data for visual assessment. To do so, predictions are made for locations in the study area based on the semivariogram and spatial arrangement of measured values that are nearby (ESRI, 2004). Kriging is a common interpolation method that forms weights from surrounding measured values to predict values at unmeasured locations (ESRI, 2004). With kriging interpolation, the closest measured values have the most influence on weights. Much like the semivariogram, sample size can greatly influence the accuracy and detail of a kriged surface map.

GIS is more common in agriculture to implement the precision agriculture (PA) concept (Rhoades, 1999; Corwin and Lesch, 2005; Thomsen et al., 2007). PA involves applying inputs, such as water, fertilizers, and cultivation only where, when, and in the amount needed (Bouma et al., 1999; Corwin and Lesch, 2005; Bullock et al., 2007). As a parallel to PA, the concept of precision turfgrass management (PTM) is gaining increasing attention for enhanced input efficiency and management decision in turfgrass (Stowell and Gelernter, 2008; Carrow et al., 2007; Bell and Xiong, 2008; Krum, 2008; Carrow et al., 2010; Krum et al., 2010). PTM was developed and based on the premise of site-specific management. To a certain degree, complex turf sites already use some degree of PTM. For example, on sports fields, management can differ

significantly depending on turf species, soil class, field usage, level of sport, and the sport itself being played. However, the evolution of PTM is based on acquiring detailed site information by intensive data sampling to offer an even more precise and efficient management of inputs, such as sub-areas within a sports field, than is currently practiced now (Carrow et al., 2010). Performance testing can be viewed as the site assessment referred to in the PTM concept.

Few researchers have used geostatistical methods to analyze spatial variability of surface and edaphic properties on natural turf sports fields; however, none evaluated turf performance (Miller, 2004; Freeland et al., 2008; Caple et al., 2012). Aside from Freeland et al. (2008), who used an electric golf cart to tow a ground penetrating radar (GPR) for the rapid assessment of soil compaction, all other data collection in these studies used handheld sensors for data collection. A disadvantage of sampling at such a high intensity with handheld sensors is that it can be timely, costly, and labor intensive.

In agriculture, mobile platforms, with built in sensors, have been developed for efficient sampling and more precise spatial analysis. For example, Stowell and Gelernter (2006) reported on a mobile system with GPS capability with combined spectral unit for measuring NDVI and an electromagnetic induction (EM) device. Recently in turfgrass, the Toro Precision Sense 6000 (PS6000) (The Toro Company, Bloomington, MN) was developed for rapid sampling on complex turfgrass sites. The PS6000 simultaneously measures NDVI (unit-less with best = 1.0), volumetric water content (VWC, %), and soil compaction (penetration resistance; N in m kg $s^{-2}$) all while using GPS to geo-reference longitudinal and latitudinal location of samples.

Currently, Krum et al. (2010) are the only researchers to utilize the PS6000 for NDVI research in turf. Their study used geostatistical techniques to identify site-specific management units (SSMU's), on two golf course fairways, to aide in the application of inputs as well as

potentially identify deficiencies in irrigation systems. Since NDVI could reflect water stress from past irrigation scheduling, NDVI surface maps were used as secondary considerations to VWC surface maps, when troubleshooting irrigation system deficiencies.

Spatial NDVI data generated from a mobile sensor could be beneficial for early detection of turf stresses associated with sports fields, such as wear, compaction, and water deficiencies. By following through with the concept of PTM, site-specific management of cultural practices could be implemented. Additionally, NDVI data can be used for coordinating game and practice schedules to spread out the level of wear between multiple fields or areas on one field. Preventing continuous wear in the same locations can decrease soil compaction and increase turf performance and the quality and longevity of sports fields.

Mobile multi-sensor devices to conduct performance tests with spatial analysis have yet to be utilized on sports fields, but can be fundamental in developing a site-specific, comprehensive sports turf management program. Site-specific information is the first requirement of spatial analysis. To the author's knowledge, the PS6000 is the first and only mobile multi-sensor device, with GPS capability, for use on turfgrass sites. However, there are currently few available for use, thus limiting data collections to handheld devices in most instances. Furthermore, an efficient sampling procedure, using either methodology, has yet to be implemented for an accurate spatial analysis. Therefore, the primary objective of this study was to utilize the PS6000 to evaluate 7 different sample grid sizes, and a sample size of 7 locations resembling previous performance testing methods, to define an effective, science-based grid spacing for an accurate spatial analysis of NDVI on natural turf sports fields.

## Materials and Methods

*Description of sports fields*

Research was conducted at the Grimes Bridge Soccer Complex in the city of Roswell, GA and at the Oconee Veterans Park in Watkinsville, GA. A total of six community level sports fields were used between the two locations. The Roswell location included three 'Tifway 419' hybrid bermudagrass (*Cynodon dactylon* x *C. transvaalensis*) soccer fields mowed two times a week at 2.54 cm with a reel mower. The Watkinsville location included three 'TifSport' bermudagrass soccer fields also mowed two times a week at 2.54 cm with a reel mower. All fields evaluated had sandy loam soils and field size ranged from 60-64 m x 95-104 m (Tables A-1 and A-2, Appendix).

Soccer was the primary sport played on all fields at both locations (Table A-1, Appendix). Fields in Roswell were constructed in tiers, with field 1 being at the top, field 2 in the middle, and field 3 below. Two concrete walls approximately 9.1 m and 3.0 m high separates fields 1 and 2, and fields 2 and 3, respectively. Field 1 is open to the public while fields 2 and 3 remain gated throughout the day and are solely used for scheduled practice and games. Fields in Watkinsville were designed in a flat open area (4.2 ha) and laid in close proximity to one another. Field 1 is directly north of field 3 with the south end zone of 1 being approximately 22.9 m from the north end zone of 3. Field 2 is centered approximately 22.9 m east of 1 and 3. All fields in Watkinsville are open to the public.

*Data collection*

NDVI data was collected in Roswell on 9 May, 2013 and in Watkinsville on 10 May, 2013 (Table A-1, Appendix). A GreenSeeker RT100 active sensor (NTech Industries, Inc. Ukiah, CA) measured NDVI on the turf surface. There are two GreenSeeker RT100 sensors

mounted to the Toro PS6000, which is a mobile multi-sensor device equipped to attach to the hitch of a utility vehicle. Only NDVI data from the sensor located on the right side of the PS6000 was used in this study. The sensor emits light pulses every 100 ms and outputs an averaged value every second. Passes made downfield with the PS6000 were 2.4 m apart and NDVI data was recorded using an on-board computer and displayed in a spreadsheet format. A NovAtel GPS (NovAtel Inc., Alberta, Canada), attached to the PS6000, was used to gather latitude and longitude information for the data.

The ArcGIS version 10.1 GIS and mapping software (ArcMap) was used to develop, display, analyze and interpret maps of the PS6000 NDVI data (ESRI, Redlands, CA). Using the editor tool in ArcMap, samples were removed from the initial data collection to create the various sample sizes evaluated in this study. For each field, a total 8 sample sizes were manipulated including 7 sampling grids as well as a sampling pattern that resembles test procedures from previous non-spatial performance testing research (Table 4.1-4.4; Figures 4.1a-4.48a).

*Statistical analysis*

Analysis of field data was done in three components. First, summary statistics were produced to evaluate central tendency, variability, and frequency distribution of data from each sample size on all fields. The mean is commonly used to measure central tendency and is calculated by:

$$\bar{x} = \frac{\sum x}{n} \qquad \text{[Eq. 4.1]}$$

where $\sum x$ is the sum of all values and $n$ is the number of samples taken. Comparison of means between sample sizes within each field was done using one-way ANOVA and Fisher's Protected LSD ($P < 0.05$). Data analysis was performed using the 'agricolae' package (Mendiburu, 2014)

in R version 2.15.2 statistical software (R Development Core Team, 2008). Skewness is a measure of degree of symmetry and determines extent of even or uneven data distribution in relation to the mean:

$$\text{Skewness} = \frac{\sum(X_i - \overline{\text{X}})^3}{ns^3} \qquad \text{[Eq. 4.2]}$$

Kurtosis measures the degree of flatness or peakness of a data set:

$$\text{Kurtosis} = \frac{\sum(X_i - \overline{\text{X}})^4}{ns^4} \qquad \text{[Eq. 4.3]}$$

Histograms (not shown) were also produced to visually assess the central tendency and shape of data distribution.

The range is the simplest measure of data variability and is simply the difference between the highest and the lowest value in the data set. The standard deviation (SD) shows how much variation of the data there is from the mean and can be found using:

$$s = \sqrt{\frac{\sum(\text{X}_i - \overline{\text{X}})^2}{n}} \qquad \text{[Eq. 4.4]}$$

where $\text{X}_i$ is the value of observation *i*. The standard error of the mean (SE) is the level of dispersion of the data from the mean and is calculated:

$$\text{SE}_{\bar{X}} = \frac{s}{\sqrt{n}} \qquad \text{[Eq. 4.5]}$$

The coefficient of variability (CV) is different from standard deviation in that it is expressed as a percentage of the mean and consequently allows for analysis between data sets with different absolute values. Therefore, the CV is valuable as a relative index of data dispersion:

$$\text{CV} = \frac{s}{\overline{\text{X}}}(100) \qquad \text{[Eq. 4.6]}$$

Next, semivariograms were created by plotting the semivariance, $\gamma(h)$, between each pair of data. Semivariance is quantified using the equation:

$$\gamma(h) = \frac{1}{2N(h)} \sum_{i=1}^{N(h)} [z(x_i) - z(x_i + h)]^2 \qquad \text{[Eq. 4.7]}$$

where $N(h)$ is the number of pairs of data separated by a lag distance $h$, and $z$ is the value of the given measurement at location $x_i$. The lag distance $h$ is the spatial range between two data points. If a grid survey is used for sampling it is common to use the grid spacing as $h$ (Oliver and Webster, 2014). Therefore, when constructing the semivariograms of the sampling grids in this study, the respective grid spacing was used as $h$. For the sampling pattern not following a grid survey $h$ was found using the Average Nearest Neighbor tool in the Spatial Statistics toolbox of ArcMap (ESRI, Redlands, CA).

The range ($A_0$), nugget ($C_0$), sill ($C_0 + C$), and partial sill ($C$) are important components of a semivariogram and are used to describe the parameters of spatial structure. The range is the finite lag distance where spatial dependency occurs (i.e. at distances beyond the range there is little to no correlation among variables). The nugget is the value that intercepts the y axis and represents independent error, measurement error, and/or microscale variation at spatial scales that are too small to detect. The sill represents the total variance of the dataset; at large distances variables become uncorrelated and the sill of the semivariogram is equal to the variance of the random variable. The partial sill is the sill minus the nugget.

There are several models that can be fit to describe semivariograms; the spherical model is considered the most commonly used model for describing spatial data and was used to fit the semivariograms in this study (Jian, 1996). This model has linear behavior at small separation

distances near the origin but flattens out at larger distances and reaches the sill at the range (Isaaks, 1989). The spherical model is calculated by:

$$\gamma(h) = \begin{cases} 0, & h = 0 \\ C_0 + (C - C_0)\left\{\frac{3h}{2A_0} - \frac{1}{2}\left(\frac{h}{A_0}\right)^3\right\}, & 0 \le h \le A_0 \\ C_0 + (C - C_0), & h \ge A_0 \end{cases} \qquad \text{[Eq. 4.8]}$$

where $C_0$ is the nugget ($C_0 \geq 0$), $C$ is the sill ($C \geq 0$), $A_0$ is the range ($A_0 \geq 0$), and $h$ is the lag distance as defined in Eq. 1 (Jian, 1996).

Lastly, visual assessment of the measured parameters was done using kriging, with the Geostatistical Analyst extension of ArcMap, to create prediction surface maps (ESRI, Redlands, CA). The formula for kriging is:

$$\hat{Z}(x_0) = \sum_{i=1}^{N} \lambda_i z(x_i) \qquad \text{[Eq. 4.9]}$$

where $\hat{Z}(x_0)$ is the predicted value at the prediction location, $N$ is the number of measured values, $\lambda_i$ is an unknown weight for the measured value at the $i$th location, and $z(x_i)$ is the measured value at the $i$th location (ESRI, 2004). There are various models of kriging, for this study simple kriging was used. Simple kriging assumes the model:

$$\hat{Z}(x) = \mu + \varepsilon(x) \qquad \text{[Eq. 4.10]}$$

where $\hat{Z}(x)$ is the variable of interest, $\mu$ is the known mean constant, and $\varepsilon(x)$ is formed from autocorrelated errors.

Following kriging, cross-validation is conducted to provide summary statistics in order to choose the most plausible model. Cross-validation is the process by which each of the $N$ data points is omitted in turn from the set of data and it value is predicted using the chosen kriging model (Oliver and Webster, 2014). Three statistics are calculated; the mean error (ME), the root

mean squared error (RMSE), and the root mean square standardized error (RMSSE). The ME is the average difference between each measured and predicted value:

$$\frac{1}{N}\sum_{i=1}^{N} z(x_i) - \hat{Z}(x_i) \qquad \text{[Eq. 4.11]}$$

The RMSE indicates how closely the model predicts the measured values:

$$\frac{1}{N}\sum_{i=1}^{N} \{z(x_i) - \hat{Z}(x_i)\}^2 \qquad \text{[Eq. 4.12]}$$

Lastly, the RMSSE is the RMSE divided by the corresponding kriging variance:

$$\frac{1}{N}\sum_{i=1}^{N} \frac{\{z(x_i) - \hat{Z}(x_i)\}^2}{\hat{\sigma}_K^2(x_i)} \qquad \text{[Eq. 4.13]}$$

where $\hat{\sigma}_K^2(x_i)$ is the kriging variance. RMSSE should be close to 1 if the prediction standard errors are valid (ESRI, 2004).

## Results

*Descriptive statistics*

According to Fisher's Protected LSD, significant differences in mean of NDVI were observed between sample sizes on all fields with exception of Roswell 2 and Watkinsville 2 (Table 4.1 and 4.2, respectively). At Roswell 1, sample grid sizes of 2.4 m x 2.4 m to 9.6 m x 9.6 m all had statistically similar means and then differences became apparent with larger grid sizes and at the 7 sample size (Table 4.1). All sample sizes at Roswell 3 were similar to one another with only the 7 sample size and the 19.2 m x 19.2 m sample grid being different (Table 4.1). Watkinsville 1 exhibited similar means with grid sizes 2.4 m x 2.4 m to 9.6 m x 9.6 m and the 7 sample size (Table 4.1). The 9.6 m x 9.6 m and 19.2 m x 9.6 m sample grids had similar means and the 19.2 m x 9.6 m and 19.2 m x 19.2 m sample grid were also similar. Lastly, on Watkinsville 3 all sample grid sizes had similar means to one another with the 19.2 m x 9.6 m

being the only different. However, grids 9.6 m x 4.8 m through 19.2 m x 19.2 m did show to be also be similar to one another (Table 4.2).

Positive skewness indicates the mass of the distribution is concentrated on the left side (i.e. lower NDVI values). A negative skewness indicates the mass of distribution is concentrated on the right side (i.e. higher NDVI values). A skewness of 0 would exhibit perfect symmetry and data falling within -1 and 1 are said to be normally distributed. In both Roswell and Watkinsville primarily negative skewness was observed indicating that the mass distribution of the data is higher NDVI values. Roswell 1 exhibited non-normal distribution with sample grids 2.4 m x 2.4 m to 9.6 m x 9.6 m (Table 4.1). On Roswell 2, the only sample grids with non-normal distribution were the 2.4 m x 2.4 m and 4.8 m x 2.4 m. The 9.6 m x 4.8 m was the single non-normal distributed grid size on Roswell 3. At Watkinsville, only field 1 had sampling schemes with non-normal distributions and those were with sample grids 2.4 m x 2.4 m through 9.6 m x 9.6 m as well as the 7 sample size (Tables 4.3).

A kurtosis value > 3.0 indicates a leptokurtic (peaked) distribution, a mesokurtic (normal) distribution has a kurtosis of 3.0, and a platykurtic (flat) distribution is < 3.0 (McGrew and Monroe, 2009). All fields at both locations tended to have leptokurtic distributions with the exception of one or two sampling schemes on each field being either mesokurtic or platykurtic (Table 4.1 and 4.2). Significantly high kurtosis values such as the 2.4 m x 2.4 m sample grid on Roswell field 2, indicates that the data is not normally distributed and is extremely peaked (i.e. centered around the mean).

Although the mean, skewness, and kurtosis can be a useful tool in understanding the data, they provide little information about variability. The range is the simplest method to determine variability, with wide ranges indicating more. From the smallest sampling grid to the largest

sampling grid the range often decreased dramatically, indicating far less variability being accounted for with larger grid spacing (Table 4.1 and 4.2). This result is expected, since low and high values can be omitted from the dataset as more samples are removed to create larger grid sizes. The range of the 7 sample sizes fluctuated in comparison to the grid sizes. On three of the fields, the range of the 7 sample size was lower than all grid sizes while on the other three fields the range was somewhere in the middle of that of their respective grid sizes (Table 4.1 and 4.2).

The SD, SE, and CV are all common measures of data variability. The SD and CV did not differ dramatically between sample sizes on Roswell fields 2 and 3 and Watkinsville fields 2 and 3, with the exception of the 7 sample size (Table 4.1 and 4.2, respectively). Roswell 1 and Watkinsville 1 SD and CV were somewhat similar from the 2.4 m x 2.4 m sample grid to the 9.6 m x 9.6 m sample grid before decreasing with the larger grid sizes (Table 4.1). The SD and CV for the sample sizes of 7 were higher than all grid sizes with exception of Roswell 3 where they did not differ significantly (Table 4.1 and 4.2). SE increased as sample size decreased for all fields (Table 4.1 and 4.2). Smaller SE indicates less sampling error and is primarily influenced by sample size. Therefore, this result was expected.

*Spatial analysis*

Semivariograms were generated for all sample sizes to describe parameters of spatial structure (Figures 4.1c-4.48c). The range represents the distance, at which once beyond, a pair of samples is no longer correlated. Sampling distances should be less than the range if data are to be spatially correlated for interpolation. The ranges for all sample grids on each field was greater than the sampling distance used indicating all were sufficient (Tables 4.7-4.12; Figures 4.1c-4.48c).

The nugget and sill provide information to determine error and variability of the models, respectively. A trend in nugget and sill values between sampling grids on each field was not observed (Table 4.3 and 4.4). Nugget and sill values also varied from field to field. Sample sizes of 7, and the 19.2 m x 19.2 m sample grid on Watkinsville 3, indicated pure nuggets (Table 4.3 and 4.4). Pure nuggets occur when the nugget equals the sill, which indicates that the distance between sampling intervals is too large and the scale of spatial dependency is determined in ranges less than the shortest sampling distance. It is not recommended to conduct interpolation on a pure nugget (Oliver and Webster, 2014).

It is common to use the nugget/sill ratio of each dataset to assess the strength of spatial dependence (< 25% indicates strong spatial dependence, 25-75% indicates moderate spatial dependence, and > 75% indicates weak spatial dependence) (Cambardella et al., 1994). A large ratio can indicate that substantial measurement errors are present or the need of a more intense sampling, or both (Oliver and Webster, 2014). Strong spatial dependence occurred for at least one sample grid on all fields except Watkinsville 2 (Table 4.3 and 4.4). On Roswell 1, all sample grids except the 19.2 m x 19.2 m grid exhibited strong spatial dependence (Table 4.3). Roswell 2 had strong spatial dependence with sample grids 9.6 m x 4.8 m through 19.2 m x 9.6 m (Table 4.3). All other grid sizes exhibited moderate spatial dependence. Sample grids 2.4 m x 2.4 m and 4.8 m x 4.8 m through 9.6 m x 9.6 m had strong spatial dependence on Roswell field 3 with all other grid sizes having moderate spatial dependence (Table 4.3). In Watkinsville, field 1 exhibited strong spatial dependence with sample grids 2.4 m x 2.4 m through 9.6 m x 9.6 m with the 19.2 m x 9.6 m and 19.2 m x 19.2 m grids being moderate (Table 4.4). Watkinsville 2 sample grids all had moderate spatial dependence except the 19.2 m x 19.2 m grid which was weak (Table 4.4). Lastly, Watkinsville 3 had strong spatial dependence for sample grids 2.4 m x 2.4 m

through 9.6 m 4.8 m, moderate spatial dependency for the 9.6 m x 9.6 m sample grid, and weak spatial dependency for all other grid sizes with the 19.2 m x 19.2 m exhibiting pure nugget (Table 4.4). All sample sizes of 7 had weak spatial dependence and each exhibited a pure nugget (Table 4.3 and 4.4).

*Visual assessment*

All fields at Roswell showed similar NDVI patterns between their respective sample grids of 2.4 m x 2.4 m and 4.8 m x 2.4 m (Figure 4.1b and 4.2b, 4.9b and 4.10b, and 4.17b and 4.18b). While the level of detailed variability decreased as sample grid size increased, generally similar patterns of NDVI across the fields were noticeable until the 9.6 m x 4.8 m sampling grid (Figure 4.1b-4.4b, 4.9b-4.12b, and 4.17b-4.20b). NDVI surface maps began to deteriorate at sample grid sizes of 9.6 m x 9.6 m and greater until ultimately exhibiting no variability with the pure nugget sample sizes of 7 (Table 4.5b-4.8b, 4.13b-4.16b, and 4.21b-4.24b).

All fields at Watkinsville also showed similar NDVI patterns for their respective sample grids of 2.4 m x 2.4 m and 4.8 m x 2.4 m (Figure 4.25b and 4.26b, 4.33b and 4.34b, and 4.41b and 4.42b). On Watkinsville 1 general patterns of NDVI were apparent through sampling grid 19.2 m x 9.6 m however detailed variability was greatly reduced as sample grid size increased (Figure 4.25b-4.30b). The 19.2 m x 19.2 m sample grid size is not an acceptable representation of NDVI in comparison to the smaller grid sizes and the 7 sample size shows no variability due to being a pure nugget (Figures 4.31b and 4.32b). Watkinsville 2 exhibited similar NDVI patterns with sample grids 2.4 m x 2.4 m though the 9.6 m x 4.8 m (Figure 4.33b-4.36b). NDVI began to deform with the 9.6 m x 9.6 m sample grid and beyond until the pure nugget sample size of 7 (Figure 4.37b-4.40b). Watkinsville 3 exhibited a decrease in detailed variability with increasing sample grid sizes up to 9.6 m x 9.6 m (Figure 4.41b-4.45b). The 19.2 m x 9.6 m

sample grid did not display an acceptable NDVI surface map and the 19.2 m x 19.2 m and 7 sample size had no variability due to a pure nugget (Figure 4.46b-4.48b).

Following kriging, cross-validation is conducted to provide prediction errors. The ME should be close to zero if the predicted values are centered around the measurement values (unbiased predictions). The ME varied between sample grids on all fields (Table 3.3 and 3.4). Pure nugget semivariograms exhibited an ME of 0, but these models have already been observed as an unacceptable option.

If predicted values being close to the measurement values would result in a low RMSE. There were no trends of RMSE between sample sizes on each field (Table 4.3 and 4.4). The lower RMSE were typical with smaller sample grid sizes and higher RMSE with larger grid sizes. However, the lowest RMSE were not always associated with small grid sizes. The highest RMSE would be expected with the 7 sampling grid, but was only true for four of the six fields.

If RMSSE are greater than 1, the variability in the predictions is underestimated; if the RMSSE are less than 1, the variability in the predictions is overestimated. RMSSE varied between sample sizes on all fields. All RMSSE were less than 1 on Roswell 1 and 2, except the 9.6 m x 9.6 m sample grid on both fields and the 9.6 m x 4.8 m on field 2 (Table 4.3). On Roswell 3 sample grids 2.4 m x 4.8 m, 19.2 m x 9.6 m, and 19.2 m x 19.2 m had a RMSSE less than 1 with all other grid sizes being greater than 1. All sample grids at Watkinsville were less than 1 except the 19.2 m x 19.2 m grid on field 1, the 9.6 m x 9.6 m grid on field 2, and the 2.4 m x 2.4 m grid on field 3 (Tables 4.4). The majority of sample grids having RMSSE less than 1 indicates that the variability of the predictions of NDVI on these fields tend to be overestimated.

## Discussion

Comprehensive insight of the spatial variation of plant performance on sports fields can be provided with descriptive statistics and geostatistical techniques. Often, as seen with previous methods of performance testing, the mean is the determinate statistic to quantify performance of a given variable on a sports field; although it is highly unpractical to predict the true value. In theory, a higher sampling intensity would be a better prediction than a low sampling intensity. However, of the six fields evaluated, two showed no significant differences in NDVI mean between sample sizes. Of the four fields that did show differences, although statistically significant, were not dramatically different aside from the 7 sample sizes. These results suggest that the central tendency of a field can be approximated with lower sampling numbers; however spatial variability of NDVI in exact locations across the field is not identified.

Defining spatial variability was better conducted using geostatistics. Ideally, the best type of model will have a low nugget with a high sill to indicate that greater micro-scale variability is accounted for with less measurement error and also to provide a low nugget/sill ratio indicating strong spatial dependence. Although, the ratio can warn us of measurement errors and/or micro-scale variability, it tells us nothing about the underlying variation of properties that vary continuously in space (Oliver and Webster, 2014). This phenomenon is better explained with interpolation.

The best indication of NDVI variation in space was with generated surface maps from kriging interpolation. Generally, as sample grid sized increased, accounted variability decreased. Results from this study show that larger sample grid sizes, such as 9.6 m x 9.6 m and 19.2 m x 9.6 m, are capable of showing similar trends of NDVI variability as smaller sample grid sizes. However, these mask detailed variability in certain locations and provide a less accurate surface

map. Thus, sampling schemes should be chosen relative to the desired degree of accounted variability, with smaller sampling grids providing the most accuracy and detail. Detailed spatial information is important when identifying why small (or large) areas of extreme (high or low) values are exhibited for a particular property.

The ME, RMSE, and RMSSE, obtained from cross-validation are good indicators of prediction errors and should be used when considering models. However, they depend on the scale of the data and should not be the sole determinate. The combination of descriptive statistics, geostatistics, and general knowledge of the site conditions and use before spatial analysis can aide in interpretation of the interpolated data and selecting the best model (Oliver and Webster, 2014).

It is important to emphasize that data collection and spatial analysis in this study was conducted after rainfall events when fields were at field capacity. At field capacity the spatial distribution of NDVI may be influenced by turf stress prior to the rain (or in other instances, a heavy irrigation event) that is severe enough to affect turf color or density (Carrow et al., 2010). NDVI relationships to soil properties, such as VWC and compaction, when data is obtained at field capacity may not be strong. However, when data is obtained at less than field capacity, these properties could be better related. Thus, for spatial analysis of NDVI on sports fields, data collection at both field capacity, and less than field capacity, give the most robust information. Since our study only evaluated sample procedures for spatial analysis of NDVI at field capacity, further research should evaluate sample procedures for spatial analysis of NDVI at less than field capacity to determine an appropriate protocol for data collection under such conditions.

Comparison of results from this study is difficult. Straw et al. (Chapters 2 and 3) have been the only researchers to use mobile devices to evaluate spatial analyses for different

sampling procedures on sports fields, but only for VWC and penetration resistance. However, similar results were observed regarding measuring central tendency with smaller sample sizes and general trends of variability decreasing with increasing sample size. Though in this study, strong spatial dependence occurred more often at larger sample grids resulting in patterns of NDVI being evident in those surface maps in comparison to maps of the smaller sample grids. These results indicate that NDVI variability in space could be detected with greater sample grids than VWC and penetration resistance.

Other researchers that have conducted spatial analysis on sports fields have not evaluated NDVI, nor used mobile devices. Handheld devices that were used for data collection in these studies may be time, cost, and labor intensive for certain facilities. The PS6000 was capable of sampling a soccer field, using a distance of 2.4 m between passes (> 2000 NDVI samples), in approximately 1 h and would be more practical for use of mapping multiple sports fields at one facility.

Handheld devices, however, should not be completely disregarded due to the development of mobile devices. Data collection for spatial analysis of a small number of fields could be feasible using handheld devices with the sample grids evaluated in this study. Our results found a minimum sampling procedure of 9.6 m x 9.6 m (~75-85 samples) can provide an acceptably accurate spatial analysis of NDVI. However, the sample grids used in this study were manipulated in GIS from data collected with the PS6000. Future research should consider using handheld devices, at these sampling grids, to determine if they correlate with analyses conducted in this study.

Moreover, spatial analysis of sports fields by Miller (2004) and Caple et al. evaluated variability of surface and edaphic properties for various soil classes. Miller observed higher

uniformity of surface hardness on sand-based fields than that of native soil. Caple et al. detected greater spatial and temporal uniformity of sand rootzone fields compared to clay loam and loamy sand for all observed properties. Due to the observed uniformity of properties on sand-based sports fields, a smaller sampling grid may be required to account for short-range variability between samples. Our study only evaluated fields with sandy loam soils; therefore, further research with varying sampling schemes on fields with different soil classes should be conducted for comparisons.

## Conclusions

Performance tests to spatially analyze surface and edaphic properties, such as plant performance, on sports fields can be fundamental in determining a site-specific sports turf management program. As a result, an increase in player safety and field playability, and the reduction of inputs can be achieved. Performance testing on sports fields in the past have used minimal amount of samples across a field. However, to better assess the variability of a property, as well as the relationship between properties, spatial analysis using geostatistics is more appropriate. This would involve implementing a more intense sampling procedure and the use of geostatistical techniques, such as semivariograms and interpolation.

The most important factor in determining the reliability, or accuracy, of a semivariogram is the sample size on which it is based (Oliver and Webster, 2014). In general, the more data you have for spatial analysis, the greater the accuracy. It is for this reason that mobile sensor platforms are the most practical means of data collection over larger areas, because of the ability to sample more intensely and the addition of an equipped GPS. With a mobile platform, like the PS6000, the user may sample as intense as desired. Our results suggest that at minimum a 9.6 m x 9.6 m sampling grid (~75-85 samples) be utilized for spatial analysis of NDVI on sports fields

using geostatistical techniques. For the PS6000, this exact sampling grid is not achievable in the field because samples are collected every ~2.4 m. We suggest distances between passes downfield be 4.8 m (an approximate 4.8 m x 2.4 m sample grid) or at most 9.6 m (an approximate 9.6 m x 2.4 m sample grid). However, due to the relatively short time for data collection with the PS6000 (~1 h), an intense sample grid such as 2.4 m x 2.4 m would be most beneficial.

Furthermore, to date, mobile sensors are not abundantly available for commercial use. Sports fields differ from agriculture and golf courses with respect to the area managed. Use of the more commonly available handheld devices to spatially analyze sports field properties could be feasible if a standard procedure is implemented. However, the sample grids used in this study were manipulated in GIS from data collected with the PS6000. Future research should consider a comparison of spatial analyses, using sample grids from this study, between handheld and mobile devices.

## References

American Society for Testing and Materials (ASTM). 2010. F1936–10, Standard specification of impact attenuation of turf playing systems as measured in the field. Annual book of ASTM standards. American Society for Testing Materials, West Conshohocken, PA.

Baker, S.W. 1991. Temporal variation of selected mechanical properties of natural turf football pitches. J. Sports Turf Res. Inst. 67:83-92.

Baker, S.W., and P.M Canaway. 1993. Concepts of playing quality: criteria and management. Int. Turfgrass Soc. Res. J. 7:172-181.

Bartlett, M.D., I.T. James, M. Ford, and M. Jennings-Temple. 2009. Testing natural turf sports surfaces: the value of performance quality standards. Proceedings of the Institution of Mechanical Engineers, Part P. J. Sports Eng. and Technol. 223:21-29.

Beard, J.B. 1973. Turfgrass: Science and culture. Prentice Hall Inc., Englewood Cliffs, NJ.

Bell, G.E., and X. Xiong. 2008. The history, role, and potential of optical sensing for practical turf management. p. 641-660. *In* M. Pessarakli (Ed.), Handbook of turfgrass management and physiology. CRC Press, NY.

Bouma, J., J. Stoorvogel, B.J. van Alphen, and H.W.G. Booltink. 1999. Pedology, precision agriculture, and the changing paradigm of agricultural research. Soil Sci. 63.6:1763-1768.

Bullock, D.S., N. Kitchen, and D.G., Bullock. 2007. Multidisciplinary teams: a necessity for research in precision agriculture systems. Crop Sci. 47:1765-1769.

Cambardella, C.A., T.B. Moorman, T.B. Parkin, D.L. Karlen, J.M. Novak, R.F. Turco, and A.E. Konopka. 1994. Field-scale variability of soil properties in central Iowa soils. Soil Sci. Soc. Am. J. 58:1501-1511.

Caple, M., I. James, and M. Bartlett. 2012. Spatial analysis of the mechanical behaviour of natural turf sports pitches. Sports Eng. 15:143-157.

Carrow, R.N., and A.M. Petrovic. 1992. Effects of traffic on turfgrasses. p. 285-330. *In* Carrow, R.N and R.C. Shearman (Eds.), Turfgrass. ASA, Madison, WI.

Carrow, R.N., V. Cline, and J. Krum. 2007. Monitoring spatial variability in soil properties and turfgrass stress: applications and protocols. Proc. of 28th Int. Irrigation Show, 9-11 Dec. 2007, San Diego, CA.

Carrow, R.N., J.M Krum, I. Flitcroft, and V. Cline. 2010. Precision turfgrass management: challenges and field applications for mapping turfgrass soil and stress. Precis. Agric, 11:115-134.

Corwin, D.L., and S.M. Lesch. 2005. Apparent soil electrical conductivity measurements in agriculture. Comput. Electron. Agric. 46:103-133.

Emery, X., and K. González. 2007. Incorporating the uncertainty in geological boundaries into mineral resources evaluation. J. Geol. Soc. India. 69:29–38.

ESRI. 2004. ArcGIS 9: Using ArcGIS Geostatistical Analyst. ESRI, Redlands, CA.

Freeland, R.S., J.C. Sorochan, M.J. Goddard, and J.S. McElroy. 2008. Using ground-penetrating radar to evaluate soil compaction of athletic turfgrass fields. Appl. Eng. Agric. 24:509-514.

Haggar, R.J., C.J. Stent, and S. Isaac. 1983. A prototype hand-held patch sprayer for killing weeds, activated by spectral differences in crop/weed canopies. J. Agric. Eng. Res. 28:349-358.

Holmes, G., and M.J. Bell. 1986. A pilot study of the playing quality of football pitches. J. Sports Turf Res. Inst. 62:74-91.

Institute of Groundsmanship (IOG). 2014. Performance Quality Test (PQS) Methods. http://www.iog.org/train-education/Technical-Library/Performance+Quality+Standards/PQS+Methods+of+Test (accessed 25 Feb 2014).

Isaaks, E.H., and R.M Srivastava. 1989. Applied geostatistics. Oxford University Press. New York, NY.

James, I.T., and R.J. Godwin. 2003. Soil, water and yield relationships in developing strategies for the precision application of nitrogen fertiliser to winter barley. Biosyst. Eng. 84:467-480.

Jennings-Temple, M., P. Leeds-Harrison, and I. James. 2006. An investigation into the link between soil physical conditions and the playing quality of winter sports pitch rootzones. *In* The engineering of sport 6. 1:315-320. Springer, NY.

Jian, X., R.A. Olea, and Y.S. Yu. 1996. Semivariogram modeling by weighted least squares. Comput. Geosci. 22:387-397.

Krum, J.M. 2008. Spatial site assessment of soil moisture and plant status on golf courses. M.S. thesis. Univ. of Georgia, Athens, GA.

Krum, J.M., R.N. Carrow, and K. Karnok. 2010. Spatial mapping of complex turfgrass sites: Site-specific management units and protocols. Crop Sci. 50:301-315.

McAuliffe, K.W. 2008. The role of performance testing and standards in the sports turf industry: A case study approach. *In* J.C. Stier, L. Han, and D. Li (Eds.). Proceedings of 2nd international conference on turfgrass management and sports fields (pp. 391-398). Int. Soc. Hort. Sci, Belgium.

McGrew Jr, J.C., and C.B Monroe. 2009. An introduction to statistical problem solving in geography. Waveland Press, Long Grove, IL.

Mendiburu, F. (2014). agricolae: Statistical Procedures for Agricultural Research. R package version 1.1-7. http://CRAN.R-project.org/package=agricolae (accessed 1 April 2014).

Miller, G.L. 2004. Analysis of soccer field surface hardness. *In* P.A. Nektarios (Ed.), Proceedings of the first International Conference on Turfgrass Management and Science for Sports Fields. ISHS, Leuven, pp. 287-294.

Oliver, M.A., and R. Webster. 2014. A tutorial guide to geostatistics: Computing and modelling variograms and kriging. Catena. 113:56-69.

R Development Core Team. 2008. R: A language and environment for statistical computing. R Foundation for Statistical Computing, Vienna, Austria. http://www.R-project.org (accessed 1 April 2014).

Rhoades, J.D., F. Chanduvi, and S.M. Lesch. 1999. Soil salinity assessment: Methods and interpretation of electrical conductivity measurements. FAO Irrigation and Drainage Paper 57. Food and Agric. Organ. of the United Nations. Rome, Italy.

Stiles, V.H., I.T. James, S.J. Dixon, and I.N. Guisasola. 2009. Natural turf surfaces. Sports Med. 39(1):65-84.

Stiles, V. H., James, I. T., Dixon, S. J., & Guisasola, I. N. (2009). Natural turf surfaces. Sports Medicine, 39(1), 65-84.

Stowell, L., and W. Gelernter. 2006. Sensing the future. Golf Course Manage. 74(3):107-110.

Stowell, L., and W. Gelernter. 2008. Evaluation of a Geonics EM38 and NTech GreenSeeker sensor array for use in precision turfgrass management. *In* Abstracts, GSA-SSSA-ASACSSA-GCAGS Int. Annu. Meet., Houston, TX, 5-9 Oct. 2008. ASA-CSSA-SSSA, Madison, WI.

Taylor, J.C., G.A. Wood, R. Earl, and R.J. Godwin. 2003. Soil factors and their influence on within-field crop variability, part II: spatial analysis and determination of management zones. Biosyst. Eng. 84:441-453.

Taylor, J.A., A.B. McBratney, and B.M. Whelan. 2007. Establishing management classes for broadacre agricultural production. Agron. J. 99:1366-1376.

Thomsen, A., K. Schelde, P. Drøscher, and F. Steffensen. 2007. Mobile TDR for geo-referenced measurement of soil water content and electrical conductivity. Precis. Agric. 8:213-223.

Trenholm, L.E., R.N. Carrow, and R.R. Duncan. 1999. Relationship of multispectral radiometry data to qualitative data in turfgrass research. Crop Sci. 39:763-769.

Webster, R., and Oliver, M.A. 2007. Geostatistics for environmental scientists. John Wiley & Sons, Hoboken, NJ.

**Table 4.1.** Descriptive statistics of normalized difference vegetative index (NDVI) on fields at Roswell for evaluated sample sizes on 9 May, 2013.

| Sample size | Sample Grid | Mean (±SE)[†] [‡] | Min[§] | Max[¶] | Range | SD[#] | CV[††] (%) | Skewness | Kurtosis |
|---|---|---|---|---|---|---|---|---|---|
| Roswell 1 | | | | | | | | | |
| | | NDVI | | | | | | | |
| 1129 | 2.4 m x 2.4 m | 0.63 ± 0.004cd | 0.12 | 0.83 | 0.71 | 0.12 | 19.7 | -1.40 | 5.04 |
| 588 | 4.8 m x 2.4 m | 0.63 ± 0.005cd | 0.12 | 0.83 | 0.71 | 0.13 | 20.1 | -1.41 | 5.14 |
| 300 | 4.8 m x 4.8 m | 0.63 ± 0.008cd | 0.12 | 0.81 | 0.69 | 0.13 | 20.9 | -1.32 | 4.80 |
| 159 | 9.6 m x 4.8 m | 0.64 ± 0.011bcd | 0.12 | 0.81 | 0.69 | 0.14 | 22.0 | -1.61 | 5.65 |
| 83 | 9.6 m x 9.6 m | 0.65 ± 0.016bc | 0.12 | 0.81 | 0.69 | 0.14 | 21.9 | -1.91 | 6.99 |
| 47 | 19.2 m x 9.6 m | 0.69 ± 0.011a | 0.48 | 0.81 | 0.33 | 0.08 | 11.2 | -0.57 | 3.13 |
| 23 | 19.2 m x 19.2 m | 0.69 ± 0.017ab | 0.48 | 0.80 | 0.32 | 0.08 | 11.8 | -0.73 | 3.07 |
| 7 | N/A | 0.54 ± 0.062d | 0.32 | 0.73 | 0.41 | 0.16 | 30.1 | -0.29 | 1.46 |
| Roswell 2 | | | | | | | | | |
| | | NDVI | | | | | | | |
| 1195 | 2.4 m x 2.4 m | 0.71 ± 0.002a | 0.21 | 0.82 | 0.61 | 0.05 | 7.7 | -1.62 | 11.67 |
| 617 | 4.8 m x 2.4 m | 0.72 ± 0.002a | 0.43 | 0.82 | 0.39 | 0.05 | 7.4 | -1.06 | 5.56 |
| 310 | 4.8 m x 4.8 m | 0.72 ± 0.003a | 0.49 | 0.82 | 0.33 | 0.05 | 7.1 | -0.97 | 5.24 |
| 154 | 9.6 m x 4.8 m | 0.72 ± 0.004a | 0.49 | 0.82 | 0.33 | 0.05 | 7.5 | -1.00 | 5.11 |
| 77 | 9.6 m x 9.6 m | 0.72 ± 0.006a | 0.49 | 0.81 | 0.32 | 0.05 | 7.0 | -0.76 | 3.88 |
| 44 | 19.2 m x 9.6 m | 0.73 ± 0.007a | 0.61 | 0.82 | 0.20 | 0.05 | 6.2 | -0.36 | 2.75 |
| 24 | 19.2 m x 19.2 m | 0.73 ± 0.010a | 0.61 | 0.80 | 0.19 | 0.05 | 6.6 | -0.78 | 3.03 |
| 7 | N/A | 0.69 ± 0.027a | 0.55 | 0.79 | 0.23 | 0.07 | 10.4 | -0.89 | 3.29 |
| Roswell 3 | | | | | | | | | |
| | | NDVI | | | | | | | |
| 1021 | 2.4 m x 2.4 m | 0.74 ± 0.001ab | 0.51 | 0.84 | 0.33 | 0.05 | 6.5 | -0.72 | 4.10 |
| 531 | 4.8 m x 2.4 m | 0.74 ± 0.002ab | 0.51 | 0.84 | 0.33 | 0.05 | 6.5 | -0.90 | 4.78 |
| 266 | 4.8 m x 4.8 m | 0.74 ± 0.003ab | 0.51 | 0.83 | 0.32 | 0.04 | 6.0 | -0.81 | 5.27 |
| 145 | 9.6 m x 4.8 m | 0.74 ± 0.004ab | 0.51 | 0.83 | 0.32 | 0.05 | 6.3 | -1.13 | 6.50 |
| 73 | 9.6 m x 9.6 m | 0.74 ± 0.005ab | 0.58 | 0.83 | 0.26 | 0.05 | 6.2 | -0.69 | 4.16 |
| 42 | 19.2 m x 9.6 m | 0.75 ± 0.006ab | 0.66 | 0.83 | 0.17 | 0.04 | 5.0 | -0.33 | 3.10 |
| 20 | 19.2 m x 19.2 m | 0.76 ± 0.008a | 0.66 | 0.83 | 0.17 | 0.04 | 4.9 | -0.63 | 3.93 |
| 7 | N/A | 0.72 ± 0.018b | 0.66 | 0.79 | 0.12 | 0.05 | 6.5 | 0.08 | 1.64 |

[†] Within columns, means followed by the same letter are not significantly different at $p \leq 0.05$ according to Fisher's Protected LSD test.
[‡] SE, standard error
[§] Min, minimum
[¶] Max, maximum
[#] SD, standard deviation
[††] CV, coefficient of variability

**Table 4.2.** Descriptive statistics of normalized difference vegetative index (NDVI) on fields at Watkinsville for evaluated sample sizes on 10 May, 2013.

| Sample size | Sample Grid | Mean (±SE)[†] [‡] | Min[§] | Max[¶] | Range | SD[#] | CV[††] (%) | Skewness | Kurtosis |
|---|---|---|---|---|---|---|---|---|---|
| Watkinsville 1 | | | | | | | | | |
| | | NDVI | | | | | | | |
| 1095 | 2.4 m x 2.4 m | 0.53 ± 0.003c | 0.14 | 0.75 | 0.61 | 0.10 | 18.8 | -1.30 | 5.20 |
| 547 | 4.8 m x 2.4 m | 0.53 ± 0.004c | 0.14 | 0.75 | 0.61 | 0.10 | 19.4 | -1.33 | 5.20 |
| 273 | 4.8 m x 4.8 m | 0.53 ± 0.006c | 0.18 | 0.73 | 0.55 | 0.10 | 18.8 | -1.26 | 5.08 |
| 148 | 9.6 m x 4.8 m | 0.54 ± 0.008c | 0.18 | 0.70 | 0.52 | 0.10 | 18.4 | -1.34 | 5.38 |
| 78 | 9.6 m x 9.6 m | 0.55 ± 0.011bc | 0.18 | 0.70 | 0.52 | 0.10 | 18.1 | -1.43 | 5.75 |
| 45 | 19.2 m x 9.6 m | 0.58 ± 0.010ab | 0.40 | 0.70 | 0.30 | 0.07 | 12.1 | -0.74 | 3.00 |
| 24 | 19.2 m x 19.2 m | 0.60 ± 0.013a | 0.45 | 0.70 | 0.25 | 0.07 | 11.0 | -0.64 | 3.11 |
| 7 | N/A | 0.48 ± 0.059c | 0.18 | 0.62 | 0.45 | 0.15 | 32.4 | -1.04 | 2.98 |
| Watkinsville 2 | | | | | | | | | |
| | | NDVI | | | | | | | |
| 1089 | 2.4 m x 2.4 m | 0.65 ± 0.002a | 0.30 | 0.82 | 0.52 | 0.06 | 9.0 | -0.75 | 5.56 |
| 541 | 4.8 m x 2.4 m | 0.66 ± 0.003a | 0.37 | 0.82 | 0.45 | 0.06 | 9.1 | -0.65 | 5.00 |
| 273 | 4.8 m x 4.8 m | 0.66 ± 0.003a | 0.45 | 0.82 | 0.37 | 0.06 | 8.6 | -0.20 | 3.88 |
| 147 | 9.6 m x 4.8 m | 0.66 ± 0.004a | 0.50 | 0.80 | 0.30 | 0.05 | 8.2 | -0.01 | 3.69 |
| 76 | 9.6 m x 9.6 m | 0.66 ± 0.006a | 0.50 | 0.78 | 0.28 | 0.05 | 7.8 | -0.10 | 3.66 |
| 43 | 19.2 m x 9.6 m | 0.67 ± 0.008a | 0.55 | 0.78 | 0.23 | 0.05 | 7.6 | 0.25 | 3.15 |
| 24 | 19.2 m x 19.2 m | 0.66 ± 0.011a | 0.55 | 0.77 | 0.21 | 0.05 | 8.3 | 0.27 | 2.86 |
| 7 | N/A | 0.62 ± 0.026a | 0.50 | 0.68 | 0.18 | 0.07 | 11.0 | -0.83 | 2.33 |
| Watkinsville 3 | | | | | | | | | |
| | | NDVI | | | | | | | |
| 1121 | 2.4 m x 2.4 m | 0.58 ± 0.002b | 0.23 | 0.75 | 0.52 | 0.08 | 13.6 | -0.88 | 4.27 |
| 584 | 4.8 m x 2.4 m | 0.58 ± 0.003b | 0.23 | 0.75 | 0.52 | 0.08 | 14.0 | -0.89 | 4.46 |
| 295 | 4.8 m x 4.8 m | 0.58 ± 0.005b | 0.28 | 0.74 | 0.45 | 0.08 | 13.8 | -0.81 | 4.12 |
| 160 | 9.6 m x 4.8 m | 0.59 ± 0.007ab | 0.29 | 0.74 | 0.44 | 0.08 | 14.1 | -0.86 | 4.08 |
| 83 | 9.6 m x 9.6 m | 0.59 ± 0.010ab | 0.33 | 0.74 | 0.40 | 0.09 | 14.8 | -0.81 | 3.64 |
| 47 | 19.2 m x 9.6 m | 0.61 ± 0.011a | 0.35 | 0.74 | 0.39 | 0.08 | 12.4 | -0.96 | 4.65 |
| 24 | 19.2 m x 19.2 m | 0.60 ± 0.019b | 0.35 | 0.74 | 0.39 | 0.09 | 15.3 | -0.71 | 3.56 |
| 7 | N/A | 0.55 ± 0.041b | 0.40 | 0.68 | 0.28 | 0.11 | 19.8 | -0.38 | 1.74 |

[†] Within columns, means followed by the same letter are not significantly different at $p \leq 0.05$ according to Fisher's Protected LSD test.
[‡] SE, standard error
[§] Min, minimum
[¶] Max, maximum
[#] SD, standard deviation
[††] CV, coefficient of variability

**Table 4.3.** Geostatistical model parameters for normalized difference vegetative index (NDVI) on fields at Roswell for evaluated sample sizes on 9 May, 2013.

| Sample size | Sample Grid | Model | Nugget ($C_0$) | Sill ($C_0 + C$) | Nugget/Sill (%) | Spatial dependence[†] | Range (m) | ME[‡] | RMSE[§] | RMSSE[¶] |
|---|---|---|---|---|---|---|---|---|---|---|
| Roswell 1 | | | | | | | | | | |
| 1129 | 2.4 m x 2.4 m | Spherical | 0.00030 | 0.0151 | 2.0 | Strong | 22.9 | -0.00005 | 0.041 | 0.90 |
| 588 | 2.4 m x 4.8 m | Spherical | 0.00028 | 0.0170 | 1.6 | Strong | 21.1 | -0.00023 | 0.044 | 0.81 |
| 300 | 4.8 m x 4.8 m | Spherical | 0.00099 | 0.0170 | 5.8 | Strong | 25.2 | -0.00045 | 0.060 | 0.87 |
| 159 | 9.6 m x 4.8 m | Spherical | 0.00338 | 0.0194 | 17.4 | Strong | 27.6 | -0.00213 | 0.080 | 0.84 |
| 83 | 9.6 m x 9.6 m | Spherical | 0.00183 | 0.0208 | 8.8 | Strong | 28.9 | -0.00155 | 0.110 | 1.08 |
| 47 | 19.2 m x 9.6 m | Spherical | 0.00115 | 0.0065 | 17.5 | Strong | 36.2 | -0.00159 | 0.051 | 0.83 |
| 23 | 19.2 m x 19.2 m | Spherical | 0.00395 | 0.0069 | 57.7 | Moderate | 36.6 | -0.00480 | 0.072 | 0.90 |
| 7 | N/A | Spherical | 0.02670 | 0.0267 | 100.0 | Weak | 61.9 | 0 | 0.151 | 0.93 |
| Roswell 2 | | | | | | | | | | |
| 1195 | 2.4 m x 2.4 m | Spherical | 0.00087 | 0.0030 | 29.2 | Moderate | 37.1 | 0.00004 | 0.032 | 0.94 |
| 617 | 2.4 m x 4.8 m | Spherical | 0.00070 | 0.0027 | 25.8 | Moderate | 36.4 | 0.00003 | 0.029 | 0.90 |
| 310 | 4.8 m x 4.8 m | Spherical | 0.00069 | 0.0025 | 27.4 | Moderate | 33.2 | -0.00021 | 0.032 | 0.93 |
| 154 | 9.6 m x 4.8 m | Spherical | 0.00045 | 0.0029 | 15.4 | Strong | 33.3 | -0.00003 | 0.065 | 1.03 |
| 77 | 9.6 m x 9.6 m | Spherical | 0.00045 | 0.0032 | 14.1 | Strong | 26.2 | -0.00020 | 0.045 | 1.03 |
| 44 | 19.2 m x 9.6 m | Spherical | 0.00030 | 0.0020 | 15.1 | Strong | 56.7 | -0.00082 | 0.024 | 0.82 |
| 24 | 19.2 m x 19.2 m | Spherical | 0.00079 | 0.0030 | 26.6 | Moderate | 84.3 | -0.00092 | 0.030 | 0.74 |
| 7 | N/A | Spherical | 0.00550 | 0.0055 | 100.0 | Weak | 85.8 | 0 | 0.067 | 0.90 |
| Roswell 3 | | | | | | | | | | |
| 1021 | 2.4 m x 2.4 m | Spherical | 0.00045 | 0.0025 | 18.4 | Strong | 30.3 | -0.00010 | 0.028 | 1.04 |
| 531 | 2.4 m x 4.8 m | Spherical | 0.00064 | 0.0025 | 25.4 | Moderate | 37.5 | -0.00016 | 0.030 | 0.96 |
| 266 | 4.8 m x 4.8 m | Spherical | 0.00028 | 0.0021 | 13.7 | Strong | 29.5 | -0.00030 | 0.028 | 1.05 |
| 145 | 9.6 m x 4.8 m | Spherical | 0.00009 | 0.0023 | 4.0 | Strong | 30.7 | 0.00004 | 0.030 | 1.15 |
| 73 | 9.6 m x 9.6 m | Spherical | 0.00001 | 0.0022 | 0.3 | Strong | 30.6 | -0.00052 | 0.033 | 1.11 |
| 42 | 19.2 m x 9.6 m | Spherical | 0.00049 | 0.0016 | 31.0 | Moderate | 50.0 | -0.00191 | 0.279 | 0.90 |
| 20 | 19.2 m x 19.2 m | Spherical | 0.00038 | 0.0014 | 27.5 | Moderate | 42.0 | -0.00144 | 0.026 | 0.78 |
| 7 | N/A | Spherical | 0.00190 | 0.0019 | 100.0 | Weak | 99.9 | 0.00000 | 0.043 | 1.00 |

[†] Spatial dependence is described as strong, moderate, or weak for nugget/sill ratios <25%, 25-75%, or >75%, respectively.
[‡] ME, mean prediction error.
[§] RMSE, root-mean square prediction error.
[¶] RMSSE, root-mean square standardized prediction error.

**Table 4.4.** Geostatistical model parameters for normalized difference vegetative index (NDVI) on fields at Watkinsville for evaluated sample sizes on 10 May, 2013.

| Sample size | Sample Grid | Model | Nugget ($C_0$) | Sill ($C_0 + C$) | Nugget/Sill (%) | Spatial dependence[†] | Range (m) | ME[‡] | RMSE[§] | RMSSE[¶] |
|---|---|---|---|---|---|---|---|---|---|---|
| Watkinsville 1 | | | | | | | | | | |
| 1095 | 2.4 m x 2.4 m | Spherical | 0.00173 | 0.0103 | 16.8 | Strong | 25.2 | -0.00015 | 0.048 | 0.88 |
| 547 | 2.4 m x 4.8 m | Spherical | 0.00049 | 0.0110 | 4.5 | Strong | 23.9 | -0.00018 | 0.044 | 0.97 |
| 273 | 4.8 m x 4.8 m | Spherical | 0.00195 | 0.0105 | 18.6 | Strong | 25.9 | -0.00059 | 0.052 | 0.79 |
| 148 | 9.6 m x 4.8 m | Spherical | 0.00183 | 0.0102 | 17.9 | Strong | 25.2 | -0.00173 | 0.059 | 0.83 |
| 78 | 9.6 m x 9.6 m | Spherical | 0.00128 | 0.0100 | 12.7 | Strong | 21.9 | -0.00515 | 0.078 | 0.84 |
| 45 | 19.2 m x 9.6 m | Spherical | 0.00146 | 0.0049 | 30.1 | Moderate | 18.8 | -0.00474 | 0.063 | 0.96 |
| 24 | 19.2 m x 19.2 m | Spherical | 0.00282 | 0.0050 | 56.9 | Moderate | 97.6 | -0.00239 | 0.063 | 1.02 |
| 7 | N/A | Spherical | 0.02060 | 0.0206 | 100.0 | Weak | 85.0 | 0 | 0.143 | 1.00 |
| Watkinsville 2 | | | | | | | | | | |
| 1089 | 2.4 m x 2.4 m | Spherical | 0.00175 | 0.0040 | 43.3 | Moderate | 57.8 | -0.00017 | 0.036 | 0.80 |
| 541 | 2.4 m x 4.8 m | Spherical | 0.00172 | 0.0040 | 42.7 | Moderate | 48.1 | -0.00014 | 0.098 | 0.83 |
| 273 | 4.8 m x 4.8 m | Spherical | 0.00136 | 0.0036 | 37.2 | Moderate | 51.4 | -0.00009 | 0.038 | 0.88 |
| 147 | 9.6 m x 4.8 m | Spherical | 0.00110 | 0.0032 | 34.2 | Moderate | 49.4 | -0.00015 | 0.037 | 0.92 |
| 76 | 9.6 m x 9.6 m | Spherical | 0.00123 | 0.0029 | 41.8 | Moderate | 55.9 | -0.00085 | 0.043 | 1.01 |
| 43 | 19.2 m x 9.6 m | Spherical | 0.00146 | 0.0030 | 48.7 | Moderate | 73.2 | -0.00048 | 0.044 | 0.97 |
| 24 | 19.2 m x 19.2 m | Spherical | 0.00248 | 0.0028 | 87.0 | Weak | 64.1 | -0.00092 | 0.052 | 0.98 |
| 7 | N/A | Spherical | 0.00470 | 0.0047 | 100.0 | Weak | 85.8 | 0 | 0.064 | 0.93 |
| Watkinsville 3 | | | | | | | | | | |
| 1121 | 2.4 m x 2.4 m | Spherical | 0.00064 | 0.0067 | 9.6 | Strong | 21.5 | -0.00054 | 0.040 | 1.03 |
| 584 | 2.4 m x 4.8 m | Spherical | 0.00025 | 0.0070 | 3.5 | Strong | 21.1 | 0.00028 | 0.036 | 0.97 |
| 295 | 4.8 m x 4.8 m | Spherical | 0.00033 | 0.0070 | 4.8 | Strong | 21.6 | -0.00021 | 0.045 | 0.96 |
| 160 | 9.6 m x 4.8 m | Spherical | 0.00064 | 0.0072 | 8.9 | Strong | 19.3 | -0.00074 | 0.047 | 0.82 |
| 83 | 9.6 m x 9.6 m | Spherical | 0.00247 | 0.0080 | 31.1 | Moderate | 21.1 | -0.00265 | 0.071 | 0.89 |
| 47 | 19.2 m x 9.6 m | Spherical | 0.00505 | 0.0057 | 89.2 | Weak | 29.0 | -0.00039 | 0.074 | 0.99 |
| 24 | 19.2 m x 19.2 m | Spherical | 0.00836 | 0.0084 | 100.0 | Weak | 97.6 | 0.00003 | 0.090 | 0.98 |
| 7 | N/A | Spherical | 0.01220 | 0.0122 | 100.0 | Weak | 88.8 | 0 | 0.101 | 0.91 |

[†] Spatial dependence is described as strong, moderate, or weak for nugget/sill ratios <25%, 25-75%, or >75%, respectively.
[‡] ME, mean prediction error.
[§] RMSE, root-mean square prediction error.
[¶] RMSSE, root-mean square standardized prediction error.

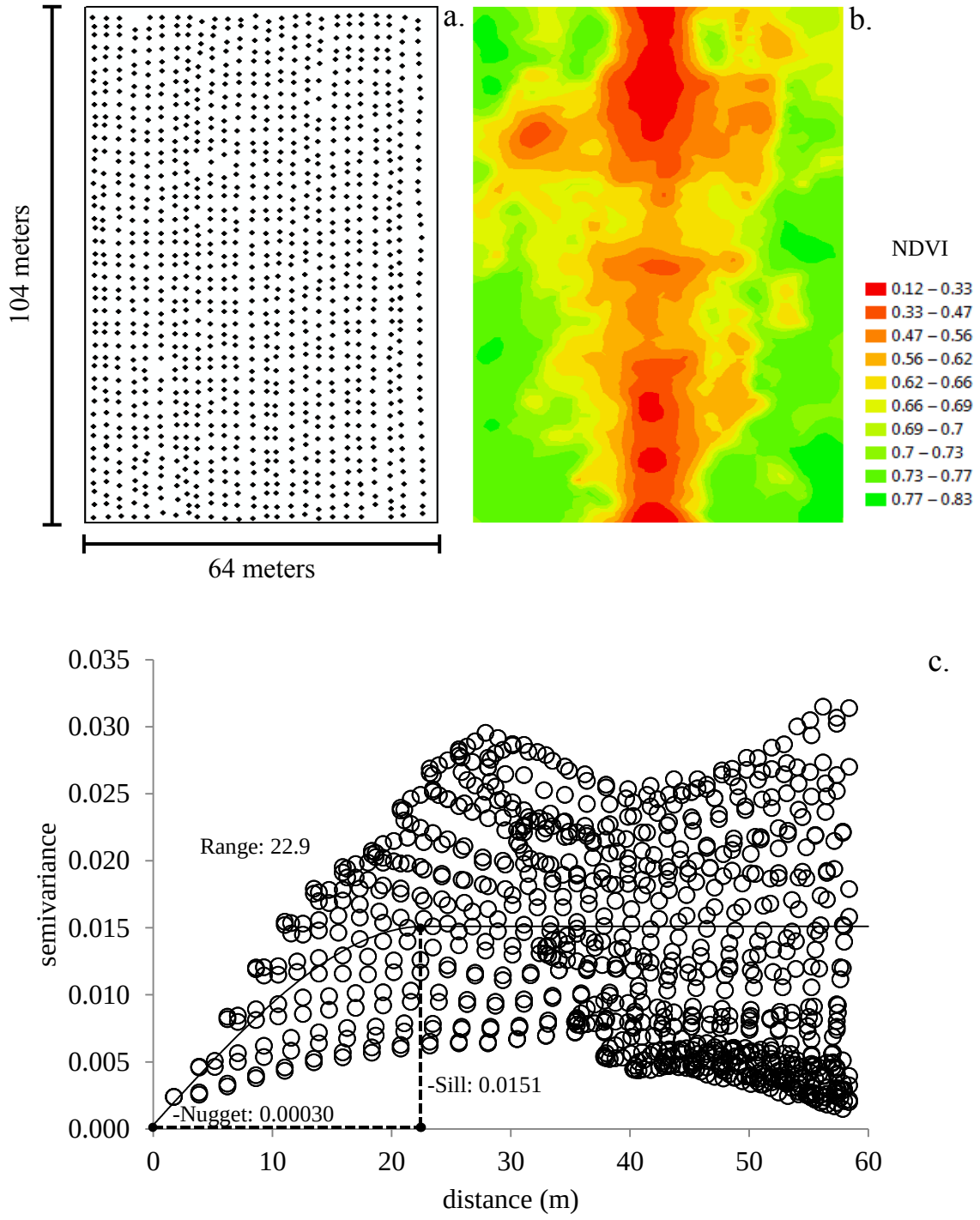


Figure 4.1. (a) Sampling locations (approximately 2.4 m x 2.4 m grid; 1129 samples), (b) kriged prediction map and (c) semivariogram including the fitted spherical model of normalized difference vegetative index (NDVI) on Roswell field 1.

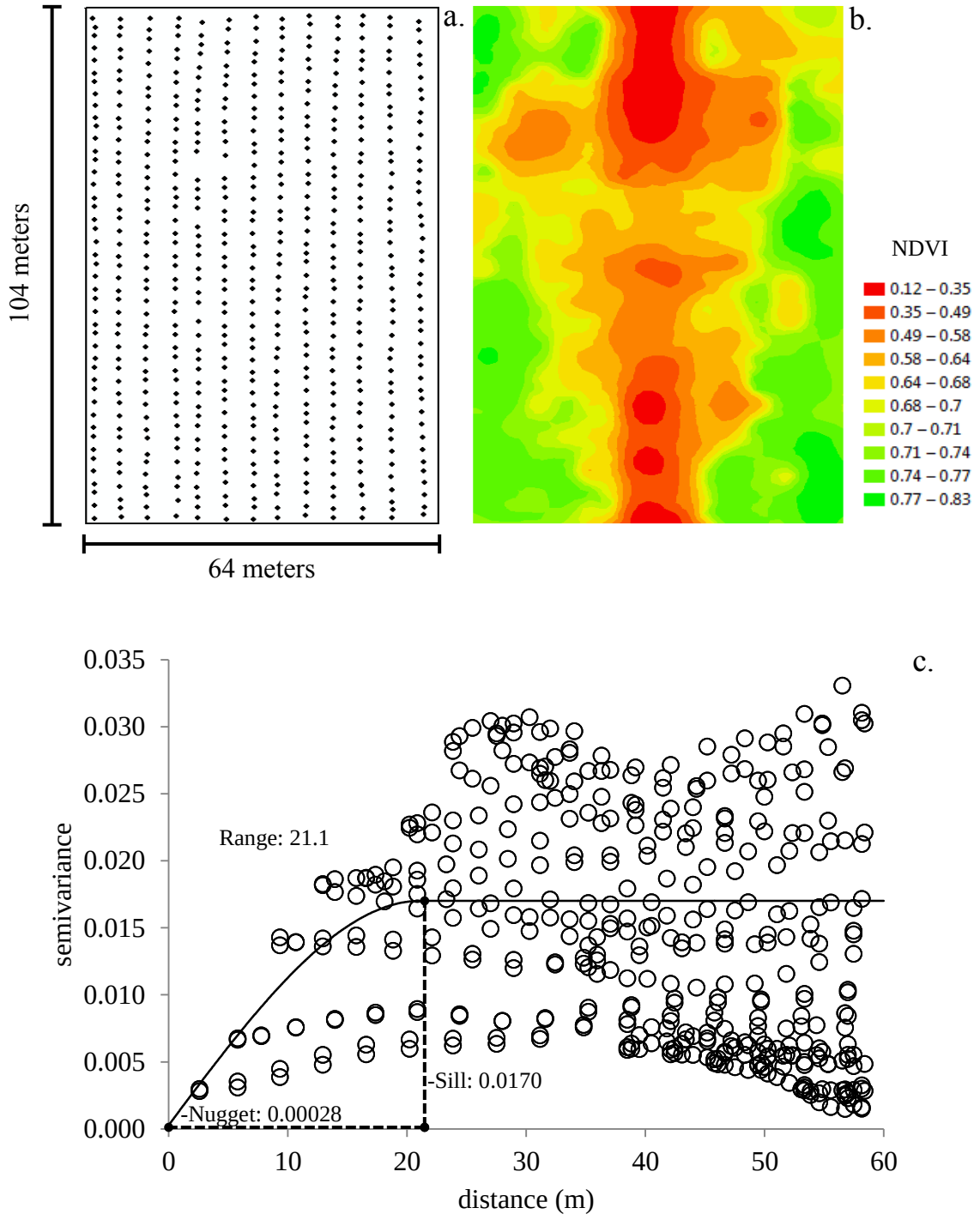


Figure 4.2. (a) Sampling locations (approximately 4.8 m x 2.4 m grid; 588 samples), (b) kriged prediction map and (c) semivariogram including the fitted spherical model of normalized difference vegetative index (NDVI) on Roswell field 1.

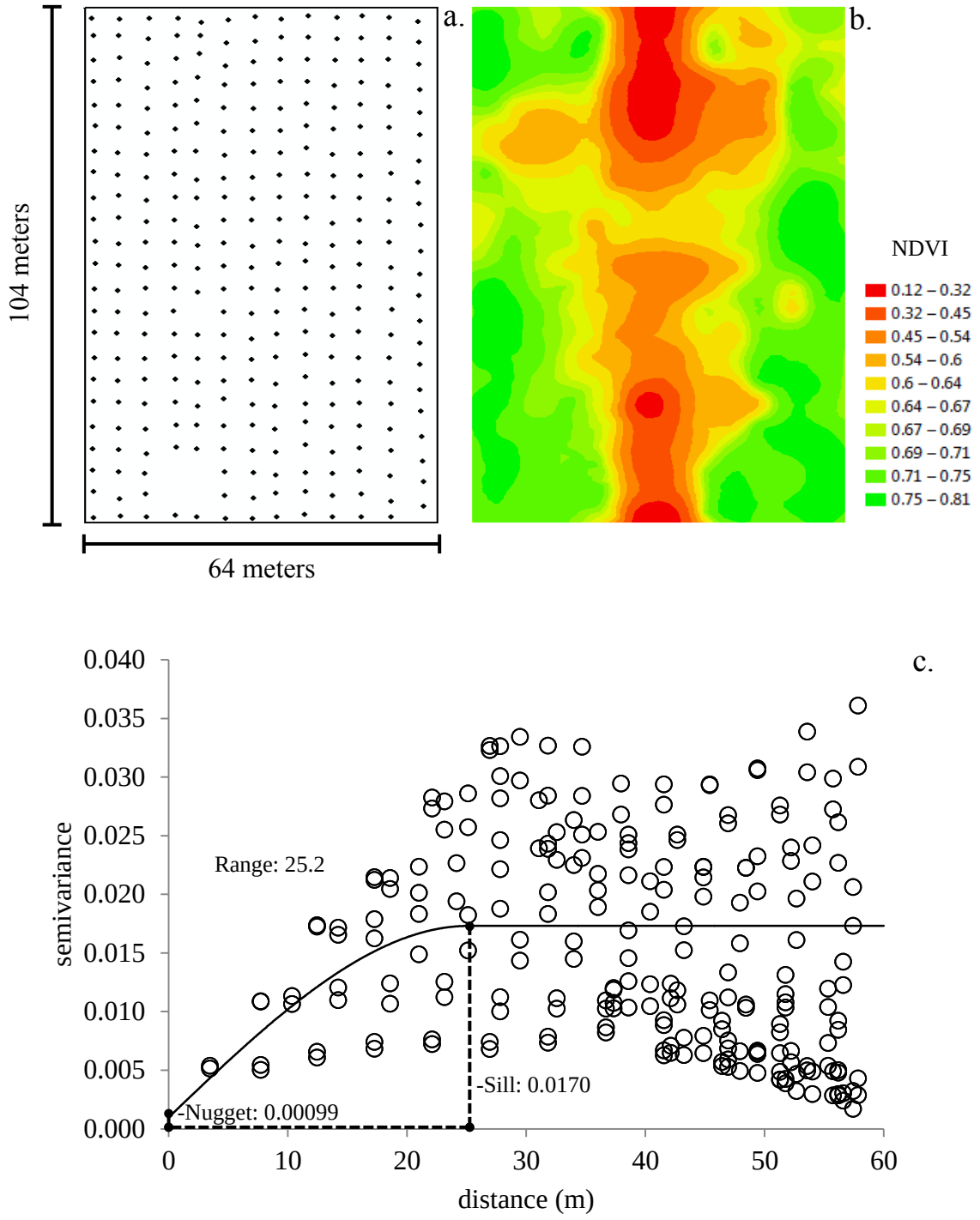


Figure 4.3. (a) Sampling locations (approximately 4.8 m x 4.8 m grid; 300 samples), (b) kriged prediction map and (c) semivariogram including the fitted spherical model of normalized difference vegetative index (NDVI) on Roswell field 1.

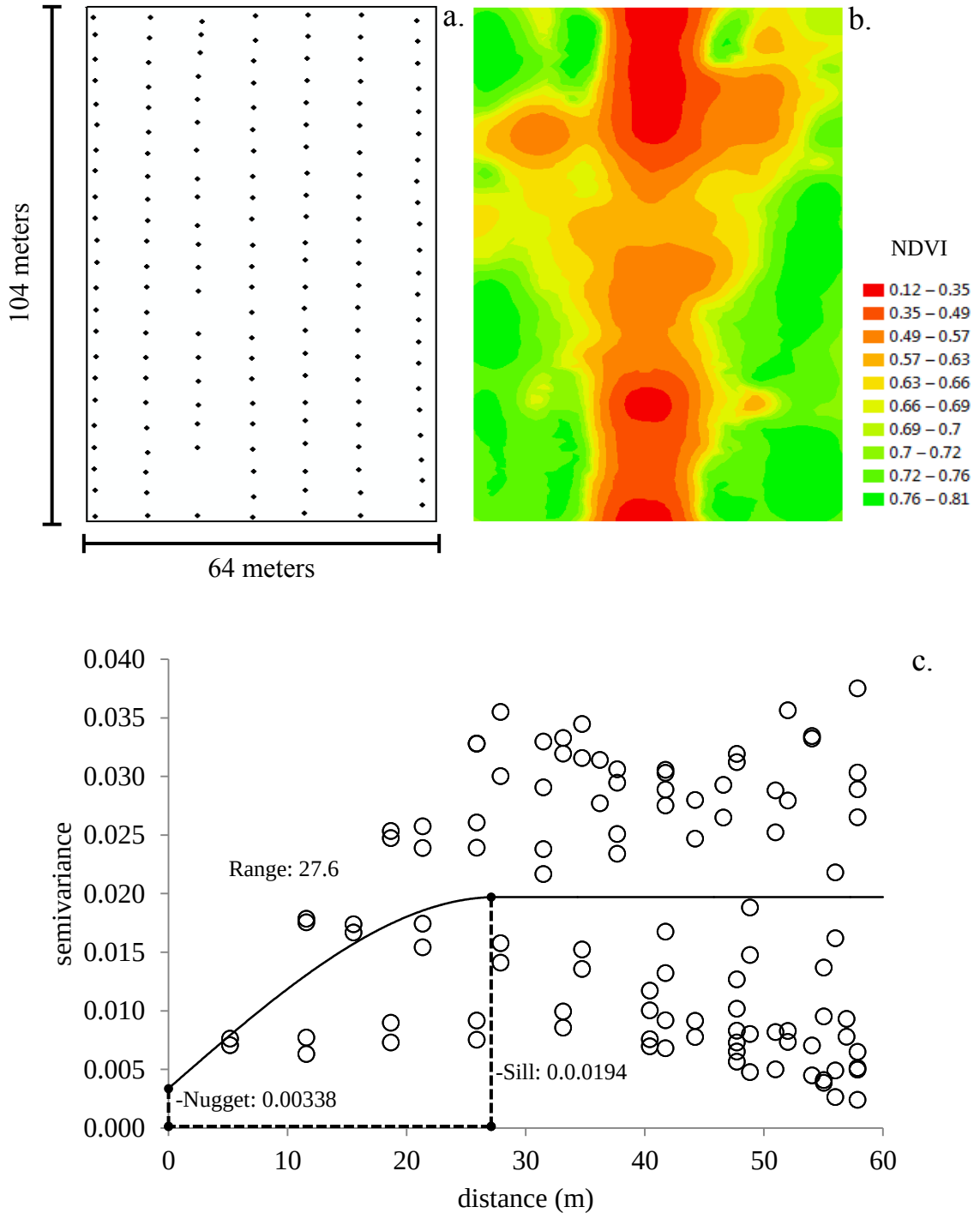


Figure 4.4. (a) Sampling locations (approximately 9.6 m x 4.8 m grid; 159 samples), (b) kriged prediction map and (c) semivariogram including the fitted spherical model of normalized difference vegetative index (NDVI) on Roswell field 1.

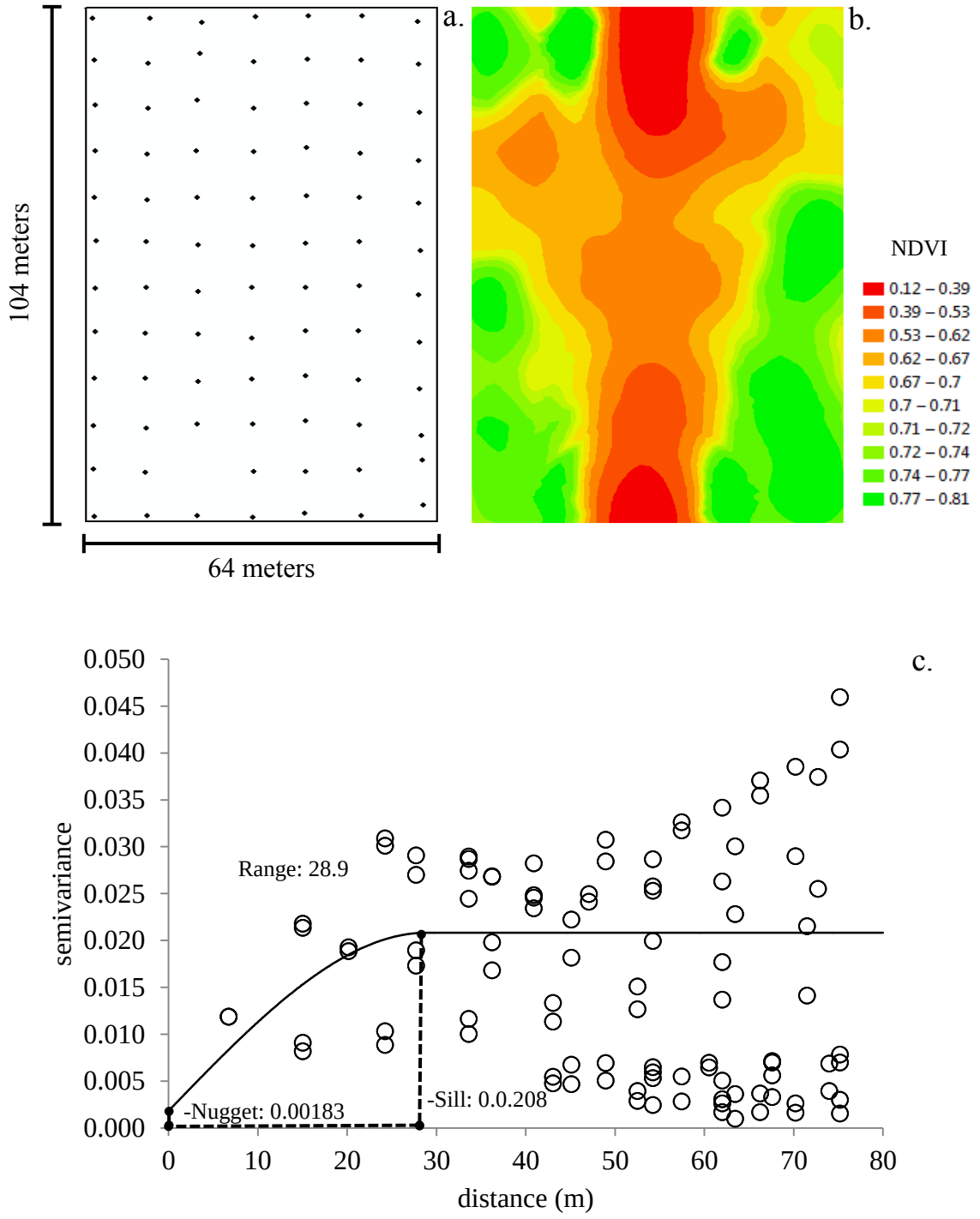


Figure 4.5. (a) Sampling locations (approximately 9.6 m x 9.6 m grid; 83 samples), (b) kriged prediction map and (c) semivariogram including the fitted spherical model of normalized difference vegetative index (NDVI) on Roswell field 1.

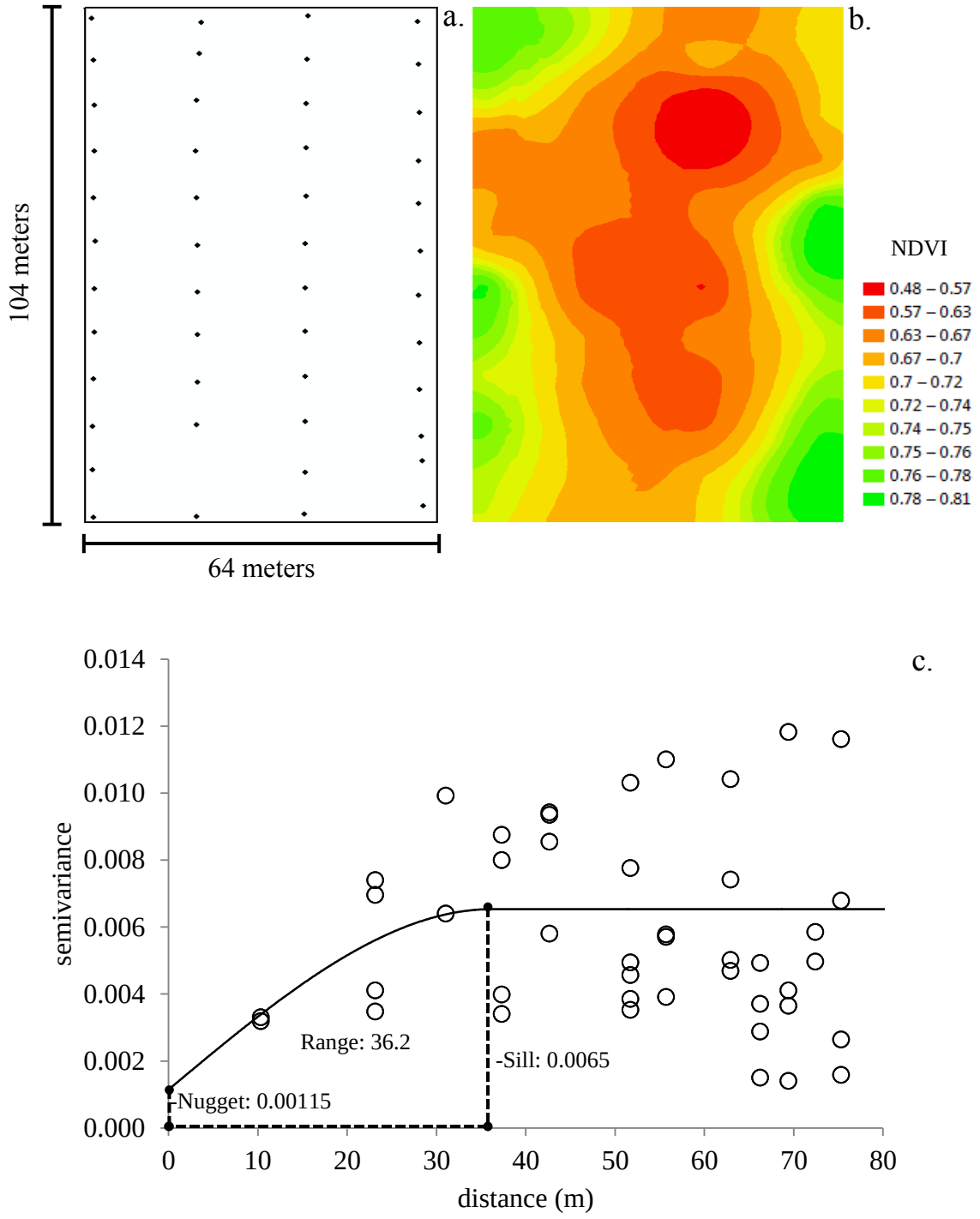


Figure 4.6. (a) Sampling locations (approximately 19.2 m x 9.6 m grid; 47 samples), (b) kriged prediction map and (c) semivariogram including the fitted spherical model of normalized difference vegetative index (NDVI) on Roswell field 1.

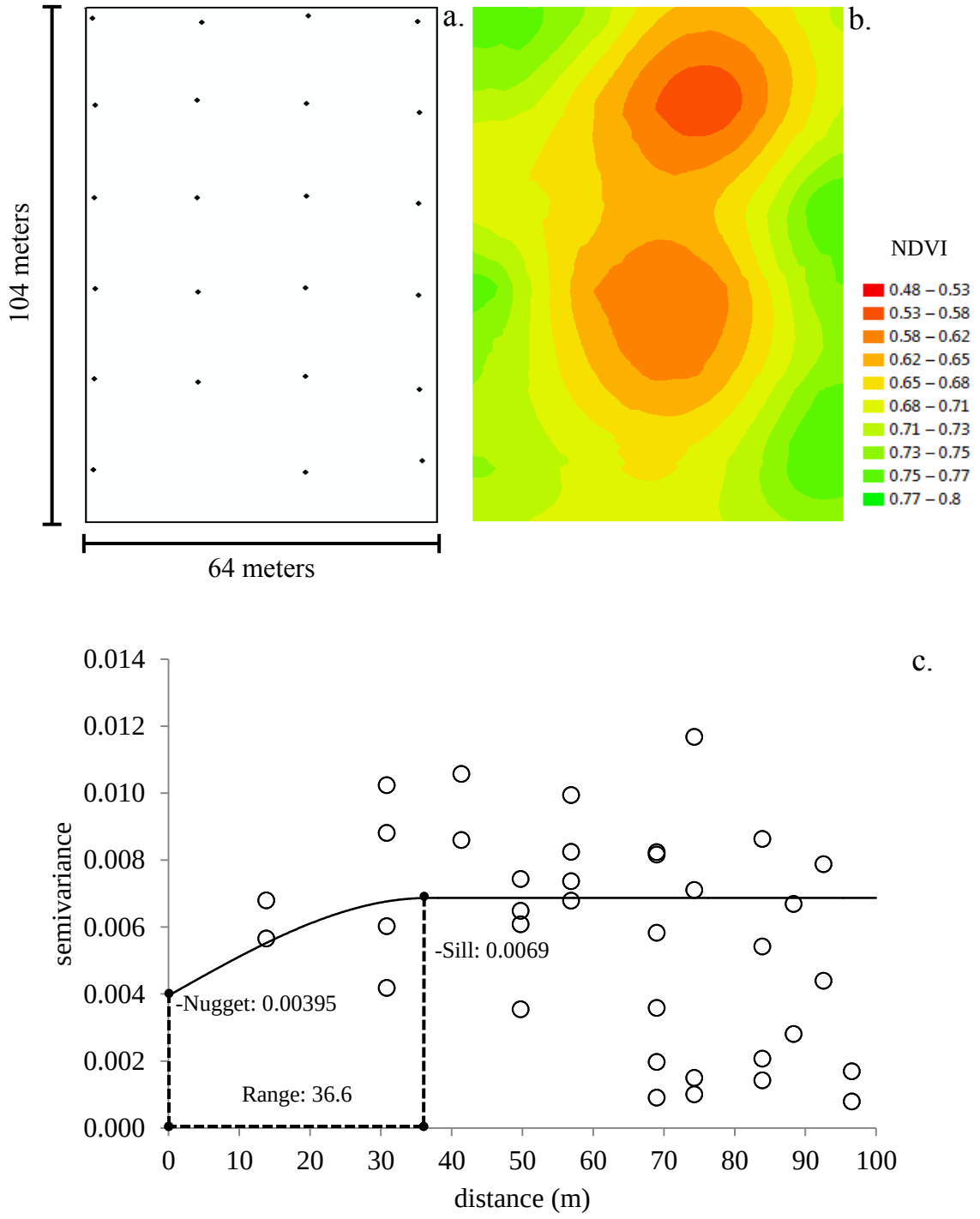


Figure 4.7. (a) Sampling locations (approximately 19.2 m x 19.2 m grid; 23 samples), (b) kriged prediction map and (c) semivariogram including the fitted spherical model of normalized difference vegetative index (NDVI) on Roswell field 1.

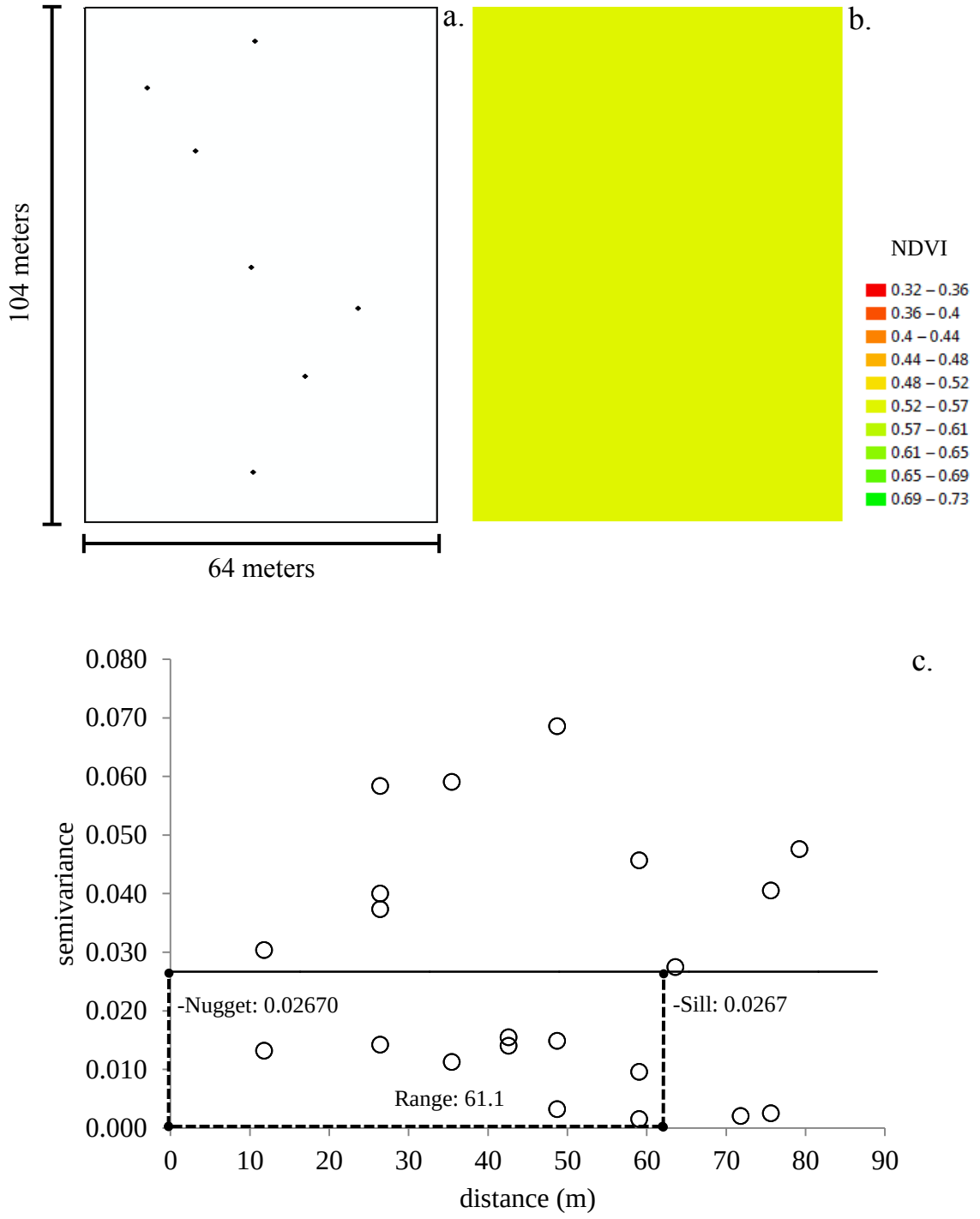


Figure 4.8. (a) Sampling locations (7 samples), (b) kriged prediction map and (c) semivariogram including the fitted spherical model of normalized difference vegetative index (NDVI) on Roswell field 1.

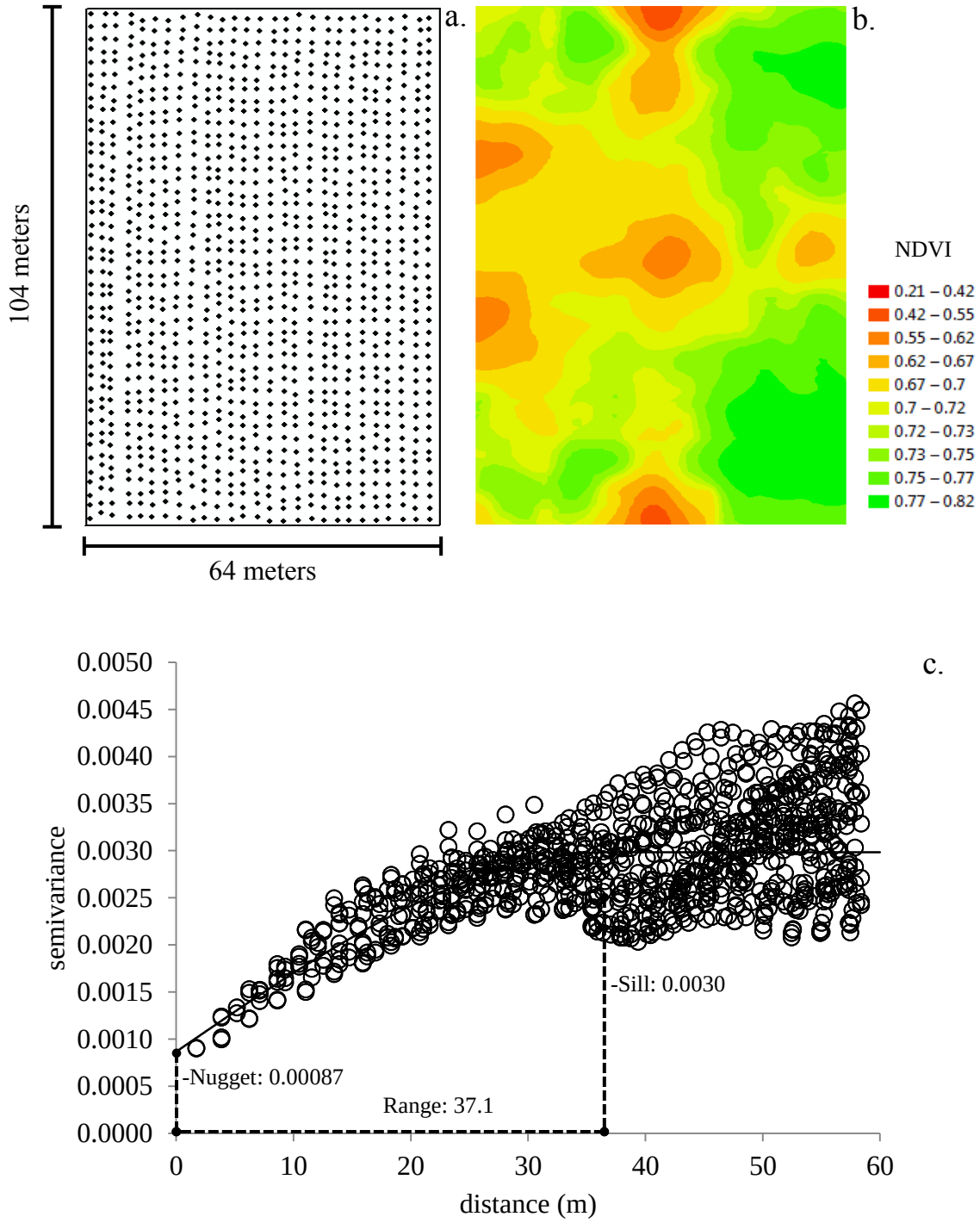


Figure 4.9. (a) Sampling locations (approximately 2.4 m x 2.4 m grid; 1195 samples), (b) kriged prediction map and (c) semivariogram including the fitted spherical model of normalized difference vegetative index (NDVI) on Roswell field 2.

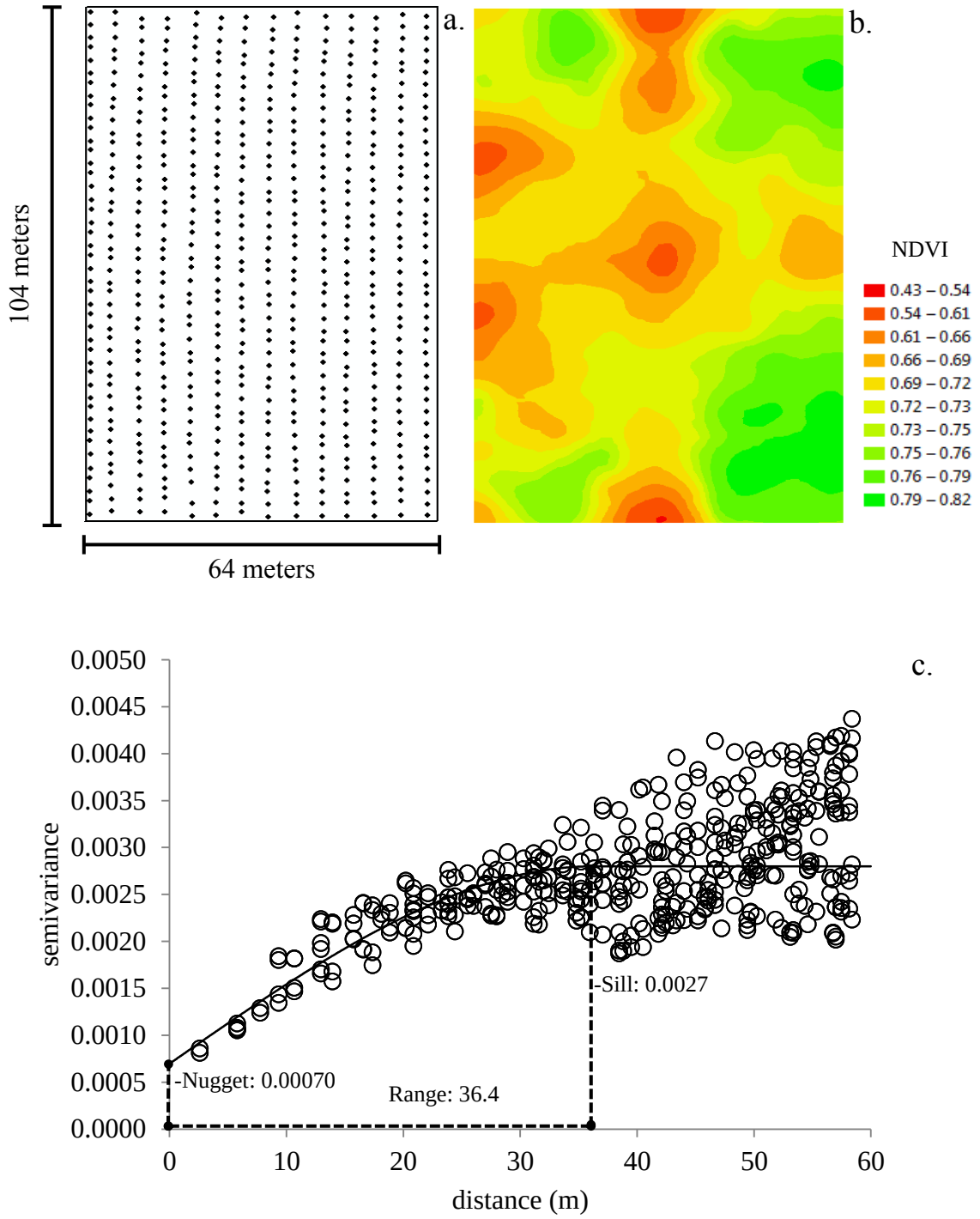


Figure 4.10. (a) Sampling locations (approximately 4.8 m x 2.4 m grid; 617 samples), (b) kriged prediction map and (c) semivariogram including the fitted spherical model of normalized difference vegetative index (NDVI) on Roswell field 2.

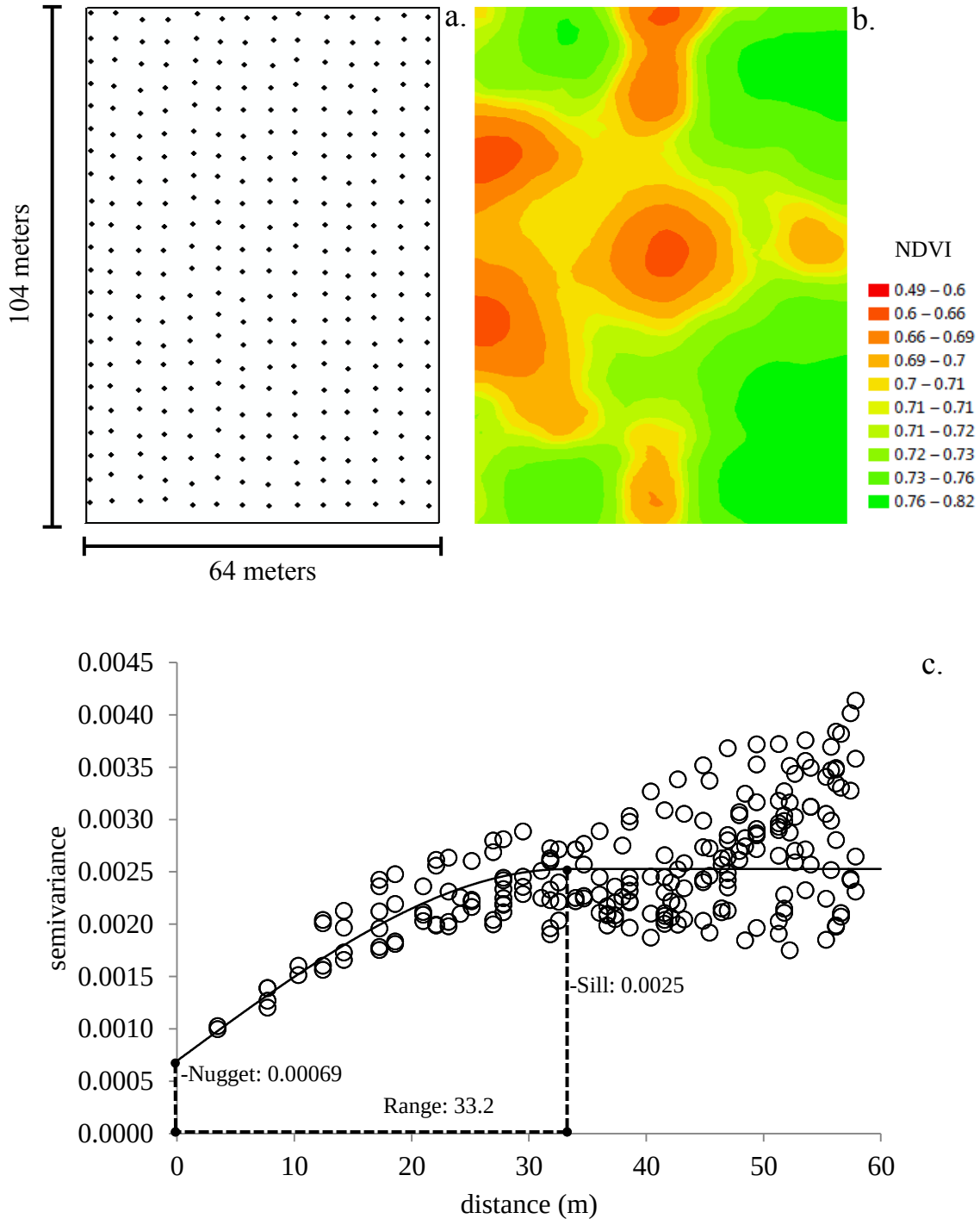


Figure 4.11. (a) Sampling locations (approximately 4.8 m x 4.8 m grid; 310 samples), (b) kriged prediction map and (c) semivariogram including the fitted spherical model of normalized difference vegetative index (NDVI) on Roswell field 2.

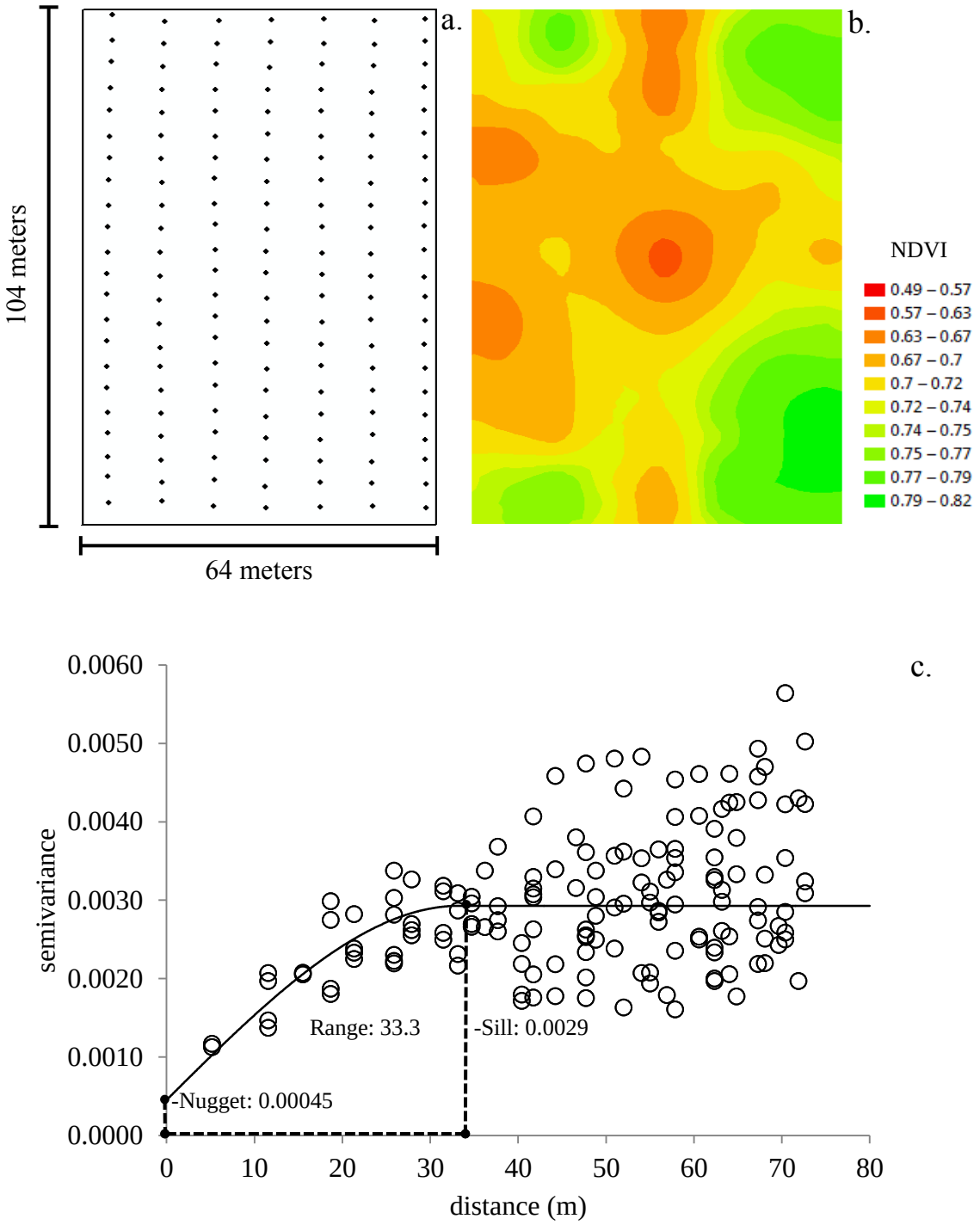


Figure 4.12. (a) Sampling locations (approximately 9.6 m x 4.8 m grid; 154 samples), (b) kriged prediction map and (c) semivariogram including the fitted spherical model of normalized difference vegetative index (NDVI) on Roswell field 2.

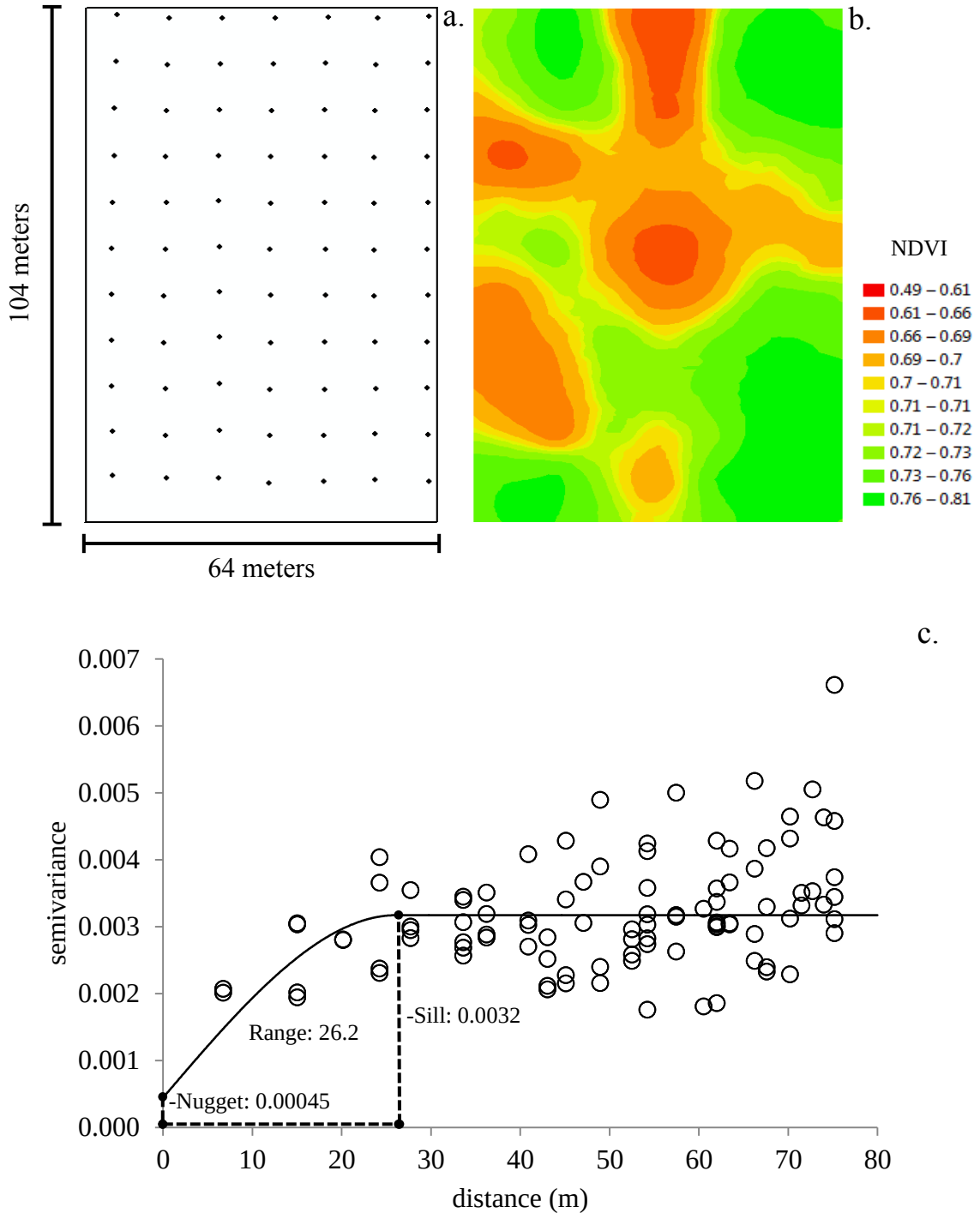


Figure 4.13. (a) Sampling locations (approximately 9.6 m x 9.6 m grid; 77 samples), (b) kriged prediction map and (c) semivariogram including the fitted spherical model of normalized difference vegetative index (NDVI) on Roswell field 2.

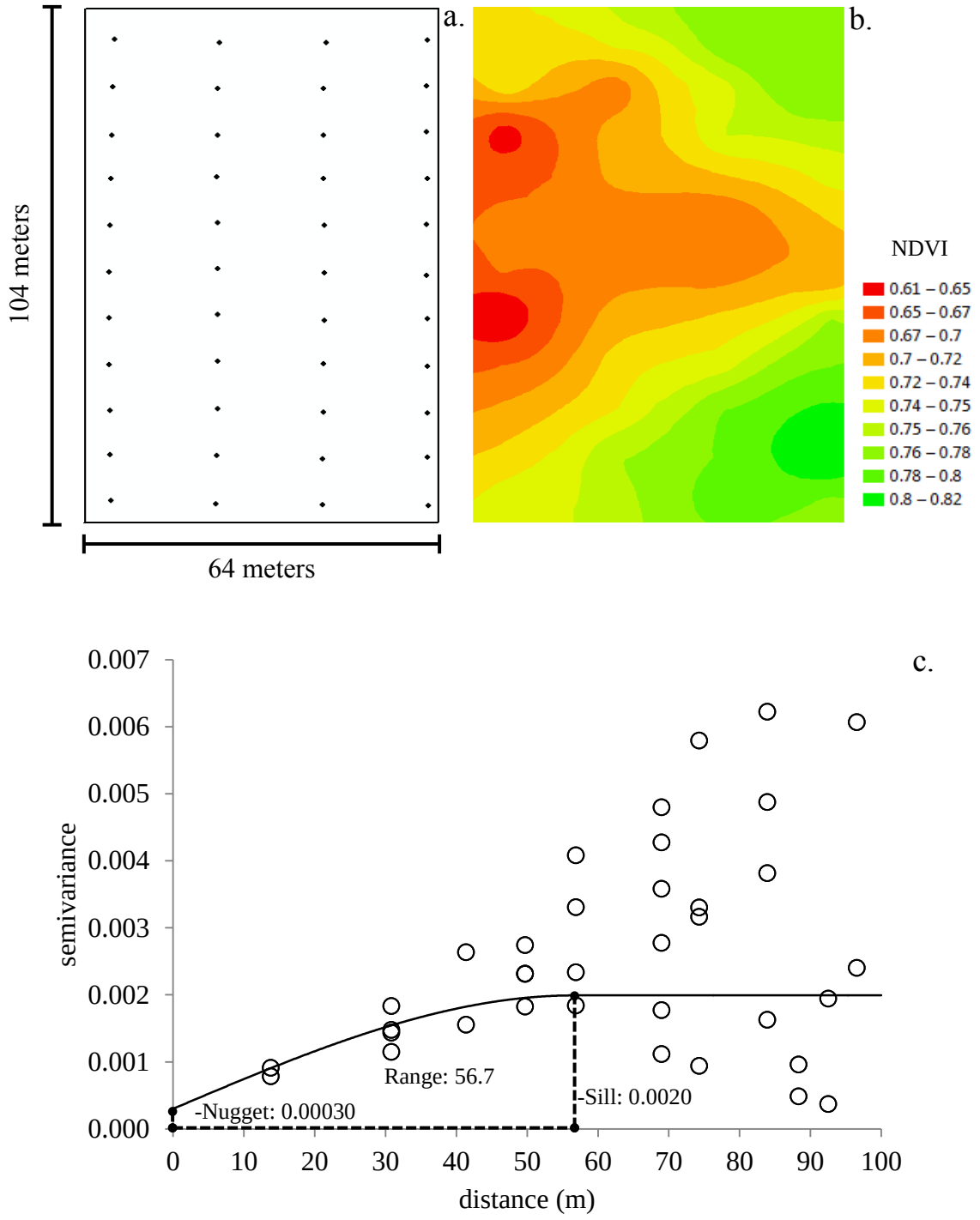


Figure 4.14. (a) Sampling locations (approximately 19.2 m x 9.6 m grid; 44 samples), (b) kriged prediction map and (c) semivariogram including the fitted spherical model of normalized difference vegetative index (NDVI) on Roswell field 2.

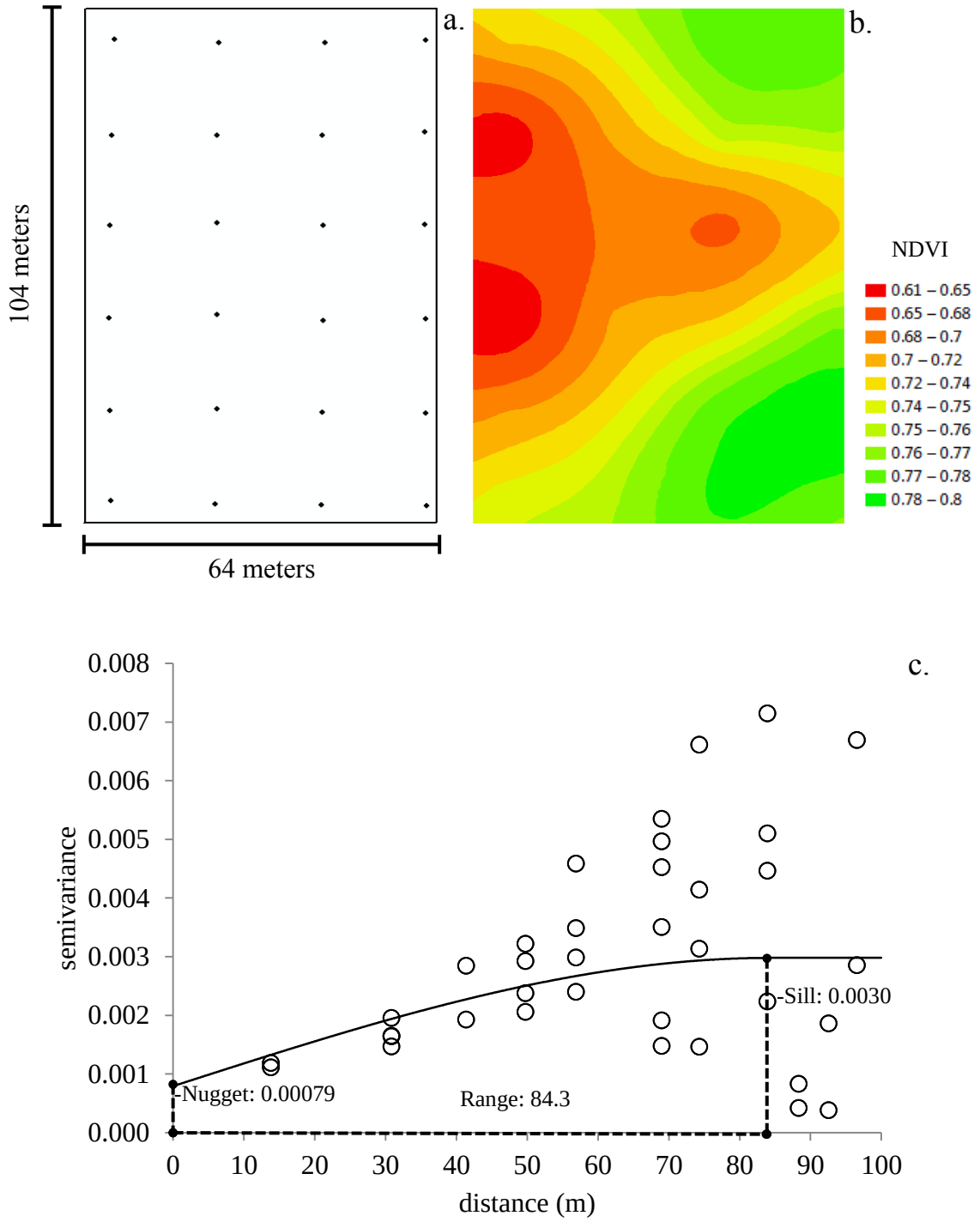


Figure 4.15. (a) Sampling locations (approximately 19.2 m x 19.2 m grid; 24 samples), (b) kriged prediction map and (c) semivariogram including the fitted spherical model of normalized difference vegetative index (NDVI) on Roswell field 2.

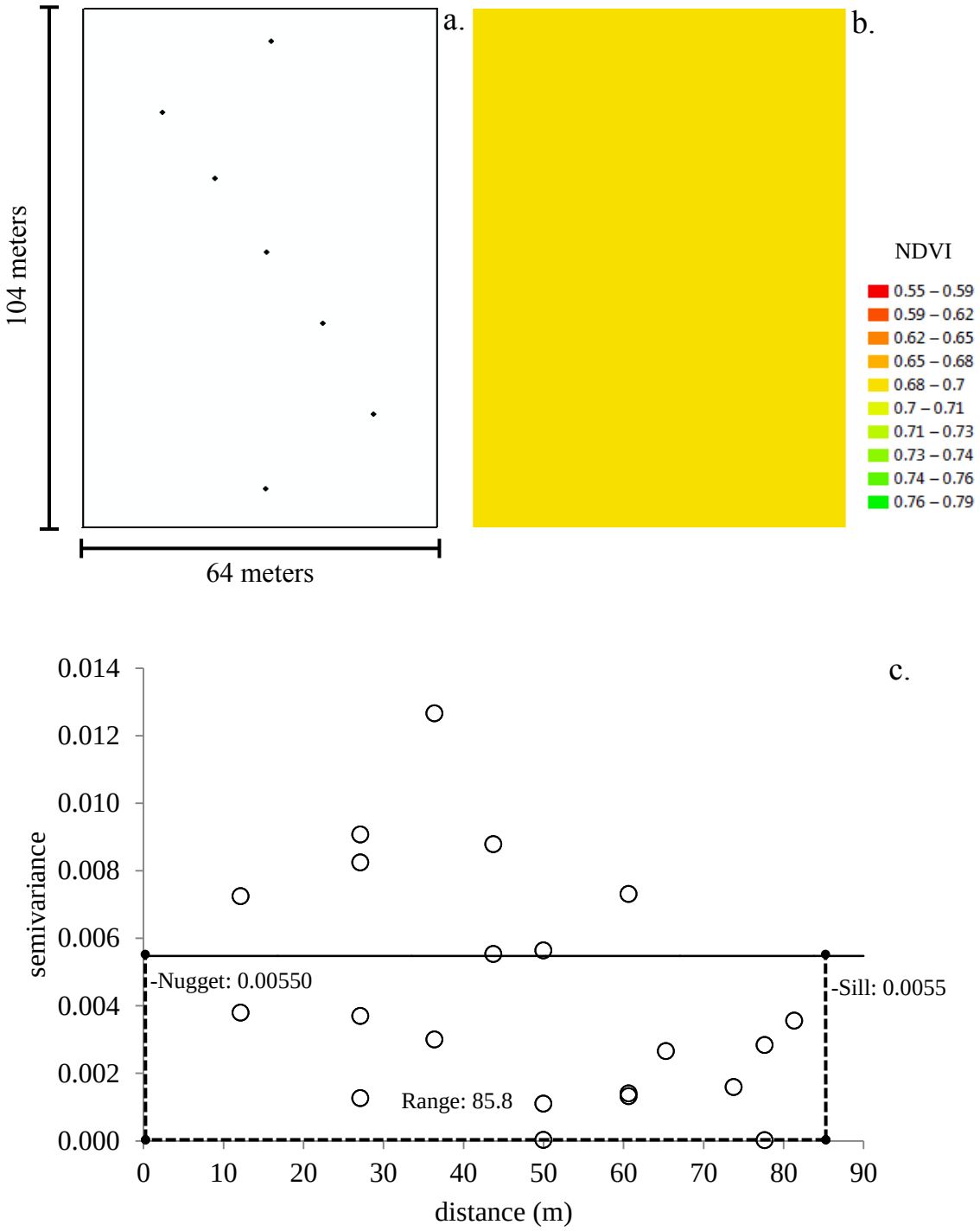


Figure 4.16. (a) Sampling locations (7 samples), (b) kriged prediction map and (c) semivariogram including the fitted spherical model of normalized difference vegetative index (NDVI) on Roswell field 2.

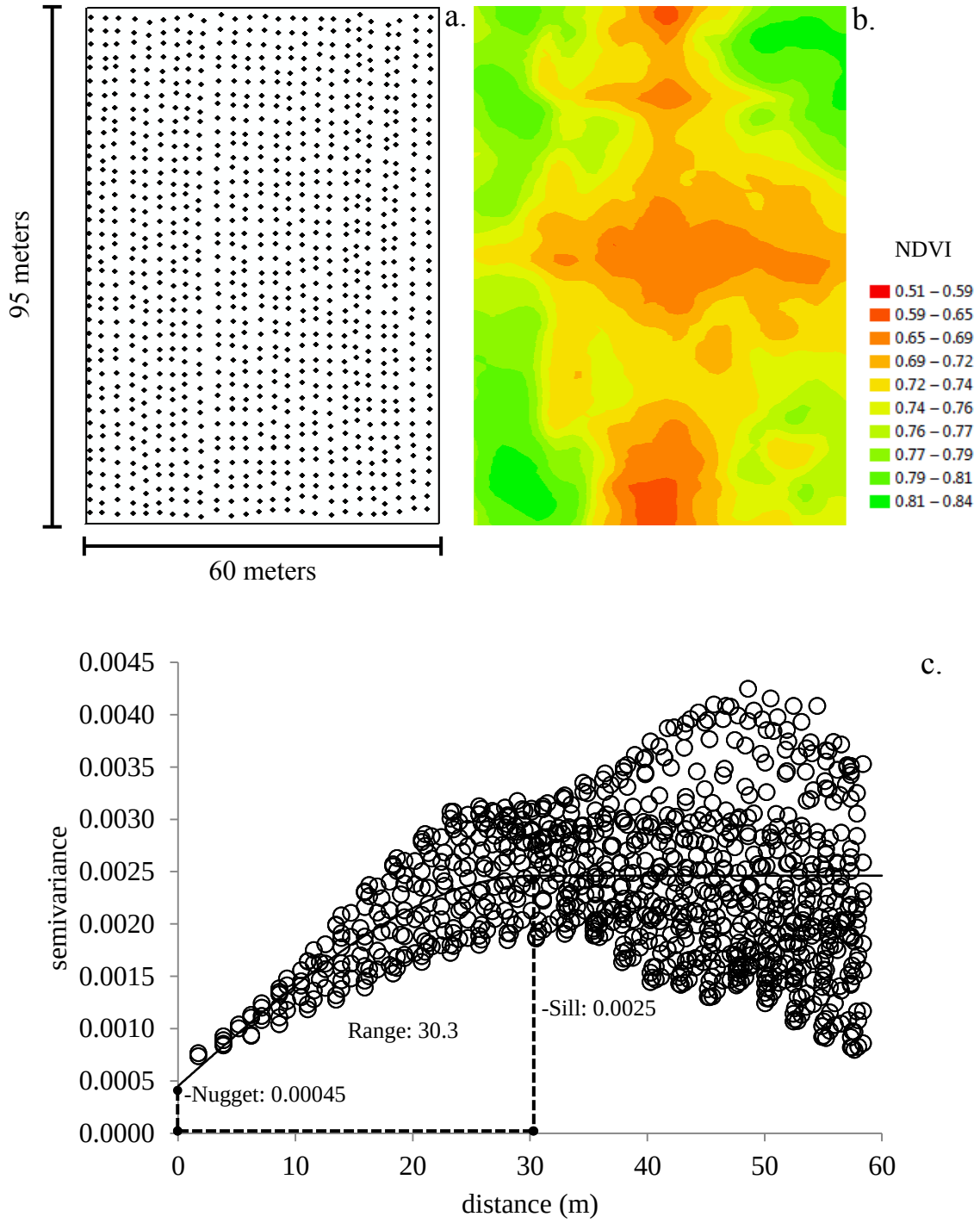


Figure 4.17. (a) Sampling locations (approximately 2.4 m x 2.4 m grid; 1021 samples), (b) kriged prediction map and (c) semivariogram including the fitted spherical model of normalized difference vegetative index (NDVI) on Roswell field 3.

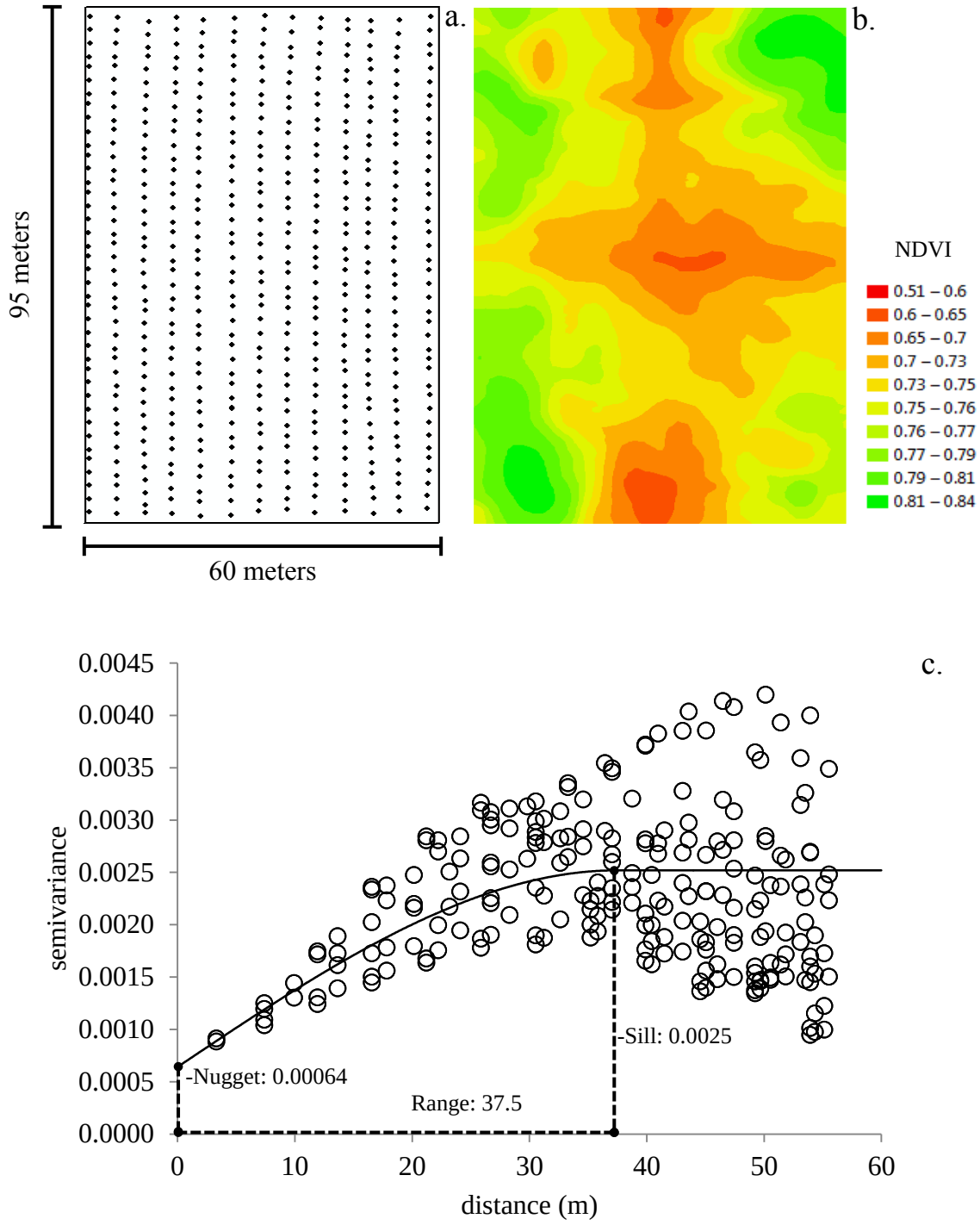


Figure 4.18. (a) Sampling locations (approximately 4.8 m x 2.4 m grid; 531 samples), (b) kriged prediction map and (c) semivariogram including the fitted spherical model of normalized difference vegetative index (NDVI) on Roswell field 3.

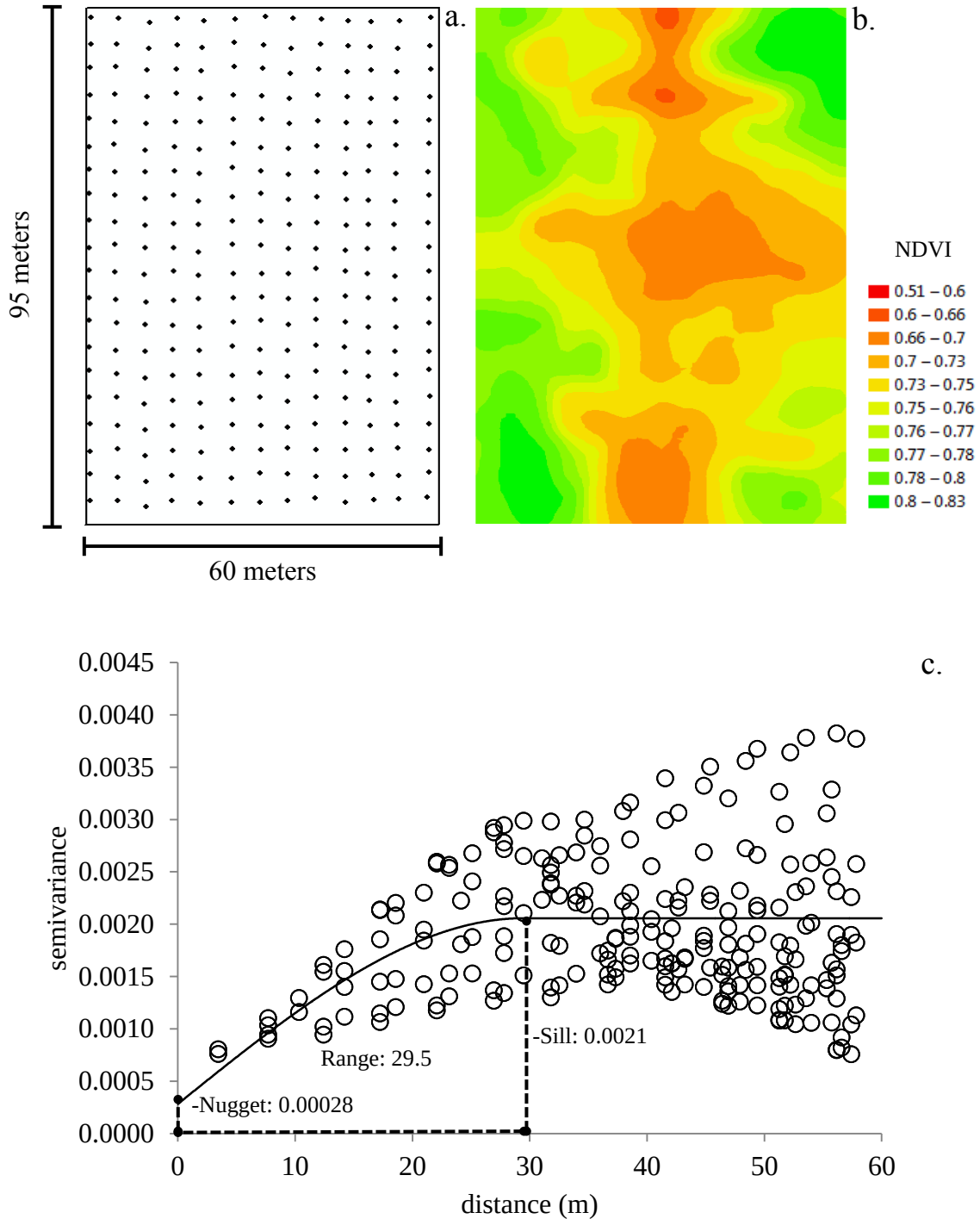


Figure 4.19. (a) Sampling locations (approximately 4.8 m x 4.8 m grid; 266 samples), (b) kriged prediction map and (c) semivariogram including the fitted spherical model of normalized difference vegetative index (NDVI) on Roswell field 3.

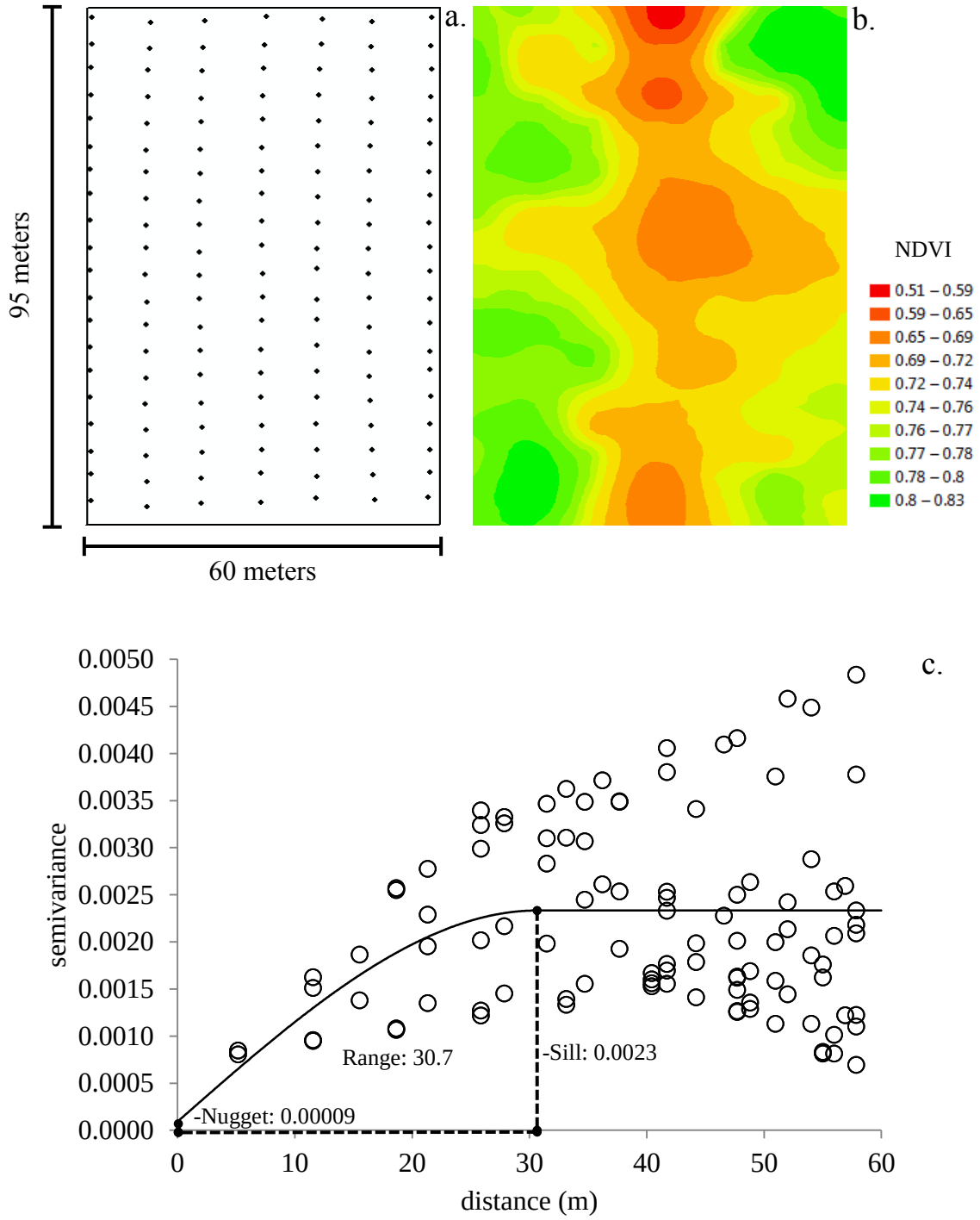


Figure 4.20. (a) Sampling locations (approximately 9.6 m x 4.8 m grid; 145 samples), (b) kriged prediction map and (c) semivariogram including the fitted spherical model of normalized difference vegetative index (NDVI) on Roswell field 3.

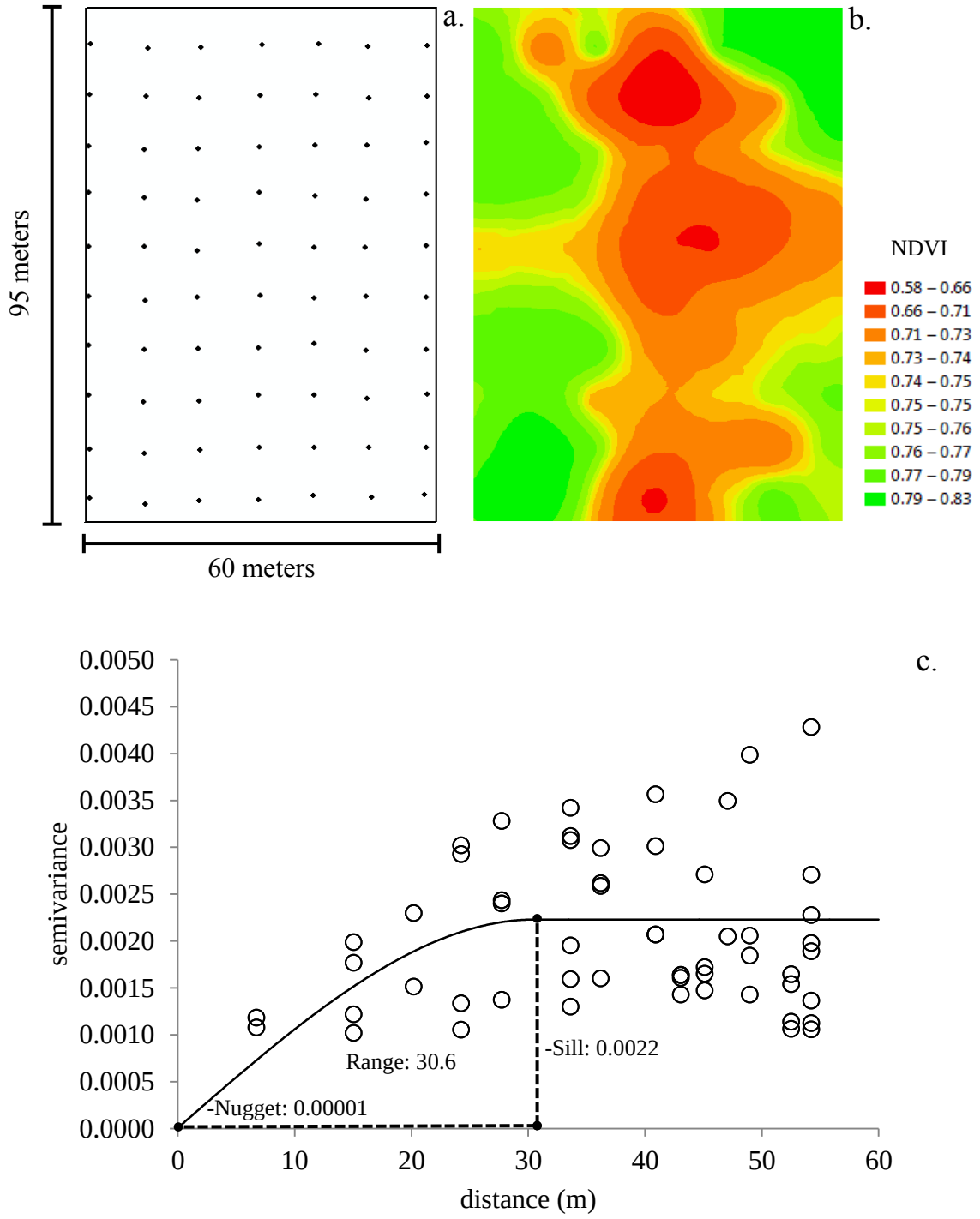


Figure 4.21. (a) Sampling locations (approximately 9.6 m x 9.6 m grid; 73 samples), (b) kriged prediction map and (c) semivariogram including the fitted spherical model of normalized difference vegetative index (NDVI) on Roswell field 3.

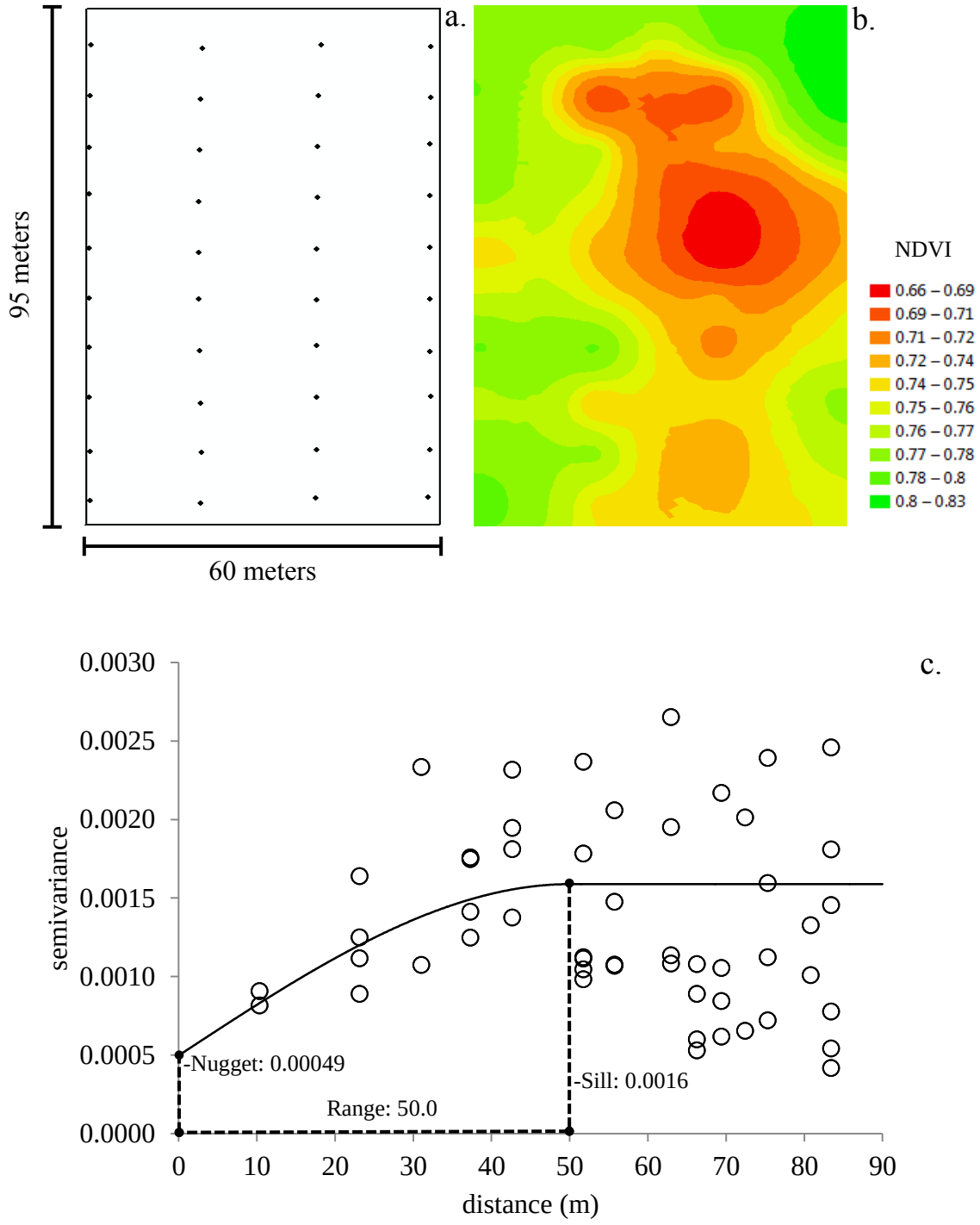


Figure 4.22. (a) Sampling locations (approximately 19.2 m x 9.6 m grid; 43 samples), (b) kriged prediction map and (c) semivariogram including the fitted spherical model of normalized difference vegetative index (NDVI) on Roswell field 3.

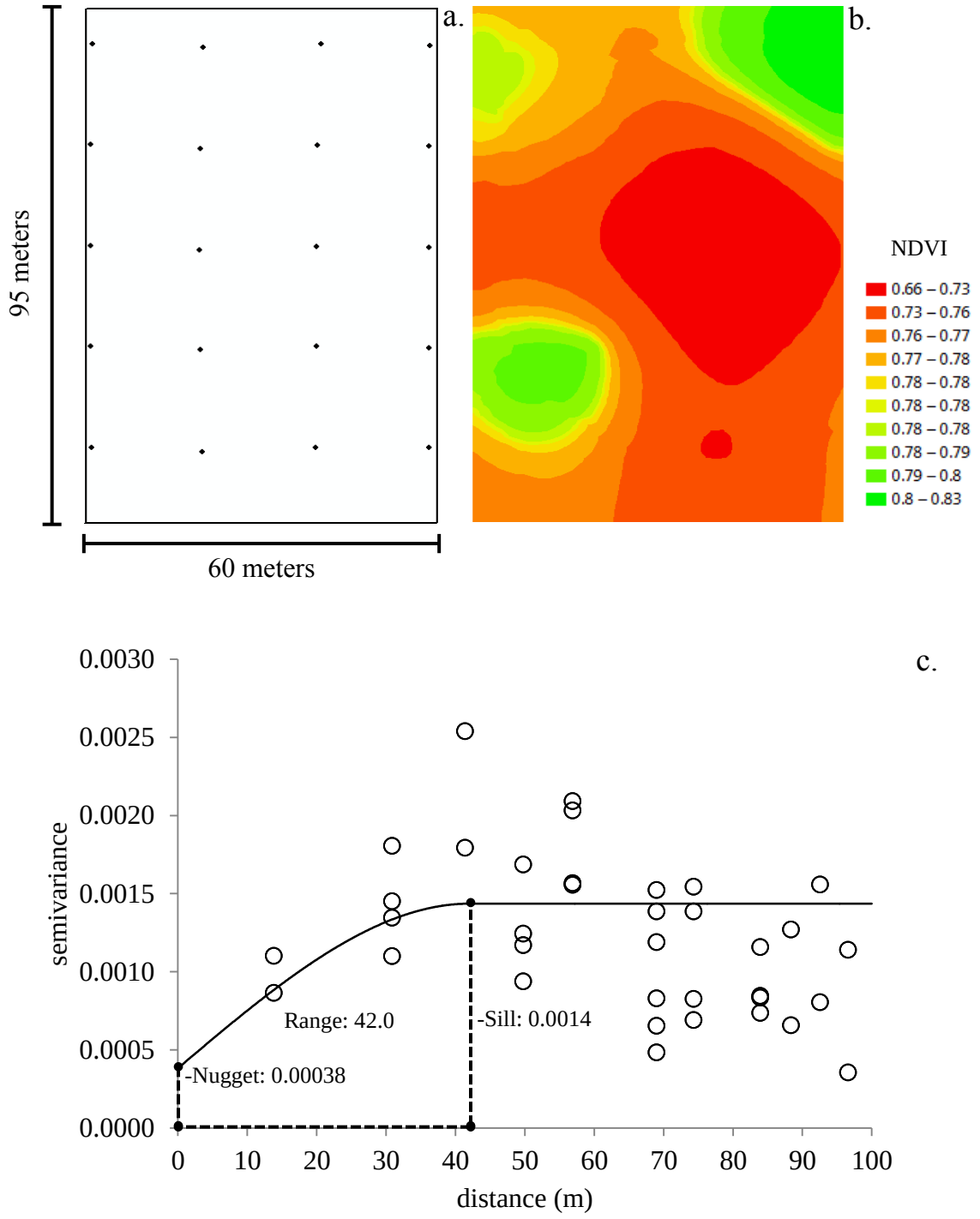


Figure 4.23. (a) Sampling locations (approximately 19.2 m x 19.2 m grid; 20 samples), (b) kriged prediction map and (c) semivariogram including the fitted spherical model of normalized difference vegetative index (NDVI) on Roswell field 3.

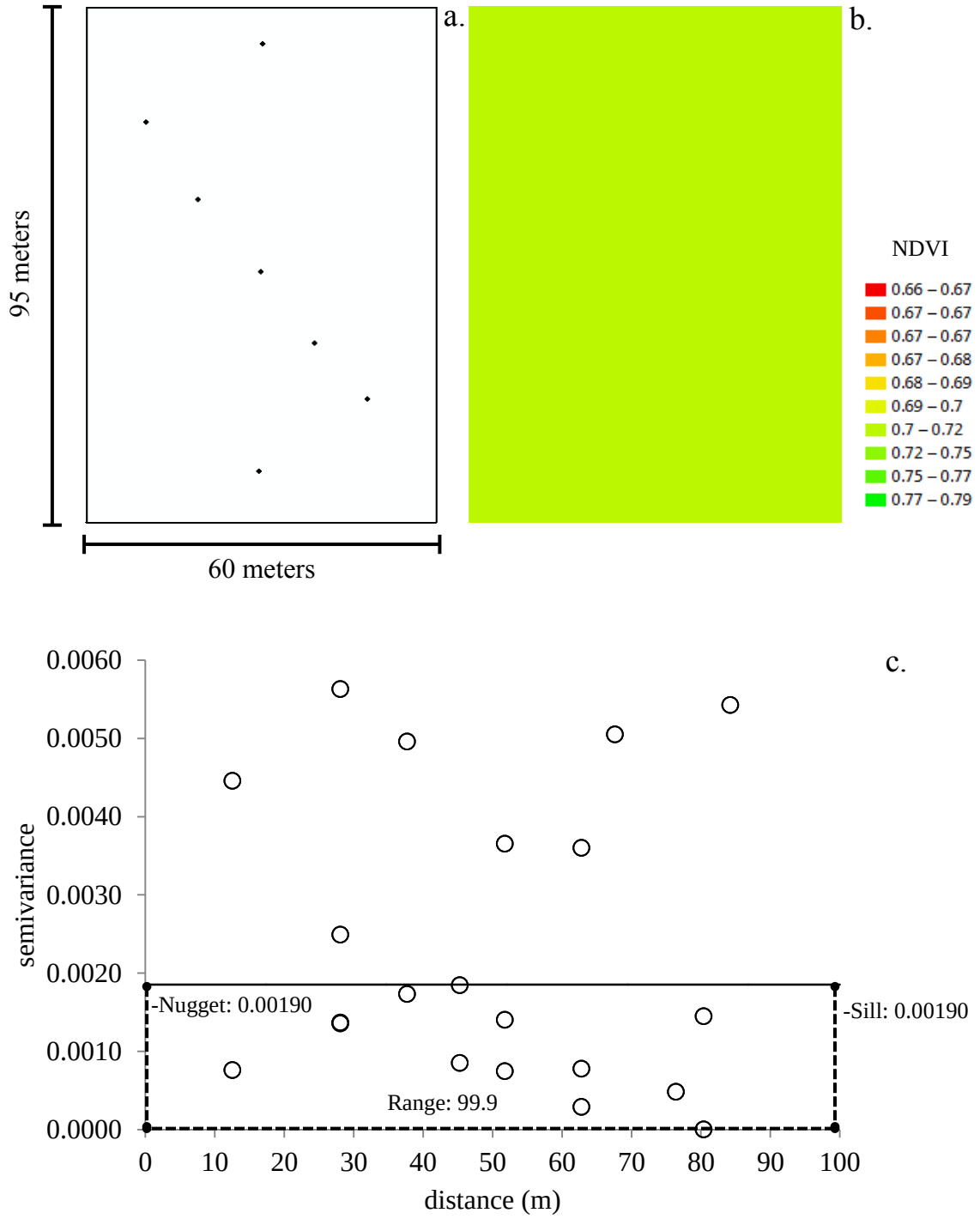


Figure 4.24. (a) Sampling locations (7 samples), (b) kriged prediction map and (c) semivariogram including the fitted spherical model of normalized difference vegetative index (NDVI) on Roswell field 3.

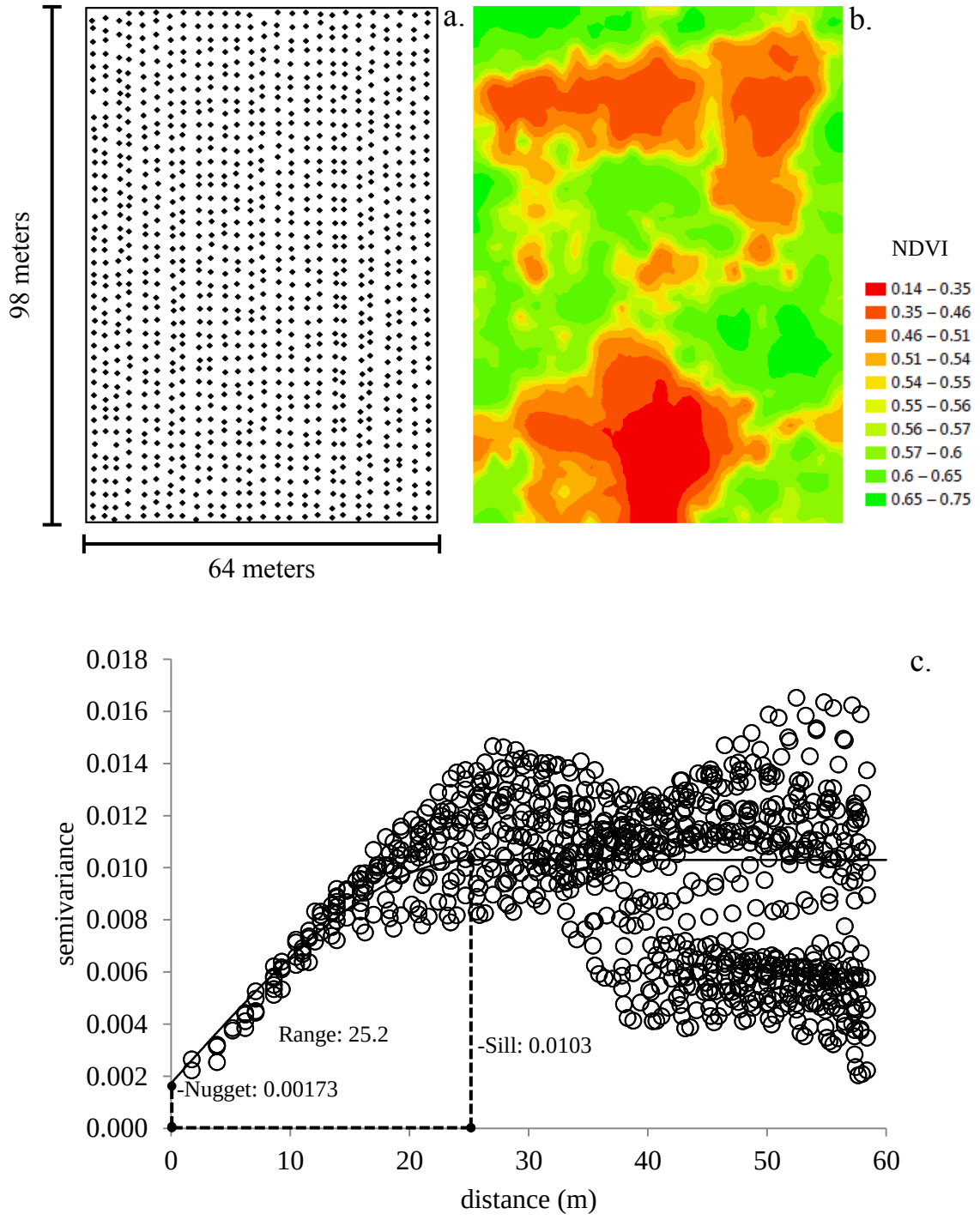


Figure 4.25. (a) Sampling locations (approximately 2.4 m x 2.4 m grid; 1095 samples), (b) kriged prediction map and (c) semivariogram including the fitted spherical model of normalized difference vegetative index (NDVI) on Watkinsville field 1.

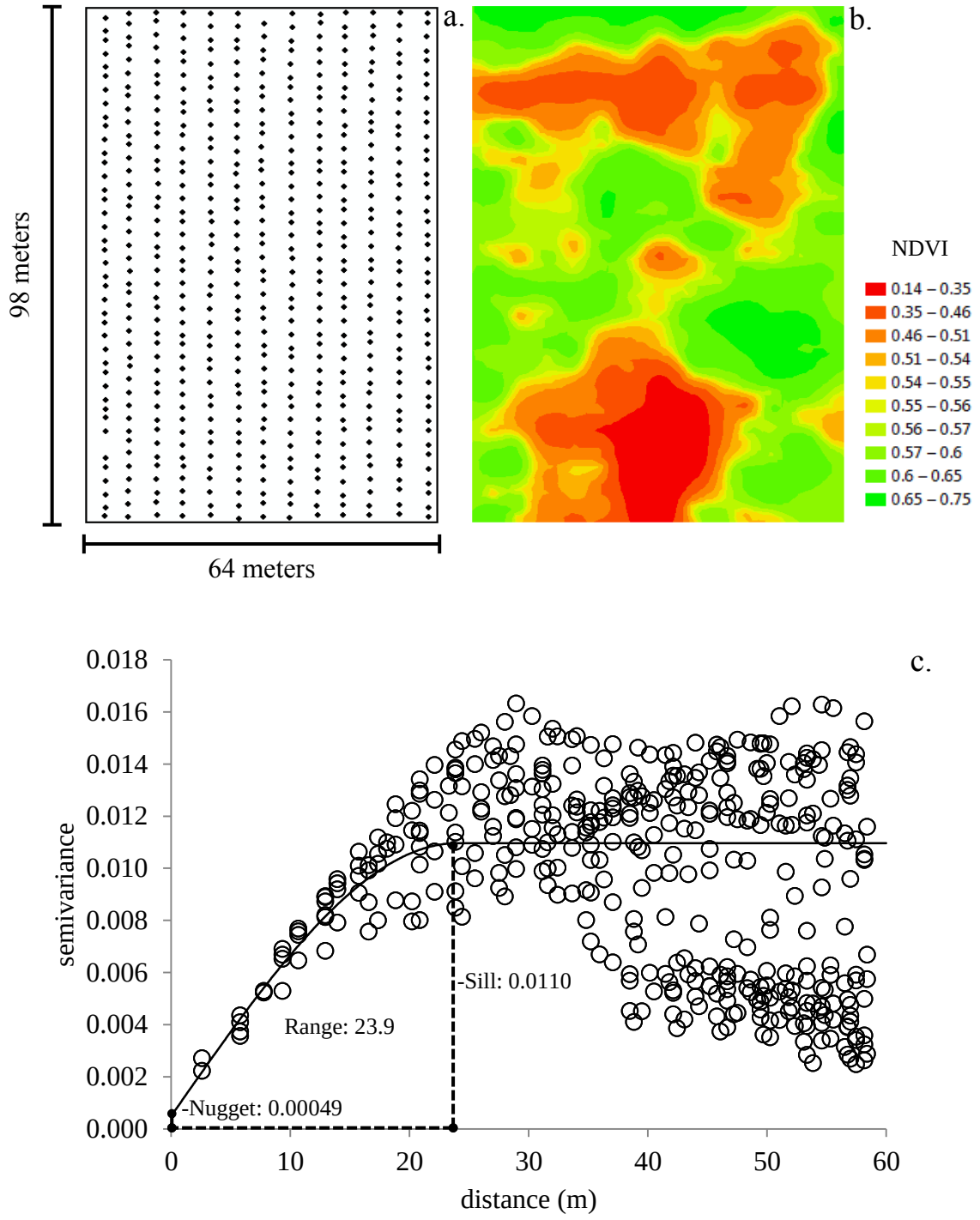


Figure 4.26. (a) Sampling locations (approximately 4.8 m x 2.4 m grid; 547 samples), (b) kriged prediction map and (c) semivariogram including the fitted spherical model of normalized difference vegetative index (NDVI) on Watkinsville field 1.

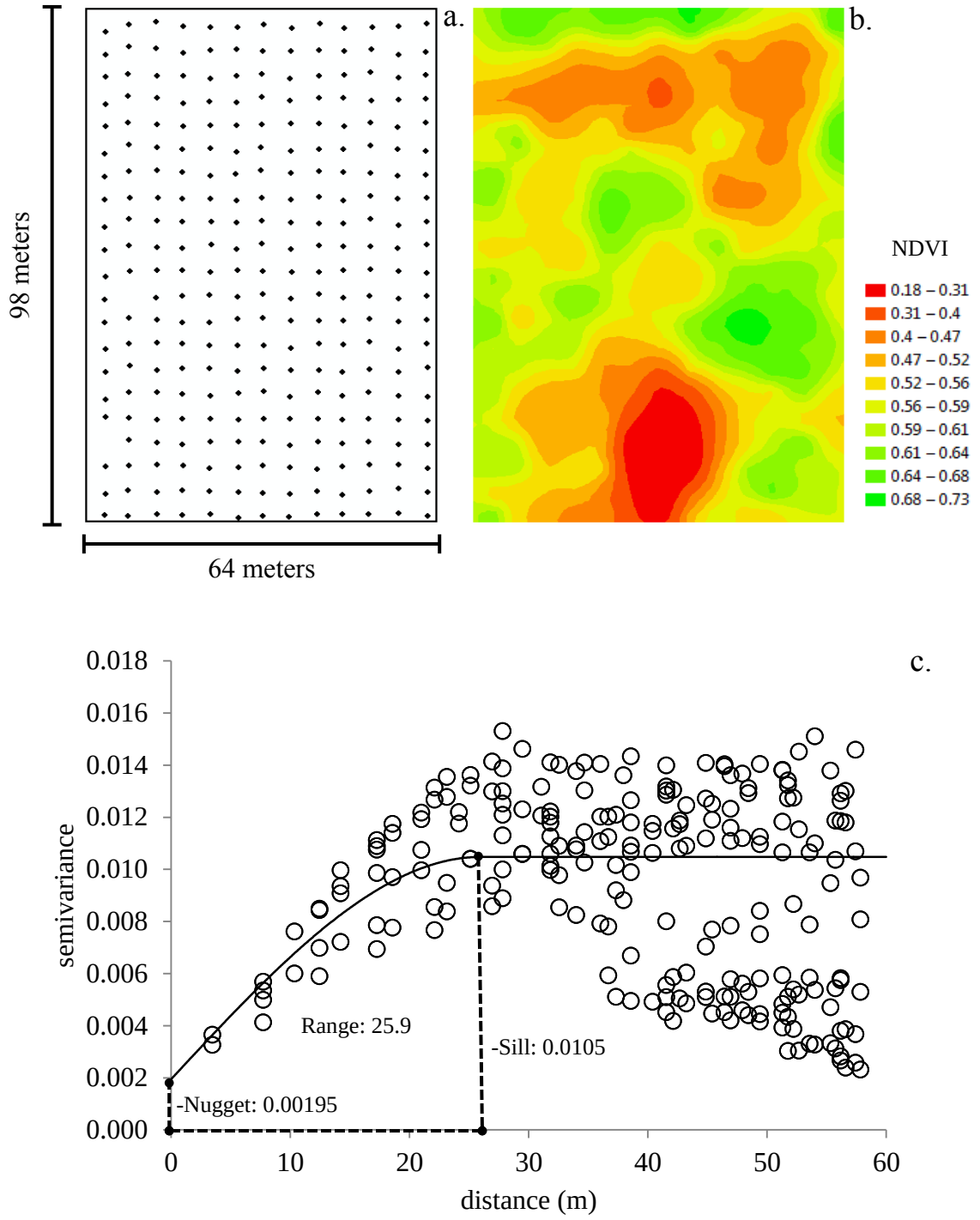


Figure 4.27. (a) Sampling locations (approximately 4.8 m x 4.8 m grid; 273 samples), (b) kriged prediction map and (c) semivariogram including the fitted spherical model of normalized difference vegetative index (NDVI) on Watkinsville field 1.

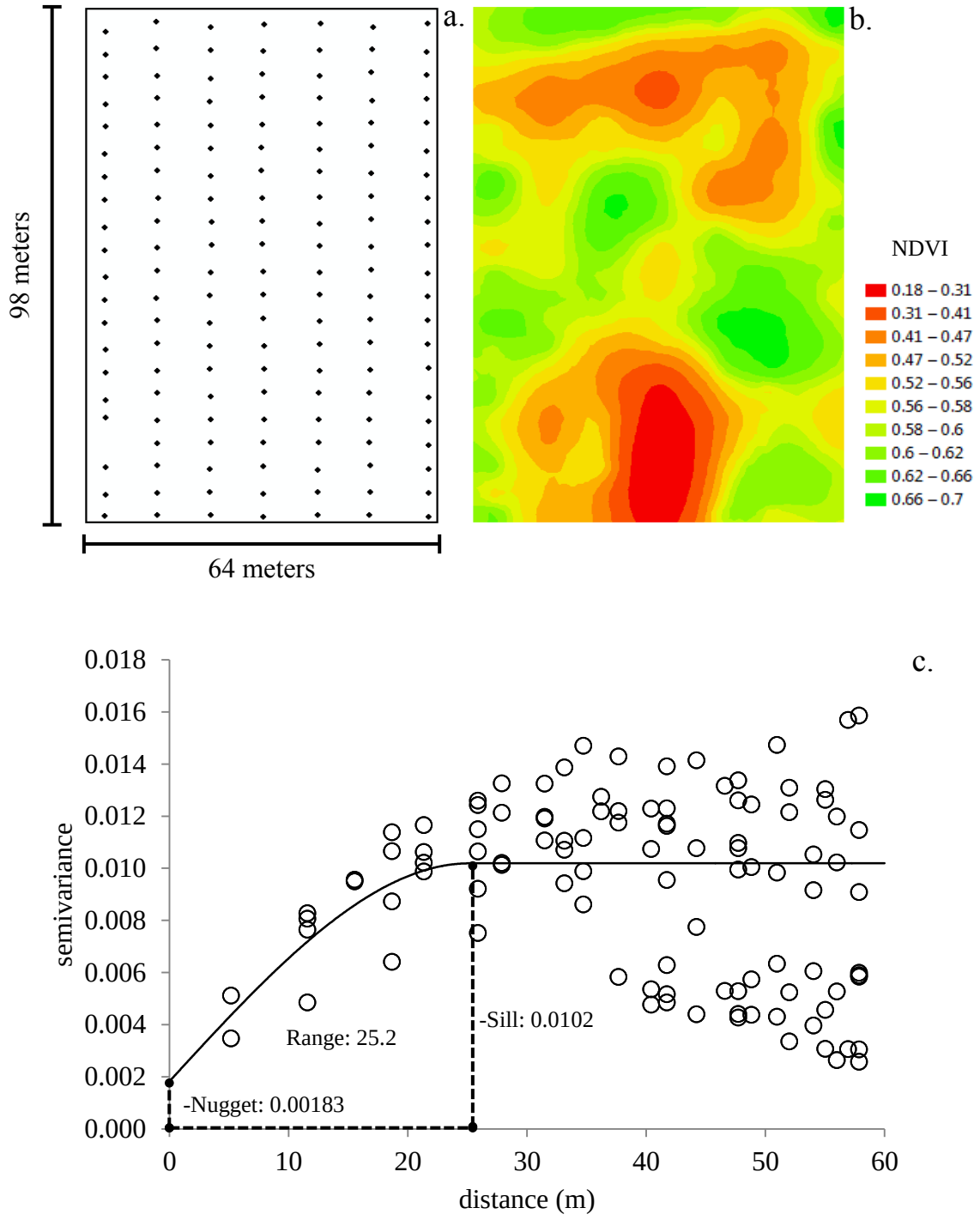


Figure 4.28. (a) Sampling locations (approximately 9.6 m x 4.8 m grid; 148 samples), (b) kriged prediction map and (c) semivariogram including the fitted spherical model of normalized difference vegetative index (NDVI) on Watkinsville field 1.

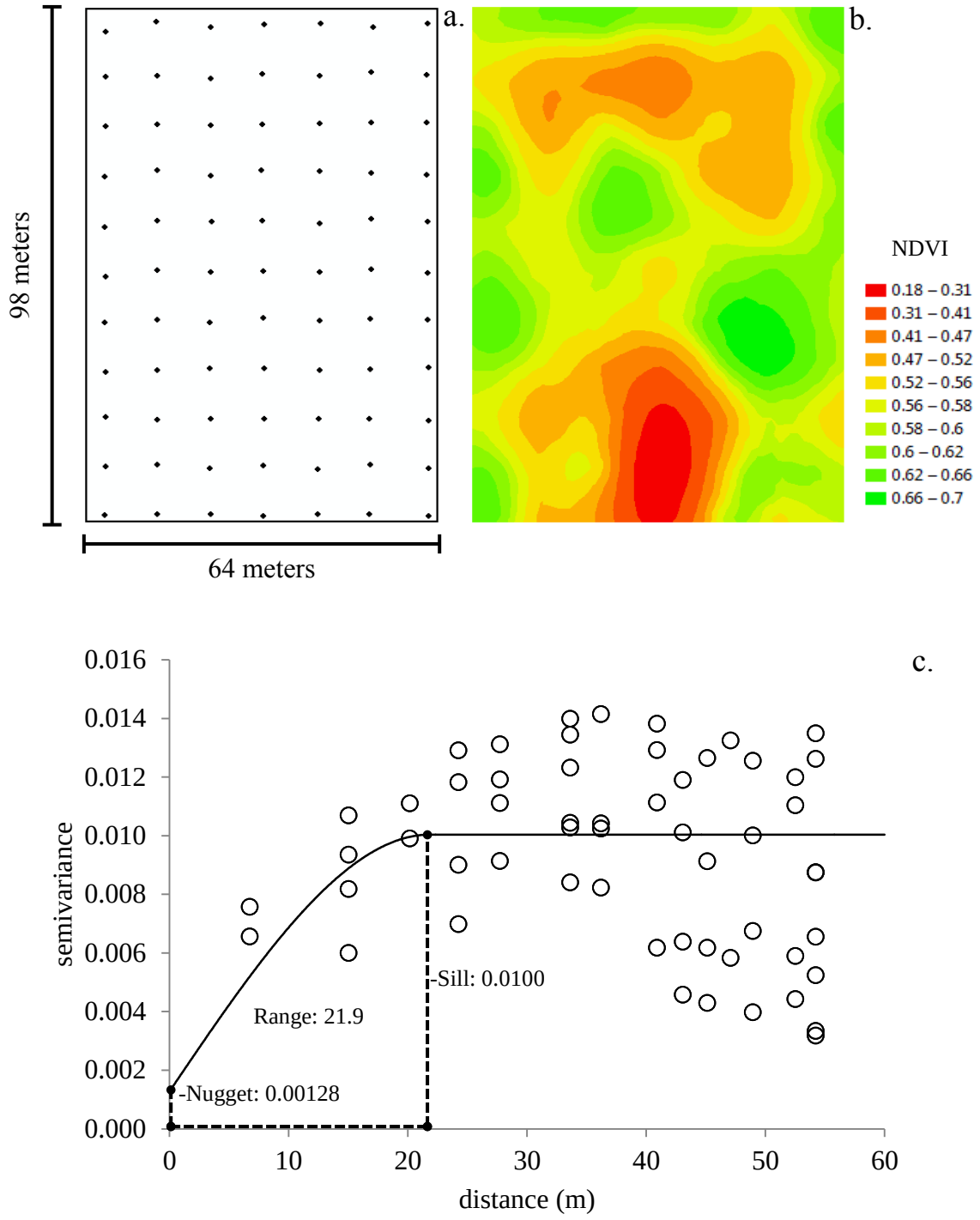


Figure 4.29. (a) Sampling locations (approximately 9.6 m x 9.6 m grid; 75 samples), (b) kriged prediction map and (c) semivariogram including the fitted spherical model of normalized difference vegetative index (NDVI) on Watkinsville field 1.

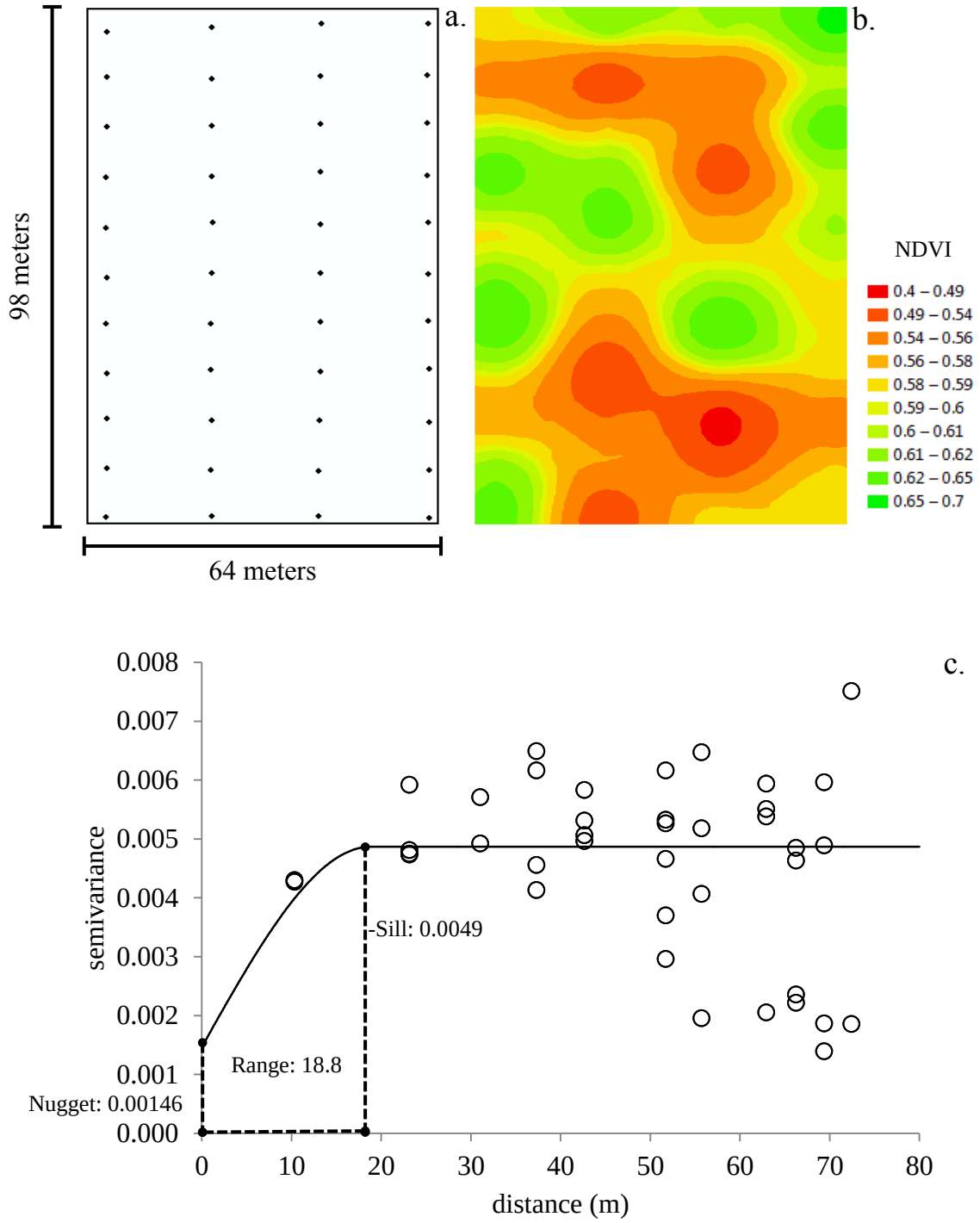


Figure 4.30. (a) Sampling locations (approximately 19.2 m x 9.6 m grid; 45 samples), (b) kriged prediction map and (c) semivariogram including the fitted spherical model of normalized difference vegetative index (NDVI) on Watkinsville field 1.

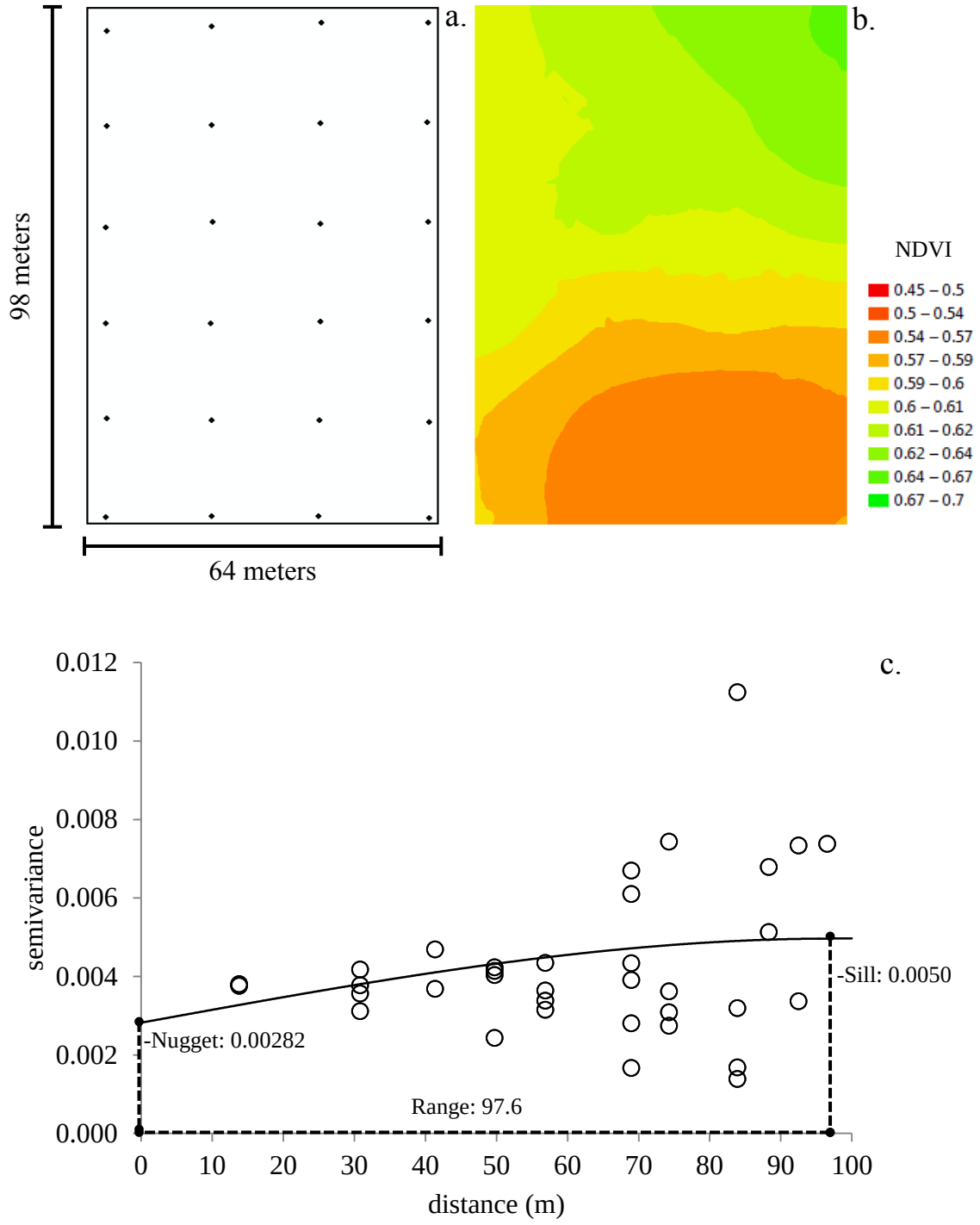


Figure 4.31. (a) Sampling locations (approximately 19.2 m x 19.2 m grid; 24 samples), (b) kriged prediction map and (c) semivariogram including the fitted spherical model of normalized difference vegetative index (NDVI) on Watkinsville field 1.

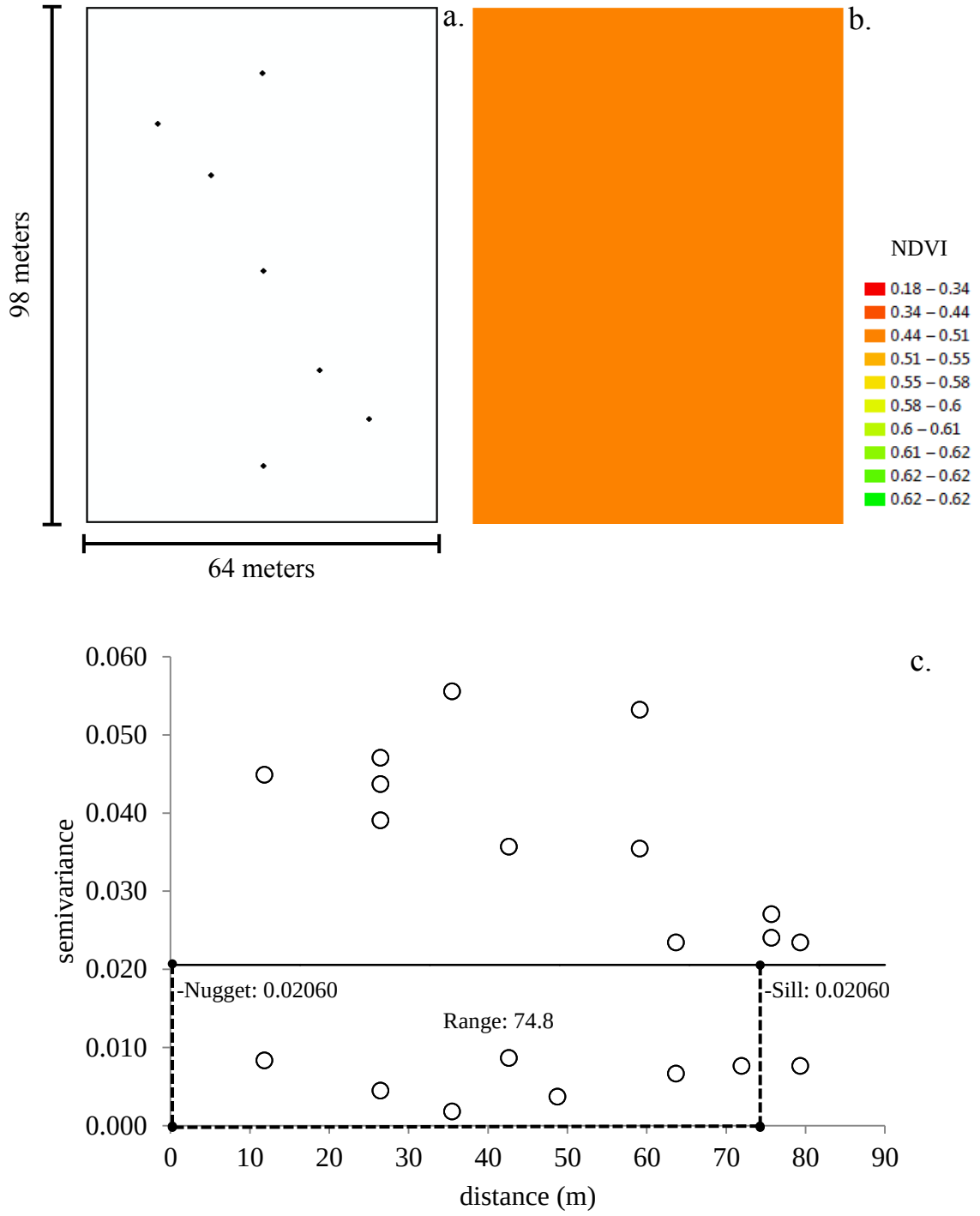


Figure 4.32. (a) Sampling locations (7 samples), (b) kriged prediction map and (c) semivariogram including the fitted spherical model of normalized difference vegetative index (NDVI) on Watkinsville field 1.

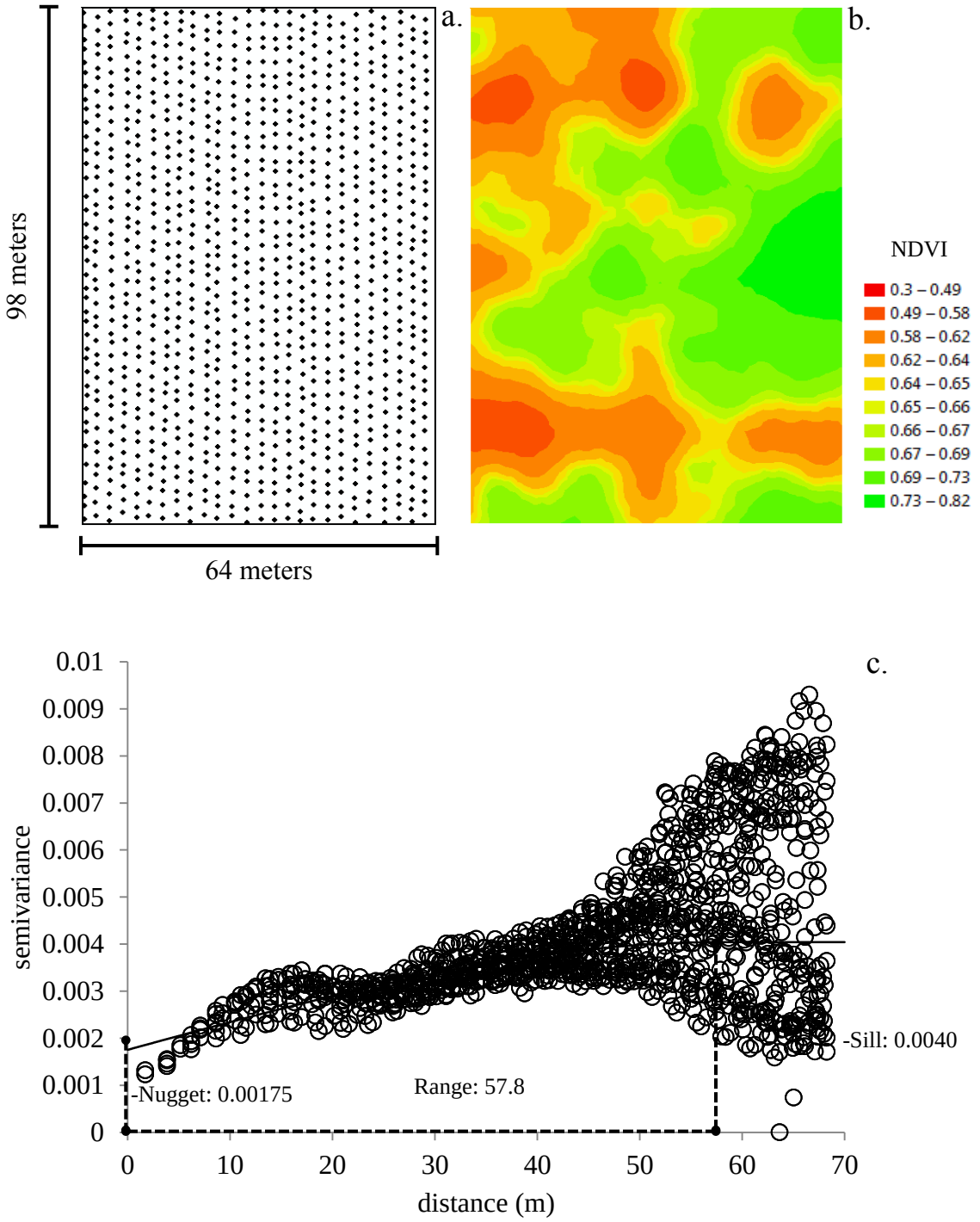


Figure 4.33. (a) Sampling locations (approximately 2.4 m x 2.4 m grid; 1089 samples), (b) kriged prediction map and (c) semivariogram including the fitted spherical model of normalized difference vegetative index (NDVI) on Watkinsville field 2.

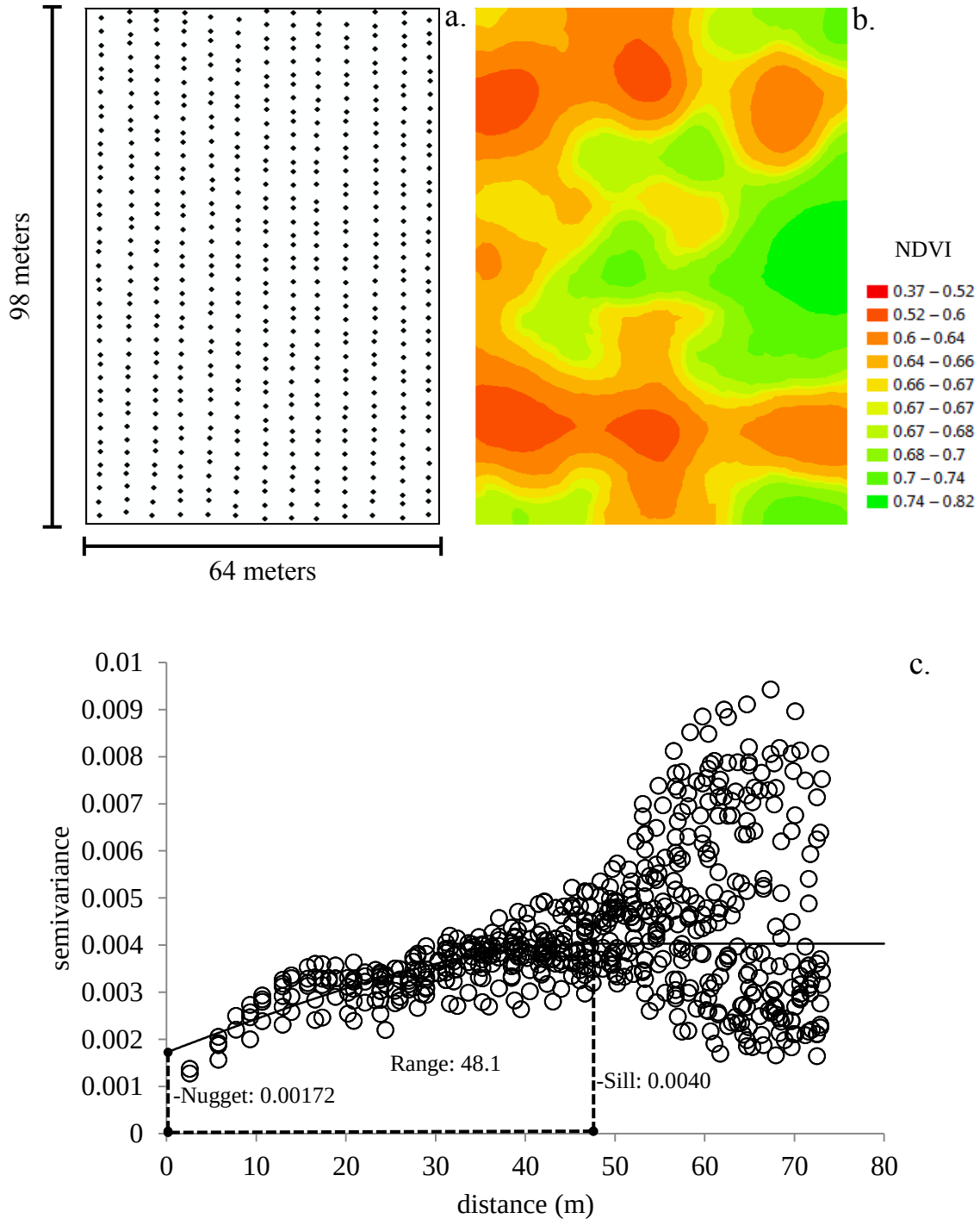


Figure 4.34. (a) Sampling locations (approximately 4.8 m x 2.4 m grid; 541 samples), (b) kriged prediction map and (c) semivariogram including the fitted spherical model of normalized difference vegetative index (NDVI) on Watkinsville field 2.

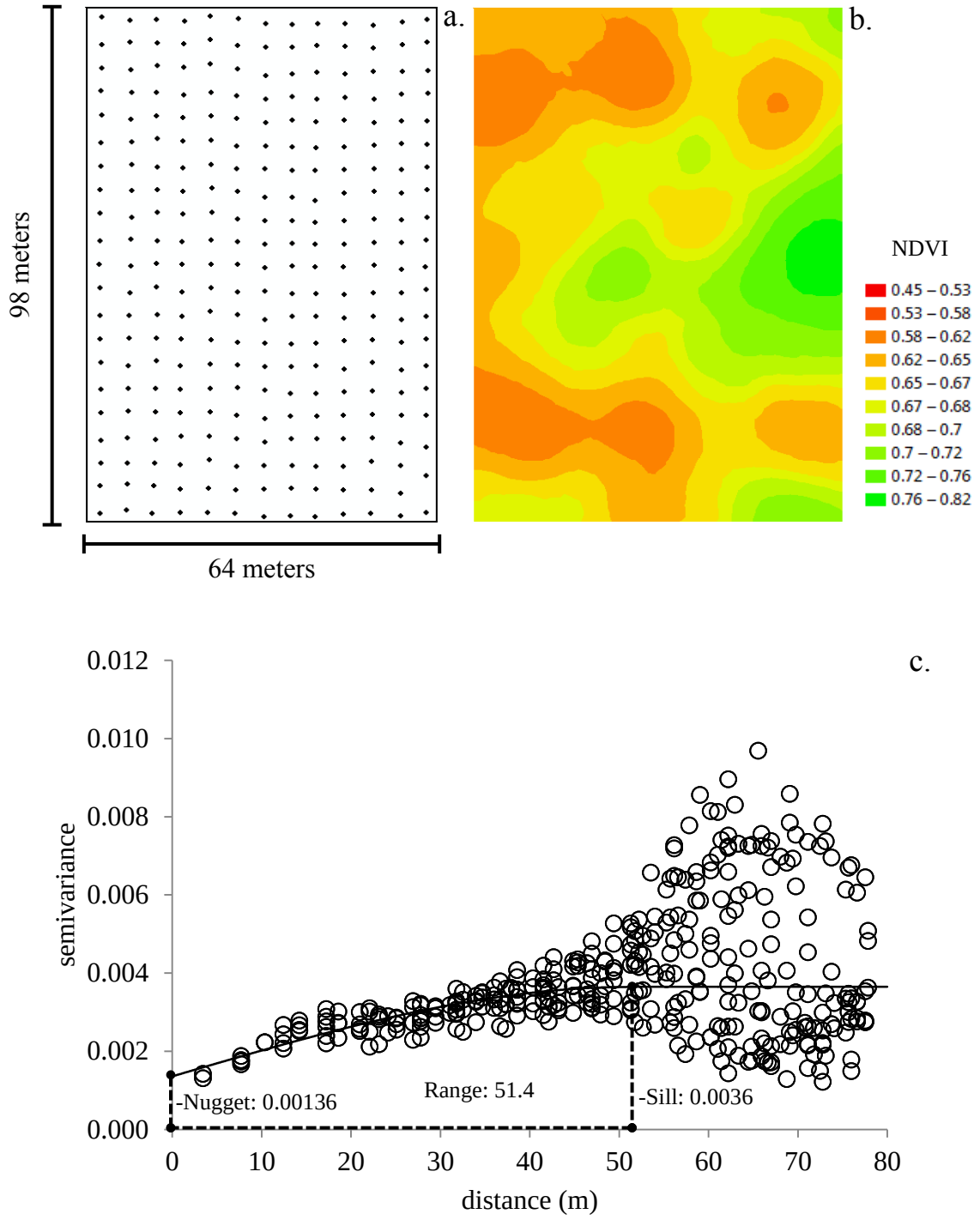


Figure 4.35. (a) Sampling locations (approximately 4.8 m x 4.8 m grid; 273 samples), (b) kriged prediction map and (c) semivariogram including the fitted spherical model of normalized difference vegetative index (NDVI) on Watkinsville field 2.

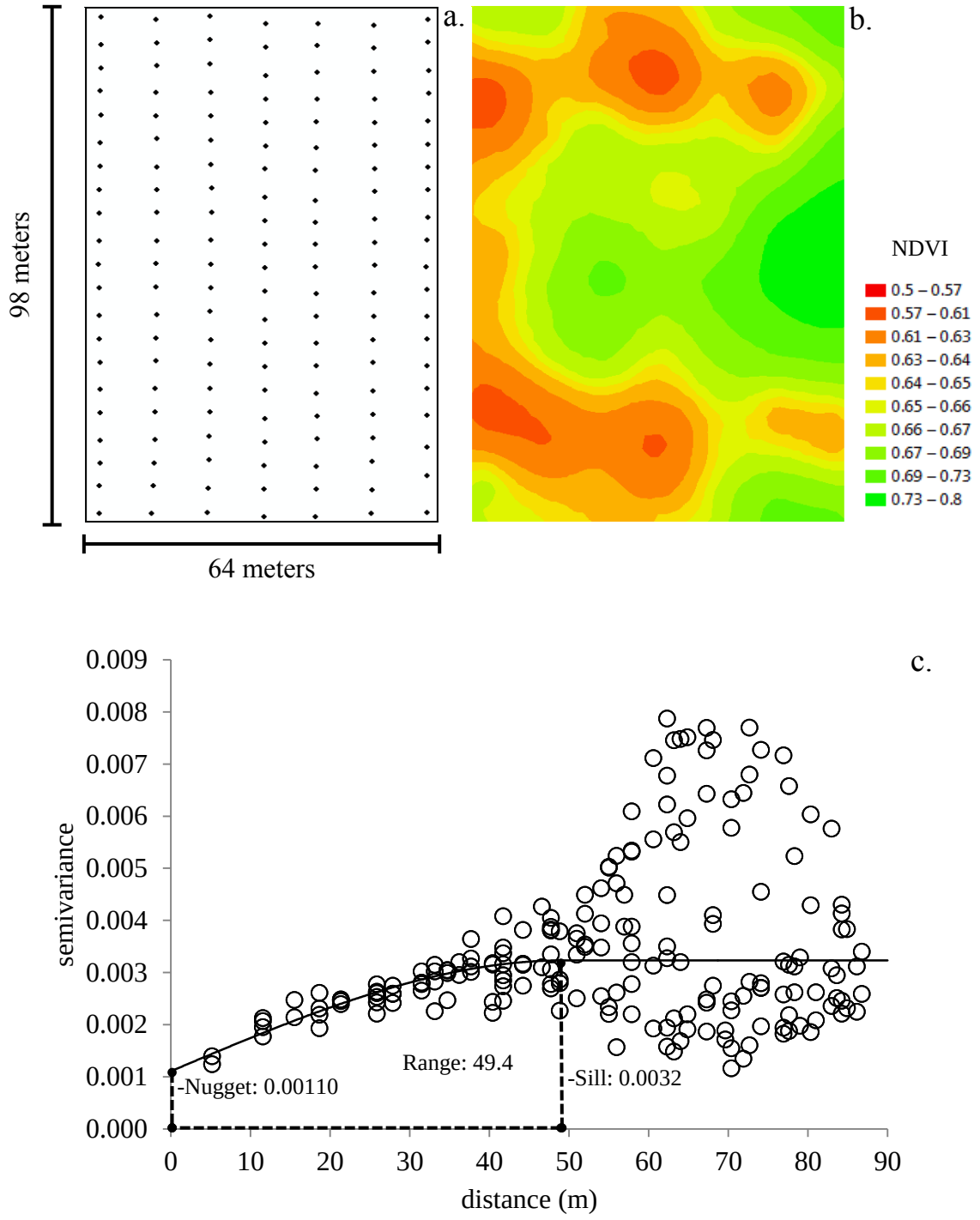


Figure 4.36. (a) Sampling locations (approximately 9.6 m x 4.8 m grid; 147 samples), (b) kriged prediction map and (c) semivariogram including the fitted spherical model of normalized difference vegetative index (NDVI) on Watkinsville field 2.

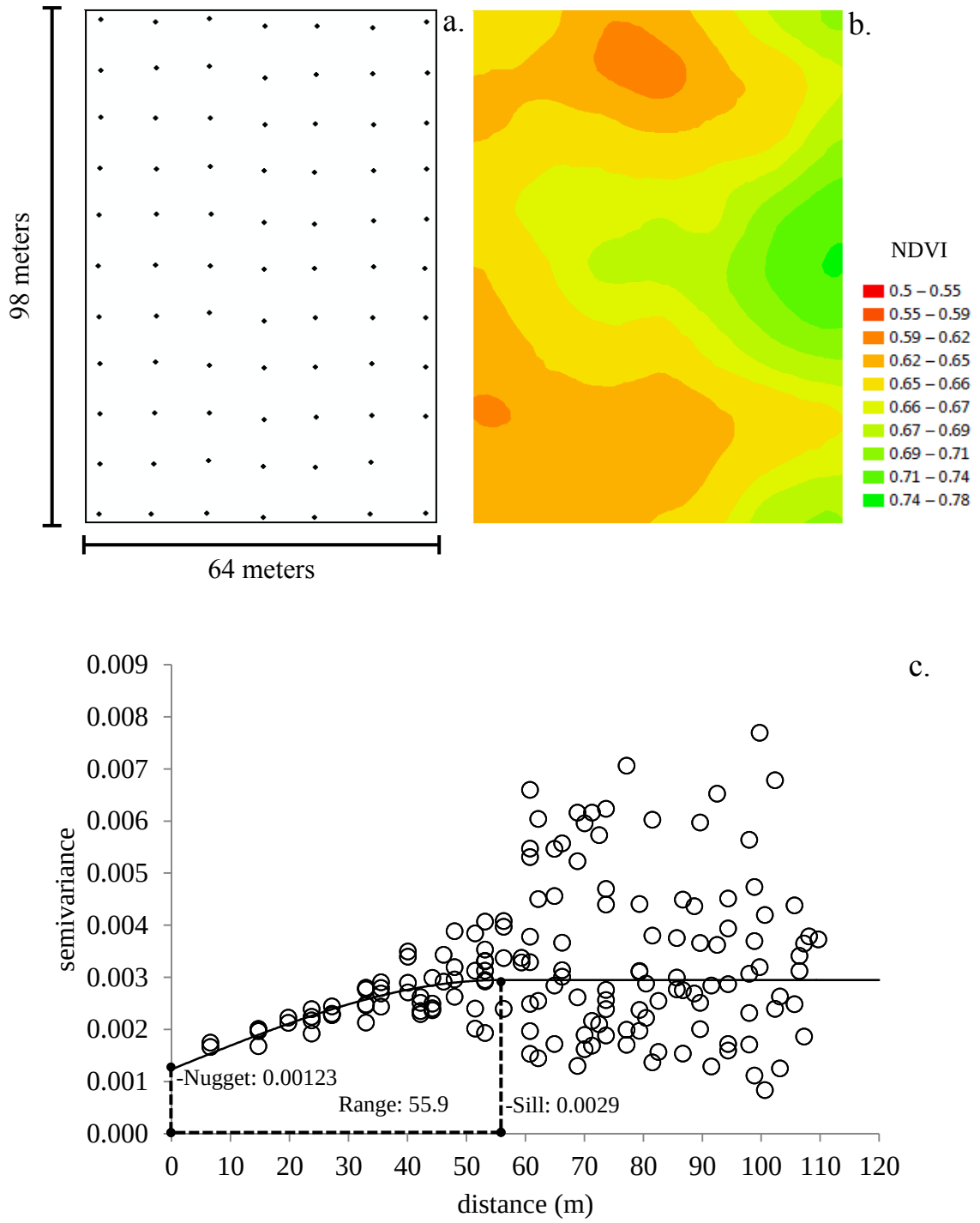


Figure 4.37. (a) Sampling locations (approximately 9.6 m x 9.6 m grid; 76 samples), (b) kriged prediction map and (c) semivariogram including the fitted spherical model of normalized difference vegetative index (NDVI) on Watkinsville field 2.

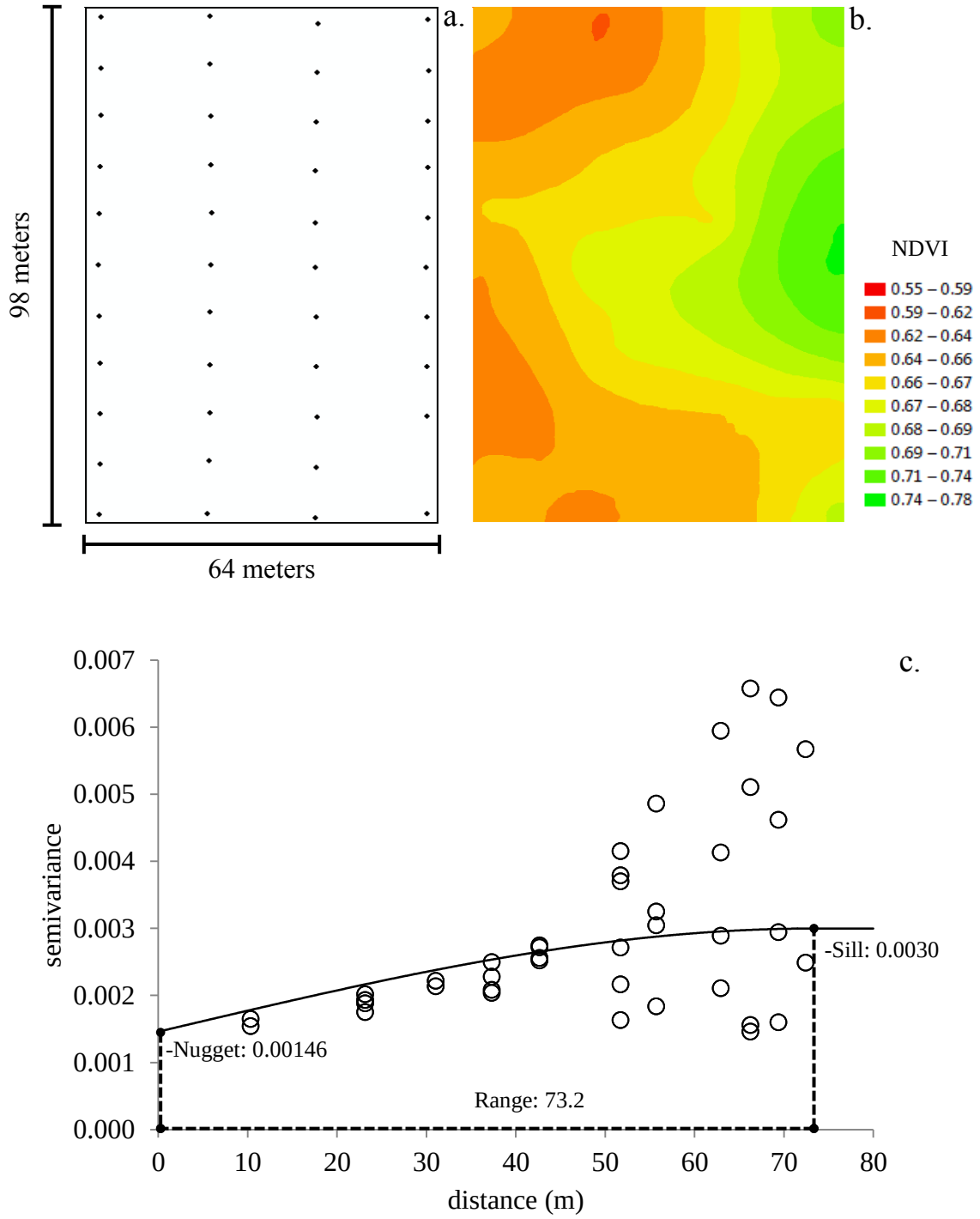


Figure 4.38. (a) Sampling locations (approximately 19.2 m x 9.6 m grid; 43 samples), (b) kriged prediction map and (c) semivariogram including the fitted spherical model of normalized difference vegetative index (NDVI) on Watkinsville field 2.

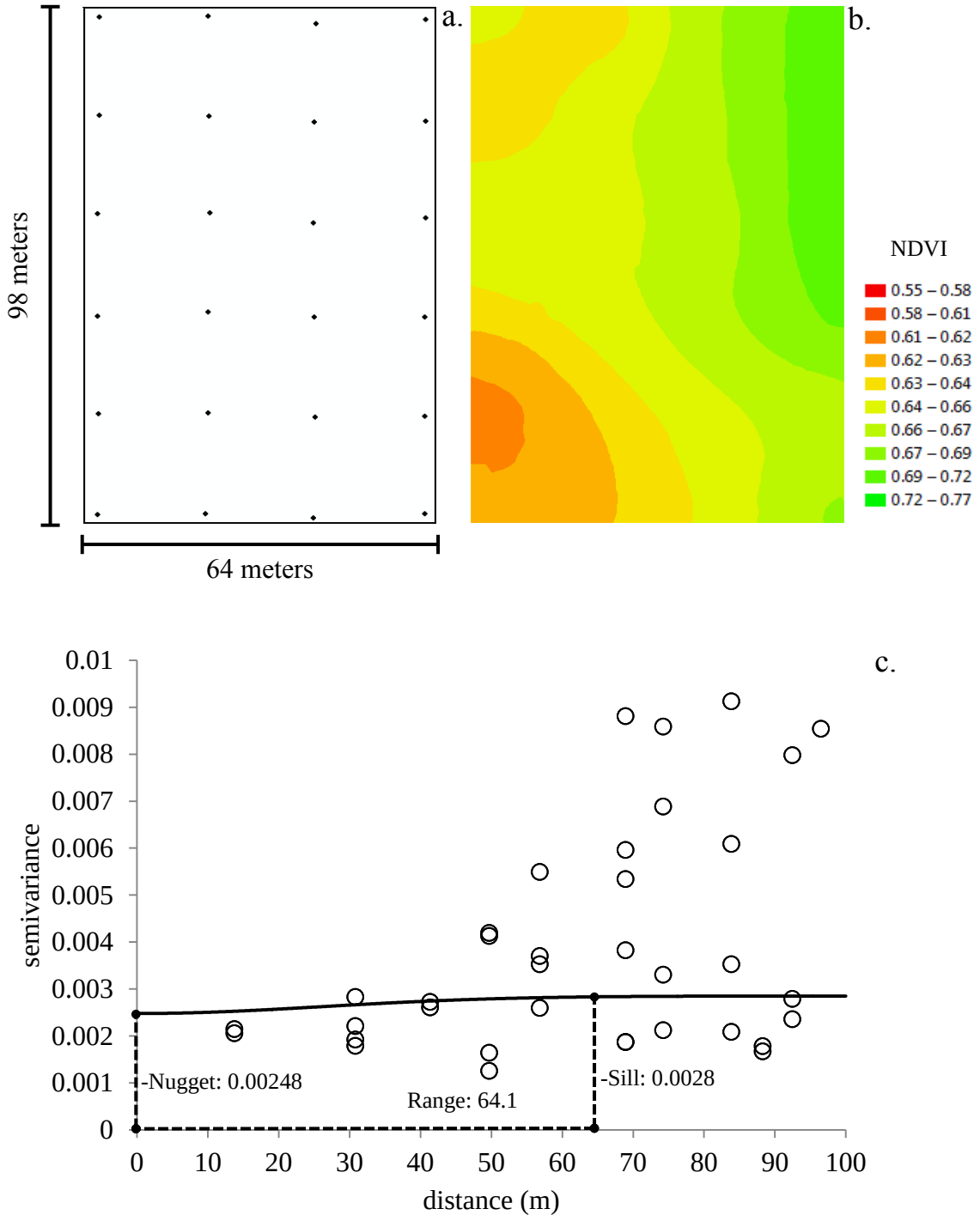


Figure 4.39. (a) Sampling locations (approximately 19.2 m x 19.2 m grid; 24 samples), (b) kriged prediction map and (c) semivariogram including the fitted spherical model of normalized difference vegetative index (NDVI) on Watkinsville field 2.

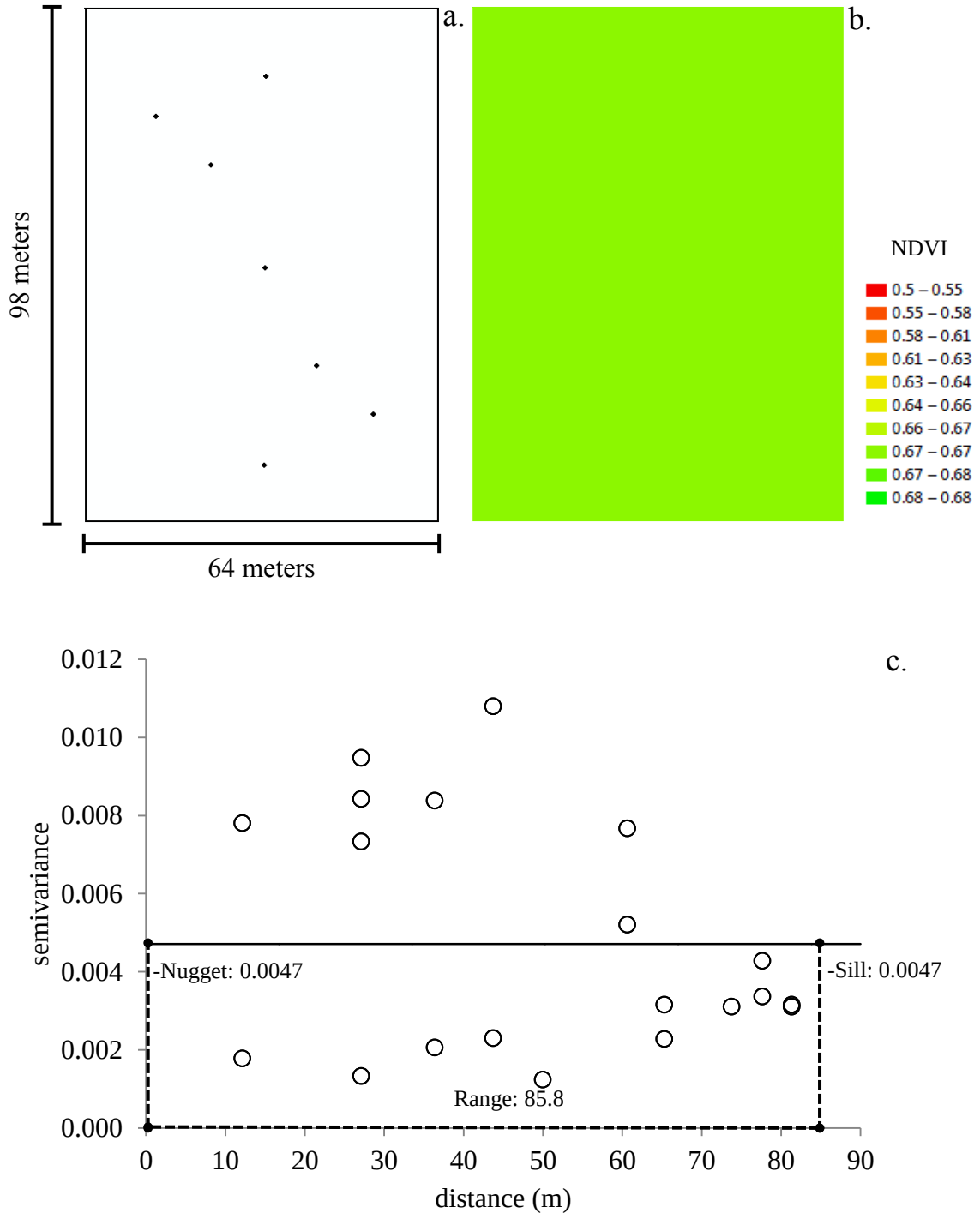


Figure 4.40. (a) Sampling locations (7 samples), (b) kriged prediction map and (c) semivariogram including the fitted spherical model of normalized difference vegetative index (NDVI) on Watkinsville field 2.

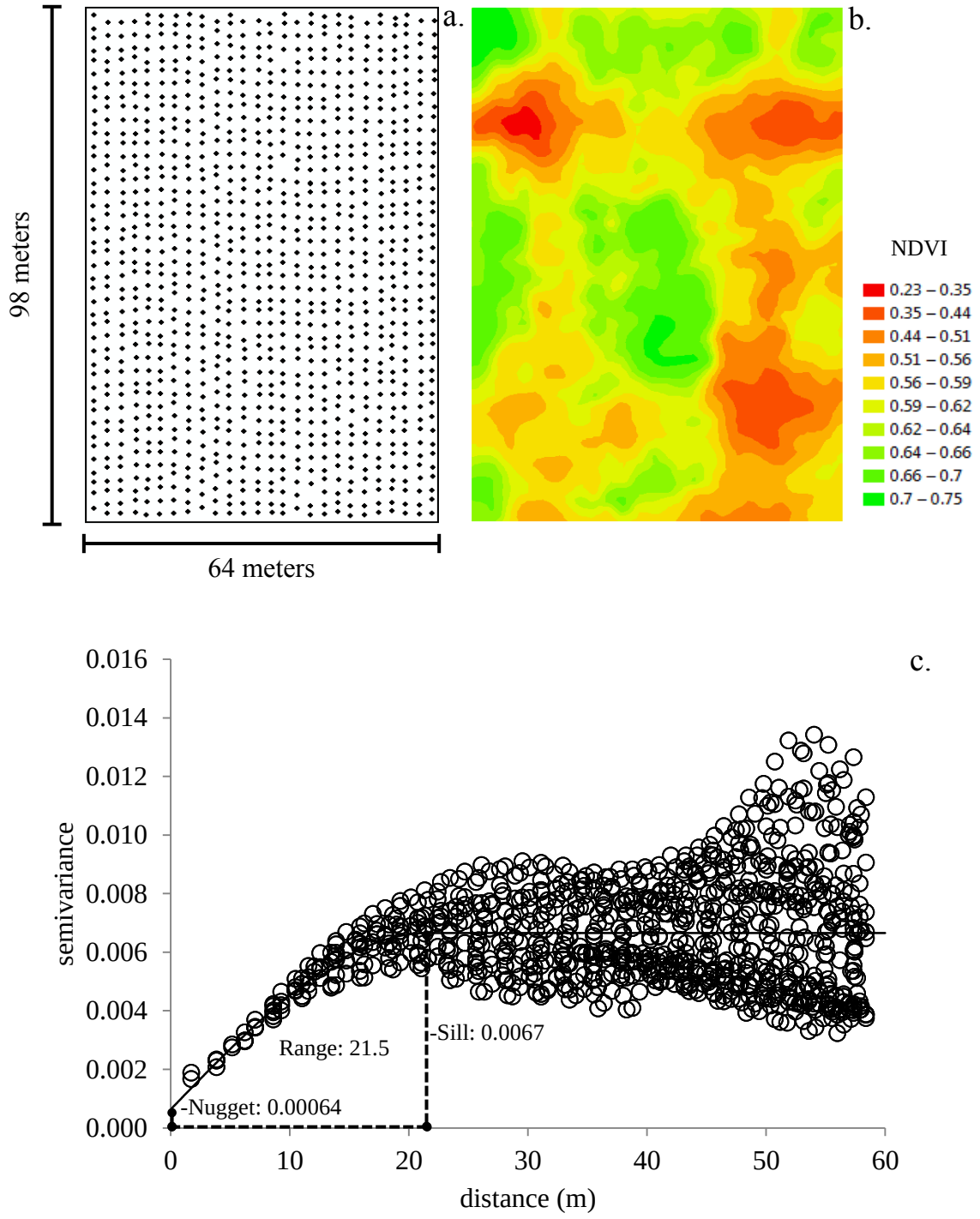


Figure 4.41. (a) Sampling locations (approximately 2.4 m x 2.4 m grid; 1121 samples), (b) kriged prediction map and (c) semivariogram including the fitted spherical model of normalized difference vegetative index (NDVI) on Watkinsville field 3.

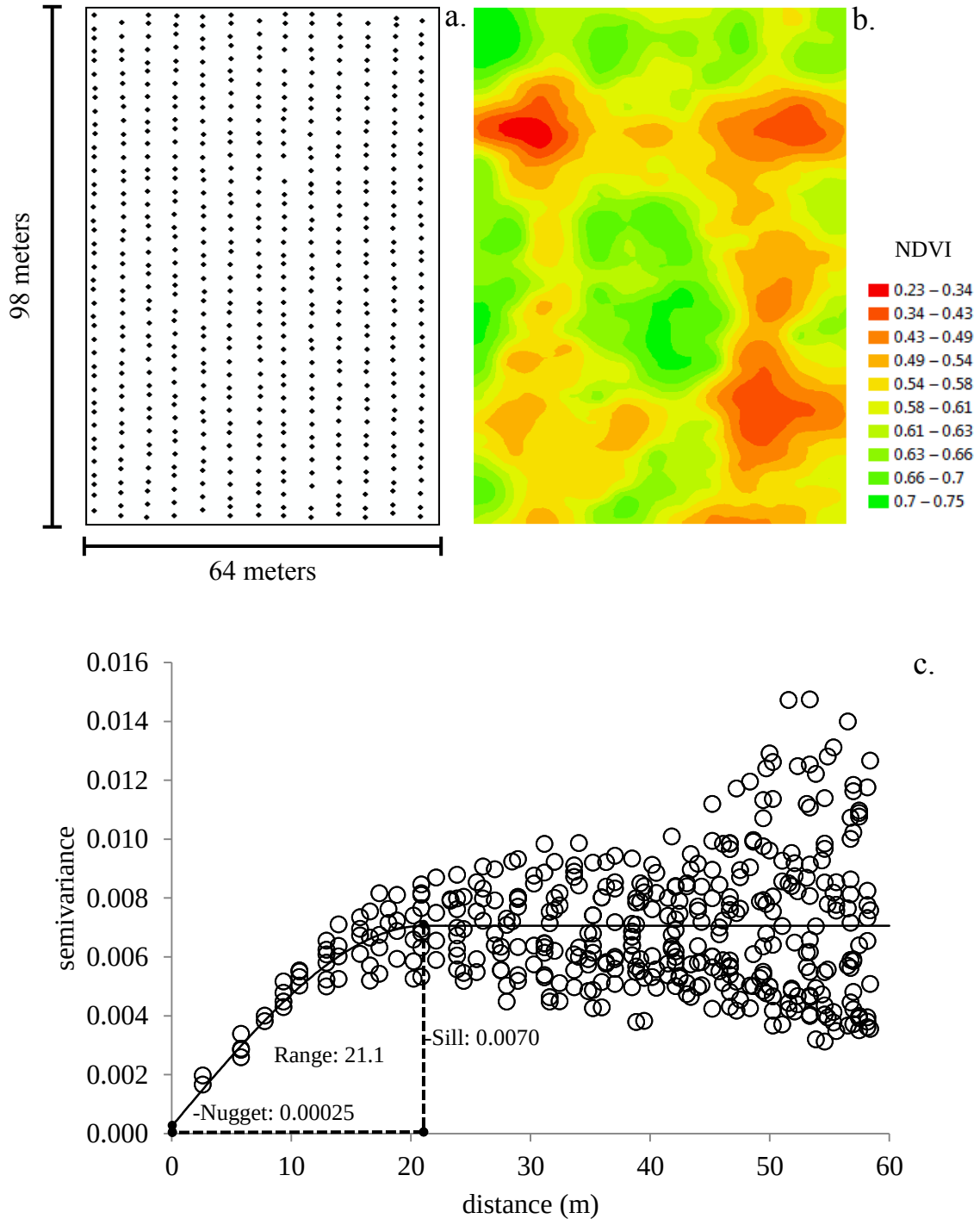


Figure 4.42. (a) Sampling locations (approximately 4.8 m x 2.4 m grid; 563 samples), (b) kriged prediction map and (c) semivariogram including the fitted spherical model of normalized difference vegetative index (NDVI) on Watkinsville field 3.

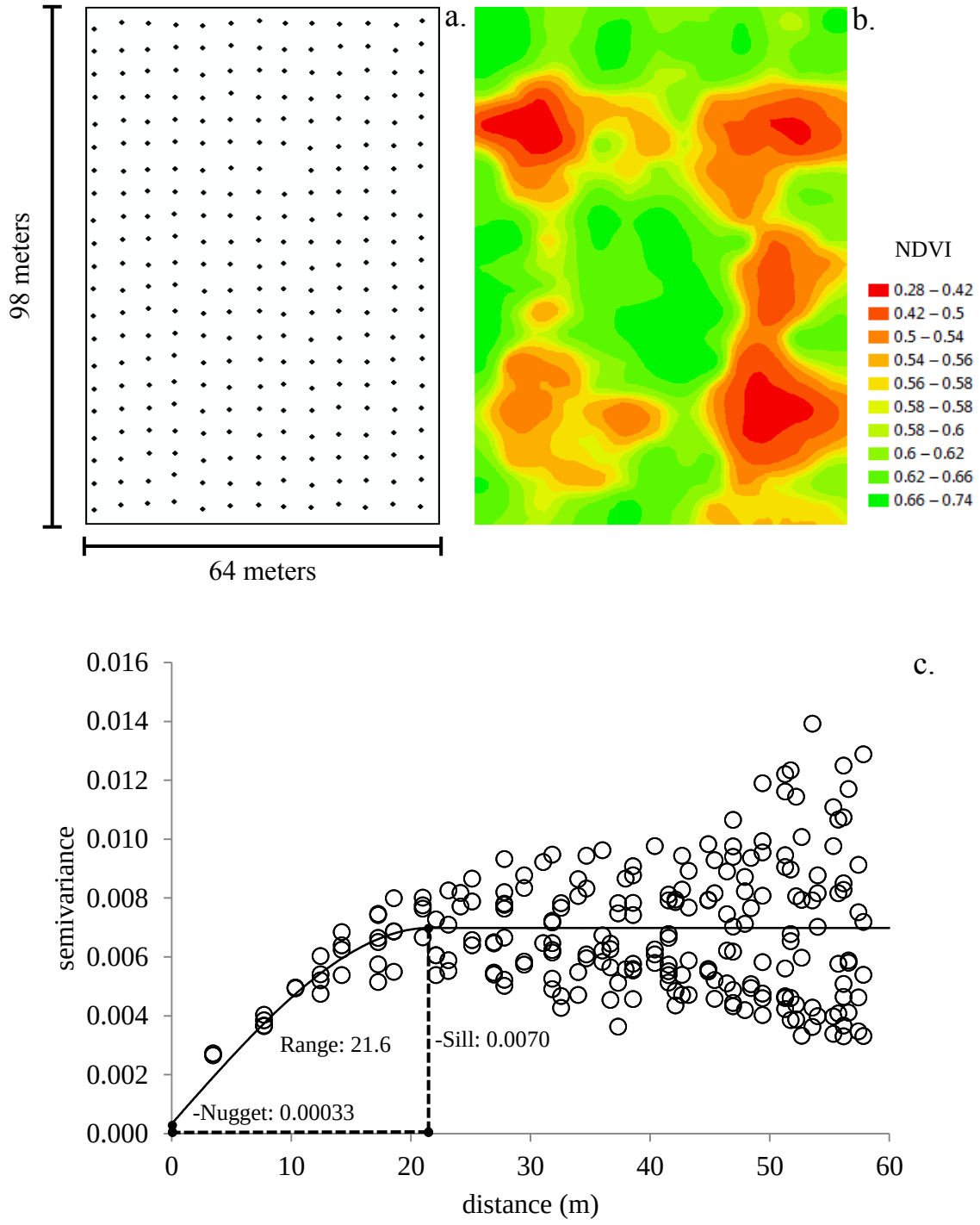


Figure 4.43. (a) Sampling locations (approximately 4.8 m x 4.8 m grid; 273 samples), (b) kriged prediction map and (c) semivariogram including the fitted spherical model of normalized difference vegetative index (NDVI) on Watkinsville field 3.

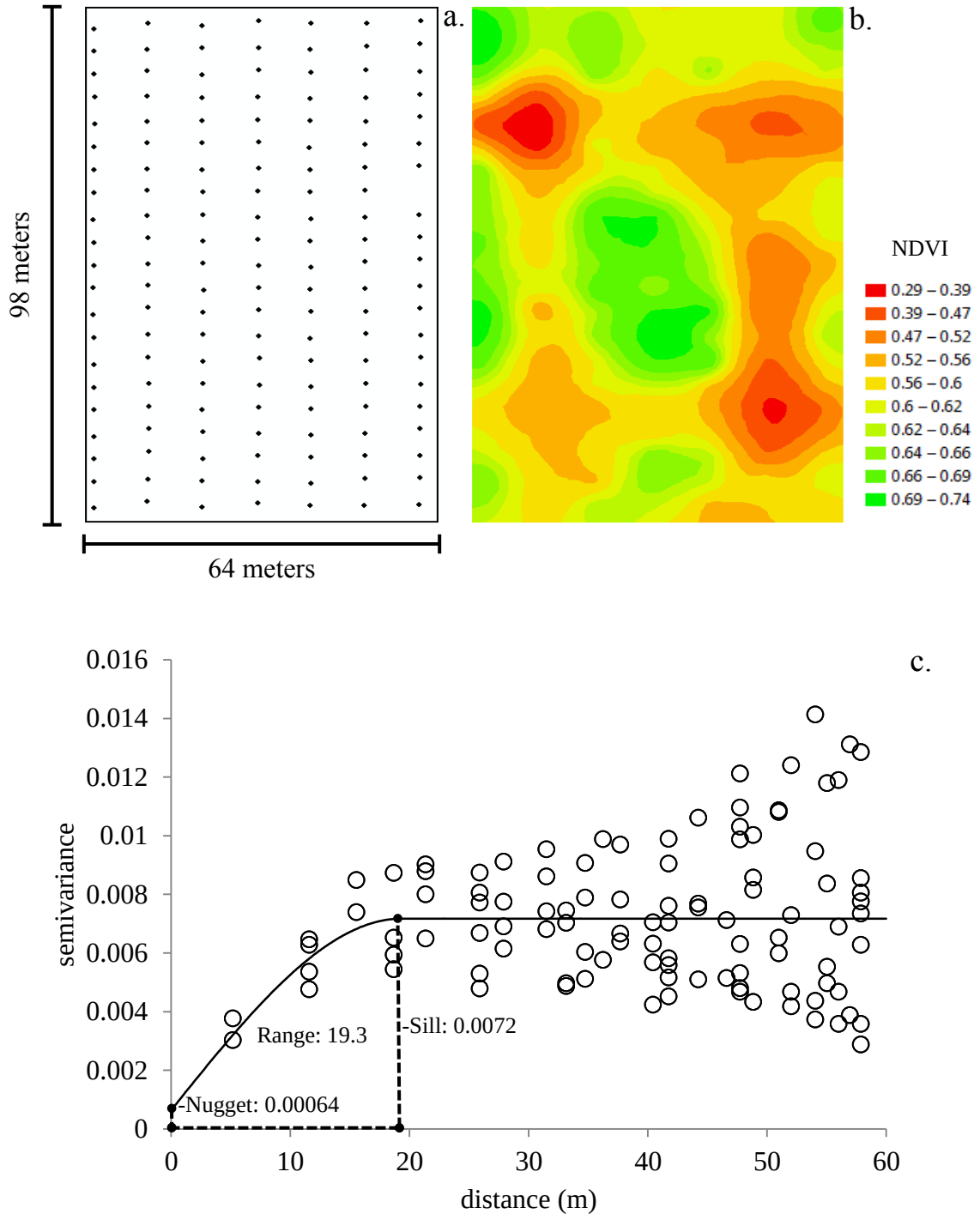


Figure 4.44. (a) Sampling locations (approximately 9.6 m x 4.8 m grid; 147 samples), (b) kriged prediction map and (c) semivariogram including the fitted spherical model of normalized difference vegetative index (NDVI) on Watkinsville field 3.

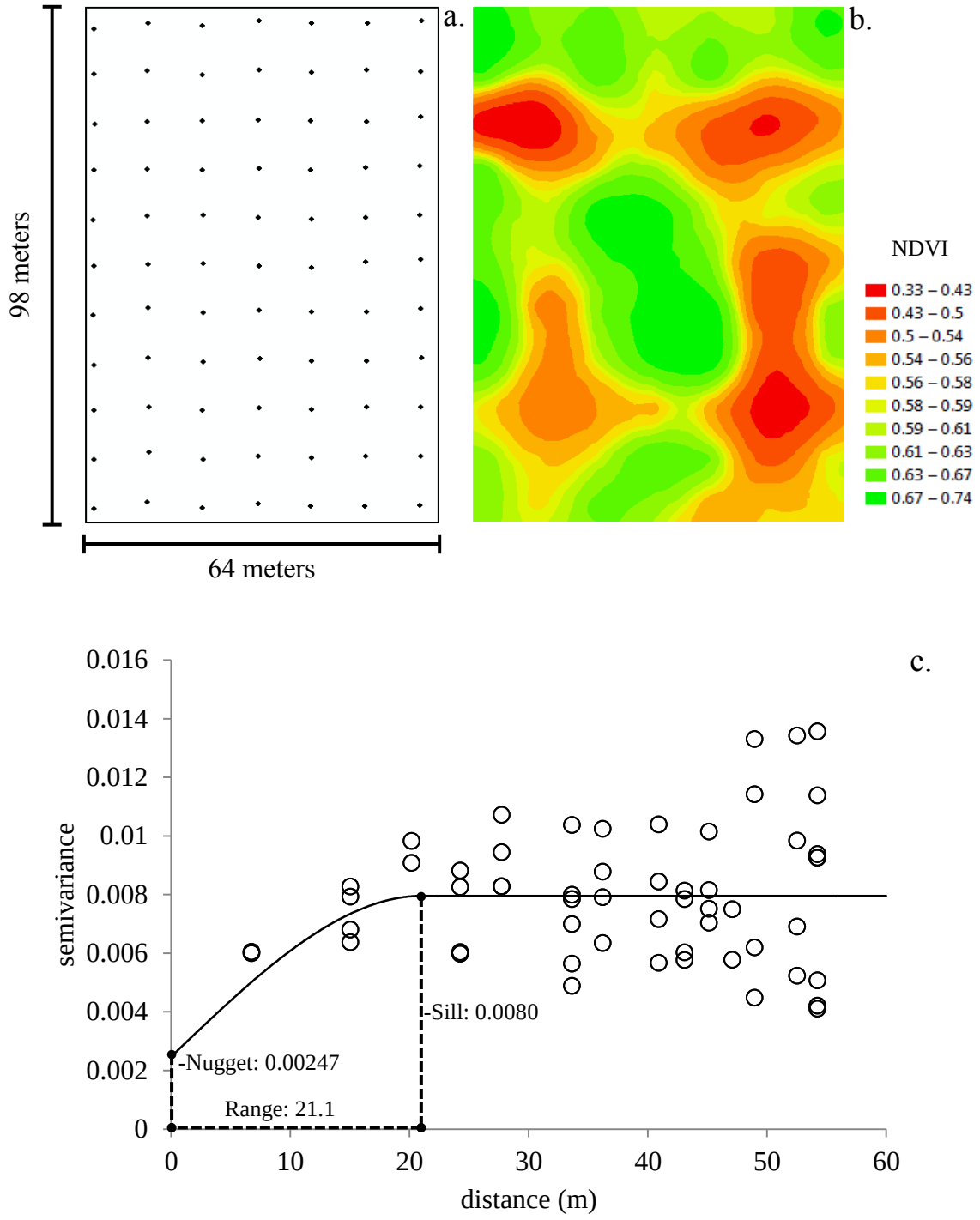


Figure 4.45. (a) Sampling locations (approximately 9.6 m x 9.6 m grid; 77 samples), (b) kriged prediction map and (c) semivariogram including the fitted spherical model of normalized difference vegetative index (NDVI) on Watkinsville field 3.

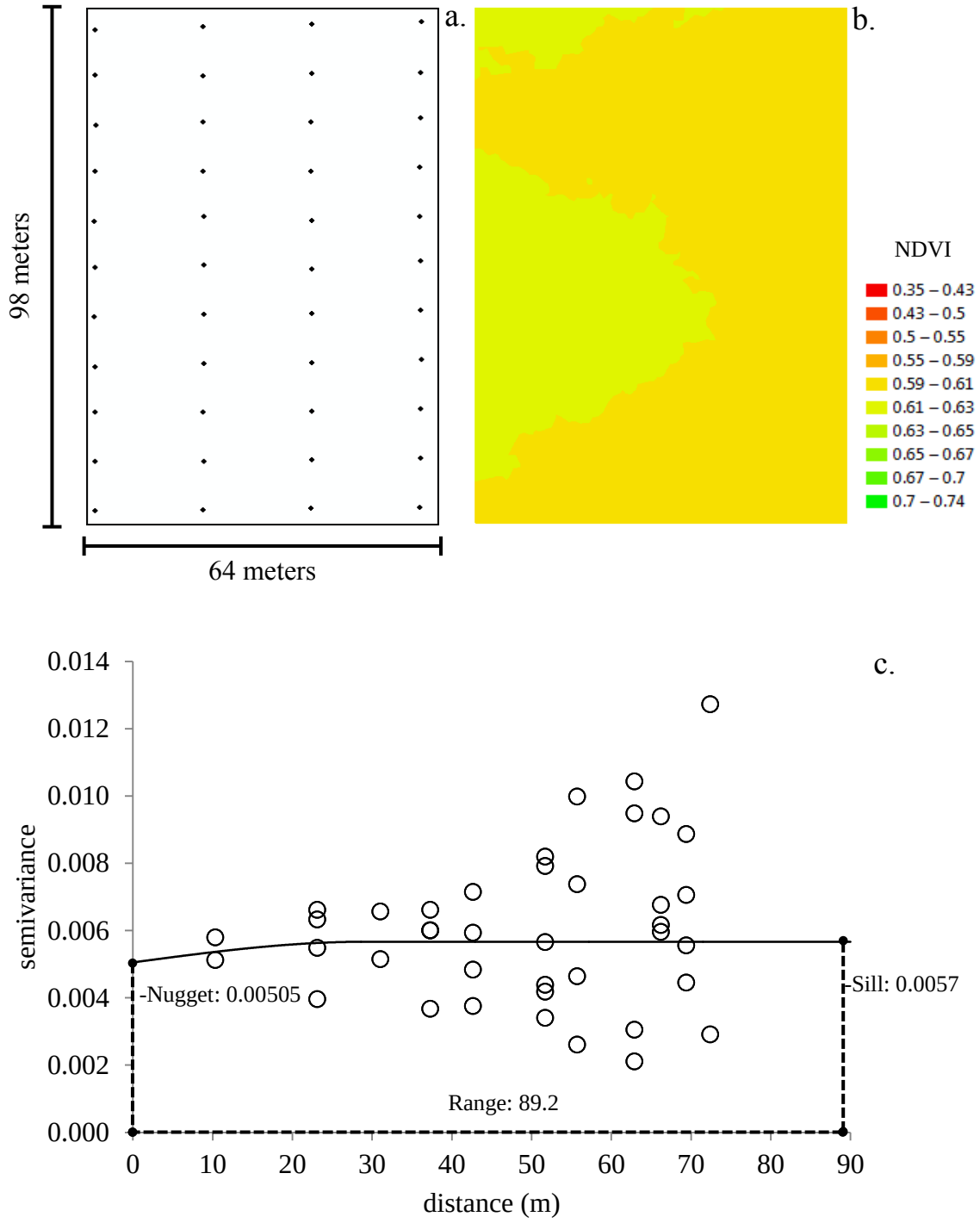


Figure 4.46. (a) Sampling locations (approximately 19.2 m x 9.6 m grid; 44 samples), (b) kriged prediction map and (c) semivariogram including the fitted spherical model of normalized difference vegetative index (NDVI) on Watkinsville field 3.

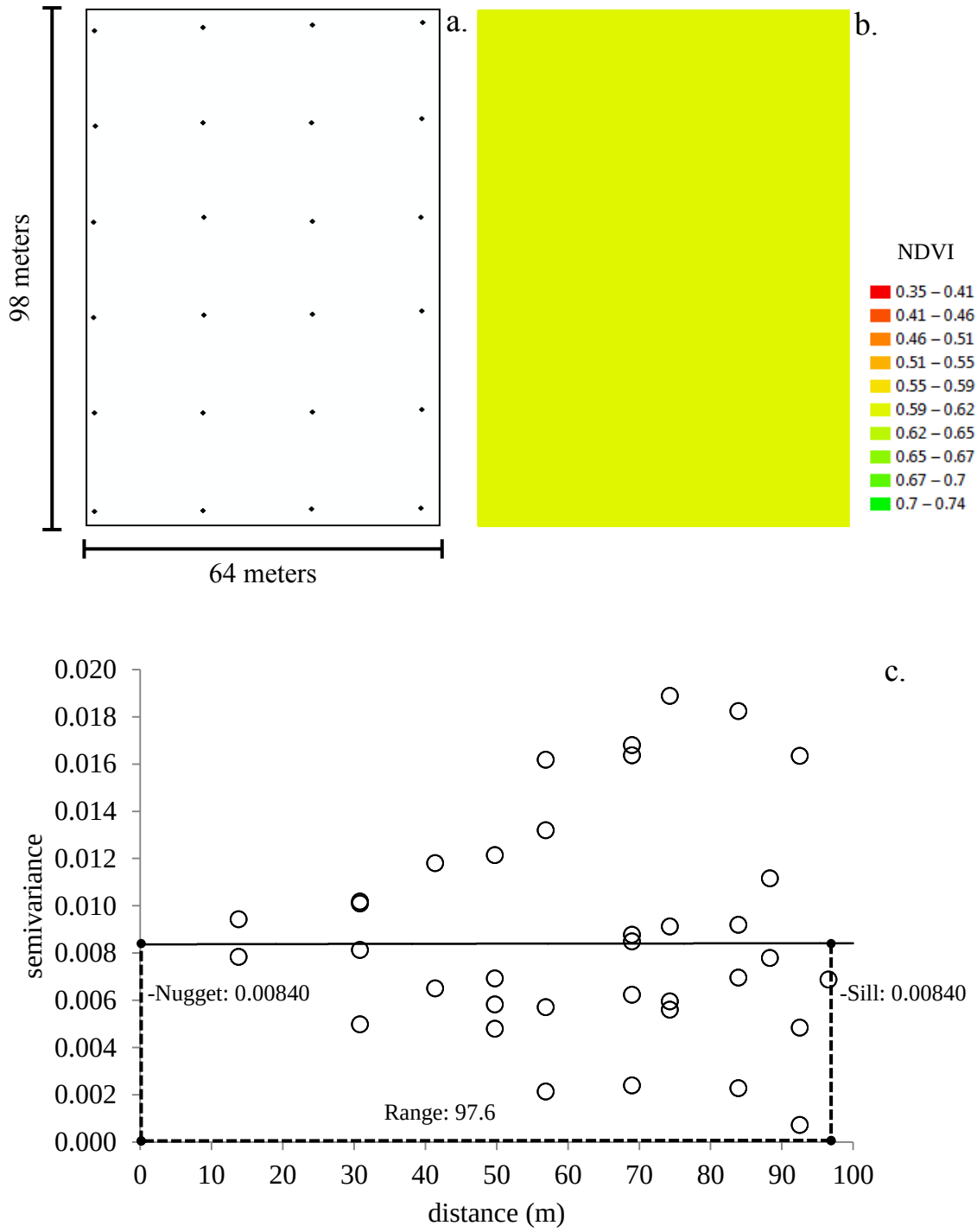


Figure 4.47. (a) Sampling locations (approximately 19.2 m x 19.2 m grid; 24 samples), (b) kriged prediction map and (c) semivariogram including the fitted spherical model of normalized difference vegetative index (NDVI) on Watkinsville field 3.

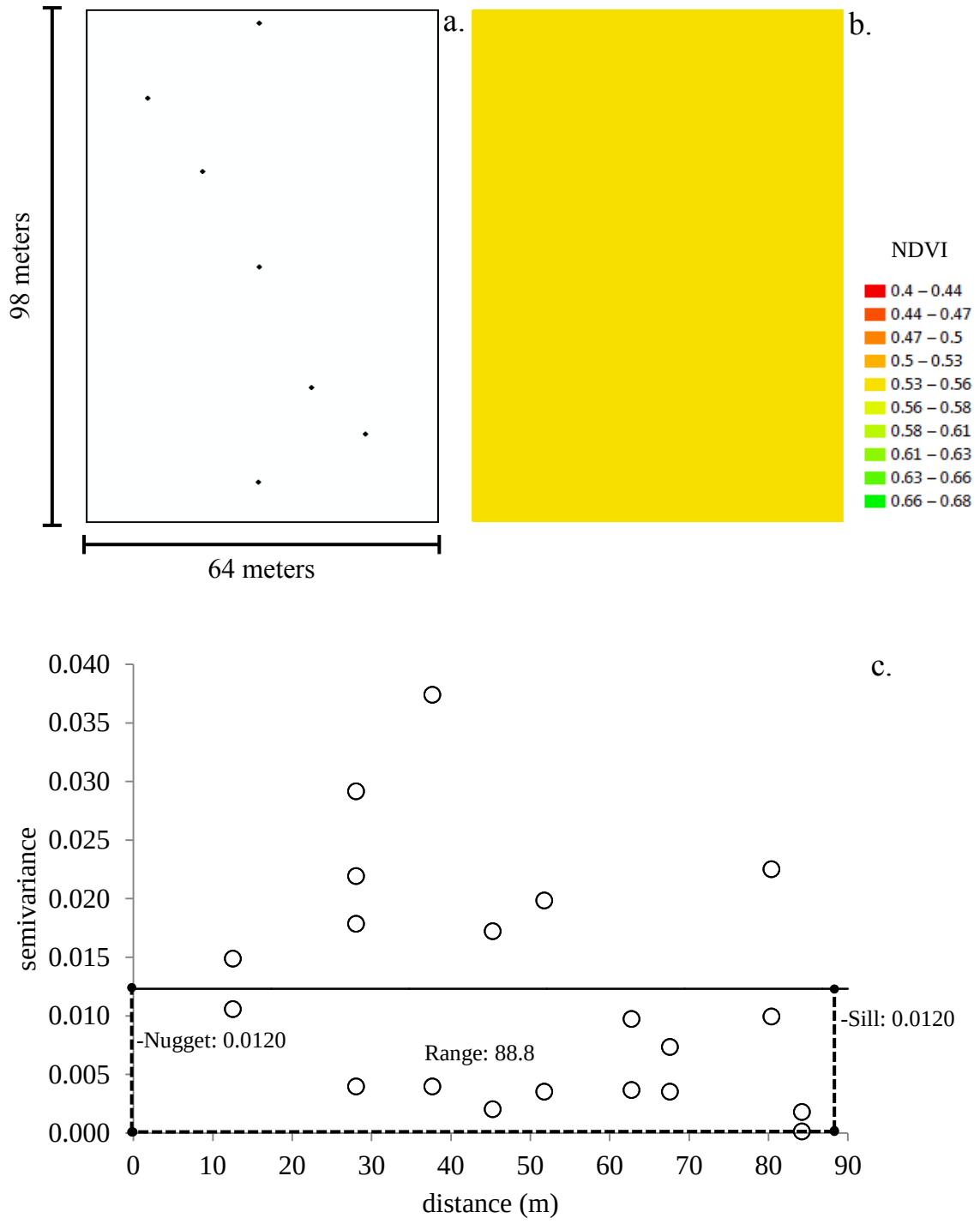


Figure 4.48. (a) Sampling locations (7 samples), (b) kriged prediction map and (c) semivariogram including the fitted spherical model of normalized difference vegetative index (NDVI) on Watkinsville field 3.

# CHAPTER 5

# PRELIMINARY COMPARISON OF MOBILE AND HANDHELD SAMPLING DEVICES FOR MEASURING SURFACE AND EDAPHIC PROPERTIES ON SPORTS FIELDS

## Introduction

High user expectations and pressure from society for improved environmental stewardship have created a demand to test the performance of sports fields (McAuliffe, 2008; Bartlett, 2009). The term "performance testing" (i.e. site assessment) is receiving increasing attention as a method to quantify the surface and edaphic properties associated with sports fields (Stiles et al., 2009; Carrow et al., 2010). Performance testing is primarily focused on synthetic turf surfaces with the assumption that natural turf surfaces are a benchmark for safety (Fédération Internationale de Football Association, FIFA, 2012; Stiles et al., 2009). However, with natural turf, the magnitude and frequency of temporal variations are considerably greater and more challenging to control because of dependency on the level of foot traffic (Baker, 1991).

There are several common methods of measuring surface and edaphic properties on sports fields using handheld devices. Surface hardness tests involve dropping a missile of known mass from a standard height, with a mounted linear accelerometer (Gramckow, 1968; Clegg, 1976; American Society for Testing and Materials, ASTM, 2010). Soil compaction tests can be conducted with a penetrometer that uses a cylindrical tip (also referred to as a "cone") of a certain length to measure the penetration resistance of the soil at a certain depth (i.e. the force it takes to insert the cone into the soil to a specific depth) (Holmes and Bell, 1986). Traction tests

use a type of studded apparatus with a certain mass and torque wrench to measure the force needed to cause the turf to fail (Canaway and Bell, 1986). Time-domain reflectometry (TDR) and capacitance sensors are two methods for determining soil moisture by measuring changes in the soil dielectric constant (ε) as water contents fluctuate (Leib et al., 2003). Lastly, a broad assessment of turf performance has been reported by Trenholm et al. (1999) using a spectral reflectance methodology referred to as normalized difference vegetative index (NDVI). NDVI has been shown to be significantly associated with visual turf quality, density, and shoot tissue injury (Trenholm et al., 1999).

Minimal procedures have been published to identify performance test locations on natural turf sports field surfaces. One procedure is the ASTM F1936, which identifies test locations to measure surface hardness (ASTM, 2010). This specification describes testing locations for all sports played on natural turf in the United States (football, soccer, lacrosse, field hockey). Generally, 10 test points are recommended in the proximity of areas such as end zones and goals, wings (a certain distance from the center line and sideline), middle of field, and one location outside the in-bound lines.

Additionally, The Performance Quality Standards (PQS) is a concept in Europe, developed by Dury (1997), to provide a complete picture of a stated facility (such as a football pitch), with the surface, sub-surface, and playing aspects being clearly defined. The Institute of Groundsmanship (IOG) provides PQS test methods to assess an extensive number of parameters (total of 19) (Bartlett et al., 2009; IOG, 2014). For each parameter, sampling numbers and test locations vary by sport, with total number of tests usually being 5-20 per field. The values from each location are averaged to determine performance of that parameter across the field.

Studies that have evaluated surface and edaphic properties have used similar performance test locations with slight variations (Bell and Holmes, 1988; Baker and Bell, 1986; Holmes and Bell, 1986; McClements and Baker, 1994; Jennings-Temple, 2006; Bartlett, 2009). Data was typically collected from 3-12 locations across their fields, with 1-10 tests per location area. Sample locations were developed from the assumption that foot traffic on a sports field creates an approximate diamond shape wear pattern (with majority of wear being in the center of the field and around goals) (Holmes and Bell, 1986). Samples were collected from sites on the field thought to receive high, intermediate, and low levels of wear to take into account inherent variability (Holmes and Bell, 1986). Summary statistics (mean, min, max, standard deviation, etc.) were the primary determinate of central tendency and variability for the data.

Previously described sampling methods are designed to be 'low technology' to enable wide usage; however, a consequence of making data assessment easier to conduct and interpret can mask variability of the data for the entire field (Bartlett et al., 2009). Geostatistics is a form of statistics used to analyze spatial data which are applied in environmental science fields such as mineral resource mapping and precision agriculture (James and Goodwin, 2003; Taylor et al., 2003; Emery and González, 2007). Global Positioning Systems (GPS) enable the data to be imported into powerful Geographic Information System (GIS) programs for spatial analysis using geostatistics. Specifically, two geostatistical techniques, variograms and interpolation, are commonly used. Semivariograms can be generated to quantify spatial autocorrelation (i.e. spatial dependence) and interpolation can create continuous surface map of a variable for visual assessment.

Geostatistics have been used recently in turfgrass to implement the concept of precision turfgrass management (PTM) (Carrow et al., 2007; Bell and Xiong, 2008; Krum, 2008; Carrow

et al., 2010; Krum et al., 2010). PTM is similar to precision agriculture in that they are based on the premise of site-specific management to apply inputs, such as water, fertilizer, and pesticides, only where, when, and in the amount needed by the plant (Bouma et al., 1999; Corwin and Lesch, 2005; Bullock et al., 2007). Complex turf sites already practice some degree of PTM. For example, on sports fields depending on turf species, soil class, field usage, level of sport, and the sport itself being played, management requirements can significantly differ. However, the evolution of PTM is based on acquiring detailed site information by intensive site assessment to offer an even more precise and efficient management of inputs, such as sub-areas with a sports field, than is currently practiced (Carrow et al., 2010). Performance testing can be viewed as the site assessment referred to in the PTM concept.

Site-specific information is the first requirement of spatial analysis using geostatistics. Few researchers have used geostatistical methods to characterize spatial structure of performance qualities on natural turf sports fields (Miller, 2004; Freeland et al., 2008; Caple et al., 2012). Aside from Freeland et al. (2008), who used an electric golf cart to tow a ground penetrating radar (GPR) for the rapid assessment of soil compaction, all other data collection in these studies used common handheld sensors for data collection. Miller (2004) evaluated the surface hardness of two soccer fields (one sand-based and one native soil) using a grid pattern of 80 cells. Each cell was 10 m x 10 m and surface hardness data was taken at the center using a Clegg Impact Soil Tester (Jolimont, Western, Australia) with a 2.25-kg missile. Caple et al. (2012) performed a more robust geostatistical analysis surveying three sports fields of different soil textures at the beginning, middle, and end of season using 135 or 150 samples of five parameters (volumetric water content, penetration resistance, shear resistance, peak deceleration (surface hardness), and

surface energy absorption). From a practical standpoint, handheld devices have been deemed to being a disadvantage when sampling at a high intensity due to the time, cost, and labor needed.

Recently, Straw et al. (Chapters 2, 3, and 4) used a mobile multi-sensor device to evaluate various sampling grids, on six community sports fields, to determine an appropriate sampling procedure for an accurate spatial analysis of soil moisture (volumetric water content (VWC)), soil compaction (penetration resistance), and plant performance (normalized difference vegetative index (NDVI)). The device used was the Toro Precision Sense 6000 (PS6000) (The Toro Company, Bloomington, MN), which has recently been developed for rapid sampling on complex turfgrass sites. To date, the PS6000 is the only mobile multi-sensor platform specifically developed for use in turfgrass. The PS6000 simultaneously measures VWC (%), soil compaction (penetration resistance; N in m kg $s^{-2}$), and NDVI (unit-less with best = 1.0), all while using GPS to geo-reference longitudinal and latitudinal location of samples.

Straw et al. concluded that the more data you have for spatial analysis, the greater the accuracy. For that reason, mobile sensor platforms are the most practical means of data collection over larger areas, because of the ability to sample more intensely and the addition of an equipped GPS. However, to date, mobile sensors are not abundantly available for commercial use. Since sports fields differ from agriculture and golf courses in that the area managed is much smaller, the more commonly used handheld devices to spatially analyze sports field properties could be feasible if a standard procedure is implemented. Straw et al. suggests a 9.6 m x 4.8 m sample grid or smaller, using the PS6000, for an accurate spatial analysis of VWC and penetration resistance and at minimum a sample grid of 9.6 m x 9.6 m for NDVI. However, further analysis using handheld devices should be evaluated, using similar sampling grids, to determine if similar results occur.

The objective of this study was to conduct a preliminary comparison of handheld devices to the PS6000. VWC, penetration resistance, and NDVI data was collected with the PS6000 and handheld devices from six community sports fields at 23 or 25 same locations per field. Although geostatistical analysis was not conducted in this study, the aim is to evaluate the correlation between sampling methods for future spatial research on sports fields.

## Materials and Methods

### *Description of sports fields*

Research was conducted at the Grimes Bridge Soccer Complex in the city of Roswell, GA and at the Oconee Veterans Park in Watkinsville, GA. A total of six community level sports fields were used between the two locations. The Roswell location included three 'Tifway 419' hybrid bermudagrass (*Cynodon dactylon* x *C. transvaalensis*) soccer fields mowed two times a week at 2.54 cm with a reel mower. The Watkinsville location included three 'TifSport' bermudagrass soccer fields also mowed two times a week at 2.54 cm with a reel mower. All fields evaluated had sandy loam soils and field size ranged from 60-64 m x 95-104 m (Tables A-1 and A-2, Appendix).

Soccer was the primary sport played on all fields at both locations (Table A-1, Appendix). Fields in Roswell were constructed in tiers, with field 1 being at the top, field 2 in the middle, and field 3 below. Two concrete walls approximately 9.1 m and 3.0 m high separates fields 1 and 2, and fields 2 and 3, respectively. Field 1 is open to the public while fields 2 and 3 remain gated throughout the day and are solely used for scheduled practice and games. Fields in Watkinsville were designed in a flat open area (4.2 ha) and laid in close proximity to one another. Field 1 is directly north of field 3 with the south end zone of 1 being approximately 22.9

m from the north end zone of 3. Field 2 is centered approximately 22.9 m east of 1 and 3. All fields in Watkinsville are open to the public.

*Data collection*

VWC, penetration resistance, and NDVI data was collected in Roswell on 9 May, 2013 and in Watkinsville on 10 May, 2013 (Table A-1, Appendix). The PS6000 was used to simultaneously measure all three parameters on each field. The PS6000 is a mobile multi-sensor device equipped to attach to the hitch of a utility vehicle. Measurements are made approximately every 2.4 m while traversing the field at a speed of 2.7 to 3.3 km $h^{-1}$. Passes downfield were made 2.4 m apart; therefore measurements were collected using an approximate 2.4 m x 2.4 m sampling grid, which resulted in ~1000-1100 readings per field. Data was recorded using an on-board computer and displayed in a spreadsheet format.

VWC measurements from the PS6000 were based on a capacitance sensor (The Toro Company, Bloomington, MN) modified for use on the PS6000 which measured VWC at a 0-to-10 cm depth. To ensure soil penetration at 10 cm, two custom stainless steel probes of 9.53 mm diameter, 3.3 cm spacing, and 10 cm length were installed on the moisture sensor located in a soil sampling head. The sensor is attached to one end of a shaft on the PS6000, while a bolt is connected to the opposite end. When the PS6000 is moving forward, the wheel-driven shaft rotates in a circular fashion. The sensor's probes enter the soil and the bolt passes by a series of magnets that triggers the data loggers to take a measurement (Krum et al., 2010).

Penetration resistance from the PS6000 is measured by a stainless steel load cell sensor located in the soil sampling head of the PS6000. The sensor measures the maximum penetration force encountered in the top 10 cm of the surface and is reported as pounds of force then converted to newton (N in m kg $s^{-2}$). Similar to VWC measurements, when the PS6000 is

moving forward, the wheel-driven shaft rotates in a circular fashion and the probes from the sampling head are inserted into the ground to collect penetration resistance data. Each probe is an individual penetrometer therefore two penetration resistance readings were made for each measurement.

Two GreenSeeker RT100 active sensors (NTech Industries, Inc. Ukiah, CA) measured NDVI on the turf surface. The sensors are equipped with internal light emitting diodes and a photodiode optical detector that measures the reflectance of red (R = 660 nm) and near-infrared (NIR = 770 nm) spectra used to calculate the vegetative index {NDVI = $[(R_{770} - R_{660})/(R_{770} + R_{660})]$}. The GreenSeeker's are mounted to the Toro PS6000 and emits light pulses every 100 ms and outputs an averaged value every second. Healthy plants have greater NIR and lower R reflectance than plants under stress.

While traversing the field, 23 or 25 exact locations where the PS6000 collected data were flagged (Figure 5.1). Handheld devices were used to collect VWC, penetration resistance, and NDVI at these locations for comparison. A FieldScout TDR 300 Soil Moisture Meter (Spectrum Technologies, Inc. Aurora, IL.) was used to measure VWC at a 7.5 cm depth with two steel probes having a diameter of 0.5 cm and spacing of 1.3 cm. The sampling volumes are elliptical cylinders extending 3 cm radially beyond the TDR probes, measuring approximately 566 $cm^3$. Penetration resistance was measured with a Lang Penetrometer (Lang Penetrometer, Inc. Gulf Shores, AL.) to a maximum depth of 12 cm into the soil profile using a probe 12 cm in length and having an approximate diameter of 0.5 cm. Lastly, NDVI was determined using a Fieldscout CM 1000 NDVI Chlorophyll Meter (Spectrum Technologies, Inc. Aurora, IL.) that measures NDVI similarly to the of the PS6000's GreenSeeker.

*Statistical analysis*

Comparison of means from the PS6000 and handheld devices for each parameter on all fields was conducted using a paired t-test analysis (two sided at alpha=0.05) in R version 2.15.2 statistical software with the t.test command (R Development Core, 2008) (Table 5.1). The *t*-value is calculated using:

$$t = \frac{\left|\bar{d} - 0\right|}{s_d/\sqrt{n}} \qquad \text{[Eq. 5.1]}$$

where $\bar{d}$ is the mean of differences within each pair of data, $s_d$ is the standard deviation of the mean of differences, and *n* is the number of pairs of data. If the calculated *t*-value exceeds the critical *t*-value then the null hypothesis that there are no differences in mean is rejected. The critical *t*-value can be determined from the critical *t*-value table using the degrees of freedom (df) from the data and a known alpha (α).

Next, simple linear regression was conducted in R (using the lm command; R Development Core, 2008) to study the strength of relationship between PS6000 and handheld devices for each parameter on all fields. Scatterplots of the data were created to visually assess the relationship between parameters. A regression line was fitted and a best fit equation was determined using the least-squares method. The equation for the regression line is:

$$y = \alpha + \beta x \qquad \text{[Eq. 5.2]}$$

where y is the dependent variable, x is the independent variable, α is the intercept, and β is the slope. The coefficient of determination ($R^2$) was then found to show how well the data points fit the regression line using the equation:

$$R^2 = 1 - \frac{SS_{residuals}}{SS_{total}} \qquad \text{[Eq. 5.3]}$$

where $SS_{residuals}$ is the sum of squares from the residuals and $SS_{total}$ is the total sum of squares.

## Results and Discussion

Paired t-test results showed that there were significant differences in means of sampling devices for all fields, with the exception of VWC and NDVI on Watkinsville field 1 (Table 5.1). Although differences in means were observed, a significant correlation ($P < 0.05$) on all fields occurred with VWC and NDVI devices (Figures 5.2 and 5.4). The significant correlations did not however result in consistently strong $R^2$ values ($R^2$ = 0.3285-0.4526 for VWC and $R^2$ = 0.35-0.9189 for NDVI) (Figures 5.2 and 5.4).

Correlation of VWC and NDVI measurements is theorized to have occurred due to the similarity in methodology of the mobile and handheld devices. For VWC, the PS6000 used a capacitance sensor while the handheld device used TDR to measure soil moisture. Since both methods measure VWC by determining the ε, the differences between the two methods are likely due to one being is mobile and one is stationary and the size of the probes that are inserted into the soil to record the measurement. The difference in probe size could be the major differential factor between methods because the PS6000 probes are 2.5 cm longer resulting in VWC data being measured at a deeper depth than with the handheld sensor. For NDVI, both sensors used spectral reflectance and since values can vary at short distances the only hypothesized reasoning for differences was the location at which the sample was collected.

Penetration resistance on Roswell 1 and Watkinsville 2 exhibited significant correlations ($P < 0.05$) between devices (Figures 5.3). However, similar to VWC and NDVI, the $R^2$ values for the significant correlations were not strong ($R^2$ = 0.4345 and $R^2$= 0.4677, respectively). It is also important to note the significant differences in mean values between devices. Aside from one device being mobile and one being stationary, differences in penetration resistant could be due to methodologies in collecting the data. The PS6000 used a load cell while the handheld device

used a tension spring. Two probes were also used on the PS6000 compared to the one on the handheld device. Furthermore, the sizes of the probes being inserted into the soil are also likely a factor in the large differences. The PS6000's two probes were each a much wider diameter, in comparison to the one probe on the handheld device, resulting in more force needed to penetrate the surface.

## Conclusion

Mobile sensor devices, such as the PS6000, provide the most rapid assessment of sports field properties. Straw et al. (Chapters 2, 3, and 4) has determined appropriate sampling procedures for spatial analysis of sports fields with the PS6000; however, to date, mobile devices are not abundantly available for commercial use. Therefore, implementing a sampling procedure with the more commonly used handheld devices is necessary.

Preliminary comparisons in this study indicate that, although not always strong, there is a correlation of VWC and NDVI with the PS6000 and the handheld devices. There were not consistently significant correlations with penetration resistance. These results provide useful information for further studies evaluating the comparison of sampling devices. Future research should use the appropriate sampling procedures determined by Straw et al. to use geostatistics for spatial comparison.

## References

American Society for Testing and Materials (ASTM). 2010. F1936–10, Standard specification of impact attenuation of turf playing systems as measured in the field. Annual book of ASTM standards. American Society for Testing Materials, West Conshohocken, PA.

Baker, S.W., and M.J. Bell. 1986. The playing characteristics of natural turf and synthetic turf surfaces for association football. J. Sports Turf Res. Inst. 62:9-35.

Baker, S.W. 1991. Temporal variation of selected mechanical properties of natural turf football pitches. J. Sports Turf Res. Inst. 67:83-92.

Bartlett, M.D., I.T. James, M. Ford, and M. Jennings-Temple. 2009. Testing natural turf sports surfaces: the value of performance quality standards. Proceedings of the Institution of Mechanical Engineers, Part P. J. Sports Eng. and Technol. 223:21-29.

Bell, M.J., and G. Holmes. 1988. The playing quality of association football pitches. J Sports Turf Res Inst. 61:19-47.

Bell, G.E., and X. Xiong. 2008. The history, role, and potential of optical sensing for practical turf management. p. 641-660. *In* M. Pessarakli (Ed.), Handbook of turfgrass management and physiology. CRC Press, NY.

Bouma, J., J. Stoorvogel, B.J. van Alphen, and H.W.G. Booltink. 1999. Pedology, precision agriculture, and the changing paradigm of agricultural research. Soil Sci. 63.6:1763-1768.

Bullock, D.S., N. Kitchen, and D.G., Bullock. 2007. Multidisciplinary teams: a necessity for research in precision agriculture systems. Crop Sci. 47:1765-1769.

Canaway, P.M., and M.J. Bell. 1986. Technical note: an apparatus for measuring traction and friction on natural and artificial playing surfaces. J. Sports Turf Res. Inst. 62:211-214.

Caple, M., I. James, and M. Bartlett. 2012. Spatial analysis of the mechanical behaviour of natural turf sports pitches. Sports Eng. 15:143-157.

Carrow, R.N., V. Cline, and J. Krum. 2007. Monitoring spatial variability in soil properties and turfgrass stress: applications and protocols. Proc. of 28th Int. Irrigation Show, 9-11 Dec. 2007, San Diego, CA.

Carrow, R.N., J.M Krum, I. Flitcroft, and V. Cline. 2010. Precision turfgrass management: challenges and field applications for mapping turfgrass soil and stress. Precis. Agric, 11:115-134.

Clegg, B. 1976. An impact testing device for in situ base course evaluation. Proc. of the Australian Road Research Board. August 1976. 8:1-6.

Corwin, D.L., and S.M. Lesch. 2005. Apparent soil electrical conductivity measurements in agriculture. Comput. Electron. Agric. 46:103-133.

Dury, P.L.K. 1997. Grounds maintenance: managing outdoor sport and landscape facilities. Thorogood, London.

Emery, X., and K. González. 2007. Incorporating the uncertainty in geological boundaries into mineral resources evaluation. J. Geol. Soc. India. 69:29–38.

Fédération Internationale de Football Association (FIFA). 2012. FIFA quality concept for football turf. Fédération Internationale de Football Association.

Freeland, R.S., J.C. Sorochan, M.J. Goddard, and J.S. McElroy. 2008. Using ground-penetrating radar to evaluate soil compaction of athletic turfgrass fields. Appl. Eng. Agric. 24:509-514.

Gramckow, J. 1968. Athletic field quality studies. Cal-Turf Inc., Camarillo, CA.

Holmes, G., and M.J. Bell. 1986. A pilot study of the playing quality of football pitches. J. Sports Turf Res. Inst. 62:74-91.

Institute of Groundsmanship (IOG). 2014. Performance Quality Test (PQS) Methods. http://www.iog.org/train-education/Technical-Library/Performance+Quality+Standards/PQS+Methods+of+Test (accessed 25 Feb 2014).

James, I.T., and R.J. Godwin. 2003. Soil, water and yield relationships in developing strategies for the precision application of nitrogen fertiliser to winter barley. Biosyst. Eng. 84:467-480.

Jennings-Temple, M., P. Leeds-Harrison, and I. James. 2006. An investigation into the link between soil physical conditions and the playing quality of winter sports pitch rootzones. *In* The engineering of sport 6. 1:315-320. Springer, NY.

Krum, J.M. 2008. Spatial site assessment of soil moisture and plant status on golf courses. M.S. thesis. Univ. of Georgia, Athens, GA.

Krum, J.M., R.N. Carrow, and K. Karnok. 2010. Spatial mapping of complex turfgrass sites: Site-specific management units and protocols. Crop Sci. 50:301-315.

Leib, B.G., J.D. Jabro, and G.R. Matthews. 2003. Field evaluation and performance comparison of soil moisture sensors. Soil Sci. 168:396-409.

McAuliffe, K.W. 2008. The role of performance testing and standards in the sports turf industry: A case study approach. *In* J.C. Stier, L. Han, and D. Li (Eds.). Proceedings of 2nd international conference on turfgrass management and sports fields (pp. 391-398). Int. Soc. Hort. Sci., Belgium.

McClements, I., and S.W. Baker. 1994. The playing quality of rugby pitches. J. Sports Turf Res. Inst. 70:29-43.

Miller, G.L. 2004. Analysis of soccer field surface hardness. *In* P.A. Nektarios (Ed.), Proceedings of the first International Conference on Turfgrass Management and Science for Sports Fields. ISHS, Leuven, pp. 287-294.

R Development Core Team. 2008. R: A language and environment for statistical computing. R Foundation for Statistical Computing, Vienna, Austria. http://www.R-project.org (accessed 1 April 2014).

Stiles, V.H., I.T. James, S.J. Dixon, and I.N. Guisasola. 2009. Natural turf surfaces. Sports Med. 39(1):65-84.

Taylor, J.C., G.A. Wood, R. Earl, and R.J. Godwin. 2003. Soil factors and their influence on within-field crop variability, part II: spatial analysis and determination of management zones. Biosyst. Eng. 84:441-453.

Trenholm, L.E., R.N. Carrow, and R.R. Duncan. 1999. Relationship of multispectral radiometry data to qualitative data in turfgrass research. Crop Sci. 39:763-769.

**Table 5.1.** Paired sample *t*-test results for percent volumetric water content (%VWC), penetration resistance (N in m kg $s^{-2}$), and NDVI (unit-less with 1.0=best) data collected with the Precision Sense 6000 (PS6000) and handheld devices from similar locations on six sports fields.

| Field | n[†] | PS6000 | | Handheld | | Dif.[§] | *t*-value | df[¶] | *p*-value |
|---|---|---|---|---|---|---|---|---|---|
| | | Mean | SD[‡] | Mean | SD | | | | |
| ----------%VWC---------- | | | | | | | | | |
| Roswell 1 | 25 | 38.4 | 6.7 | 30.9 | 5.1 | 7.5 | 7.56 | 24 | 0.000[*] |
| Roswell 2 | 25 | 56.7 | 10.29 | 42.2 | 7.21 | 14.5 | 9.24 | 24 | 0.000[*] |
| Roswell 3 | 25 | 61.2 | 11.7 | 48.0 | 6.6 | 13.2 | 7.48 | 24 | 0.000[*] |
| Watkinsville 1 | 23 | 21.1 | 3.5 | 22.3 | 3.3 | -1.2 | -1.98 | 22 | 0.060 |
| Watkinsville 2 | 25 | 21.7 | 3.3 | 24.9 | 2.6 | -3.2 | -5.69 | 24 | 0.000[*] |
| Watkinsville 3 | 25 | 19.5 | 3.7 | 23.9 | 3.7 | -4.4 | -7.00 | 24 | 0.000[*] |
| ----------penetration resistance---------- | | | | | | | | | |
| Roswell 1 | 25 | 1256.0 | 507.0 | 69.9 | 14.0 | 1186.1 | 11.9 | 24 | 0.000[*] |
| Roswell 2 | 25 | 900.8 | 347.46 | 62.8 | 8.9 | 838.0 | 12.1 | 24 | 0.000[*] |
| Roswell 3 | 25 | 652.9 | 212.8 | 60.0 | 10.9 | 592.9 | 14.0 | 24 | 0.000[*] |
| Watkinsville 1 | 23 | 2513.2 | 556.6 | 83.9 | 8.0 | 2429.3 | 21.0 | 22 | 0.000[*] |
| Watkinsville 2 | 25 | 1726.4 | 480.7 | 81.3 | 8.0 | 1645.1 | 17.3 | 24 | 0.000[*] |
| Watkinsville 3 | 25 | 2356.3 | 465.5 | 87.1 | 8.1 | 2269.2 | 24.5 | 24 | 0.000[*] |
| ----------NDVI---------- | | | | | | | | | |
| Roswell 1 | 25 | 0.64 | 0.16 | 0.68 | 0.17 | -0.04 | -3.98 | 24 | 0.000[*] |
| Roswell 2 | 25 | 0.72 | 0.05 | 0.76 | 0.05 | -0.04 | -4.37 | 24 | 0.000[*] |
| Roswell 3 | 25 | 0.73 | 0.10 | 0.77 | 0.10 | -0.04 | -4.66 | 24 | 0.000[*] |
| Watkinsville 1 | 23 | 0.50 | 0.09 | 0.53 | 0.11 | -0.03 | -1.73 | 22 | 0.097 |
| Watkinsville 2 | 25 | 0.65 | 0.05 | 0.71 | 0.06 | -0.06 | -7.05 | 24 | 0.000[*] |
| Watkinsville 3 | 25 | 0.59 | 0.06 | 0.62 | 0.08 | -0.03 | -3.39 | 24 | 0.002[*] |

[†]n, number of samples collected
[‡]SD, standard deviation
[§]Dif., differences in mean
[¶]df, degrees of freedom
[*]significantly different at the $p \leq 0.05$ level (two-tailed)

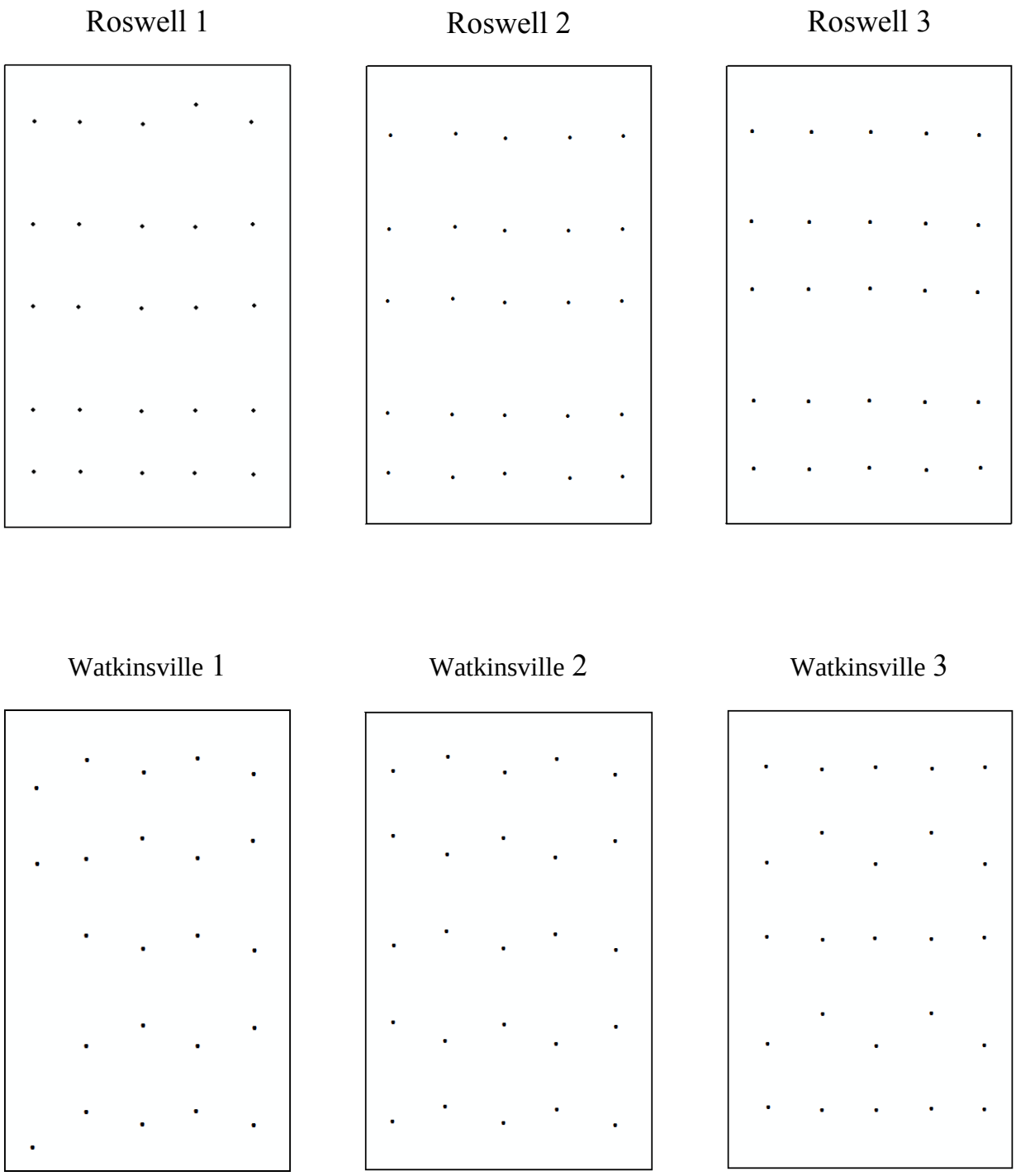


**Figure 5.1.** Sampling locations of percent volumetric water content (%VWC), penetration resistance, and normalized difference vegetative index (NDVI), collected with the PS6000 and handheld devices on six sports fields.

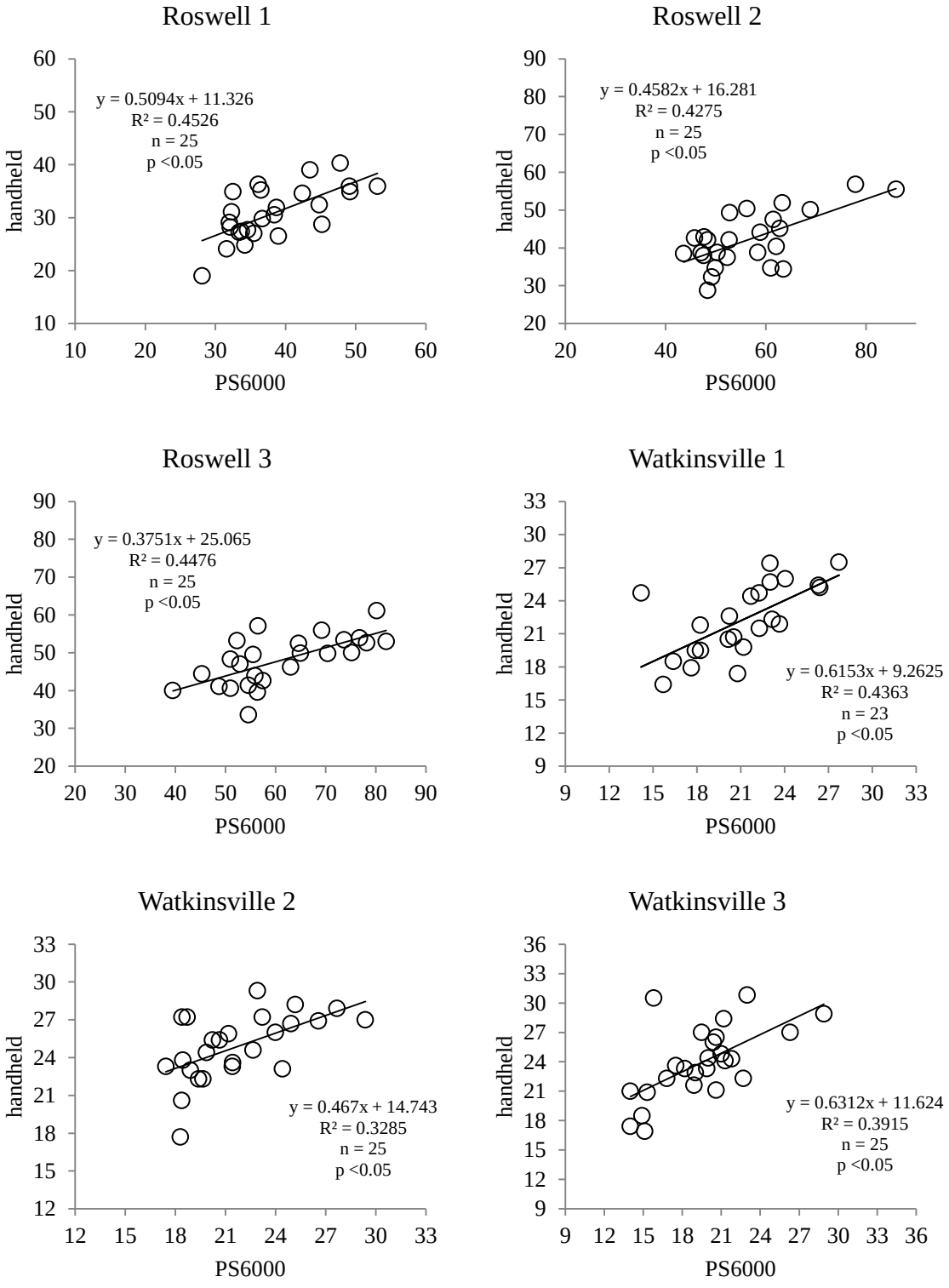


**Figure 5.2.** Linear regression of percent volumetric water content (%VWC) data collected with the Precision Sense 6000 (PS6000) and handheld TDR sensor from similar locations on six sports fields.

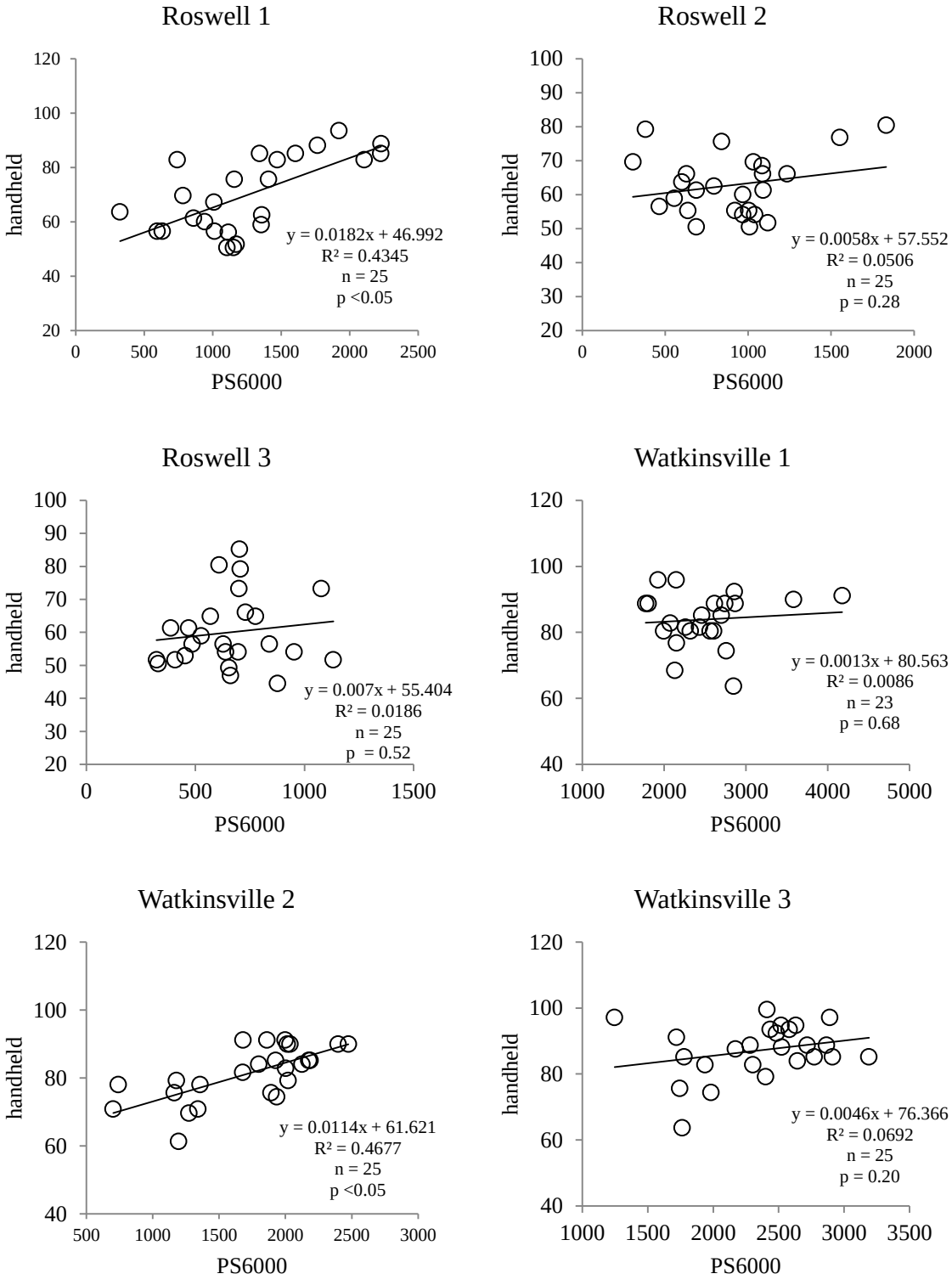


**Figure 5.3.** Linear regression of penetration resistance (N) data collected with the Precision Sense 6000 (PS6000) and handheld penetrometer from similar locations on six sports fields.

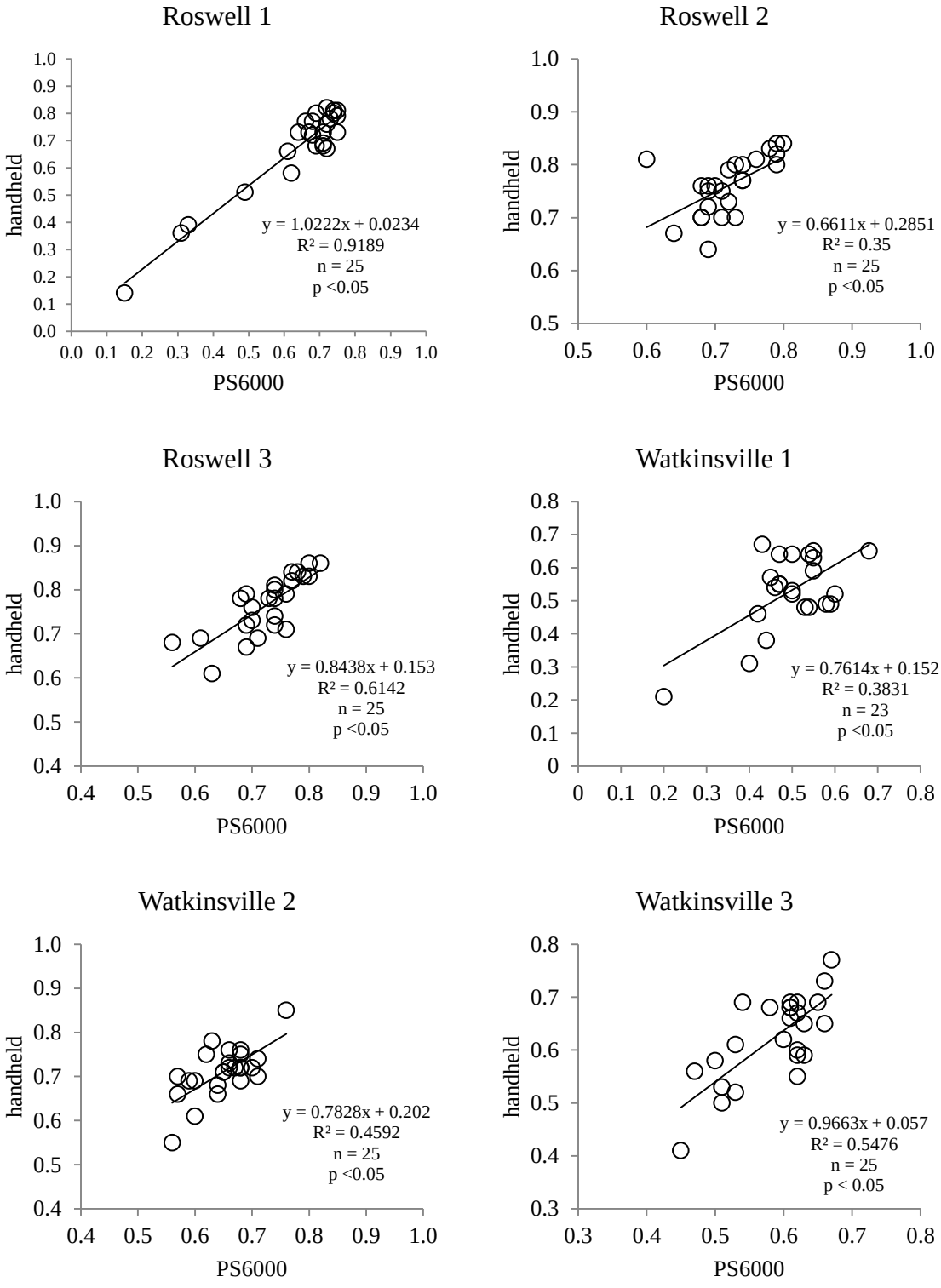


**Figure 5.4.** Linear regression of normalized difference vegatative index (NDVI) data collected with the Precision Sense 6000 (PS6000) and handheld NDVI sensor from similar locations on six sports fields.

# CHAPTER 6

# CONCLUSIONS

Sports turf managers aspire for homogeneous surface and edaphic properties to enhance player safety and field playability. Turf managers world-wide are also interested in ways to improve input efficiency to minimize costs and reduce any potential negative environmental aspects. The concept of precision turfgrass management (PTM) is gaining increasing attention for enhanced management decisions and input efficiency in turfgrass. PTM is based on acquiring detailed site information by intensive data sampling. As an implementation of PTM, performance testing to conduct spatial analysis on sports field properties can be fundamental in determining a site-specific management program.

Previous performance test procedures involved data collection from few locations on a field (6-12) using handheld devices. However, with the recent introduction of the Toro Precision Sense 6000 (PS6000), a more rapid and intense data collection can be achieved in a timely manner. The PS6000 simultaneously measures volumetric water content (VWC; %), soil compaction (penetration resistance; N in m kg $s^{-2}$), and plant performance (normalized difference vegetative index (NDVI; unit-less with best = 1.0) all while using global positioning systems (GPS) to geo-reference longitudinal and latitudinal location of samples. With the geo-referenced data, Geographic Information Systems (GIS) can be utilized for spatial analysis using geostatistical techniques. Common techniques include semivariograms to explain spatial structure, and interpolation to create continuous surface amps for visual assessment.

Few researchers have conducted spatial analysis on sports fields; therefore, a standard sampling procedure has yet to be implemented. The objective of chapters 2, 3, and 4 was to utilize the PS6000 to identify what sample grid is needed to achieve an accurate spatial analysis of soil moisture (VWC), soil compaction (penetration resistance), and plant performance (NDVI), respectively. The study was conducted on three 'Tifway 419' hybrid bermudagrass (*Cynodon dactylon* x *C. transvaalensis*) fields and three 'TifSport" hybrid bermudagrass fields. 8 sample sizes were evaluated on each field for each property. Results suggested that the more data you have the greater the accuracy; however, minimal sample grids were also identified. For VWC and penetration resistance, sample grid size of 9.6 m x 4.8 m or smaller was determined. NDVI exhibited a stronger spatial structure and a sample grid size of 9.6 m x 9.6 m or smaller was deemed acceptable. However, with a mobile device, such as the PS6000, a more intense sample grid would be most beneficial due to the relatively short time for data collection (~1 h/field).

To date, mobile sensors are not abundantly available for commercial use. Since sports fields differ from agriculture and golf courses in that the area managed is much smaller, the more commonly available handheld devices to spatially analyze sports field properties could be feasible if a standard procedure is implemented. However, the sample grids used in this study were manipulated in GIS from data collected with the PS6000. The minimal sample grids identified in chapters 2, 3, and 4 should be utilized in future research for comparison using mobile and handheld devices. If strong correlations are made then the sample grids found in previous chapters would be appropriate for both methods.

In chapter 5 preliminary comparisons of the PS6000 and handheld devices were conducted. Commonly used handheld VWC, penetration resistance, and NDVI devices were

used. Data was collected from 23 or 25 locations on six sports fields (the same used in previous chapters) for comparison of means and to determine if correlations existed. Means were not statistically similar ($P<0.05$) with any property on most fields. Although not strong, significant correlations ($P<0.05$) existed with VWC and NDVI. Only two of the six fields evaluated showed significant correlation ($P<0.05$) in penetration resistance. These results indicate that correlation does exist; however, they were not strong and therefore provide a reason for further evaluation to conduct spatial analysis with handheld devices.

The most important factor in determining the reliability, or accuracy, of a semivariogram and surface map is the sample size on which it is based. It is for this reason that mobile sensor platforms are the most practical means of data collection over larger areas, because of the ability to sample more intensely and the addition of an equipped GPS. Handheld devices, however, should not be completely disregarded due to the development of mobile devices. However, further spatial studies of sampling procedures are needed**.** Once a standard procedure is implemented, spatial analysis can be an extremely powerful management tool on sports fields.

## APPENDIX

**Table A-1.** Mapping dates, grass species, primary field use, and sizes of evaluated athletic fields.

| Field | Date mapped | Grass species | Primary field use | Field length (m) | Field width (m) |
|---|---|---|---|---|---|
| Roswell 1 | 9 May, 2013 | 'Tifway 419' bermudagrass | Soccer | 104 | 64 |
| Roswell 2 | 9 May, 2013 | 'Tifway 419' bermudagrass | Soccer | 104 | 64 |
| Roswell 3 | 9 May, 2013 | 'Tifway 419' bermudagrass | Soccer | 95 | 60 |
| Oconee 1 | 10 May, 2013 | 'Tifway Sport' bermudagrass | Soccer | 98 | 64 |
| Oconee 2 | 10 May, 2013 | 'Tifway Sport' bermudagrass | Soccer | 98 | 64 |
| Oconee 3 | 10 May, 2013 | 'Tifway Sport' bermudagrass | Soccer | 98 | 64 |

**Table A-2.** Description of soil characteristics of evaluated athletic fields.

| Field | Sand | Silt | Clay | Soil class |
|---|---|---|---|---|
| | ----------%---------- | | | |
| Roswell 1 | 59.9 | 24.1 | 16.0 | Sandy Loam |
| Roswell 2 | 73.9 | 18.1 | 8.0 | Sandy Loam |
| Roswell 3 | 71.9 | 18.1 | 10.0 | Sandy Loam |
| Oconee 1 | 76.0 | 12.0 | 12.0 | Sandy Loam |
| Oconee 2 | 69.9 | 14.1 | 16.0 | Sandy Loam |
| Oconee 3 | 71.9 | 14.1 | 14.0 | Sandy Loam |